



Effects of dredging-related stressors on sponges: laboratory experiments

Mari-Carmen Pineda^{1,2}, Brian Strehlow^{2,3}, Alan Duckworth^{1,2}, Nicole S. Webster^{1,2}

¹ Australian Institute of Marine Science, Townsville, Queensland, Australia

² Western Australian Marine Science Institution, Perth, Western Australia, Australia

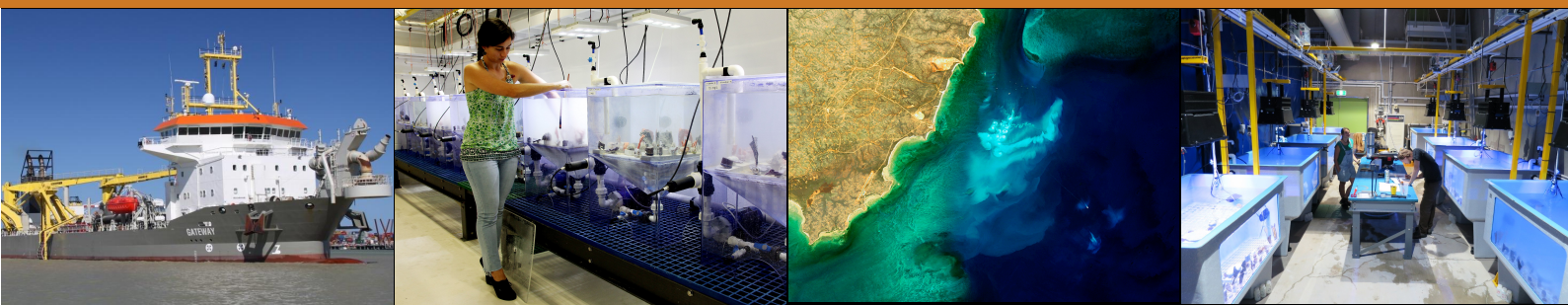
³ School of Plant Biology & Centre for Microscopy Characterisation and Analysis: University of Western Australia, Perth, Western Australia, Australia

WAMSI Dredging Science Node

Theme 6 Report

Project 6.4

November 2017



Front cover images (L-R)

Image 1: Trailing Suction Hopper Dredge *Gateway* in operation during the Fremantle Port Inner Harbour and Channel Deepening Project. (Source: OEPA)

Image 2: AIMS scientist, Dr Mari-Carmen Pineda working on an experiment investigating the effects of suspended sediment on sponges. (Source: AIMS)

Image 3: Dredge Plume at Barrow Island. Image produced with data from the Japan Aerospace Exploration Agency (JAXA) Advanced Land Observing Satellite (ALOS) taken on 29th August 2010.

Image 4: Large tank experimental set-up at the National Sea Simulator (SeaSim), Australian Institute of Marine Science, for investigating the combined effects of light attenuation, turbidity and sediment smothering on sponges. (Source: AIMS)

WAMSI Dredging Science Node

The WAMSI Dredging Science Node is a strategic research initiative that evolved in response to uncertainties in the environmental impact assessment and management of large-scale dredging operations and coastal infrastructure developments. Its goal is to enhance capacity within government and the private sector to predict and manage the environmental impacts of dredging in Western Australia, delivered through a combination of reviews, field studies, laboratory experimentation, relationship testing and development of standardised protocols and guidance for impact prediction, monitoring and management.

Legal Notice

The Western Australian Marine Science Institution advises that the information contained in this publication comprises general statements based on scientific research. The reader is advised and needs to be aware that such information may be incomplete or unable to be used in any specific situation. This information should therefore not solely be relied on when making commercial or other decision. WAMSI and its partner organisations take no responsibility for the outcome of decisions based on information contained in this, or related, publications.

Ownership of Intellectual property rights

Unless otherwise noted, any intellectual property rights in this publication are owned by the Western Australian Marine Science Institution, the Australian Institute of Marine Science and the University of Western Australia.

Copyright

© Western Australian Marine Science Institution. All rights reserved.

Unless otherwise noted, all material in this publication is provided under a Creative Commons Attribution 3.0 Australia Licence. (<http://creativecommons.org/licenses/by/3.0/au/deed.en>)



Funding Sources

The \$20million Dredging Science Node is delivering one of the largest single issue environmental research programs in Australia. This applied research is funded by **Woodside Energy, Chevron Australia, BHP Billiton and the WAMSI Partners** and designed to provide a significant and meaningful improvement in the certainty around the effects, and management, of dredging operations in Western Australia. Although focussed on port and coastal development in Western Australia, the outputs will also be broadly applicable across Australia and globally.

This remarkable **collaboration between industry, government and research** extends beyond the classical funder-provider model. End-users of science in regulator and conservation agencies, and consultant and industry groups are actively involved in the governance of the node, to ensure ongoing focus on applicable science and converting the outputs into fit-for-purpose and usable products. The governance structure includes clear delineation between end-user focussed scoping and the arms-length research activity to ensure it is independent, unbiased and defensible.

And critically, the trusted across-sector collaboration developed through the WAMSI model has allowed the sharing of hundreds of millions of dollars worth of environmental monitoring data, much of it collected by environmental consultants on behalf of industry. By providing access to this usually **confidential data**, the **Industry Partners** are substantially enhancing WAMSI researchers' ability to determine the real-world impacts of dredging projects, and how they can best be managed. Rio Tinto's voluntary data contribution is particularly noteworthy, as it is not one of the funding contributors to the Node.

Funding and critical data

Critical data



Year of publication: 2017

Metadata: <http://catalogue.aodn.org.au/geonetwork/srv/eng/metadata.show?uuid=8a3520ee-c696-4165-b99e-5ecdedfa17f2>

Citation: Pineda MC, Strehlow B, Duckworth A, Webster NS (2017) Effects of dredging-related stressors on sponges: laboratory experiments. Report of Theme 6 - Project 6.4 prepared for the Dredging Science Node, Western Australian Marine Science Institution, Perth, Western Australia, 157 pp.

Author Contributions: MCP, BS, AD and NSW conceived and designed the experiments. MCP and BS performed the experiments. MCP and BS performed laboratory and data analyses. MCP, BS, AD and NSW wrote the manuscripts.

Corresponding author and Institution: Mari-Carmen Pineda (Australian Institute of Marine Science, Townsville). Email: M.Pineda@aims.gov.au or N.Webster@aims.gov.au

Competing Interests: The commercial investors and data providers had no role in the data analysis, data interpretation, the decision to publish or in the preparation of the manuscript. The authors have declared that no competing interests exist.

Acknowledgements: We are thankful to the Node Leaders (Dr. R Jones and Dr. R Masini) and Theme 6 leader (Dr. MA Abdul Wahab) for their advice and discussion of results. We are in debt to P Bessell-Browne, N Giofre and SeaSim staff for their time and efforts on the WAMSI tank prototyping and sediment delivery systems. We would like to thank the crew of the San Miguel for helping with the sponge collection for this study. J Doyle provided valuable advice on the chlorophyll analysis. Dr. C Schönberg and Dr. J Fromont contributed to the species identification. Dr. D Francis and V Mocellin provided advice for the lipid analysis. Dr. H Luter, Dr. L Moitinho-Silva, Dr. P Laffy, C Astudillo and G Millar provided useful advice on the microbial community data analyses. Finally, special thanks to M Sternal, J Kamp and E Arias for help in the field, laboratory and while running the experiments.

Collection permits/ethics approval: All collections were performed under Great Barrier Reef Marine Park Regulations 1983 (Commonwealth) and Marine Parks regulations 2006 (Queensland) Permit G12/35236.1 (re-issue) issued to the Australian Institute of Marine Science (AIMS, PMB No. 3 Townsville MC QLD 4910) on 19 July 2013 to cover the period 19 July 2013 to 1 August 2015 for ‘...conduct of a research program’ associated with the AIMS 2011-2015 Research Plan...’ and Permit G13/35758.1 (re-issue) to AIMS from 4 June 2013 to 31 Jan 2016 for “...effects of sediment on corals and sponges...”

Publications supporting this work:

Pineda MC, Duckworth A, Webster N (2016) Appearance matters: sedimentation effects on different sponge morphologies. *Journal of the Marine Biological Association of the UK*, 96 (2): 481-492 DOI: 10.1017/S00253154140001787

Pineda MC, Strehlow B, Duckworth A, Doyle J, Jones R, Webster NS (2016) Effects of light attenuation on the sponge holobiont-implications for dredging management. *Scientific Reports*. 6:39038. DOI:10.1038/srep39038.

Pineda MC, Strehlow B, Sternal M, Duckworth A, Jones R, Webster NS (2017) Effects of suspended sediments on the sponge holobiont with implications for dredging management. *Scientific Reports*. 7: 4925 | DOI:10.1038/s41598-017-05241-z

Pineda MC, Strehlow B, Sternal M, Duckworth A, den Haan J, Jones R, Webster NS (2017) Effects of sediment smothering on the sponge holobiont with implications for dredging management. *Scientific Reports*. | 7: 5156 | DOI:10.1038/s41598-017-05243-x

Pineda MC, Strehlow B, Kamp J, Duckworth A, Jones R, Webster NS (2017) Effects of combined dredging-related stressors on sponges: a laboratory approach using realistic scenarios. *Scientific Reports*. 7: 5155 | DOI:10.1038/s41598-017-05251-x

Strehlow BW, Jorgensen D, Webster NS, Pineda MC, Duckworth A (2016) Using a thermistor flowmeter with attached video camera for monitoring sponge excurrent speed and oscular behaviour. *PeerJ*. 4:e2761. DOI:10.7717/peerj.2761

Strehlow BW, Pineda MC, Duckworth A, Kendrick GA, Renton M, Abdul Wahab M, Webster NS, Clode P (2017) Sediment tolerance mechanisms identified in sponges using advanced imaging techniques. *PeerJ*. 5:e3904; DOI 10.7717/peerj.3904

Contents

- EXECUTIVE SUMMARY I**
- CONSIDERATIONS FOR PREDICTING AND MANAGING THE IMPACTS OF DREDGING IV**
- RESIDUAL KNOWLEDGE GAPS XI**
- PUBLICATIONS 1**
- 1. APPEARANCE MATTERS: SEDIMENTATION EFFECTS ON DIFFERENT SPONGE MORPHOLOGIES1
- 2. EFFECTS OF LIGHT ATTENUATION ON THE SPONGE HOLOBIONT-IMPLICATIONS FOR DREDGING MANAGEMENT13
- 3. EFFECTS OF SUSPENDED SEDIMENTS ON THE SPONGE HOLOBIONT WITH IMPLICATIONS FOR DREDGING MANAGEMENT...33
- 4. EFFECTS OF SEDIMENT SMOTHERING ON THE SPONGE HOLOBIONT WITH IMPLICATIONS FOR DREDGING MANAGEMENT...55
- 5. EFFECTS OF COMBINED DREDGING-RELATED STRESSORS ON SPONGES: A LABORATORY APPROACH USING REALISTIC SCENARIOS.....77
- 6. USING A THERMISTOR FLOWMETER WITH ATTACHED VIDEO CAMERA FOR MONITORING SPONGE EXCURRENT SPEED AND OSCULAR BEHAVIOUR94
- 7. SEDIMENT TOLERANCE MECHANISMS IDENTIFIED IN SPONGES USING ADVANCED IMAGING TECHNIQUES..... 116

Executive Summary

The responses of sponges to dredging-related pressures are not well known, posing a significant challenge to their effective management. Sponges can be differentially affected by dredging-related pressures depending on their nutritional mode, their overall morphology and their behavioural and physical adaptations to exclude sediment¹. For instance, due to their high filter-feeding activity, heterotrophic sponges may be affected by elevated suspended sediment concentrations (SSCs) with long term exposure to high SSCs clogging their aquiferous systems and reducing the flow of oxygenated seawater to the sponge. In parallel, phototrophic sponges may be affected by the reduction in benthic light availability that occurs during dredging plumes. Sediment deposition may also cause smothering and suffocation of recruits and adult sponges, especially encrusting, massive, cup and plate-like morphologies which can trap sediments. These effects are expected to have flow on consequences for host energetics, health and reproductive output, potentially impacting community structure and functioning.

The identification of cause-effect pathways and derivation of dose:response relationships are essential for effective dredging management and impact-prediction. For this purpose, and in order to avoid confounding interactions of stressors, light attenuation, SSCs and sediment smothering were tested in isolation. Results of these individual experiments contributed to the derivation of trigger values that can be used to interrogate models for impact prediction and in water quality monitoring programs to alert dredging proponents to levels of stressors that, if continued, could detrimentally impact sponge populations. However, during dredging operations these three pressures occur in combination which may have additive or synergistic negative effects on sponges under realistic field conditions. Therefore, a final experiment which investigated the combined effects of these stressors under different dredging scenarios was also performed.

Five laboratory experiments were performed at the National Sea Simulator (SeaSim; Australian Institute of Marine Science, Townsville, QLD). Experiments were conducted in custom-designed small and large tank systems that provided reliable automated sediment delivery, and continuous monitoring of turbidity, light intensity and sediment deposition (i.e. sediment falling out of suspension). The state of the art laboratory infrastructure at SeaSim is globally unique, hence these experiments could not have been performed elsewhere in Australia. To ensure direct transferability of experimental results to Western Australia, a number of procedures were established; 1) 5 out of the 6 selected sponge species (*Cliona orientalis*, *Carteriospongia foliascens*, *Coscinoderma matthewsi*, *lanthella basta* and *Stylissa flabelliformis*) are common throughout the Indo-Pacific, including the east and west coasts of tropical Australia. The sixth species, *Cymbastela coralliophila* has not been reported from outside Queensland, however a closely related sister species, *Cymbastela stipitata* with similar morphology and symbiont composition² is known to occur across the Northern Territory and tropical Western Australia, including areas where dredging occurred. The shared morphology and symbiont composition infer similar responses to dredging-related pressures in the two species. 2) Sediment used in Experiments 3 (suspended sediment), 4 (smothering) and 5 (combined) was selected after an initial comparison (Experiment 1; range finding) between the siliclastic sediment collected subtidally from Onslow (WA) and the calcareous sediment collected from the lagoon of Davies Reef, a mid-shelf reef centrally located in the GBR (QLD), showed similar responses in sponges from comparative dosing. Of note, the sediment from Onslow was only representative of a specific location in WA, subjected to high terrestrial influence, while the sediment from Davies Reef was representative of most reef environments where dredging occurs in WA. Taking all this into consideration, the calcareous sediment from Davies Reef was selected for use in Experiments 3 – 5. Most importantly, all sediments were ground to ~30 µm (with 80% of the sediment 3 – 65 µm), being predominantly silt-sized, typical for dredge plumes, to ensure environmental relevance. Finally, experimental treatments

¹ See review by Schönberg CHL (2016) Effects of dredging on filter feeder communities, with a focus on sponges. Report of Theme 6 – Project 6.1 prepared for the Dredging Science Node, Western Australian Marine Science Institution, Perth, Western Australia. 139 pp.

² See Report for Project 6.2: Fromont J et al. (2016) Patterns of sponge biodiversity in the Pilbara, Northwestern Australia. Diversity 8(4):21 doi:10.3390/d8040021

incorporated in these experiments were based on field data from dredging sites in WA (water quality analysis from WAMSI DSN Theme 4).

Experiments were conducted from Oct 2013 – Oct 2016. Experiment 1 – 4 tested dredging related pressures in isolation to establish cause:effect pathways and determine thresholds of stress for adult sponges to individual stressors; Experiment 5 tested the combined effects of these stressors under realistic dredging scenarios. The effects of dredging-related pressures on sponges were determined using a suite of response variables, with a particular focus on sponge health and feeding strategies (growth, bleaching, necrosis, mortality, respiration rates, lipids, histology), and changes in sponge symbiosis (pigment analyses and chlorophyll fluorescence for assessing phototrophy and molecular analyses for assessing the composition of the entire sponge microbial community).

Experiment 1 (range-finding; Project 6.4_1) was performed in Oct 2013 and tested the effects of a single pulse of sediments (0, 250 and 500 mg L⁻¹; resulting in 0, 8 and 16 mg cm⁻² of settled sediment, respectively) on ten sponge species encompassing the 4 main morphologies (massive, erect, cup and encrusting) over a 14 d period. The effects of high sedimentation included mortality of cup shaped *Callyspongia confederata* and small areas of tissue necrosis in other species, with massive, encrusting and wide cup morphologies particularly affected. However, the sediment concentrations tested did not cause changes in the concentration of sponge pigments or the structure of the symbiotic microbial community in any species. Experiment 1 facilitated selection of the most appropriate species for further experimental work, based on their ability to survive in aquaria under experimental conditions. Results also indicated that a single pulse of sediments less than 16 mg cm⁻² is not detrimental to most sponge species.

Experiment 2 (light attenuation; Project 6.4_2) was performed in May 2014 and tested the effects of five different light levels (daily light integrals [DLIs] of 0, 0.8, 3.1, 8.1 mol photons m⁻² d⁻¹ and a natural light control of ~3.2–6.5 mol photons m⁻² d⁻¹) on a selection of three phototrophic (*Carteriospongia foliascens*, *Cymbastela coralliophila* and *Cliona orientalis*) and two heterotrophic (*Ianthella basta* and *Stylissa flabelliformis*) sponge species for 28 d, followed by a 14 d recovery period under natural light. Increases in chlorophyll fluorescence under low light intensity treatments (≤ 3.1 mol photons m⁻² d⁻¹) during the first weeks revealed a potential for short term acclimation to different light levels (photoacclimation) among the phototrophic species. Light reduction impacted the three phototrophic species differently: 1) *C. orientalis* bleached after 72 h in the 0 DLI treatment, concomitant with reduced fluorescence yields and chlorophyll concentrations, but recovered completely after 14 d under natural light conditions, 2) *C. foliascens* bleached after 7 d in the 0 DLI treatment, concomitant with significantly reduced fluorescence yields, reduced chlorophyll concentrations, a significant shift in the composition of the microbial community and was unable to recover under natural light, with bleached individuals dying during the recovery period, 3) *C. coralliophila* was least affected by low light, exhibiting a slight decrease in photosynthetic pigments and growth rates, but with all individuals fully recovering under natural light conditions. As expected, the heterotrophic species were unaffected by light attenuation over the course of the experiment.

Experiment 3 (suspended sediments; Project 6.4_3) was performed in Dec 2014 and tested the effects of five different SSCs (0, 3, 10, 30 and 100 mg L⁻¹) on the same species used in Experiment 2 (note: *I. basta* was replaced by *Coscinoderma matthewsi* to include a massive morphology) for 28 d, followed by a 14 d recovery period in clear seawater. Light intensity was adjusted so that it was similar across SSC treatments (all sponges experienced a daily light integral of 5 mol photons m⁻²). Most sponges survived the experimental conditions, although an overall reduction in size and lipid reserves along with increased bleaching/necrosis was observed in most individuals exposed to high SSC (≥ 30 mg L⁻¹). Mortality was only observed in *C. foliascens* and *C. matthewsi* exposed to ≥ 30 and 100 mg L⁻¹, respectively. At high SSC, phototrophic sponges relied more on photosynthesis to obtain energy indicated by 1) a reduction in the number of choanocyte chambers, 2) increased *Symbiodinium* sp. cells in *C. orientalis*, 3) increased Chl d concentrations (i.e. Cyanobacteria) in both *C. foliascens* and *C. coralliophila* and 4) increased OTUs affiliated to the *Cyanobacteria* among the phototrophic species.

Following the experimental exposure, most of the five sponges tested recovered after 14 d in control conditions. However, the phototrophic *C. foliascens* exposed to $\geq 30 \text{ mg L}^{-1}$ exhibited necrosis and subsequent mortality, and 20% mortality was recorded for the heterotrophic *C. matthewsi* at the end of the recovery periods when exposed to 100 mg L^{-1} SSC.

Experiment 4 (smothering; Project 6.4_4) was undertaken in May 2015 with the same sponge species used in Experiment 3 to test the effects of sediment smothering ($\sim 50 \text{ mg cm}^{-2}$ every $\sim 4 \text{ d}$) for 4, 16 and 30 d, followed by a 14 d recovery period. All sponges survived the 30 d smothering period and subsequent recovery phase and, in most species, sediment smothering did not cause any visible signs of stress (i.e. necrosis). While partial bleaching was observed in some specimens of the phototrophic species *C. orientalis* after exposure to 16 and 30 d of smothering, full recovery was evident at the end of the observational phase. Smothering varied among sponge morphologies with massive and cup shaped species covered most by deposited sediments. Some sponge species produced mucus sheets that would bind deposited sediment, which water flow subsequently sloughed off. Most sponges exposed to 16 or 30 days of sediment smothering shrunk in size. However, sediment smothering (even for up to 30 days) did not cause lipid depletion or overall changes in sponge respiration rates and did not affect the photosymbiont activity or microbiome composition of any of the five sponge species.

Experiment 5 (combined effects; Project 6.4_5) was undertaken in April 2016 and tested combined elevated SSCs, light attenuation and sedimentation under realistic dredging scenarios based on field data. Experimental treatments ranged from scenarios of a high impact site (SSC of $\sim 70 \text{ mg L}^{-1}$ and DLI of 0.11, i.e., twilight or near darkness) to a low impact reference site (SSC of $< 3 \text{ mg L}^{-1}$ and DLI of > 3). The experiment ran for 28 d followed by a 14 d observational period in clean seawater, and focussed on three of the six species used in previous experiments, including the phototrophic *C. foliascens* and *C. orientalis*, and the heterotrophic *I. basta*. These species represent different morphologies, nutritional modes and showed disparate responses to the individual dredging-related stressors tested previously. High levels of bleaching/partial mortality (90%) and total mortality (20%) were reported in *C. foliascens* and *C. orientalis* respectively, after 28 d exposure to the high impact treatment (SSC of $\sim 70 \text{ mg L}^{-1}$ and DLI of 0.11). In *C. foliascens*, stress responses were observed in all treatments $\geq 10 \text{ mg L}^{-1}$, with an LC_{50} of 47.02 mg L^{-1} (95 % confidence interval range: $39.8\text{--}56.0 \text{ mg L}^{-1}$) with $0.266 \text{ mol photons m}^{-2} \text{ day}^{-1}$ (range: $0.214\text{--}0.334$), and an LC_{10} of 22.50 mg L^{-1} (range: $13.9\text{--}30.6 \text{ mg L}^{-1}$) with DLI of $0.861 \text{ mol photons m}^{-2} \text{ day}^{-1}$ (range: $0.615\text{--}1.256 \text{ mol photons m}^{-2} \text{ day}^{-1}$). Although *C. orientalis* was adversely affected in the high impact dredging scenario, this species fully recovered during the 14 d observational period. *Ianthella basta* showed signs of stress including tissue regression and mucus production when exposed to $\geq 10 \text{ mg L}^{-1}$, but this species did not experience any mortality and showed high potential for recovery during the post-exposure observational period. Hence, the combination of stressors simulating field conditions at a dredging site had a higher impact on sponges than turbidity, smothering or light attenuation alone. However, the impacts were highly species-specific and were most detrimental to the phototrophic species *C. foliascens*. In contrast, the phototrophic *C. orientalis* exhibited 100% survival for up to 21 d under the high impact dredging scenario, reducing to 80% survival after 28 days of exposure, while the heterotrophic species *I. basta* tolerated even longer periods (i.e. up to 28 d) and was able to recover once returned to pre-dredging conditions.

Appendix Experiment 6 (thermistor; Project 6.4_Appendix). Sponge pumping rates have been shown to significantly decrease or arrest when exposed to elevated SSCs. A digital, four-channel thermistor flowmeter integrated with time-lapse cameras was therefore developed to provide an experimental tool for measuring pumping rates in marine sponges, particularly those with small excurrent openings (oscula) such as *Cliona orientalis*. Combining flowmeters with time-lapse imagery yielded valuable insights into the contractile behaviour of oscula in sponges. Osculum cross-sectional area in *C. orientalis* was positively correlated to measured excurrent speeds, indicating that sponge pumping and osculum contraction are coordinated behaviours. Both osculum area and excurrent speed are positively correlated to sponge pumping rate. Diel trends in pumping activity and osculum contraction were observed, with sponges increasing their pumping activity to peak at midday and decreasing pumping and contracting oscula at night. Short-term elevation of SSC initially decreased

pumping rates in sponges by up to 90%, ultimately resulting in closure of the oscula and cessation of pumping after ~1 hour. The development of the thermistor flowmeter has provided a methodological platform for future quantification of changes in sponge pumping due to dredging-related stressors.

Considerations for predicting and managing the impacts of dredging

Sponges respond to dredging-related stressors in a highly species-specific way, making it difficult to predict the population level consequences of dredging activity. Across all dredging pressures, the phototrophic cup sponge *Carteriospongia foliascens* was the most sensitive species, exhibiting rapid bleaching and mortality under low light and high impact dredging scenarios. **Due to the broad geographic range of *C. foliascens*, we propose this species as a sensitive bioindicator for dredging-related stress.** Notably, phototrophic cup sponges (*Carteriospongia* spp. and the sister genus *Phyllospongia* spp.) have previously been shown to be depth limited in clear water reefs of the GBR, presumably influenced by light attenuation at >30 m; as these species rely on phototrophy for >50% of their carbon needs^{3,4,5}.

Pre-development Surveys

Identifying sensitive bioindicators and relevant monitoring sites

As phototrophic sponges are expected to be the most sensitive filter feeders to dredging pressures, areas/habitats where these sponges occur should be identified as part of pre-dredging surveys and then regularly monitored over the course of the dredging activity. **In particular, phototrophic sponges at proposed reference sites and within the modelled Zone of Influence (Zoi), Zone of Moderate Impact (ZoMI) and Zone of High Impact (ZoHI) should be identified to allow for sub-lethal stress detection.** For example, *Carteriospongia foliascens* or *Carteriospongia* spp., which can be easily identified in high resolution photographs of the benthos, can be surveyed over large spatial scales using towed video surveys or ROVs. **Water quality monitoring loggers should be deployed at the reference and impact monitoring sites to assess baseline water quality parameters before the start of dredging and maintained during dredging activity.**

Assessing the baseline health of sponges

Based on laboratory experiments, bleaching and necrosis are relevant visual indicators of sub-lethal stress in sponges. **These visual indicators can be incorporated into pre-dredging surveys to establish the baseline health of sponge populations, and would facilitate the interpretation of impacts from dredging activity, as opposed to effects from pre-existing sub-optimal biological conditions.** Baseline surveys should be performed at sufficient temporal (e.g. ≥1 year) and spatial scales (e.g. 20 km) to allow for the assessment of natural disturbance events on sponge health over different seasons.

Impact Prediction

A detailed summary of how sponges respond to dredging-related stressors, including experimentally derived stress thresholds are provided in Table 1.

Light attenuation and associated reduced light availability as a predictor of impact

Experimental results indicate that light attenuation is an important dredging-related parameter affecting sponge health in phototrophic species. Phototrophic and heterotrophic sponge species survived under low light intensities (DLI ≤3.1 mol photons m⁻² d⁻¹) for 28 d. However, some phototrophic species bleach within 72 h and the health of other species is seriously impaired after 7–14 d of complete darkness. Species-specific mortalities were detected within the phototrophic sponges, with *C. orientalis* fully recovering when returned to natural light after 28d of continuous darkness (DLI 0 mol photons m⁻² d⁻¹). In contrast, *C. foliascens* exhibited 100% mortality

³ Wilkinson C (1983) Net primary productivity in coral reef sponges. *Science*. 219(4583):410–412

⁴ Wilkinson C (1988) Foliose Dictyoceratida of the Australian Great Barrier Reef. II. Ecology and distribution of these prevalent sponges. *Biomass* 9:321–327

⁵ Wilkinson C and Evans E (1989) Sponge distribution across Davies Reef, Great Barrier Reef, relative to location, depth, and water movement. *Coral Reefs* 8:1-7.

under the same experimental and recovery conditions. **This highlights the complex and variable sensitivities of sponges to light attenuation and the importance of considering species-specific thresholds when managing dredging-related stressors. *C. foliascens* is highly susceptible to prolonged acute light reduction, bleaches readily and has low recovery potential.**

Relevance of SSCs and smothering to impact prediction

Most sponges can survive short-term (<28d) exposure to elevated SSC, although an overall reduction in size and lipid reserves and increased bleaching/necrosis occurred in most species at high SSC ($\geq 30 \text{ mg L}^{-1}$). In addition to the adverse effects on sponge feeding behavior (with associated depletion of energy reserves), mortality of *C. foliascens* and *C. matthewsi* occurred at SSC of $\geq 30 \text{ mg L}^{-1}$. The LC_{50} in *C. foliascens*, for SSC in isolation, was 40.6 mg L^{-1} (95 % CI: $28.9\text{--}57.0 \text{ mg L}^{-1}$) and the LC_{10} was 21.5 mg L^{-1} (95 % CI: $13.1\text{--}35.2 \text{ mg L}^{-1}$). These values were slightly lower than when all stressors were applied in combination; however the confidence intervals for both overlap, with narrower intervals in the combined experiment. LC values could not be determined for *C. matthewsi* because mortality in the highest treatment, i.e. 70 mg L^{-1} , after 28 days was only 20%. However, it is expected that a longer term exposure would result in greater mortality. **Overall, $\text{SSC} \leq 10 \text{ mg L}^{-1}$ (in isolation) for <28 d was tolerated by most species and could be established as a reasonable sub-lethal threshold for adult sponges.**

Sponges were able to survive smothering from a single pulse of sediment exposure $<16 \text{ mg cm}^{-2}$ for 14 d, however necrosis was detected in massive, encrusting and horizontal cup morphologies. Additionally, while negative growth rates were observed in most sponges exposed to 16 and 30 d of non-continuous smothering (where sponges were exposed to sediment every 4 days, simulating intermittent stress under dredging scenarios), the 30 d sediment smothering period did not cause any mortality, visible signs of host stress, lipid depletion or overall changes in sponge respiration rates, and this treatment did not affect the photosymbiont activity or microbiome composition of any of the five sponge species. **Non-continuous sediment smothering for up to 30 days did not alter the health of adult sponges as most species possessed either active or passive self-cleaning strategies which allowed them to continue feeding. Nevertheless, symptoms of sub-lethal SSC and sedimentation stress which could be used as indicators of dredging impact include the reduction of lipids, bleaching, necrosis, tissue regression, mucus production and oscula closure.**

Combined effects of light attenuation, SSC and smothering

A faster and greater sponge stress response was observed when all three dredging-related pressures (light attenuation, suspended sediments and sedimentation) were tested in combination, simulating near dredging site conditions. Overall, stress responses (i.e. bleaching, necrosis, tissue regression, mucus production and oscula closure) were detected in sponges exposed to $\text{SSC} \geq 10 \text{ mg L}^{-1}$ with DLI of $\leq 1 \text{ mol photons m}^{-2} \text{ d}^{-1}$ for up to 28 d exposure, corresponding to a “moderate impact” treatment, although extensive mortality was only observed in one species and under higher impact scenarios ($\geq 30 \text{ mg L}^{-1}$ with DLI of $\leq 0.5 \text{ mol photons m}^{-2} \text{ d}^{-1}$ for 28 d; Experiment 5).

Most sponges can survive under low-moderate dredging impact scenarios (i.e. $\leq 30 \text{ mg L}^{-1}$, ≥ 0.5 DLI) for up to 28 d, with 20% and 90% mortality observed in *C. orientalis* and *C. foliascens* under the highest impact scenario (i.e. 70 mg L^{-1} , 0.1 DLI). The combination of high SSCs and low light availability accelerated and increased mortality in both phototrophic species, although most sponges presented mechanisms or adaptations to effectively deal with dredging-related pressures in the short term. However, these tolerance mechanisms come at a cost, as evidenced by reduced lipids and deterioration of sponge health in all species towards the end of the experiment, suggesting that longer term exposure to similar conditions is likely to result in higher mortality.

Monitoring

Environmental monitoring

The laboratory experiments identified the physical factors of light attenuation and SSC as relevant dredging-related stressors for sponges. **Therefore, light (DLI; mol photons m⁻² d⁻¹) and SSCs (mg L⁻¹) at distances from dredging or within the Zones of Influence, Moderate Impact and High Impact as described in EPA (2016)⁶ should be monitored before and during the dredging program, to facilitate the management of dredging on sponge communities.** Other contributing factors, such as water depth and ambient light which would inevitably influence the amount of light reaching the benthos through time should also be considered and monitored. The threshold levels for light attenuation and SSCs are provided (Table 1).

Biological monitoring

In addition to environmental monitoring, changes in the visible biological health status of sponge communities should also be monitored through time. **The potential visual indicators of sponge health are tissue discolouration (i.e. bleaching), tissue necrosis, mucus sheet production and tissue regression, which can be detected using high resolution photographs or *in-situ* observations by diving, towed video or remotely operated underwater vehicles (ROVs).** Oscula closure, which was a stress response observed in sponges under dredging-related stress in the laboratory, is expected to be technically challenging to implement in non-diver based monitoring programs.

From this present study, *C. orientalis* and *C. foliascens* represent robust bioindicator species for monitoring programs, as they showed different sensitivities (i.e. fast and reversible bleaching versus slow and irreversible bleaching and necrosis, respectively) to stress associated with dredging activity. These bioindicator species should therefore be included in routine monitoring programs for dredging operations.

Management

The thresholds and pressure:response relationships derived from this experiment can be used in management guidelines, however it is important to note that considerable inter-species variability exists in how sponges respond to dredging pressures. **It is therefore imperative to assess the sensitivity of ecologically important or endemic species at planned dredging sites.**

Although most phototrophic sponge species showed short-term (i.e. hrs–days) light acclimation potential, longer-term (i.e. days–weeks) light attenuation events led to detrimental and in some cases irreversible effects on the sponge holobiont (host sponge and associated microbiome). **Considering the abundance and ecological importance of photosynthetic sponges in marine ecosystems, the maximum duration of dredging-related light attenuation to complete darkness should be limited to <7 d to enable phototrophic sponges to recover between events.** The LC₅₀ (SSCs: 47.02 mg L⁻¹; DLI: 0.266 mol photons m⁻² d⁻¹, for 28 d) and LC₁₀ (SSCs: 22.50 mg L⁻¹; DLI: 0.861 mol photons m⁻² d⁻¹, for 28 d) values derived for *C. foliascens* can be used by managers and dredging proponents **when implementing zones of impact based on dredge plume models.** Similarly, exposure to high SSC (≥ 23 mg L⁻¹) for extended periods (28 d) had a negative effect on sponge feeding behaviour and associated depletion of energy reserves, while an exposure to SSCs ≤ 10 mg L⁻¹ (in isolation) was tolerated by most species. **The monitoring of light attenuation and SSCs using *in-situ* loggers and real-time sentinel monitoring stations would allow for the detection of detrimental stressor trajectories approaching threshold levels, and can inform managers and proponents when corrective measures are required.**

⁶ EPA (2016) Technical Guidance: Environmental Impact Assessment of Marine Dredging Proposals. Environmental Protection Authority, Perth, Western Australia.

Table 1: Summary of biological responses and dredging-related pressure thresholds in six sponge species investigated in the laboratory experiments of WAMSI DSN Theme 6.4. Light attenuation (DLI; mol photons m⁻² d⁻¹), suspended sediment concentrations (SSCs; mg L⁻¹) and sediment smothering (mg cm⁻²) were tested in isolation and in combination on three phototrophic (*Cliona orientalis*, *Carteriospongia foliascens* and *Cymbastela coralliophila*) and three heterotrophic (*Coscinoderma matthewsi*, *Ianthella basta* and *Stylissa flabelliformis*) sponge species.

		Thresholds for dredging related pressures in sponges											
		Light attenuation			Suspended sediments (SS)			Sediment smothering			Combined stressors		
Species	Morphology / Nutritional mode	Sub-lethal stress	Recovery?	Mortality	Sub-lethal stress	Recovery?	Mortality	Sub-lethal stress	Recovery?	Mortality	Sub-lethal stress	Recovery?	Mortality
<i>Cliona orientalis</i> (RESILIENT : sensitive indicator species with potential for recovery)	Encrusting (endolithic)/ Phototrophic	100% survival in DLI 0–8.1 for 28 d Bleaching under low light (in <7 d, under DLI <0.8), but 100% recovery	Yes	Not observed	100% survival in SSCs >70 mg L ⁻¹ for 28 d Bleaching under high SSCs but 100% recovery No effects <23 mg L ⁻¹	Yes	Not observed	100% survival to 28 d smothering Partial bleaching under smothered tissue but 100% recovery	Yes	Not observed	100% survival under low-moderate impact scenarios (≤30 FNU, ≥0.5 DLI)	Yes	Yes, 20% mortality after 7 d under high impact scenarios (70 FNU, 0.1 DLI)
		<u>Mechanism</u> : Ability to switch between nutritional modes (compensates with heterotrophic feeding)			<u>Mechanism</u> : Ability to increase phototrophic feeding (decrease choanocyte chambers and increase symbiont activity) under high SSCs as long as light is available.			<u>Mechanism</u> : High sediment removal rates (probably due to its microhispid surface and large exhalant oscula).			<u>Mechanism</u> : Oscula closure under high SSCs led to lipid depletion, but photosymbiont activity partially compensated, likely contributing to its high survival. Possesses passive self-cleaning strategy (microhispid surface). Good recovery once returned to control conditions.		

Table 1. continued.

		Light attenuation			Suspended sediments (SS)			Sediment smothering			Combined stressors		
Species	Morphology / Nutritional mode	Sub-lethal stress	Recovery?	Mortality	Sub-lethal stress	Recovery?	Mortality	Sub-lethal stress	Recovery?	Mortality	Sub-lethal stress	Recovery?	Mortality
<i>Carteriospongia foliascens</i> (SENSITIVE: highly vulnerable indicator species)	Cup (wide) / Phototrophic	100 % survival under >0.8 DLI Bleaching in 7 d under low light (<0.8 DLI)	Yes, for DLI ≥0.8 No, for DLI 0	Yes, 100% mortality after 28 d at DLI 0	80% survival at SSCs <23 mg L ⁻¹ for 28 d 90% necrosis and mortality at >23 mg L ⁻¹ from 7 d	Yes, for SSCs <23 mg L ⁻¹ No, for SSCs >23 mg L ⁻¹	Yes, >80% mortality at SSCs >70 mg L ⁻¹ for 28 d (necrosis from 7 d at SSC>23 mg L ⁻¹) LC ₅₀ =40 mg L ⁻¹ LC ₁₀ =21 mg L ⁻¹	100% survival to 28 d smothering No necrosis observed.	Yes	Not observed	100% survival under low impact scenarios (<10 FNU, >1 DLI)	Yes, under <10 FNU No, under ≥30 FNU treatments	Yes, 90% mortality after moderate-high impact scenarios (≥10 FNU) LC ₅₀ =47 mg L ⁻¹ , 0.2 DLI LC ₁₀ =22mg L ⁻¹ , 0.8 DLI
		<u>Mechanism</u> : Total loss of photosymbionts. Highly specialised microbiome. Energy depletion.			<u>Mechanism</u> : Decreased respiration rates and lipids. Disruption of the holobiont under high SSCs. Energy depletion.			<u>Mechanism</u> : Mucus production and sediment sloughing			<u>Mechanism</u> : Mucus production and sediment sloughing; likely metabolically taxing. No phototrophic feeding under low light conditions.		
<i>Cymbastela coralliophila</i> (TOLERANT species)	Encrusting-Cup (tabulate) / Phototrophic	100% survival in DLI 0–8.1 for 28d (<0.8 DLI minor bleaching)	Yes	Not observed	100% survival under SSCs ≤70 mg L ⁻¹ for 28 d	Yes	Not observed	100% survival to 28 d smothering	Yes	Not observed	[Not tested]		
		<u>Mechanism</u> : Ability to feed heterotrophically. No changes observed in microbiome.			<u>Mechanism</u> : Ability to increase phototrophic feeding under high SSCs as long as light is available.			<u>Mechanism</u> : Unknown. Potential self-cleaning strategies? (e.g. moving and shedding sediment from the edges)					

Table 1. continued.

Species	Morphology / Nutritional mode	Light attenuation			Suspended sediments (SS)			Sediment smothering			Combined stressors		
		Sub-lethal stress	Recovery?	Mortality	Sub-lethal stress	Recovery?	Mortality	Sub-lethal stress	Recovery?	Mortality	Sub-lethal stress	Recovery?	Mortality
<i>Coscinoderma matthewsi</i> (slightly SENSITIVE species)	Massive (simple) / Heterotroph.	[Not tested]			100% survival under SSCs ≤ 23 mg L ⁻¹ for 28 d, but regression under any SSC	Yes, at SSCs ≤ 23 mg L ⁻¹	20% mortality at SSCs 70 mg L ⁻¹ for 28 d	100% survival to 28 d smothering	Yes	Not observed	[Not tested]		
					<u>Mechanism:</u> Reduced feeding ability with depletion of energy reserves under high SSC			<u>Mechanism:</u> Potential development of new oscula. Removal of sediment by infauna (e.g. brittle stars)					
<i>Ianthella basta</i> (RESILIENT species)	Erect (laminar) / Heterotroph.	No effect. 100% survival in DLI 0–8.1 for 28 d			[Not tested]			[Not tested]			100% survival under high impact scenarios	Yes	Not observed
		<u>Mechanism:</u> Heterotrophic feeding									<u>Mechanism:</u> Tissue regression (i.e. dormant state) to avoid clogging. Mucus production. Lipid reduction and some energy depletion.		

Table 1. continued.

Species	Morphology / Nutritional mode	Light attenuation			Suspended sediments (SS)			Sediment smothering			Combined stressors		
		Sub-lethal stress	Recovery?	Mortality	Sub-lethal stress	Recovery?	Mortality	Sub-lethal stress	Recovery?	Mortality	Sub-lethal stress	Recovery?	Mortality
<i>Stylissa flabelliformis</i> (Highly <u>TOLERANT</u> species)	Erect (laminar) / Heterotroph.	No effect. 100% survival in DLI 0–8.1 for 28 d			100% survival under SSCs ≤ 70 mg L ⁻¹ for 28d Regression under any SSC	Yes	Not observed	100% survival to 28 d smothering No necrosis observed.	Yes	Not observed	[Not tested]		
		<u>Mechanism:</u> Heterotrophic feeding			<u>Mechanism:</u> Reduced feeding ability with depletion of energy reserves under high SSC			<u>Mechanism:</u> High sediment removal rates (probably due to its erect morphology and mucus production)					
Main Conclusions:		<ul style="list-style-type: none"> -Light reduction had an impact on some phototrophic species -Bleaching can be used as an stress bioindicator -Limit low <u>DLI (<0.8)</u> to <u><7 d</u> during dredging events to prevent sponge bleaching 			<ul style="list-style-type: none"> -High SSC can have an impact on the filter feeding mode of nutrition. -Different sponges have evolved strategies to prevent clogging (e.g. closing oscula and arresting pumping), although this can compromise energy stores in the long term -<u>High SSCs (≥ 23 mg L⁻¹)</u> for 28 d cause lower survival, increased necrosis and reduced feeding in some species -<u>SSCs ≤ 10 mg L⁻¹</u> is suggested as a reasonable sub-lethal threshold for SSCs in adult sponges -For <i>C. foliascens</i>: LC₅₀=40 mg L⁻¹; LC₁₀=21 mg L⁻¹ (SSCs) 			<ul style="list-style-type: none"> -Sediment smothering for up to 30 d did not alter the health of adult sponge holobionts as most species possess either active or passive self-cleaning strategies which allow them to continue with their feeding activity -Strategies included sediment sloughing via mucus production and removal of sediment by infauna. -Although sediment smothering did not appear to impact symbiont health and composition, continuous and complete smothering which results in prolonged light attenuation may affect the symbiont community and therefore the host in the longer term 			<ul style="list-style-type: none"> -The combination of stressors (especially, high SSC and low light) accelerated mortality in <i>C. foliascens</i> and <i>C. orientalis</i> -Stress responses occur in sponges exposed to “moderate-high impact” (≥ 10 mg L⁻¹ with DLI≤ 1, for 28 d) -90% and 20% mortality in <i>C. foliascens</i> and <i>C. orientalis</i> under high impact scenarios (≥ 30 mg L⁻¹, DLI≤ 0.5, for 28 d). -Most sponges survived and recovered under low-moderate dredging impact (≤ 10 mg L⁻¹, DLI≥ 1, for 28 d) -For <i>C. foliascens</i>: LC₅₀=47 mg L⁻¹, DLI 0.2; LC₁₀=22mg L⁻¹, DLI 0.8 -Suggested sub-lethal bioindicators: bleaching, necrosis, mucus production, oscula closure and tissue regression 		

Residual Knowledge Gaps

The WAMSI DSN 6.4 experimental research has enhanced our understanding of the tolerance of adult phototrophic and heterotrophic sponges to dredging related stressors and elucidated a variety of tolerance mechanisms (see Table 1 for summary). However, our experimental research focussed on adult sponges in short term (<28 day) experimental exposures, and a number of knowledge gaps still exist to fully understand the extent of dredging impacts on marine filter feeders.

Assessing longer term impacts

Most of the 6 species used in this study were relatively resistant to dredging-related stressors over the 28 day maximum experimental period, with the exception of *C. foliascens* which had high mortality when exposed to low light and high SSC. Interestingly, while some indication of sub-lethal stress, such as bleaching, was detected in the phototrophic sponge *C. orientalis* when exposed to the highest level of stressors; this species exhibited a remarkable capacity to recover to its pre-treatment state within 14 day under natural conditions. It is currently unknown whether a longer term exposure, to various degrees or frequencies of these stressors would cumulatively incur an irreversible condition leading to eventual mortality. As capital dredging programs can last for durations of months to years, it is still necessary to assess the responses of sponge species over realistic extended timeframes. In the first instance, it would be beneficial to develop LC₁₀ and LC₅₀ values for sponges which have intermediate sensitivities to the stressors, such as the phototrophic *C. orientalis* and heterotrophic *C. matthewsi*.

Assessing impacts across different life history stages

The early life history stages of benthic sessile invertebrates are important for the replenishment and maintenance of populations, and are expected to be more sensitive to dredging-related pressures than adults. Periods when sponges are reproductive and spawning, and when larvae are developing or being released into the water column are critical steps in the sponge life cycle that represent important ecological windows. However, to date, little is known about the response of sponge gametes and larvae to dredging-related pressures and there is almost no data about the effects of sediment smothering on gametes, larvae, settlement substrate, and settled recruits or juveniles. Future research aimed at building our understanding of the sensitivity of different sponge life history stages would allow for a more holistic approach to managing dredging-related impacts on sponge populations.

Assessing impacts on broader filter feeder taxa

The present research focussed on sponges as the primary filter feeding taxa in northwestern Australia, hence findings may not be directly applicable to other filter feeding taxa such as ascidians, bryozoans and gorgonians. The field research component of this Theme⁷, which surveyed filter feeder communities before and after a 2-year capital dredging program highlighted differences in the responses of the different taxonomic groups, with colonial ascidians and hydrozoans potentially more sensitive to dredging related stressors than sponges. Similar experimental approaches to those employed in this present study should be applied to other filter feeder taxa to build upon our knowledge of thresholds, and the response of communities under dredging pressure.

⁷ See Report for Project 6.3: Abdul Wahab et al. (2017) Comparisons of benthic filter feeder communities before and after a large-scale capital dredging program. Report of Theme 6 - Project 6.3 prepared for the Dredging Science Node, Western Australian Marine Science Institution, Perth, Western Australia.

Appearance matters: sedimentation effects on different sponge morphologies

M. CARMEN PINEDA^{1,2}, ALAN DUCKWORTH^{1,2} AND NICOLE WEBSTER^{1,2}

¹Australian Institute of Marine Science, PMB3, Townsville 4810, Queensland, Australia, ²Western Australian Marine Science Institution, Entrance 2 Brockway Rd., Floreat 6014, WA, Australia

*Dredging activity poses an environmental risk to sponges as sediments from the dredge or disposal site may smother the sponge surface, potentially affecting water filtration and light penetration. Dredge related sedimentation effects may also vary between sponge morphologies, potentially impacting community structure and functioning. To test this, 10 sponge species encompassing four different morphologies (massive, erect, cup and encrusting), were exposed to a single pulse treatment of three different sediment concentrations (0, 250 and 500 mg l⁻¹) and followed over 2 weeks, in 1000 l tanks. Total suspended solids (TSS) and sedimentation rates (SR) were recorded throughout the study. A sharp decrease in TSS was recorded within the first 2–3 h and a total settlement of sediments occurred within the first 48 h of the pulse exposure (0, 8 and 16 mg cm⁻² in the control, medium and high sediment treatments, respectively). The effects of high sedimentation included mortality of cup shaped *Callyspongia confederata* and small areas of tissue necrosis in other species, with massive, encrusting and wide cup morphologies particularly affected. However, the sediment concentrations tested in this experiment did not cause changes in the concentration of sponge pigments or the structure of the symbiotic microbial community in any species. These results indicate that a single pulse of sediments less than 16 mg cm⁻² is not detrimental to most of the sponge species studied.*

Keywords: Australia, chlorophyll, dredging, sedimentation, sponge, symbiont

Submitted 31 July 2014; accepted 2 November 2014

INTRODUCTION

Dredging of the sea bed is required for the development and maintenance of harbours and offshore petrochemical facilities around the world (Morton, 1977; DEWHA, 2009). However, this activity requires the removal and subsequent dumping of millions of cubic metres of spoil into proximate areas, posing an environmental risk for marine communities (Morton, 1977; Desprez, 2000). One of the main physical effects of dredging is the temporary increase in suspended sediment concentrations at both dredge and disposal sites (Morton, 1977). Dredged sediments can remain in suspension for minutes to days depending on their particle size and composition, and local environmental conditions, before settling on the seafloor and benthic communities (Newell *et al.*, 1998). Increased sedimentation and levels of total suspended solids (TSS) are considered major causes of worldwide degradation of important marine ecosystems such as coral reefs (Rogers, 1990; McClanahan & Obura, 1997; McCulloch *et al.*, 2003), rocky assemblages (Airoldi, 2003; Balata *et al.*, 2005) and estuaries (Wilber & Clarke, 2001). The effects of high sedimentation and TSS range from the immediate burial and smothering of benthic organisms to negative effects on life history processes such as settlement, recruitment, feeding and growth (Airoldi, 2003; Fabricius, 2005; Lohrer *et al.*, 2006). Competitive and predator prey

interactions may also be affected by high sedimentation (Airoldi, 2003).

Sponges are sessile filter feeding organisms that play important roles in marine ecosystems including occupying and eroding substrate, benthic pelagic energy transfer, and positive and negative associations with other organisms (Bell, 2008; de Goeij *et al.*, 2013). Sponges are highly diverse and can even be the dominant fauna in many regions including some coral reefs, inter reef habitats and deep water environments (e.g. Wilkinson & Evans, 1989; Bell & Barnes, 2000a; Diaz & Rützler, 2001; Pawlik, 2011; Murillo *et al.*, 2012). In areas of particularly high sponge abundance (sponge gardens), these organisms can fulfil ecological roles comparable to coral reefs (Schönberg & Fromont, 2011). However, sponge assemblages can also be sensitive to global and local pressures including climate change (Przeslawski *et al.*, 2008; Bell *et al.*, 2013; Webster *et al.*, 2013) and dredging associated increases in sediment suspension and deposition (Gerrodette & Flechsig, 1979; Wilkinson & Cheshire, 1989; Roberts *et al.*, 2006; Bannister *et al.*, 2012).

The effects of sediments on sponges include clogging of the aquiferous canals and chambers (Bakus, 1968), reduced pumping activity (Gerrodette & Flechsig, 1979; Tompkins MacDonald & Leys, 2008), reduced growth rates (Roberts *et al.*, 2006; Whalan *et al.*, 2007) and increased respiration rates (Bannister *et al.*, 2012). High sediment deposition can also smother sponge recruits (Maldonado *et al.*, 2008) and even bury adults (Wulff, 1997). In addition, sponges host dense and diverse microbial symbionts that contribute to the health, fitness and nutrition of the host (Webster & Taylor, 2012). Many of these symbionts are photosynthetic which may make sponges particularly sensitive to

Corresponding author:
M.C. Pineda
Email: mcarmen.pineda@gmail.com

dredge related light reduction due to increased turbidity (Thacker, 2005; Roberts *et al.*, 2006; Bell, 2008). High sedimentation can therefore greatly influence the structure, abundance and diversity of sponge assemblages (Bell & Barnes, 2000a, b; Carballo, 2006).

Effects of sedimentation will vary between sponge species with morphology or shape likely to be a major contributor to this inter species variation. For example, high sediment deposition may smother thin, encrusting sponges while having little impact on upright or erect sponges. The overall aim of this study was to investigate responses of different sponge morphologies to a range of controlled sedimentation treatments simulating conditions associated with dredging activity.

MATERIALS AND METHODS

Sponge species and morphology

Ten sponge species (Table 1), representing four general morphologies (massive, erect, cup and encrusting), were collected from Broadhurst Reef, Great Barrier Reef (18°51.891'S 147°41.660 E), in September 2013. Of these, *Stylissa flabelliformis*, *Cliona orientalis*, *Ianthella basta* and *Carteriospongia foliascens* are also widely distributed throughout the Indo Pacific (Fromont, 2004). Sponges were transported to the Australian Institute of Marine Science and acclimated in 1000 l tanks for >2 weeks with 5 µm filtered flow through seawater at 25°C and 36‰ salinity, environmental conditions comparable to the collection site.

Experimental set up

The experiment was conducted in three 1000 l tanks, each dosed at one of three sediment levels: 0 mg l⁻¹ (control), 250 mg l⁻¹ (medium) and 500 mg l⁻¹ (high). The siliciclastic sediment used in this experiment was collected sub tidally from Onslow, Western Australia (21°38'S 114°56'E) and ground to 63 µm. Particle size distribution analysis determined that the ground sediment ranged from 1–130 µm in size, with the majority between 30 and 80 µm. Heavy metal analysis determined that the grinding process did not contaminate sediments but that they were naturally rich in Fe and Al.

For the medium and high treatments, ground sediment was blended with seawater, forming a sediment slurry that was poured slowly into each tank in a single pulse at Day 0 to

reach desired treatment concentrations. Water flow in the tanks was standardized to ~300 ml min⁻¹, resulting in a complete renewal of seawater in 48 h.

One to four replicates of each sponge species were randomly placed in each tank, with all sponges separated by ≥10 cm to prevent any antagonistic interactions. All species were placed in their natural orientation. For example, *I. basta*, *Haliclona* sp., *S. flabelliformis* and *Callyspongia confederata* were fixed to coral plugs using non toxic underwater putty (Knead IT® Aqua Selleys, NSW Australia) and placed in plastic racks, so that they were exposed to sediments in their natural upright position. Sponges were exposed to sediments for 15 days.

No significant differences in initial size of replicates among treatments were observed for any of the species (ANOVA: $P > 0.05$ for all species), thus excluding initial sponge size influencing the results.

Studied parameters

PHYSICAL PARAMETERS

Total Suspended Solids (TSS) were recorded immediately following sediment addition ($T = 0$ h), $T = 8$, 24 and 32 h, and then after 7 and 14 days. For TSS analysis, triplicate water samples (200 ml) were collected from each tank and filtered through previously weighed 0.4 µm polycarbonate filters (Advantec MFS, Inc.). Filters were dried overnight at 60°C and dry weights were recorded the following morning.

Sedimentation Rates (SR) were measured by collecting and filtering sediments that accumulated on five SedPods (Surface Area = 25.16 cm²) (Field *et al.*, 2013) randomly placed in each tank. To examine sedimentation rates throughout the experiment, SedPods were removed after 1, 2, 7 and 15 days.

DETERMINATION OF SMOTHERING AND ASSESSMENT OF SPONGE HEALTH

Underwater pictures of each sponge were taken with an Olympus C 5050 digital camera prior to sediment addition and after 2, 7 and 15 days. Image analysis software (Image J) was then used to measure the percentage of surface area covered by sediments for each sponge during the experiment (Figure 1).

To determine the weight of sediment remaining on each sponge by the end of the experiment, each sponge was carefully placed into a plastic zip lock bag underwater, and then inverted and shaken so that all sediment fell off the sponge

Table 1. List of species, morphologies and number of replicates per treatment.

Species name	Functional morphology	Replicates
<i>Callyspongia confederata</i> (<i>sensu</i> Ridley, 1884)	Cup (narrow cup or tube)	2
<i>Carteriospongia foliascens</i> (Pallas, 1766)	Cup (wide cup)	2
<i>Cliona orientalis</i> Thiele, 1900	Encrusting (bioeroding)	3
<i>Cymbastela coralliophila</i> Hooper & Bergquist, 1992	Encrusting (thick)/Cup (table)	2
<i>Haliclona</i> sp. Grant, 1836	Cup (narrow cup or tube)	2
<i>Ianthella basta</i> (Pallas, 1976)	Erect (laminar)	2
<i>Ircinia irregularis</i> (Polejaeff, 1884)	Massive (simple)	1
<i>Neopetrosia exigua</i> (Kirkpatrick, 1900)	Massive/Encrusting	2
<i>Rhopaloeides odorabile</i> Thompson, Murphy, Bergquist & Evans, 1987	Massive (simple)	4
<i>Stylissa flabelliformis</i> (Hentschel, 1912)	Erect (laminar)	2

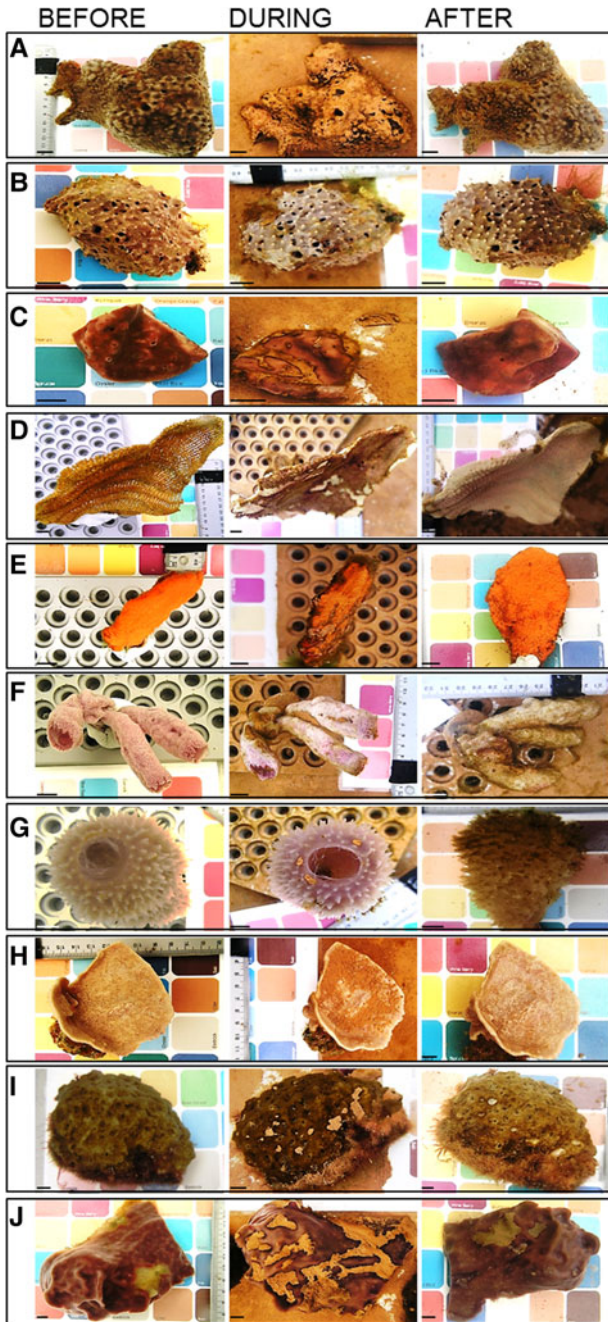


Fig. 1. Tested sponge species prior to the sediment addition (before), during the experiment (during) and after removal of sediments (after) in the high sediment treatment: (A) *R. odorabile*; (B) *I. irregularis*; (C) *N. exigua*; (D) *I. basta*; (E) *S. flabelliformis*; (F) *Haliclona* sp.; (G) *C. confoederata*; (H) *C. foliascens*; (I) *C. orientalis*; (J) *C. coralliophila*. Scale bars: 1 cm.

surface into the bag. The water and sediment within each plastic bag was filtered and weighed as described above.

Following the removal of sediments and any attached algae, additional pictures were taken of each sponge to confirm sponge mortality, determine colour changes and calculate the percentage of necrosed tissue. The change in sponge surface area from day 0 to day 15 was measured for each sample to determine approximate sponge growth (Figure 1). Importantly however, inferred growth based on surface area could be underestimated, especially in sponges with a three dimensional structure such as cups and erect morphologies.

Changes in surface area (i.e. growth), percentage of necrosed tissue, percentage of area covered by sediments on day 2 and total sedimentation on sponges were studied separately for those species with sufficient levels of replication to enable statistical testing (i.e. ≥ 3 replicates: *Rhopaloeides odorabile* and *C. orientalis*) with a one way analysis of variance (ANOVA) using treatment as the fixed factor. For all four variables, we performed a two way general linear model (GLM) ANOVA with sponge morphology (as per Table 1) and treatment as fixed factors. Logit and arcsine transformations were performed to meet the assumptions for ANOVA. Transformed data had homogeneity of variances in all data sets, although in some instances normality was not accomplished. GLM ANOVA tests were still conducted as they are robust to departures from normality when variances are homogeneous (Underwood, 1997). Statistical analysis and graphs were performed using the software SigmaPlot v.11.0 (Systat Software Inc.) and NCSS v 9 (NCSS, USA).

PIGMENT ANALYSIS

At the completion of the experiment, two $1 \times 0.5 \times 0.5$ cm pieces of healthy tissue per sponge individual were excised using sterile scalpels, cutting from the pinacoderm through to the mesohyl. Excised pieces were briefly rinsed in clean seawater to remove surface sediments, placed into two 2 ml cryo vials and snap frozen in liquid nitrogen for subsequent analysis of pigments and microbial symbionts.

Chlorophyll and carotenoid concentrations were used as a proxy for host stress and photosynthetic potential after exposure to sediments. Samples were allowed to thaw slightly and approximately 0.25 g wet weight of each sample was finely cut and extracted in 2 ml of 95% ethanol. Three stainless steel beads were added to each vial, and samples were shaken in a Bead Beater (Bio Spec Products Inc., Bartlesville, USA) for 3 min. Triplicate 300 μ l extracts, and the 95% ethanol blank, were then pipetted into a microplate.

The extraction method using 95% ethanol was less toxic and more time efficient than extractions with acetone or methanol and also yielded greater extraction concentrations (data not shown). As ethanol is less volatile than methanol or acetone, it can be used in 96 well microplates for assessment using the spectrophotometer.

Absorbance at 470, 632, 649, 665, 696 and 750 nm (i.e. turbidity) was read on a Power Wave Microplate Scanning Spectrophotometer (BIO TEK® Instruments Inc., Vermont, USA). Using the blank corrected absorbance readings minus the absorbance at wavelength 750 nm (E_x), Chl *a*, Chl *b*, Chl *c*, Chl *d*, Total Chl and Total Carotenoids were calculated using the following equations (Lichtenthaler, 1987; Ritchie, 2008):

$$\text{Chl } a (\mu\text{g ml}^{-1}) = [(-0.9394 \times E_{632}) + (-4.2774 \times E_{649}) + (13.3914 \times E_{665})]/0.794$$

$$\text{Chl } b (\mu\text{g ml}^{-1}) = [(-4.0937 \times E_{632}) + (25.6865 \times E_{649}) + (-7.3430 \times E_{665})]/0.794$$

$$\text{Chl } c (\mu\text{g ml}^{-1}) = [(28.5073 \times E_{632}) + (-9.9940 \times E_{649}) + (-1.9749 \times E_{665})]/0.794$$

$$\text{Chl } d (\mu\text{g ml}^{-1}) \quad [(-0.2007 \times E_{632}) + (0.0848 \times E_{649}) \\ + (-0.1909 \times E_{665}) \\ + (12.1302 \times E_{696})]/0.794$$

$$\text{Total Chl } (\mu\text{g ml}^{-1}) \quad [(24.1209 \times E_{632}) + (11.2884 \times E_{649}) \\ + (3.7620 \times E_{665}) + (5.8338 \\ \times E_{696})]/0.794$$

$$\text{Total carotenoids } (\mu\text{g ml}^{-1}) \quad [((1000 \times E_{470})/0.794) \\ - (2.13 \times \text{Chl } a) - (97.64 \\ \times \text{Chl } b)]/209$$

The factor 0.794 is a path length correction, determined by the ratio of the absorbance of the microplate measurement divided by the absorbance of the 1 cm cuvette at a given wave length, using ethanol as solvent and for a volume of 300 μl of sample extract.

Pigment concentrations were normalized to wet weight using the calculation:

$$[\text{Chl } a (\mu\text{g ml}^{-1}) \times \text{extraction volume (ml)}]/\text{wet weight (g)}$$

MICROBIAL SYMBIONTS ANALYSIS

Assessment of host associated microbial communities was performed for all sponge species that had ≥ 2 replicates alive in all treatments at the completion of the experiment (i.e. *C. foliascens*, *C. orientalis*, *Cymbastela coralliophila*, *I. basta*, *Neopetrosia exigua*, *R. odorabile* and *S. flabelliformis*). DNA extractions were performed using the Power Plant® Pro DNA Isolation Kit (MoBio Laboratories, Carlsbad, CA) and a fragment of the 16S rRNA gene was amplified with the primer set 1055F and 1392r containing a GC clamp (Muyzer *et al.*, 1993; Ferris *et al.*, 1996). Total reaction volume was 50 μl , including 10 μl of 5 \times Buffer (containing 5 mM dNTPs and 15 mM MgCl_2), 0.4 μl of BSA (10 mg ml⁻¹), 0.25 μl (1.25 units) of My Taq DNA Polymerase (Bioline®, London, UK), 1 μl of each primer (10 μM), ~10 ng of template DNA and sterile Milli Q water. PCR conditions were as follows: 1 cycle at 95°C for 1 min; 32 cycles at 94°C for 30 s, 54°C for 30 s and 72°C for 1 min, and a final elongation at 72°C for 7 min. PCR products were visualized on 1% agarose gels to assess amplification specificity and initial product quantity. 15 μl of each PCR product were applied to 8% w/v polyacrylamide (37.5:1) gels containing a 50–70% denaturing gradient of formamide and urea. Gels were electrophoresed at 65°C for 16 h in 1 \times TAE (Tris acetic acid EDTA) buffer at 75 V using the Ingeny D Code system (Goes, the Netherlands). Gels were stained with 1 \times Sybr Gold for 10 min, visualized under UV illumination and photographed. Individual band numbers were assigned based on their migration. Bands assigned the same number had identical migration end points, and were used to build a presence/absence matrix. Three factors were determined (i.e. species, morphology, sediment treatment). principal component analysis (PCA) of microbial community profiles was performed on square root transformed data.

The same matrix was used for SIMPER analysis (similarity/distance percentages), which examined the contribution of each variable to average resemblances between sample groups. A distance matrix was obtained using Bray Curtis similarity and used for PERMANOVA (Permutational multivariate ANOVA based on distances). All analyses were performed on Primer 6 (PRIMER E Ltd, Plymouth, UK).

RESULTS

Physical parameters

Levels of TSS measured at Time 0 (directly after addition of sediments to the tanks) were 1.8 ± 0.3 , 217 ± 7 and 542 ± 87 mg l⁻¹ (mean \pm SE) in the control, medium and high treatment tanks, respectively. Thus, measured TSS values were close to expected values of 0, 250 and 500 mg l⁻¹. TSS dropped ~80% in 8 h and 99% in 48 h in both treatment tanks.

Total sedimentation levels at the end of the experiment were 0.27 ± 0.01 , 8.7 ± 0.7 and 16.3 ± 0.3 mg cm⁻² (mean \pm SE) in the control, medium and high treatment tanks, respectively. Similar to the TSS levels, a ~98% decline in SR was observed within 24 h in both sediment treatments with all sediments settling within 48 h. The primary main physical effect on sponges in this study was therefore sediment deposition.

Determination of smothering and assessment of sponge health

With the exception of individuals of *Haliclona* sp. and *Callyspongia confederata*, all sponges in all treatments survived until the end of the experiment. *Haliclona* sp. died after 7 days in the medium and high sedimentation treatments and after 15 days in the control, indicating that this species is unsuitable for further aquarium based experimentation. In contrast, *C. confederata* survived in the control treatment, but died after 7 days in the high sediment treatment and after 15 days in the medium sediment treatment, indicating sensitivity to elevated sediment levels (Figure 1).

With the exception of *Ianthella basta*, *Haliclona* sp. and *C. confederata*, all species showed positive growth (i.e. surface area) in the control treatment (Figure 2). In contrast, null or negative growth was observed in the medium and high sediment treatment for all species except *Cliona orientalis* which exhibited positive growth in the medium treatment but negative growth in the high treatment (Figure 2). Although differences in growth between treatments were not statistically significant for *Rhopaloeides odorabile* and *C. orientalis* (ANOVA: $P > 0.05$), both morphology and treatment had a significant effect on growth when comparing all individuals grouped by morphology (Table 2). Massive and encrusting species showed a significantly higher growth than cups and erect sponges. Sponges exposed to medium and high sediment treatments grew significantly less than sponges in the control treatment (Table 2, Figure 2).

Individuals of some species in the medium and high sediment treatments developed areas of necrotic tissue (e.g. 2–15% of *R. odorabile* tissue and 2.6–5% of *Cymbastela coralliophila* tissue) although there was no significant difference between treatments (ANOVA: $P > 0.05$). Tissue necrosis

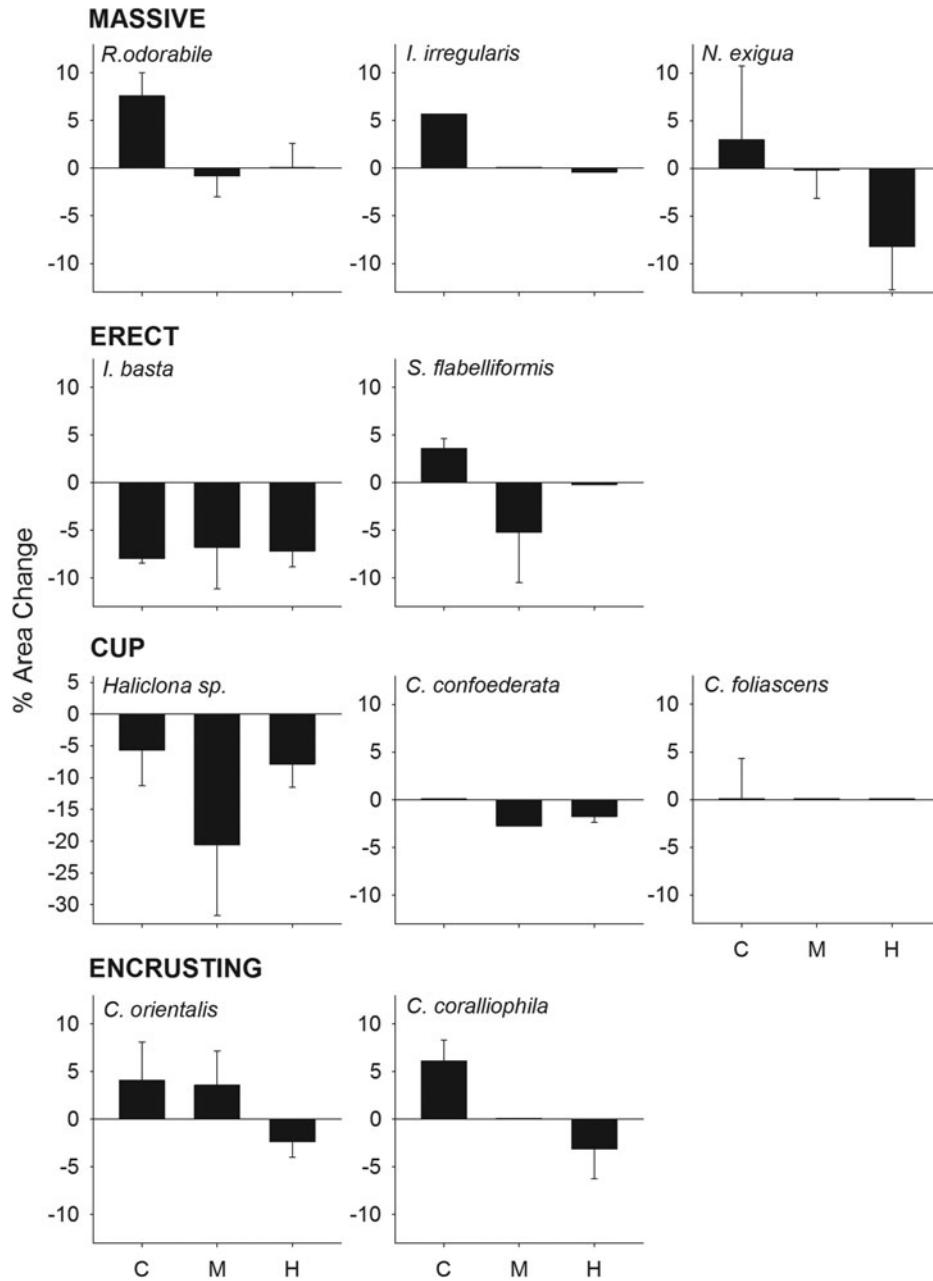


Fig. 2. Percentage of area change (growth) at the end of the experiment for all species grouped by morphologies, at the three sediment treatments (control, medium and high).

was not observed in any individual of the erect species *Stylissa flabelliformis* and *I. basta* and the encrusting species *C. orientalis*. Significant differences in percentage of necrosis were

only observed when comparing among morphologies, with cups experiencing the highest percentage of necrosis (Table 3, Figure 1).

Table 2. ANOVA examining the effects of treatment on size (growth) among the sponge morphologies after 15 days.

Source	df	MS	F	P
Morphology	3	0.0198	4.034	0.012
Treatment	2	0.0172	3.511	0.037
Morphology × Treatment	6	0.00478	0.974	0.452
Error	53	0.00491		

Significant Pairwise Multiple Comparisons (Holm Sidak method).
 MAS, ENC > CUP ($P = 0.009, 0.010$).
 C > M ($P = 0.017$), H ($P = 0.025$).

Table 3. ANOVA examining the effects of treatment on the percentage of tissue affected by necrosis among the sponge morphologies after 15 days.

Source	df	MS	F	P
Morphology	3	2.964	18.027	<0.001
Treatment	2	0.301	0.301	0.301
Morphology × Treatment	6	0.126	0.769	0.598
Error	53	0.164		

Significant Pairwise Multiple Comparisons (Holm Sidak method).
 CUP > ENC ($P = 0.009$), MAS ($P = 0.010$), ERE ($P = 0.013$).

Table 4. ANOVA examining the differences in percentage of sponge surface covered by sediments among the sponge morphologies after 48 h.

Source	df	MS	F	P
Morphology	3	0.255	5.346	0.003
Treatment	2	2.149	45.016	<0.001
Morphology × Treatment	6	0.103	2.163	0.061
Error	53	0.0477		

Significant Pairwise Multiple Comparisons (Holm Sidak method).

MAS > CUP ($P = 0.009$), ERE ($P = 0.010$).

C < M ($P = 0.025$), H ($P = 0.017$).

The percentage of sponge surface covered by sediments after 48 h differed significantly between treatments

(ANOVA: $P < 0.001$, 0.03 for *R. odorabile* and *C. orientalis*, respectively) and morphologies (Table 4, Figure 3), with massive species having a greater coverage of sediments than cup and erect species. Nevertheless, the percentage of sponge surface covered by sediments decreased over time for most species, indicating an ability to remove some sediment from their surface tissue (Figure 4). This ability differed between species with *R. odorabile* removing less than 20% of the surface sediment and *Ircinia irregularis* removing 85% of the surface sediment after 15 days (Figure 4).

Total sedimentation onto sponges was significantly higher in the sediment treatments than the control (ANOVA: $P < 0.001$, 0.04 for *R. odorabile* and *C. orientalis*, respectively) and also differed significantly between the four main sponge morphologies (Figure 5, Table 5). Erect species received the

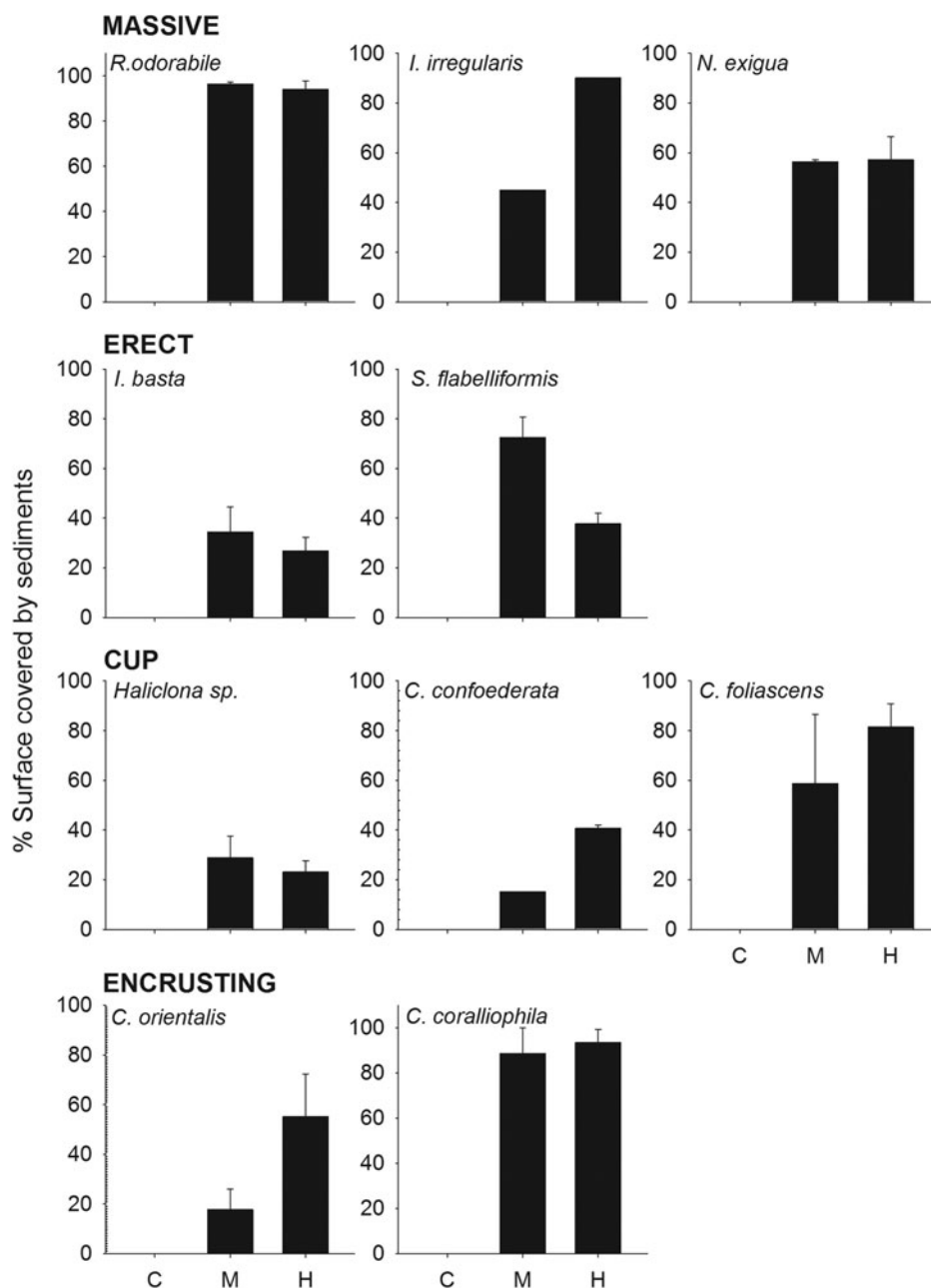


Fig. 3. Percentage of sponge surface covered by sediments 2 days after the sediment pulse for all species, grouped by morphologies, at the three sediment treatments (control, medium and high).

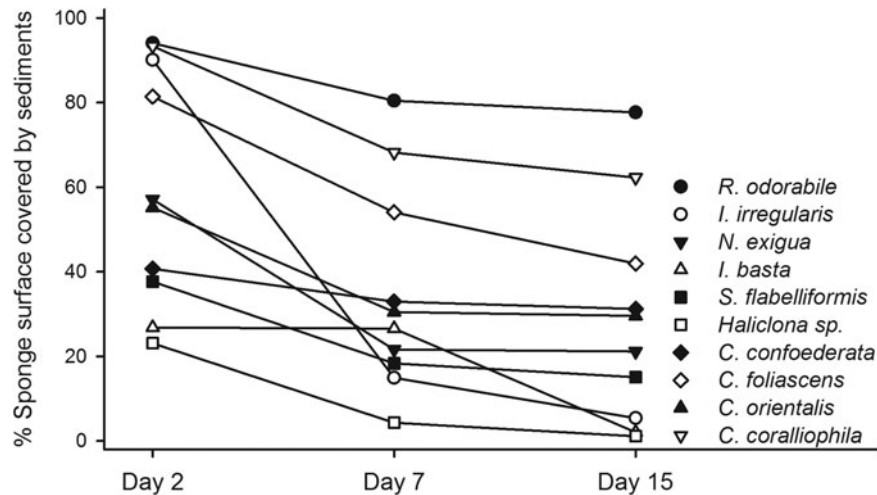


Fig. 4. Mean percentage of surface covered by sediments at day 2, 7 and 15 after sediment addition, for each sponge species at the high sediment treatment.

minimum amount of deposited sediment while cup shaped sponges, particularly those with a wide cup morphology, collected the highest amount of sediment (Figure 5, Table 5). No correlation existed between total sedimentation and sponge tissue surface area covered by sediments ($R^2 = 0.218$, $P = 0.022$).

Pigment analysis

Due to high rates of mortality, pigment concentrations were not analysed for *Haliclona sp.* and *C. confoederata*. For the remaining species, the concentration of photosynthetic pigments did not differ significantly between treatments (ANOVA: $P > 0.05$ for all species). However, pigment concentrations and types varied between species and treatments. For example, *R. odorabile* had an extremely low concentration of chlorophylls and carotenoids, consistent with the absence of photosymbionts previously described for this species (Bannister *et al.*, 2011) whereas *I. basta* and *S. flabelliformis* had low concentrations of chlorophylls, but high concentrations of carotenoids that decreased slightly with increasing sedimentation (Figure 6). The relatively high concentrations of Chl *a* in *C. orientalis* did not vary among treatments, while Chl *b* in this species was reduced slightly in the high sediment treatment (Figure 6). A slight increase in chlorophyll concentration in the sediment treatment compared with the control was observed in *I. irregularis* and *Neopetrosia exigua* (Figure 6). In general, concentrations of photosynthetic pigments were not reduced by the increasing sediment concentrations, although every species and every pigment responded differently.

Microbial symbiont analysis

Microbial community profiling of replicate samples from *Carteriospongia foliascens*, *C. orientalis*, *C. coralliophila*, *I. basta*, *N. exigua*, *R. odorabile* and *S. flabelliformis* revealed 44 unique bands (corresponding to different microbial symbionts). The microbial profiles grouped according to species although some minor clustering according to sediment treatment was observable for *C. foliascens*, *R. odorabile* and *C. coralliophila* (Figure 7). The first two factors in the principal

component analysis (PCA) explained 39.3% of the total variation (Figure 7). SIMPER analysis indicated high levels of similarity within species and moderate to high levels of similarity within morphologies: $\geq 50\%$ for erect and encrusting, and $\geq 80\%$ for massive and cup morphologies. PERMANOVA analysis of the microbial profiles revealed that microbial communities were significantly affected by host species and host morphology, but not by sedimentation treatment (Table 6).

DISCUSSION

Rapid deposition of sediments after an initial sediment pulse combined with a rapid drop in TSS within 48 h indicates that the primary pressures on sponges in this study were sediment covering the surface tissue or clogging of their aquiferous system. Although the tested sedimentation treatments are consistent with values observed near dredging operations (e.g. 300 mg l^{-1} ; Simpson, 1988), these sedimentation levels did not cause mortality during the 2 week experiment, except for *Callyspongia confoederata*. However, low levels of replication for this species precluded chlorophyll and symbiont analyses, making it difficult to reach definitive conclusions regarding the nature of the sediment sensitivity. Colour changes, generally indicating loss of photosynthetic symbionts or bleaching (Thacker, 2005; Roberts *et al.*, 2006), were not detected in any of the sponges that survived the experiment. Bleaching due to light attenuation may have occurred if there had not been such a rapid decrease in TSS or if the sediments had completely smothered the sponges.

All sponge morphologies shrunk when exposed to the high sediment treatment. Decreased or negative growth is likely linked to reduced feeding efficiency due to sediments clogging the sponge aquiferous systems (Gerrodette & Flechsig, 1979; Tompkins MacDonald & Leys, 2008). For example, the glass sponge *Rhabdocalyptus dawsoni* arrests pumping entirely in response to sediments (Tompkins MacDonald & Leys, 2008), the pumping rate of *Veronia lacunosa* has been shown to reduce with a sediment load as low as 11 mg l^{-1} (Gerrodette & Flechsig, 1979) and similar responses have previously been observed in other species of demosponges

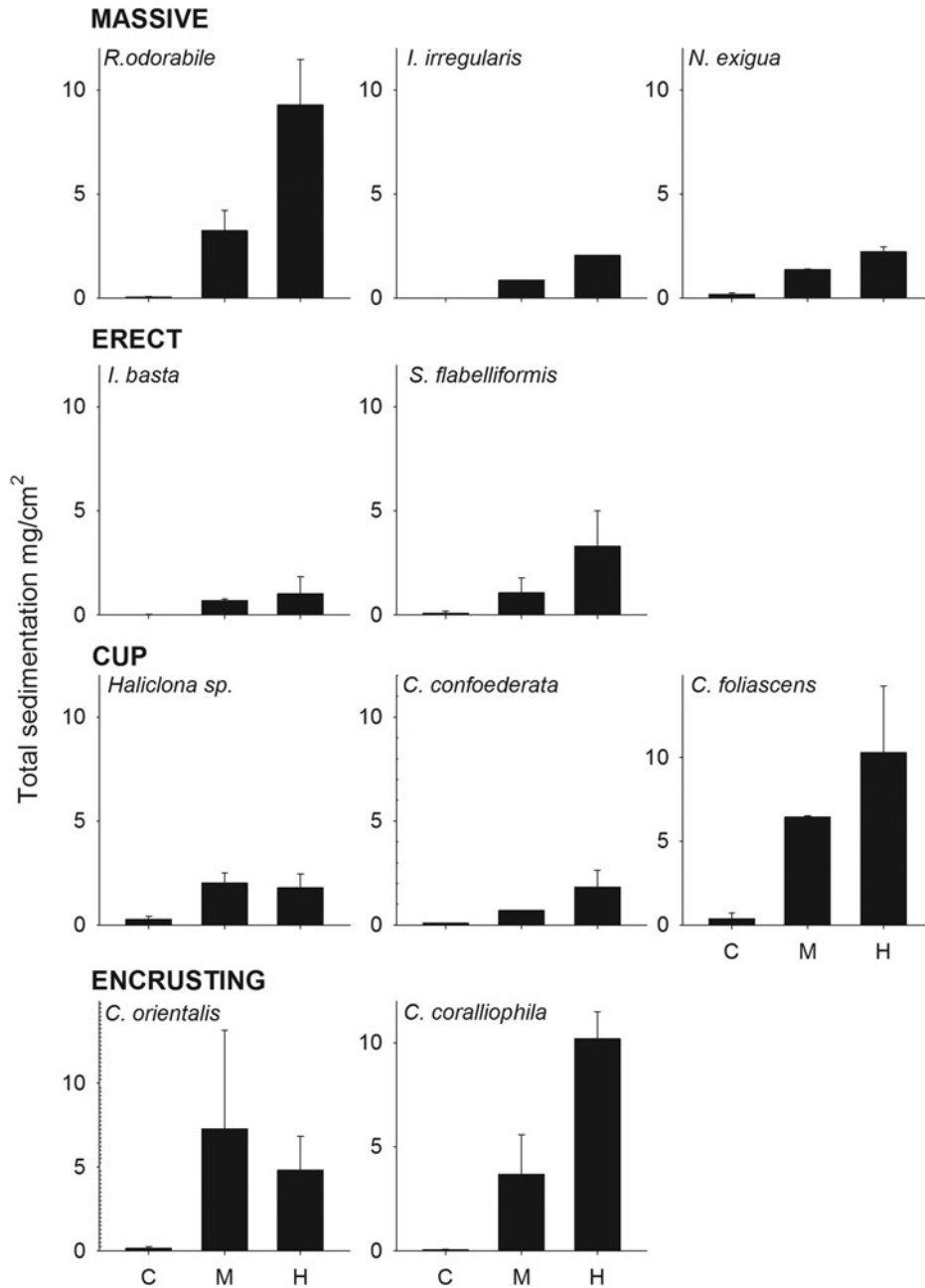


Fig. 5. Total sedimentation (mg cm^{-2}) at the end of the experiment for all species grouped by sponge morphology, at the three sediment treatments (control, medium and high).

(Reiswig, 1971; Lohrer *et al.*, 2006). Additionally, sponges living under high sediment conditions can become energetically stressed with efforts to expel unwanted material, contributing to a depletion of their reserves in comparison to individuals inhabiting areas less affected by sediment (Roberts *et al.*, 2006; Tompkins MacDonald & Leys, 2008; Bannister *et al.*, 2012).

Notable differences in the total amount of entrapped sediments and the percentage of sponge surface covered by sediments were observed between the different sponge species and sponge morphologies. In general, massive, encrusting and wide cup morphologies accumulated more sediment than erect species and the narrow cup morphology. This is consistent with what has previously been reported for other

sponge species (Gerrodette & Flechsig, 1979; Bell & Barnes, 2000b; Carballo, 2006). Although specific mechanisms were not elucidated within the context of this study, the reduction in sediment covering the sponges over time suggests that either the sponges are actively removing the sediment from their surface (i.e. through their pumping activity, production of mucus, protrusion of spicules) or other in fauna organisms are doing it for them. For instance, *Iricinia irregularis* in this study had many brittle stars living inside their oscula, which may have indirectly cleaned their surfaces as found for other species (e.g. Hendler, 1984; Turon *et al.*, 2000).

The weak correlation between total sedimentation and sponge area covered by sediments could be explained by the presence of algae overgrowing some of the sponge individuals

Table 5. ANOVA examining the differences in total sedimentation among the sponge morphologies after 15 days.

Source	df	MS	F	P
Morphology	3	5.747	4.109	0.011
Treatment	2	101.757	72.757	<0.001
Morphology × Treatment	6	1.282	0.917	0.490
Error	53	1.399		

Significant Pairwise Multiple Comparisons (Holm Sidak method).
 CUP > ENC ($P = 0.049$) > MAS ($P = 0.025$) > ERE ($P = 0.013$).
 C < M ($P = 0.025$), H ($P = 0.017$).

by the end of the experiment. Algae attached to the surface of some sponges may have immobilized the sediments, making it difficult to remove and quantify the sediments. This would

explain the observed underestimation in total sedimentation and highlights the critical importance of controlling algal growth in future experiments.

Chlorophyll and carotenoid analysis provided valuable data on pigment concentrations in each of the target sponge species. A reduction in Chl *a* has previously been reported in 90 days sediment exposed (Roberts *et al.*, 2006) and 2 weeks shaded sponges (Thacker, 2005), although these results were not statistically significant. However, elevated sediment concentrations did not appear to affect the production of any photosynthetic pigments in sponges over the 15 day exposure period. Moreover, the results were extremely variable among species and between pigments and no discernible trends in pigment behaviour could be determined according to sediment treatment. Therefore, the analyses of chlorophylls and carotenoids did not appear to be a valid

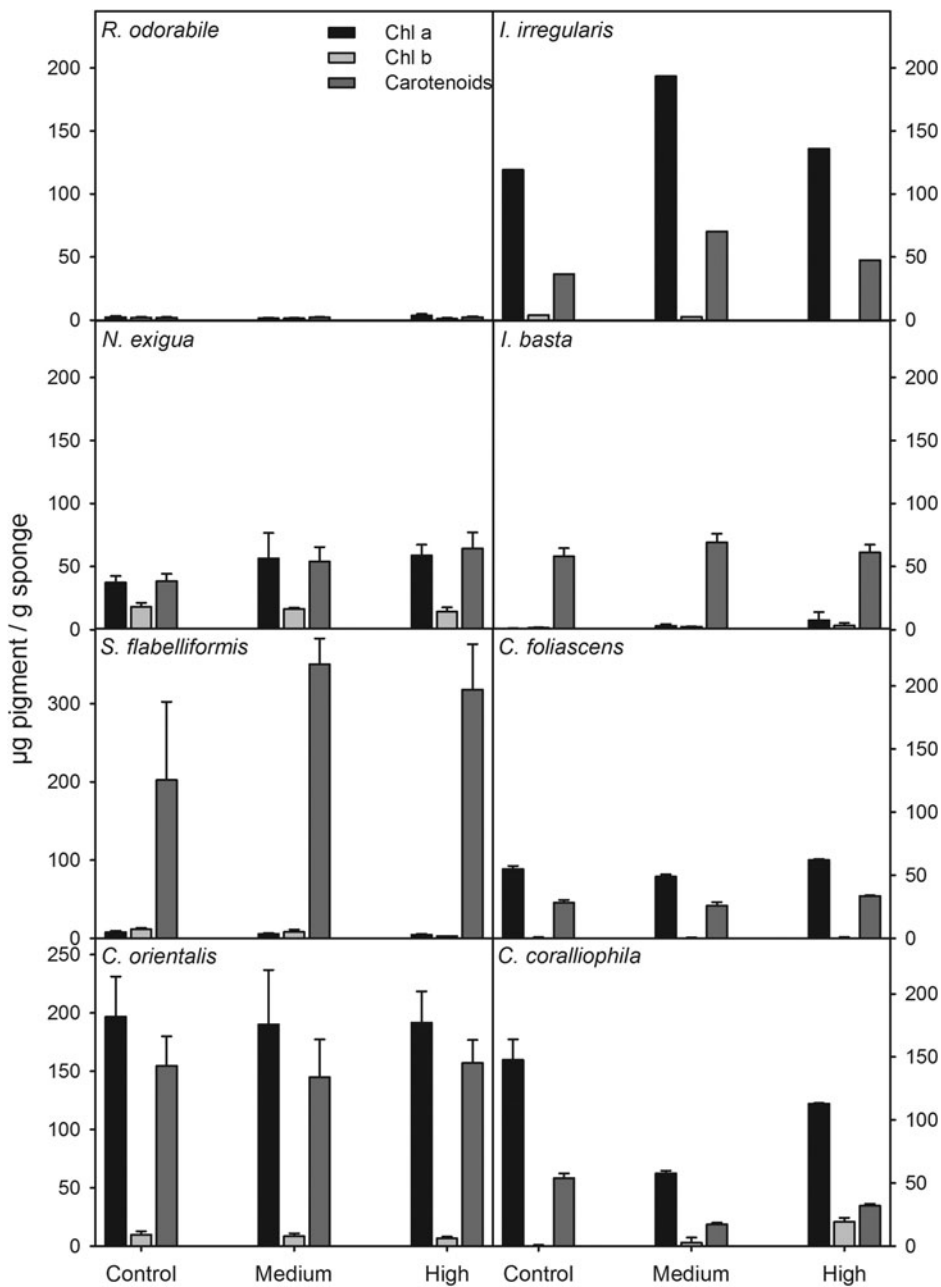


Fig. 6. Chlorophylls *a*, *b* and carotenoids (µg pigment/g sponge tissue) for all species at the three sediment treatments (control, medium and high).

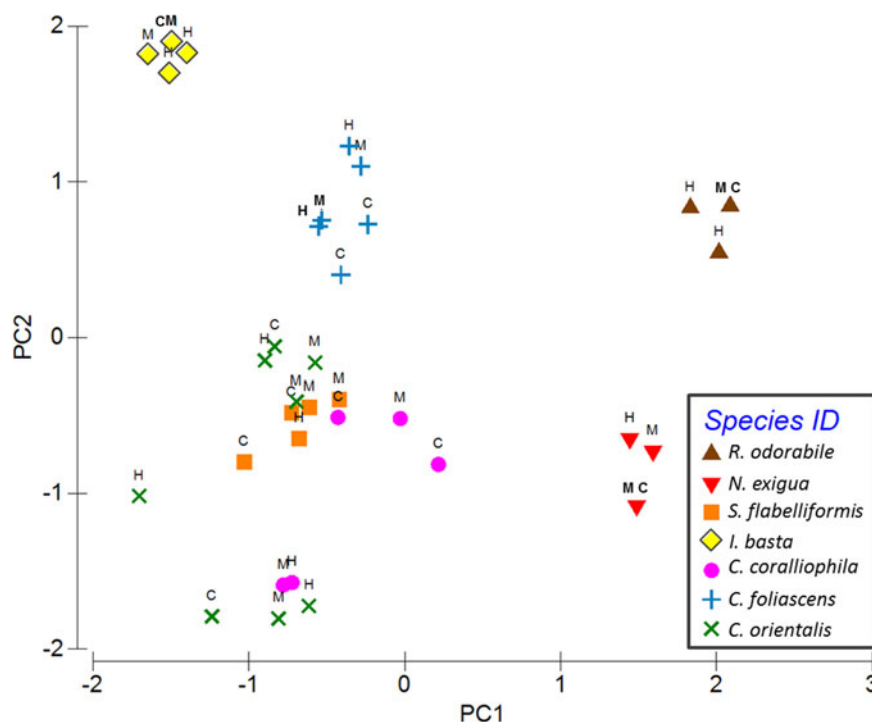


Fig. 7. Principal component analysis (PCA) of DGGE banding pattern profiles. Labels correspond to the sediment treatment (C, M and H).

proxy for sedimentation stress in sponges following a short term sediment pulse. Nevertheless, longer term experiments with higher levels of replication per species may result in more meaningful conclusions about the effect of sediments on sponge photosynthetic pigment production.

Assessment of microbial symbionts in the studied species revealed generally stable and species specific communities with some similarity observed within morphologies. Shifts in the microbial communities of sponges have previously been reported in association with temperature and contamination stress (Webster *et al.*, 2001, 2008; Simister *et al.*, 2012a; Fan *et al.*, 2013) although highly stable populations have also been reported in response to nutrient and sediment stress (Luter *et al.*, 2012, 2014; Simister *et al.*, 2012b). Consistent with these latter findings, sedimentation treatments assessed in this study did not cause large shifts in the microbial communities of any species. Small differences between control sponges and sediment treated sponges were detected in the two photosynthetic species *Carteriospongia foliascens* and *Cymbastela coralliophila* as well as the heterotrophic species *Rhopaloeides odorabile*, although greater replication would be required to determine if these shifts are truly significant. In addition, whilst we don't see the appearance of foreign microbes or the loss of stable microbes associated with

sediment treatment, a shift in the relative abundance of the microbes within the host (not detectable using a DGGE approach) may still have functional implications for the holobiont. Further research using next generation sequencing approaches would help elucidate whether higher sediment concentrations or longer exposure periods would trigger shifts in the sponge associated microbial communities.

Dredging programmes often last for many weeks or months, possibly exposing benthic organisms to periodically high sediment loads, with sedimentation rates affected by TSS, sediment size and local hydrodynamics. In addition, residual plumes can persist in the area for months before TSS returns to ambient levels. In conclusion, our results show that high sedimentation primarily affected massive, encrusting and wide cup sponge morphologies. However, the sediment concentrations tested in this experiment did not appear to cause shifts in the pigment concentrations or microbial community structure of the sponges. These results indicate that a single short term pulse of high TSS levels resulting in a sediment deposition rate of 16 mg cm⁻² could be tolerated by most of the sponge species studied. Nevertheless, the long term effects of high sedimentation, high TSS and light attenuation on sponges should be assessed before final conclusions on the effect of dredging on sponge communities can be drawn.

Table 6. PERMANOVA analysis for each factor separately.

Source	df	MS	Pseudo F	P (perm)
Sedimentation	2	258.62	0.10636	0.998
Error	43	2431.7		
Morphology	3	17,980	14.767	0.001
Error	42	1217.6		
Species	6	14,172	27.569	0.001
Error	39	514.04		

ACKNOWLEDGEMENTS

This research was funded by Woodside Energy, BHP Billiton, Chevron and the WAMSI partners as part of the WAMSI Dredging Science Node. The views expressed herein are those of the authors and not necessarily those of WAMSI. We are thankful to the Node leaders (Dr R. Jones and Dr R. Masini) for their advice and discussion of results. We are

also grateful to A. Severati and J. Gioffre for assistance in the field. J. Doyle provided valuable advice on the chlorophyll analysis. Dr C. Schönberg contributed to the species identification and facilitated access to the dredging related literature. B. Strehlow commented on a previous version of the manuscript.

REFERENCES

- Airoidi L.** (2003) The effects of sedimentation on rocky coast assemblages. *Oceanography and Marine Biology* 41, 161–236.
- Bakus G.** (1968) Sedimentation and benthic invertebrates of Fanning Island, central Pacific. *Marine Geology* 6, 45–51.
- Balata D., Piazzì L., Cecchi E. and Cinelli F.** (2005) Variability of Mediterranean coralligenous assemblages subject to local variation in sediment deposition. *Marine Environmental Research* 60, 403–421.
- Bannister R.J., Battershill C.N. and de Nys R.** (2012) Suspended sediment grain size and mineralogy across the continental shelf of the Great Barrier Reef: impacts on the physiology of a coral reef sponge. *Continental Shelf Research* 32, 86–95.
- Bannister R.J., Hoogenboom M.O., Anthony K.R.N., Battershill C.N., Whalan S., Webster N.S. and de Nys R.** (2011) Incongruence between the distribution of a common coral reef sponge and photosynthesis. *Marine Ecology Progress Series* 423, 95–100.
- Bell J.J.** (2008) The functional roles of marine sponges. *Estuarine, Coastal and Shelf Science* 79, 341–353.
- Bell J. and Barnes D.** (2000a) A sponge diversity centre within a marine “island”. *Hydrobiologia* 440, 55–64.
- Bell J. and Barnes D.** (2000b) The distribution and prevalence of sponges in relation to environmental gradients within a temperate sea lough: vertical cliff surfaces. *Diversity and Distributions* 6, 283–303.
- Bell J.J., Davy S.K., Jones T., Taylor M.W. and Webster N.S.** (2013) Could some coral reefs become sponge reefs as our climate changes? *Global Change Biology* 19, 2613–2624.
- Carballo J.L.** (2006) Effect of natural sedimentation on the structure of tropical rocky sponge assemblages. *Ecoscience* 13, 119–130.
- de Goeij J.M., van Oevelen D., Vermeij M.J., Osinga R., Middelburg J.J., de Goeij A.F.P.M. and Admiraal W.** (2013) Surviving in a marine desert: the sponge loop retains resources within coral reefs. *Science* 342, 108–110.
- Desprez M.** (2000) Physical and biological impact of marine aggregate extraction along the French coast of the Eastern English Channel: short and long term post dredging restoration. *ICES Journal of Marine Science* 57, 1428–1438.
- DEWHA (Department of the Environment Water Heritage and the Arts)** (2009) National Assessment Guidelines for Dredging 2009, 92 pp.
- Diaz M.C. and Rützler K.** (2001) Sponges: an essential component of Caribbean coral reefs. *Bulletin of Marine Science* 69, 535–546.
- Fabricius K.E.** (2005) Effects of terrestrial runoff on the ecology of corals and coral reefs: review and synthesis. *Marine Pollution Bulletin* 50, 125–146.
- Fan L., Liu M., Simister R., Webster N.S. and Thomas T.** (2013) Marine microbial symbiosis heats up: the phylogenetic and functional response of a sponge holobiont to thermal stress. *ISME Journal* 7, 991–1002.
- Ferris M.J., Muyzer G. and Ward D.M.** (1996) Denaturing gradient gel electrophoresis profiles of 16S rRNA defined populations inhabiting a hot spring microbial mat community. *Applied and Environmental Microbiology* 62, 340–346.
- Field M.E., Chezar H. and Storlazzi C.D.** (2013) SedPods: a low cost coral proxy for measuring net sedimentation. *Coral Reefs* 32, 155–159.
- Fromont J.** (2004) Porifera (sponges) of the Dampier Archipelago, Western Australia: habitats and distribution. *Records of the Western Australian Museum* 66, 69–100.
- Gerrodette T. and Flechsig A.** (1979) Sediment induced reduction in the pumping rate of the tropical sponge *Verongia lacunosa*. *Marine Biology* 55, 103–110.
- Hendler G.** (1984) The association of *Ophiothrix lineata* and *Callyspongia vaginalis*: a brittlestar sponge cleaning symbiosis? *PSZN I: Marine Ecology* 5, 9–27.
- Lichtenthaler H.** (1987) Chlorophylls and carotenoids pigments of photosynthetic biomembranes. *Methods in Enzymology* 148, 350–382.
- Lohrer A.M., Hewitt J.E. and Thrush S.F.** (2006) Assessing far field effects of terrigenous sediment loading in the coastal marine environment. *Marine Ecology Progress Series* 315, 13–18.
- Luter H.M., Gibb K. and Webster N.S.** (2014) Eutrophication has no short term effect on the *Cymbastela stipitata* holobiont. *Frontiers in Microbiology* 5, Art. 216.
- Luter H.M., Whalan S. and Webster N.S.** (2012) Thermal and sedimentation stress are unlikely causes of brown spot syndrome in the coral reef sponge, *Ianthella basta*. *PLoS ONE* 7, e39779.
- Maldonado M., Giraud K. and Carmona C.** (2008) Effects of sediment on the survival of asexually produced sponge recruits. *Marine Biology* 154, 631–641.
- McClanahan T.R. and Obura D.** (1997) Sedimentation effects on shallow coral communities in Kenya. *Journal of Experimental Marine Biology and Ecology* 209, 103–122.
- McCulloch M., Fallon S., Wyndham T., Henty E., Lough J. and Barnes D.** (2003) Coral record of increased sediment flux to the inner Great Barrier Reef since European settlement. *Nature* 421, 727–730.
- Morton W.** (1977) *Ecological effects of dredging and dredge spoil disposal: A literature review*. Washington, DC: United States Department of the Interior. Fish and Wildlife Service, 37 pp.
- Murillo F.J., Muñoz P.D., Cristobo J., Ríos P., González C., Kenchington E. and Serrano A.** (2012) Deep sea sponge grounds of the Flemish Cap, Flemish Pass and the Grand Banks of Newfoundland (Northwest Atlantic Ocean): distribution and species composition. *Marine Biology Research* 8, 842–854.
- Muyzer G., de Waal E.C. and Uitterlinden A.G.** (1993) Profiling of complex microbial populations by denaturing gradient gel electrophoresis analysis of polymerase chain reaction amplified genes coding for 16S rRNA. *Applied and Environmental Microbiology* 59, 695–700.
- Newell R.C., Seiderer L.J. and Hitchcock D.R.** (1998) The impact of dredging works in coastal waters: a review of the sensitivity to disturbance and subsequent recovery of biological resources on the sea bed. *Oceanography and Marine Biology* 36, 127–178.
- Pawlik J.R.** (2011) The chemical ecology of sponges on Caribbean reefs: natural products shape natural systems. *BioScience* 61, 888–898.
- Przeslawski R., Ah Yong S., Byrne M., Wörheide G. and Hutchings P.** (2008) Beyond corals and fish: the effects of climate change on non coral benthic invertebrates of tropical reefs. *Global Change Biology* 14, 2773–2795.
- Reiswig H.** (1971) Particle feeding in natural populations of three marine demosponges. *Biological Bulletin* 141, 568–591.

- Ritchie R.** (2008) Universal chlorophyll equations for estimating chlorophylls a, b, c, and d and total chlorophylls in natural assemblages of photosynthetic organisms using acetone, methanol, or ethanol solvents. *Photosynthetica* 46, 115–126.
- Roberts D., Davis A. and Cummins S.** (2006) Experimental manipulation of shade, silt, nutrients and salinity on the temperate reef sponge *Cymbastela concentrica*. *Marine Ecology Progress Series* 307, 143–154.
- Rogers C.** (1990) Responses of coral reefs and reef organisms to sedimentation. *Marine Ecology Progress Series* 62, 185–202.
- Schönberg C.H.L. and Fromont J.** (2011) Sponge gardens of Ningaloo Reef (Carnarvon Shelf, Western Australia) are biodiversity hotspots. *Hydrobiologia* 687, 143–161.
- Simister R., Taylor M.W., Tsai P., Fan L., Bruxner T.J., Crowe M.L. and Webster N.** (2012a) Thermal stress responses in the bacterial biosphere of the Great Barrier Reef sponge, *Rhopaloeides odorabile*. *Environmental Microbiology* 14, 3232–3246.
- Simister R., Taylor M.W., Tsai P. and Webster N.** (2012b) Sponge microbe associations survive high nutrients and temperatures. *PLoS ONE* 7, e52220.
- Simpson C.J.** (1988) *Ecology of scleractinian corals in the Dampier Archipelago, Western Australia*. Technical Series No. 23. Perth, Western Australia: Environmental Protection Authority.
- Thacker R.** (2005) Impacts of shading on sponge cyanobacteria symbioses: a comparison between host specific and generalist associations. *Integrative and Comparative Biology* 45, 369–376.
- Tompkins MacDonald G.J. and Leys S.P.** (2008) Glass sponges arrest pumping in response to sediment: implications for the physiology of the hexactinellid conduction system. *Marine Biology* 154, 973–984.
- Turon X., Codina M., Tarjuelo I., Uriz M.J. and Becerro M.** (2000) Mass recruitment of *Ophiotrix fragilis* (Ophiuroidea) on sponges: settlement patterns and post settlement dynamics. *Marine Ecology Progress Series* 200, 201–212.
- Underwood A.J.** (1997) *Experiments in ecology: their logical design and interpretation using analysis of variance*. Cambridge: Cambridge University Press.
- Webster N., Pantile R., Botté E., Abdo D., Andreakis N. and Whalan S.** (2013) A complex life cycle in a warming planet: gene expression in thermally stressed sponges. *Molecular Ecology* 22, 1854–1868.
- Webster N.S., Cobb R.E. and Negri A.P.** (2008) Temperature thresholds for bacterial symbiosis with a sponge. *ISME Journal* 2, 830–842.
- Webster N.S. and Taylor M.W.** (2012) Marine sponges and their microbial symbionts: love and other relationships. *Environmental Microbiology* 14, 335–346.
- Webster N.S., Webb R.I., Ridd M.J., Hill R.T. and Negri A.P.** (2001) The effects of copper on the microbial community of a coral reef sponge. *Environmental Microbiology* 3, 19–31.
- Whalan S., Battershill C. and Nys R.** (2007) Variability in reproductive output across a water quality gradient for a tropical marine sponge. *Marine Biology* 153, 163–169.
- Wilber D.H. and Clarke D.G.** (2001) Biological effects of suspended sediments: a review of suspended sediment impacts on fish and shellfish with relation to dredging activities in estuaries. *Journal of Fisheries Management* 21, 855–875.
- Wilkinson C.R. and Cheshire A.C.** (1989) Patterns in the distribution of sponge populations across the central Great Barrier Reef. *Coral Reefs* 8, 127–134.
- Wilkinson C.R. and Evans E.** (1989) Coral reefs relative to location, depth, and water movement. *Coral Reefs* 8, 1–7.
- and
- Wulff J.** (1997) Mutualisms among species of coral reef sponges. *Ecology* 78, 146–159.


Correspondence should be addressed to:

M.C. Pineda

Australian Institute of Marine Science, PMB3, Townsville
4810, Queensland, Australia

email: mcarmen.pineda@gmail.com

SCIENTIFIC REPORTS



OPEN

Effects of light attenuation on the sponge holobiont- implications for dredging management

Mari-Carmen Pineda^{1,2}, Brian Strehlow^{1,2,3}, Alan Duckworth^{1,2}, Jason Doyle¹, Ross Jones^{1,2} & Nicole S. Webster^{1,2}

Received: 08 June 2016
Accepted: 17 November 2016
Published: 13 December 2016

Dredging and natural sediment resuspension events can cause high levels of turbidity, reducing the amount of light available for photosynthetic benthic biota. To determine how marine sponges respond to light attenuation, five species were experimentally exposed to a range of light treatments. Tolerance thresholds and capacity for recovery varied markedly amongst species. Whilst light attenuation had no effect on the heterotrophic species *Stylissa flabelliformis* and *Ianthella basta*, the phototrophic species *Cliona orientalis* and *Carteriospongia foliascens* discoloured (bleached) over a 28 day exposure period to very low light (<0.8 mol photons $m^{-2} d^{-1}$). In darkness, both species discoloured within a few days, concomitant with reduced fluorescence yields, chlorophyll concentrations and shifts in their associated microbiomes. The phototrophic species *Cymbastela coralliophila* was less impacted by light reduction. *C. orientalis* and *C. coralliophila* exhibited full recovery under normal light conditions, whilst *C. foliascens* did not recover and showed high levels of mortality. The light treatments used in the study are directly relevant to conditions that can occur *in situ* during dredging projects, indicating that light attenuation poses a risk to photosynthetic marine sponges. Examining benthic light levels over temporal scales would enable dredging proponents to be aware of conditions that could impact on sponge physiology.

Sponges are filter-feeding organisms with important ecosystem roles including habitat provision, seawater filtration, primary production and binding and/or erosion of the carbonate reef structure¹. This diversity of functional roles means that changes to the abundance or composition of sponge assemblages is likely to significantly impact other reef organisms and overall ecosystem functioning². Importantly, sponges host dense and diverse microbial symbionts that are intimately linked to their health, fitness and nutrition^{3,4}. Many of these sponge symbionts are photosynthetic and in some cases they produce $>50\%$ of the energy requirements of the host^{5,6}. In these mutually beneficial partnerships, the photosymbionts obtain energy from sunlight and provide the host with glucose, glycerol and amino acids and, in return, are provided with a protected environment and many of the compounds required for photosynthesis^{7–10}. These sponges are described as ‘phototrophic’ or ‘mixotrophic’ depending on their degree of nutritional dependence from the symbiont primary production^{6,11}.

Phototrophic sponges are common in shallow tropical reef environments world-wide, including the Mediterranean, Red Sea and the Caribbean^{3,6} and can comprise up to 80% of individuals and biomass in some coral reefs in the Indo-West Pacific and the Great Barrier Reef (GBR)^{3,12}. In these regions phototrophic sponges have important ecological roles as net primary producers as well as in recycling organic carbon through shedding of cellular material which is rapidly consumed by detritivores^{3,13}.

Due to their nutritional dependence on the products of photosynthesis, phototrophic sponges may be particularly sensitive to turbidity (water cloudiness) and light reduction caused by increased suspended sediments in the water column^{14–17}. One cause of high turbidity is dredging of the sea bed and the subsequent disposal of the sediment at offshore dredge material placement sites¹⁸. Recent analyses of the effects of plumes from dredging have shown the marked effects the suspended sediments can have on benthic light levels^{19–21}. Close to working dredges all benthic light can be extinguished during the daytime; however, a more common feature is very low ‘caliginous’ or daytime twilight periods, which can occur over extended periods (i.e., days to weeks)¹⁹. The high

¹Australian Institute of Marine Science, Townsville, QLD, and Perth, WA, Australia. ²Western Australian Marine Science Institution, Perth, WA, Australia. ³Centre for Microscopy Characterisation and Analysis, UWA Oceans Institute, and School of Plant Biology: University of Western Australia, Crawley, WA, Australia. Correspondence and requests for materials should be addressed to M.C.P. (email: mcarmen.pineda@gmail.com)

suspended sediment concentrations (SSCs), and the resulting light attenuation, decreases with increasing distance from dredging and understanding the impact of light reduction at different degrees is important for environmental impact assessments and managing dredging programs when underway.

The impacts of light reduction are likely to vary between sponge species, and this is likely to depend on the flexibility of their feeding strategy. For example, whilst the nutrition of some phototrophic sponges can be adversely affected by light reduction and a reduction of photosymbiont derived carbon, other species may have the ability to increase heterotrophic feeding rates to compensate for the decrease in photosynthetic yields^{6,7}. Although cyanobacteria are the dominant photosymbiont taxa in most sponges^{10,22}, dinoflagellates (i.e., *Symbiodinium* spp.) are also found in association with clonoid sponges^{23,24}; and rhodophytes, chlorophytes and diatoms have been reported from a diverse range of sponges^{22,25,26}. Therefore, responses to light attenuation may also differ depending on the symbiont composition within the host. Furthermore, highly specialised, host-specific symbionts often provide a greater benefit to their hosts than generalist symbionts¹⁴, and thus any negative effects from light attenuation will have a greater relative impact on those sponge species that host obligate photosymbionts.

Close to dredging, sponges will be exposed to low light conditions in combination with high SSCs and sedimentation²⁰. This makes it difficult to identify cause-effect pathways, to identify potential bio-indicators and to establish the dose-response relationships needed for impact-prediction purposes. The effects of sedimentation on different sponge species, with a focus on sponge morphology, have been described previously²⁷. In the current study, we examined the effects of light reduction alone on five abundant and geographically widespread sponge species^{1,28}, spanning heterotrophic and phototrophic nutritional modes. In future studies, the effects of elevated SSC alone, sediment smothering alone and a combination of all dredging related factors will be described.

Using environmentally relevant exposure scenarios is essential for risk assessment purposes, and we used light reduction scenarios recently reported in several large-scale capital dredging projects on reefs in Western Australia^{19,21}. The Daily Light Integral (DLI), which is the total photosynthetically active radiation (PAR) received each day as a function of light intensity and duration ($\text{mol photons m}^{-2} \text{d}^{-1}$), was calculated over different running mean time periods from 1–30 days. For several shallow water sites (~6–9 m depth) located <1 Km from the dredge, the 5th percentile (P_5) of DLIs ranged from 1.3–2.1 $\text{mol photons m}^{-2} \text{d}^{-1}$ before dredging, but was 0.4–0.7 $\text{mol photons m}^{-2} \text{d}^{-1}$ during the dredging phase. The number of consecutive days of very low light (<0.8 $\text{mol photons m}^{-2} \text{d}^{-1}$) ranged from 0–10 d before dredging, but from 11–25 d during the dredging phase. For near complete loss of all light, the worst case scenario during the baseline phase was 2 consecutive days increasing to 5 consecutive days during the dredging phase¹⁹.

In this study, a suite of different response variables were used to examine the effects of environmentally realistic light reduction over an extended period (30 d), with a particular focus on changes in sponge symbiosis.

Results

Host response (health). All sponges survived the 28 d experimental treatments, with no observable partial mortality (tissue necrosis). Changes in colour were observed in two of the three phototrophic species. *Cliona orientalis* discoloured after 72 h in the 0 $\text{mol photons m}^{-2} \text{d}^{-1}$ treatment, and milder discolouration occurred in some individuals in the 0.8 $\text{mol photons m}^{-2} \text{d}^{-1}$ treatment (see Supplementary Fig. S1). Despite this rapid response, the colouration returned to normal when returned to natural light for the 14 d observational period. *Carterospongia foliascens* also discoloured in the 0 $\text{mol photons m}^{-2} \text{d}^{-1}$ treatment after 7 d, and whilst there was no partial mortality at the end of the experimental period (Supplementary Fig. S1), all discoloured individuals died during the observational period. The third phototrophic sponge species, *Cymbastela coralliophila*, and the heterotrophic species *Stylissa flabelliformis* and *Ianthella basta*, showed no signs of discolouration throughout the experimental or recovery periods (Supplementary Fig. S1).

Host response (growth). *S. flabelliformis*, *I. basta*, *C. coralliophila* and *C. foliascens* grew, or gained weight, over the experimental period and 14 d observational period in almost all treatments (Fig. 1a). Some individuals of *C. foliascens* from the 0 and 0.8 $\text{mol photons m}^{-2} \text{d}^{-1}$ treatments lost weight during the recovery phase. The buoyant weight of the bioeroding, encrusting sponge *C. orientalis* decreased across all treatments (Fig. 1a), reflecting active bioerosion of the coral substrate. The percentage change in buoyant weight from the start of the experimental period to the end of the observational period was not significantly different between treatments for any species except *C. orientalis* (Table 1A). *C. orientalis* exposed to the 0 and 0.8 $\text{mol photons m}^{-2} \text{d}^{-1}$ treatments lost significantly less weight than individuals in the 8.1 $\text{mol photons m}^{-2} \text{d}^{-1}$ treatment. Accordingly, the mass of excavated substrate per unit area (i.e., surface area) in *C. orientalis* was the lowest under the 0 $\text{mol photons m}^{-2} \text{d}^{-1}$ treatment, although this was not statistically significant (ANOVA: $P = 0.870$).

No change in sponge surface area between treatments could be detected at the end of the experimental period for any species and, with the exception of *C. foliascens*, no significant differences in surface area were detected between treatments from the start of the experimental period until the end of the observational period (Table 1B). A significant reduction in surface area was observed for *C. foliascens* at the end of the observational period (consistent with partial mortality in some individuals exposed to the 0 $\text{mol photons m}^{-2} \text{d}^{-1}$ treatment, see Supplementary Fig. S2). Surface area could not be measured in *C. orientalis* which grows deeper into the coral substrate whilst still maintaining a constant surface area due to its bioeroding nature.

Microbial community response (pigment analyses). Chlorophyll a concentrations of the phototrophic species *C. coralliophila*, *C. foliascens* and *C. orientalis* were typically higher than ~100 $\mu\text{g Chl a/g}$ sponge, and concentrations in the heterotrophic species *S. flabelliformis* and *I. basta* were negligible (overall, < 10 $\mu\text{g Chl a/g}$ sponge) (Fig. 1b). The only exception to this occurred in the 3.2 and 8.1 $\text{mol photons m}^{-2} \text{s}^{-1}$ treatments for *I. basta* during the observational period, in which an algal bloom corresponded with the time of sampling (Fig. 1b). In both heterotrophic species, no significant difference in Chl a was detected between light treatments

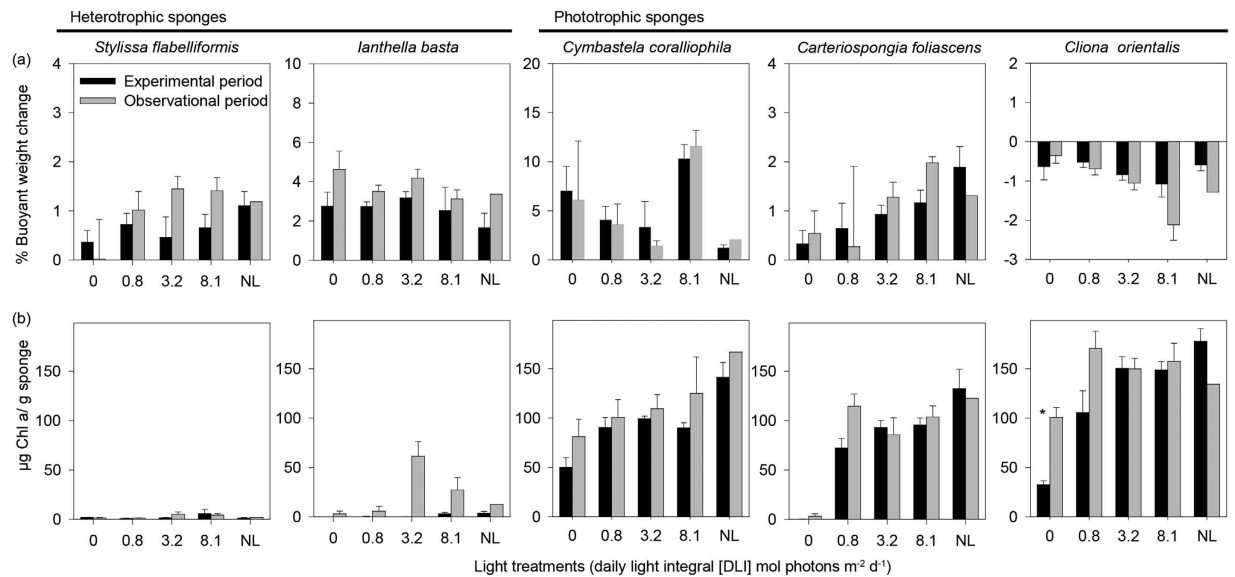


Figure 1. Physiological responses of sponges to light conditions. (a) Percentage buoyant weight change (note: y-axis scales differ between species), and (b) Chlorophyll a concentrations, for the five species, after the 28 d experimental period and 14 d observational period (mean ± SE). Asterisks show statistically significant differences between the experiment and recovery phase (T-tests: $P < 0.05$). Light treatments include 0, 0.8, 3.2, 8.1 mol photons $m^{-2} d^{-1}$ and natural light (NL, 3.2–6.5 mol photons $m^{-2} d^{-1}$).

Source	df	<i>Styllissa flabelliformis</i>		<i>Ianthella basta</i>		<i>Cymbastela coralliophila</i>		<i>Carteriospongia foliascens</i>		<i>Cliona orientalis</i>	
		F	P	F	P	F	P	F	P	F	P
(A) Buoyant weight at the end of the observational phase											
Treatment	3	1.923	0.204	1.377	0.318	1.902	0.208	0.691	0.586	9.506	0.005
Error	8										
Significant Pairwise Multiple Comparisons (Holm-Sidak)										0,0.8,3.2 > 8.1	
(B) Surface area at the end of the experimental and observational phases											
Experimental phase											
Treatment	4	2.271	0.093	1.199	0.338	0.310	0.869	1.695	0.186		
Error	23										
Observational phase											
Treatment	3	1.789	0.227	1.330	0.331	0.943	0.464	4.186	0.047		
Error	8										
Significant Pairwise Multiple Comparisons (SNK)								8.1, NL, 3.2 > 0			
(C) Chl a at the end of the experimental phase											
Treatment	6	1.792	0.173	1.472	0.257	6.072	0.003	31.163	< 0.001	17.271	< 0.001
Error	14										
Significant Pairwise Multiple Comparisons (SNK)						NL, F, T0 > 0		T0, NL, F > 8.1, 3.2, 0.8 > 0		NL, F, 8.1, 3.2, 0.8 > 0	

Table 1. ANOVA examining the effect of treatment on A) Total change in sponge buoyant weight at the end of the observational phase, B) Changes in surface area for each species at the end of experimental and observational periods (surface area was not considered a relevant metric for growth of *C. orientalis*), and C) Chl a concentration at the end of the 28 d experimental period. Holm-Sidak and Student Newman-Keuls (SNK) tests have been performed for significant pairwise multiple comparisons. In pair-wise tests, F: field control; t = 0: time 0 control; 0, 0.8, 3.2 and 8.1 mol photons $m^{-2} d^{-1}$ treatments and natural light controls (NL).

after the experimental or observational period (T-tests: $P > 0.1$) (Table 1C). The Chl a concentration of the phototrophic species under natural light was similar to the freshly collected field samples and t = 0 controls (ANOVA: $P > 0.05$). There were significant differences between the light treatments in the phototrophic species, and the highest Chl a concentration was observed in the natural light controls, followed by the 8.1, 3.2, 0.8 and 0 mol photons $m^{-2} d^{-1}$ treatments (Fig. 1b, Table 1C). In the lower light treatments (0 and 0.8 mol photons $m^{-2} d^{-1}$) there was an overall increase in Chl a concentration after the observational period in natural light (Fig. 1b).

Total chlorophyll was highly correlated to Chl a in the three phototrophic species ($R^2 = 0.834, 0.992, 0.994$ for *C. coralliophila*, *C. foliascens* and *C. orientalis*, respectively, $P < 0.001$). However, total chlorophyll was also marginally

Source	df	MS	Pseudo-F	P (perm)
A) Spectrophotometry				
Species	2	85.707	13.234	0.001
Treatments	2	47.827	7.3848	0.002
Sp × Treatm.	4	14.589	2.2526	0.019
Residuals	18	6.4765		
Pair-wise Tests				
CYM: D ≠ C ($P = 0.022$); CAR: L ≠ D ≠ C ($P < 0.05$); CLI: D ≠ C ($P = 0.046$)				
B) UPLC				
Species	2	27.666	20.451	0.001
Treatments	2	29.407	21.738	0.001
Sp × Treatm.	4	4.3757	3.2345	0.003
Residuals	18	1.3528		
Pair-wise Tests				
CYM: L, D ≠ C ($P < 0.05$); CAR: L ≠ D ≠ C ($P < 0.05$); CLI: L, C ≠ D ($P < 0.05$)				

Table 2. Two-way PERMANOVA of pigment data with species and treatment as factors, for A) Spectrophotometry and B) UPLC analyses. In pair-wise tests, D: Dark (0 mol photons $m^{-2} d^{-1}$), L: low light (0.8 mol photons $m^{-2} d^{-1}$) and C: natural light controls (CLI for *C. orientalis*, CAR for *C. foliascens* and CYM for *C. coralliophila*).

correlated to Chl d in *C. coralliophila* ($R^2 = 0.305$, $P = 0.07$), and highly correlated to Chl d in *C. foliascens* ($R^2 = 0.847$, $P < 0.001$), and to Chl c in *C. orientalis* ($R^2 = 0.906$, $P < 0.001$), consistent with the abundance of cyanobacteria in *C. foliascens* and *C. coralliophila* and *Symbiodinium* sp. in *C. orientalis*^{23,24}. Accordingly, significantly lower values of Chl d and c were retrieved from *C. foliascens* and *C. orientalis*, respectively, in the 0 mol photons $m^{-2} d^{-1}$ treatment (ANOVA: $P < 0.001$), while no significant differences in Chl d were observed in *C. coralliophila* (ANOVA: $P < 0.681$).

Ultra Performance Liquid Chromatography (UPLC) analysis detected Chl a, Chl b, Chl c, Pheophytin a and six Carotenoids (i.e., Peridinin, Neoxanthin, Violaxanthin, Diadinoxanthin, Dincoxanthin and Zeaxanthin) with distinct, species-specific pigment profiles. Non-metric Multi-Dimensional Scaling (nMDS) analysis of the normalized spectrophotometry data and UPLC data showed that both approaches resulted in comparable sample groupings (see Supplementary Fig. S3) and were significantly correlated ($R^2 \geq 0.8$ and $P < 0.001$ in all cases). *C. foliascens* and *C. coralliophila* samples showed greater similarity in pigment profiles than *C. orientalis*, consistent with the presence of cyanobacterial photosymbionts in the former species and *Symbiodinium* sp. in the latter (Supplementary Fig. S3).

Non-metric MDS ordination analysis revealed that most sponge samples in the zero light treatment grouped closely together irrespective of species (Supplementary Fig. S3). PERMANOVA confirmed significant differences between species and treatments for both methods (Table 2). Subsequent pair-wise tests showed significant differences between samples in the dark and the natural light controls in all cases (Table 2) and *C. foliascens* samples in the 0.8 mol photons $m^{-2} d^{-1}$ treatment differed from samples in the control and dark treatments.

Zeaxanthin is a pigment commonly related to the presence of Cyanobacteria²⁹. Accordingly, it was significantly higher in *C. coralliophila* and *C. foliascens* than in *C. orientalis* (ANOVA: $P = 0.002$), while no significant differences between *C. coralliophila* and *C. foliascens* were detected (ANOVA: $P > 0.05$). This pigment was lowest in samples of *C. coralliophila* and *C. foliascens* in the zero light treatment (ANOVA: $P = 0.103$, < 0.005 , respectively), followed by samples in the 0.8 mol photons $m^{-2} d^{-1}$ and the natural light treatments. While Zeaxanthin concentration in *C. orientalis* was not significantly different between treatments (ANOVA: $P = 0.469$), concentrations dropped to zero in samples in the 0 mol photons $m^{-2} d^{-1}$ treatment. On the other hand, Peridinin, which is an additional light harvesting pigment common in *Symbiodinium* sp., was exclusively present in *C. orientalis*. Whilst Peridinin was lowest in samples exposed to zero light, differences between treatments were not significant (ANOVA: $P = 0.085$).

Additional correlations were performed to determine which pigments best explained trends in sponge growth (i.e., based in buoyant weights at the end of the experimental period) within each phototrophic species. No significant correlations between any pigment and buoyant weight were detected in *C. coralliophila* and *C. orientalis*. However, growth rates were significantly correlated to all pigments in *C. foliascens* (i.e., Chl a, Chl d, Pheophytin, Zeaxanthin, Carotenoids and Total Chl; $R^2 > 0.7$, $P < 0.05$), corroborating the higher degree of *C. foliascens* dependence on phototrophic nutrition.

Microbial community response (chlorophyll fluorescence). Chlorophyll fluorescence was not significantly different between treatments at the start of the experiment for any species (Fig. 2). After 7 d, maximum quantum yields varied significantly among light intensities for all of the phototrophic species. Overall, individuals exposed to the 0.8 and 3.2 mol photons $m^{-2} d^{-1}$ treatments exhibited increased photosynthetic efficiency during the first weeks (Fig. 2). Subsequently, both *C. orientalis* and *C. foliascens* showed a significant decrease in chlorophyll fluorescence in the 0 mol photons $m^{-2} d^{-1}$ treatment. With the exception of *C. foliascens* in the zero light

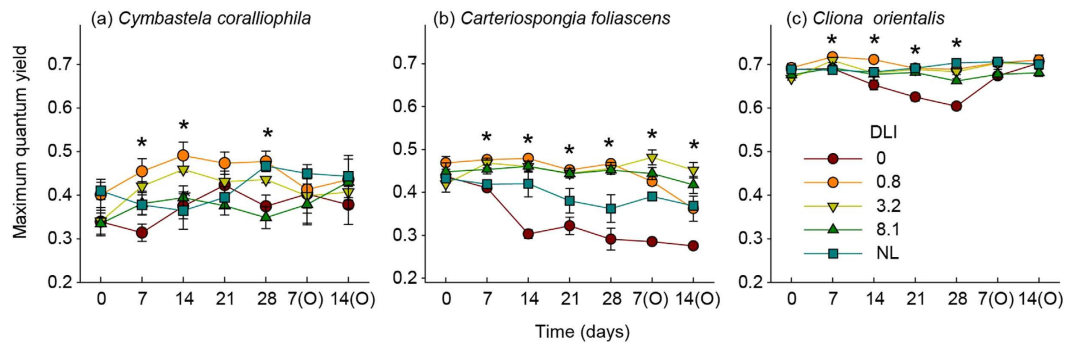


Figure 2. Temporal evolution of fluorescence levels. Mean values (\pm SE) of fluorescence (maximum quantum yield) for the three phototrophic species per light treatment 0, 0.8, 3.2, 8.1 mol photons $m^{-2} d^{-1}$ and natural light (NL, 3.2–6.5 mol photons $m^{-2} d^{-1}$). Measurements were taken at the start of the experiment and then weekly until the end of the experimental and observational (O) periods. Asterisks show statistically significant differences among treatments (ANOVA: $P < 0.05$).

treatment, which suffered 100% mortality, fluorescence values of all other samples returned to normal during the observational phase under natural light conditions.

Microbial community response (microbiome). A total of 13,240,437 high quality 16S rRNA gene amplification sequences were recovered from the 5 sponge species ($n = 168$ individual samples) and 5 seawater samples (environmental controls). Following quality filtering, 25 samples with low (< 4906) read numbers were eliminated from the dataset which included 6 from *S. flabelliformis*, 10 from *I. basta*, 8 from *C. coralliophila*, and 1 seawater environmental control. The remaining samples were sub sampled down to the lowest read number (6587). Each sponge species maintained a unique microbial community (Table 3A, Fig. 3, see also Supplementary Fig. S4) that was distinct from the seawater microbiome (Table 3B, Fig. 3, Supplementary Fig. S4). Aquarium acclimation (for ~6 weeks) did not affect the sponge-associated microbial community of any species, as evidenced by the microbiome similarity of the field controls and the $t = 0$ experimental samples (Table 3A). Overall, the microbial community of the heterotrophic species *S. flabelliformis* and *I. basta*, and the phototrophic species *C. coralliophila*, was consistent amongst all sampling times (Table 3A). Highly significant differences in microbial community composition were observed in the phototrophic species *C. foliascens* and *C. orientalis* over time (i.e., from $t = 0$ until the end of the experimental period) (Table 3A).

Microbial community composition did not differ between light treatments for either heterotrophic species or the phototrophic *C. coralliophila*, but differed between treatments in the phototrophic *C. foliascens* and *C. orientalis* (Table 3C, Fig. 3). Whilst no significant microbial shifts were detected in *C. orientalis* under different light treatments when all sample times were compared together (experimental and observational periods), differences were evident within sampling times when analysed independently (particularly in the zero light treatment) (Table 3C, Figs 3 and 4).

At the Phylum level, the microbiome of *C. coralliophila* was primarily comprised of *Alpha* and *Gammaproteobacteria*, *Acidobacteria* and *Cyanobacteria* with only a small decrease in the relative abundance of *Cyanobacteria* occurring in *C. coralliophila* in the absence of light (Fig. 3). In contrast, the microbial community of *C. foliascens* in the zero light treatment showed a complete loss of *Cyanobacteria* and no recovery after the observational period (Table 3C, Figs 3 and 4). The prokaryotic microbiome of *C. orientalis* was primarily comprised of *Alpha* and *Gammaproteobacteria* and while minor representation of *Cyanobacteria* was evident in *C. orientalis* from most light treatments, this taxa was absent in the zero light treatment (Figs 3, 5 and Table S1). However, *C. orientalis* was able to re-establish its native microbiome after recovery under natural light (Fig. 4).

Network analyses of the 100 most discriminatory operational taxonomic units (OTUs) were performed on *C. foliascens* and *C. orientalis*, for the 0, 0.8 mol photons $m^{-2} d^{-1}$ and natural light treatments. The microbial community in *C. foliascens* was comprised of a large core microbiome (i.e., the component shared between samples in all treatments) that was unaffected by light treatment (Fig. 5). However, the three dominant *Cyanobacteria* OTUs (836, 5342 and 7813) were highly sensitive to light attenuation, being exclusively present in samples from the natural light treatment only. In contrast, *Cyanobacteria* OTUs 6 and 173 could tolerate the 0.8 mol photons $m^{-2} d^{-1}$ treatment, but disappeared in the absence of light. This species also appears to shift its photosymbiont community under reduced light, with samples at the 0.8 mol photons $m^{-2} d^{-1}$ acquiring novel *Cyanobacteria* OTUs 568 and 2339 which were exclusively present in *C. foliascens* from this treatment. Network analysis of the *C. orientalis* microbiome revealed a much smaller core community, and a large number of OTUs that were highly specific to samples in each light treatment (Fig. 5). As in *C. foliascens*, some *Cyanobacteria* OTUs (6 and 110) persisted under the natural light and 0.8 mol photons $m^{-2} d^{-1}$ treatments, but disappeared in the zero light treatment, while *Cyanobacteria* OTU 61 was highly light sensitive and persisted in *C. orientalis* only under natural light conditions. Apart from the *Cyanobacteria*, the light sensitive community (i.e., taxa which were exclusively present in samples under natural light) included representatives of the Phyla *Proteobacteria*, *Bacteroidetes*, *Chlamydiae*, *Verrucomicrobia* and *Acidobacteria* as well as the candidate phylum SBR1093 and the *Archaea*. In contrast, in the zero light treatment, *C. orientalis* was colonised by novel OTUs within the *Actinobacteria*, *Planctomycetes*, *Spirochaetes*, *Chloroflexi* and additional OTUs affiliated to the *Proteobacteria* and *Acidobacteria*.

Source	df	MS	Pseudo-F	P (perm)
A)				
Species	4	58196	40.879	0.001
Time	3	3161.1	2.2205	0.001
Species x Time	11	2291.3	1.6095	0.001
Residuals	124	1423.6		
Pair-wise Tests				
STY: F ≠ E, O ($P < 0.005$); IAN: F ≠ E ($P < 0.005$); CAR: F, T0 ≠ E, O ($P < 0.005, < 0.05$); CLI: T0 ≠ E ≠ O ($P < 0.005$)				
B)				
Source	1	11984	2.8389	0.003
Residuals	145	4221.3		
C)				
<i>S. flabelliformis</i>				
Light	4	905.26	1.0564	0.35
Time (Light)	5	856.69	0.9997	0.449
Residuals	13	856.95		
<i>I. basta</i>				
Light	4	1066.9	0.68538	0.763
Time (Light)	5	1033.4	0.66389	0.805
Residuals	8	1556.6		
<i>C. coralliophila</i>				
Light	4	2860.3	1.1666	0.266
Time (Light)	5	1116.7	0.45548	0.998
Residuals	15	2451.8		
<i>C. foliascens</i>				
Light	4	1901.4	1.8751	0.001
Time (Light)	5	1105.5	1.0903	0.202
Residuals	18	1014		
Pair-wise Tests				
0 ≠ 0.8, 3.2, 8.1, NL ($P < 0.005$)				
<i>C. orientalis</i>				
Light	4	2325.8	1.0689	0.286
Time (Light)	5	3815.6	1.7536	0.001
Residuals	18	2175.9		
Pair-wise Tests				
Within 0 mol photons $m^{-2} d^{-1}$; E ≠ O ($P = 0.093$)				

Table 3. PERMANOVA analyses of the microbiome community with A) species and time as factors, B) source as factor (sponge host vs. environmental control) and, C) light treatment and time (nested to light) as fixed factors for all five sponge species. In pair-wise tests, F: field control, T=0: time 0 control, E: sampling after the 28 d experimental period, O: sampling after the 14 d observational period; STY for *S. flabelliformis*, IAN for *I. basta*, CYM for *C. coralliophila*, CAR for *C. foliascens* and CLI for *C. orientalis*; 0, 0.8, 3.2, 8.1 mol photons $m^{-2} d^{-1}$ and natural light (3.2–6.5 mol photons $m^{-2} d^{-1}$) within light treatments.

Discussion

Prolonged periods of low light caused by natural sediment resuspension events or dredging activities have the potential to adversely affect phototrophic sponges, although tolerance thresholds and capacity for recovery varied markedly in this study amongst sponge species. In contrast, heterotrophic sponge species appear unaffected by light attenuation as indicated by highly stable microbiomes, similar growth rates across all treatments and no visible signs of stress, including pigmentation changes or partial mortality.

The photosynthetic bioeroding sponge *C. orientalis* discoloured within as little as 7 d in darkness and exhibited minor discolouration after 28 d in the highly light attenuated treatment (0.8 mol photons $m^{-2} d^{-1}$). These visible effects were accompanied by a significant decrease in chlorophyll a concentrations and changes in maximum quantum yields. This discolouration was 'sponge bleaching'³⁰, caused by loss of all *Cyanobacteria* and a marked reduction in the concentration of Chlorophyll a-containing *Symbiodinium* sp. Although bleaching occurred rapidly, *C. orientalis* still maintained quite high fluorescence values and also showed a rapid recovery of pigmentation on return to natural light conditions. *Cliona varians*, a congeneric species from the Caribbean, can also rapidly recover its native symbionts (within 2 weeks) following 8 months of exposure to total darkness³¹. Histological analysis of the *C. orientalis* tissues revealed the presence of some *Symbiodinium* deep in the tissue even after 28 d in darkness. Bioeroding *Cliona* sponges appear to be able to cope with extended periods of light reduction by retracting tissue and symbionts deep into the host coral skeleton³². This behavioural response could also have

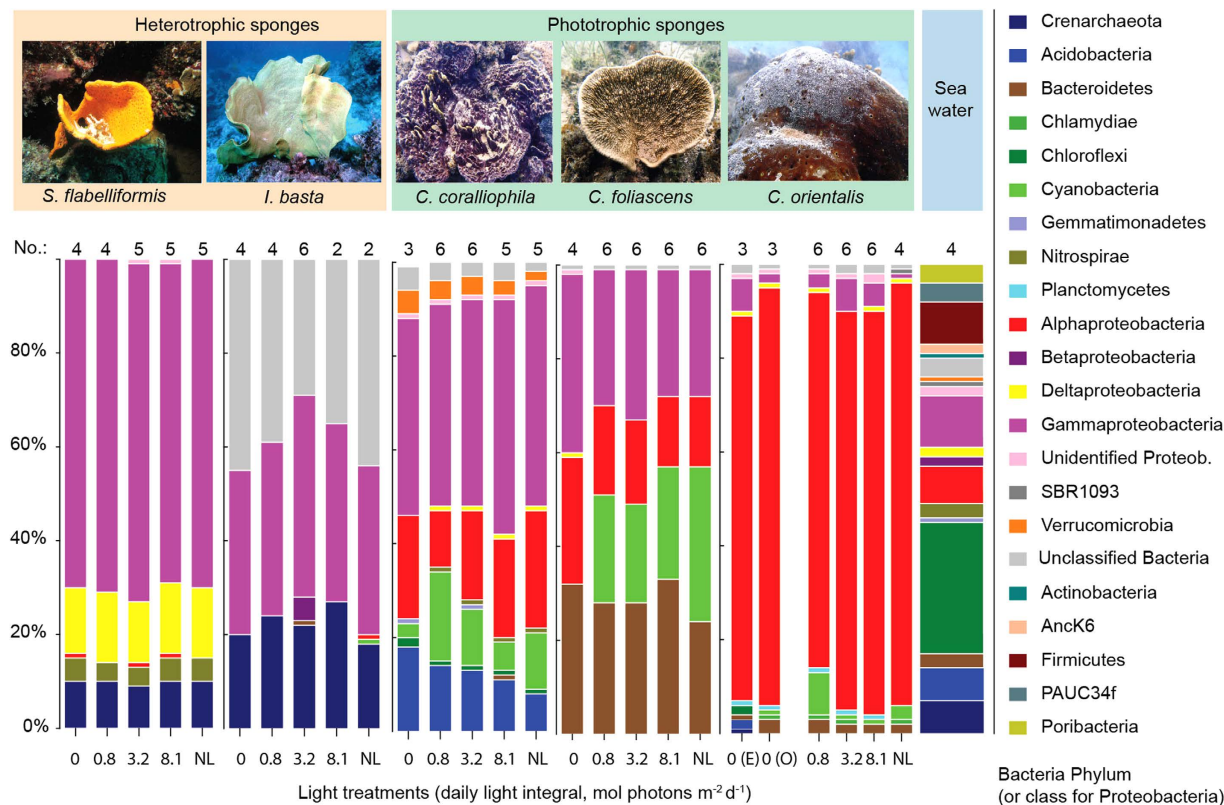


Figure 3. Phylum-level bar chart. Average relative abundance of each bacteria phylum (and class for Proteobacteria) for each species and light treatment (0, 0.8, 3.2, 8.1 mol photons $m^{-2} d^{-1}$ and natural light: NL, 3.2–6.5 mol photons $m^{-2} d^{-1}$). Only OTUs representing greater than 1% of the overall community were included. When significant differences in time were detected, samples from experimental (E) and observational (O) periods were plotted separately (i.e., 0 mol photons $m^{-2} d^{-1}$ in *C. orientalis*, Table 3).

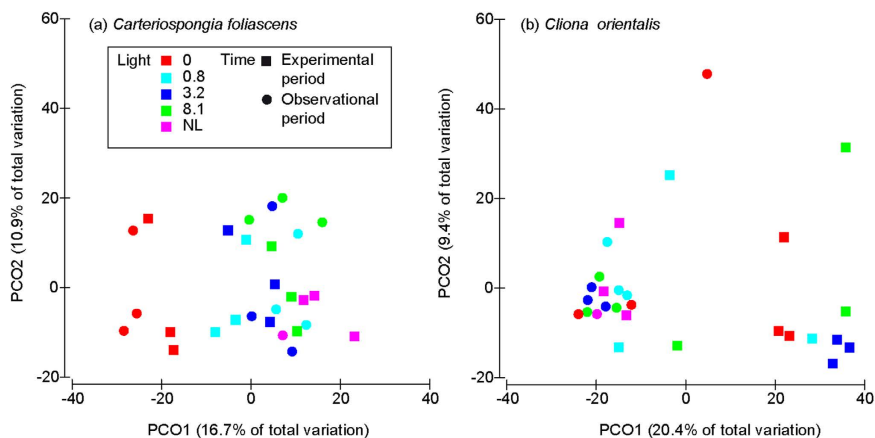


Figure 4. PCO analyses of *C. foliascens* and *C. orientalis*. Principal coordinate analysis plots for *C. foliascens* and *C. orientalis* which showed significant differences based on light treatment or time according to PERMANOVA analysis (Table 3C). Square symbols represent samples at the end of 28 d experimental period, circles are samples at the end of the observational period and colours indicate the 5 light treatments (0, 0.8, 3.2, 8.1 mol photons $m^{-2} d^{-1}$ and natural light: NL, 3.2–6.5 mol photons $m^{-2} d^{-1}$).

contributed to at least some of the discolouration, similar to effects observed with scleractinian corals where extreme retraction of the *Symbiodinium* spp. containing tissues during sub-aerial exposure can cause them to pale. This bleaching in corals is rapidly reversible (within hours) on return to more benign conditions.

It is not clear how the *Symbiodinium* sp. in *C. orientalis* could survive such periods of complete darkness. In culture, *Symbiodinium* spp. have been reported to undertake heterotrophic feeding³³, although it remains to be

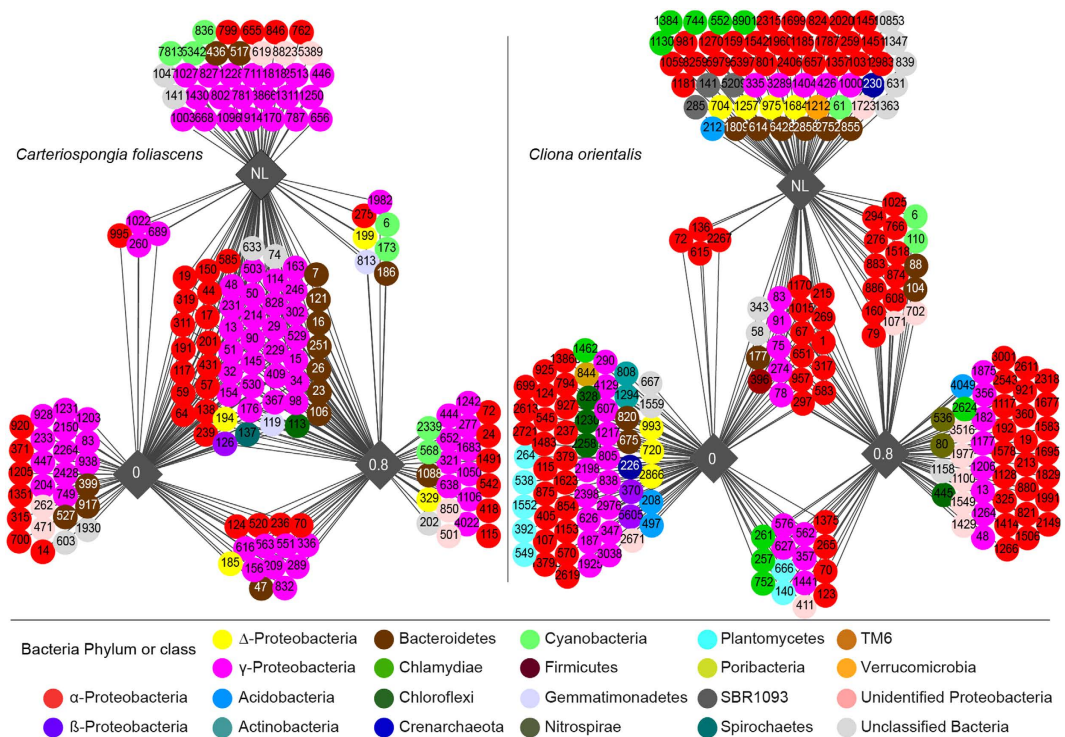


Figure 5. Cytoscape networks of *C. foliascens* and *C. orientalis* microbiome. Networks of the microbiome community on 3 light treatments (0, 0.8 and natural light ($3.2\text{--}6.5\text{ mol photons m}^{-2}\text{ d}^{-1}$)) for the phototrophic species *C. foliascens* and *C. orientalis*. Circles correspond to different OTUs (with OTU numbers) and colours relate to their Phylum or Class level in the case of *Proteobacteria*. Only samples at the end of the 28 d experimental period were used ($n = 3$ per treatment).

determined whether this can occur *in hospite*. Nevertheless, the remnant symbiont population is significant, as the rapid division of this population can mean a relatively quick recovery from bleaching on return to the more favourable conditions.

C. foliascens survived the 28 d exposure to complete darkness, but underwent a loss of photosymbionts, a large shift in the microbiome and subsequently died in the observational period on return to natural light conditions. In contrast, the phototrophic *C. coralliophila* showed a high tolerance to reduced light as evidenced by only minor bleaching, slight reductions in chlorophyll a, minor changes in quantum yield values and a decrease in the relative abundance of *Cyanobacteria* in darkness. No significant changes were observed in the overall microbiome and complete recovery was observed within two weeks under natural light conditions.

Light is a critical factor controlling the growth and population demographics of phototrophic sponges as photosynthetic productivity from symbiotic microbes can provide between 48–80% of a sponge's energy requirements³. Reduced light availability is therefore linked to energy depletion and associated mass reduction, as observed here for *C. foliascens* and as previously reported for other sponge species^{12,14}. Light is also considered an important factor influencing excavation rates by bioeroding species^{1,24}, and although some *Symbiodinium* sp. remained deep in the tissue even after four weeks without light, *C. orientalis* exposed to low light intensity also appeared to have reduced bioerosion capability, as inferred by a significantly smaller reduction in buoyant weight compared to control samples.

Although most phototrophic sponge species rely primarily on symbiotic relationships for their energy needs^{6,12}, some have the ability to activate their heterotrophic metabolism under certain conditions. This switch to heterotrophy would enable sponges to survive under reduced light conditions, as has been reported in *Petrosia ficiformis* (Poiret, 1789), *Aplysina fulva* (Pallas, 1766) and *Neopetrosia subtriangularis* (Duchassaing, 1850)^{6,7}. The same switching has also been observed in photosymbiotic corals during low light associated with natural turbidity events³⁴.

The different responses of the three phototrophic sponges under low light conditions may be related to different degrees of dependency on the photosynthetic symbionts. For instance, *Phyllospongia lamellosa* (Esper, 1794), a foliaceous phototrophic sponge closely related to *C. foliascens*³⁵, relies on photosynthesis for the majority of its respiratory carbon requirements¹². In *C. foliascens* the symbiosis is highly specialized and largely driven by a *Synechococcus* sp. (OTU 6)³⁶. The strong correlation between photopigments and growth rates in *C. foliascens* provides further support for a high degree of nutritional dependence on photosymbionts. In contrast, *C. coralliophila* tolerated the 4-week light attenuation and its growth rate showed no correlation with any pigment, suggesting that it may have the ability to increase its heterotrophic feeding rates when ambient light conditions change and photosynthetic activity of symbionts is reduced. However, longer-term experiments are still required as a 90 day

light attenuation study on a congeneric species, *Cymbastela concentrica* (Lendenfeld, 1887), resulted in bleaching, necrosis, and significant reductions in growth, reproductive status and concentration of chlorophyll a^{15} .

While many sponge species host highly stable microbiomes irrespective of environment^{37–40}, recent research has also indicated that shifts in the sponge-associated microbial community may confer a mechanism for local host acclimation to different environmental conditions⁴¹. The large shifts in the microbiome of *C. foliascens* and *C. orientalis* under low light conditions, including the appearance of novel photosynthetic microorganisms under highly light attenuated conditions (DLI of 0.8 mol photons $m^{-2} d^{-1}$), may indicate an attempt at symbiont shuffling to a community better able to function under reduced irradiance. The rapid microbiome recovery of both *C. orientalis* and *C. coralliophila* under natural light further indicates significant flexibility in symbiosis in these species. However, while some species may have the ability to successfully alter the composition of their microbial community under different environmental conditions⁴², an extensive body of literature also highlights that species with intimate and/or potentially obligate symbioses can be adversely impacted by disruption of the microbiome^{43,44} or loss of symbiotic function⁴⁵. The rapid deterioration in health of *C. foliascens* following the microbiome shift is consistent with its intimate reliance on a highly specialised microbial community.

The levels of light reduction attained close to dredging activities were recently described in a large-scale capital project on reefs in Western Australia^{19,21}. The light treatments used in the present study are clearly relevant to conditions that can occur during dredging, showing that light attenuation is not only a hazard to photosynthetic sponges but also a risk in close proximity to dredging operations⁴⁶. This study examined the specific effects of light reduction on sponges, with the combined effects of elevated SSCs and light attenuation being investigated in subsequent experiments. Nevertheless, based on light reduction alone, the rapid bleaching response observed in *C. foliascens* (irreversible) and *C. orientalis* (reversible) suggests that discolouration of sponges would be an effective bioindicator during dredging operations, as long as natural variations in colour are taken into consideration. The results of this study could be used in conjunction with water quality monitoring programs to alert dredging proponents to levels of light reduction that, if continued, could result in harm to phototrophic sponges. In combination with sediment plume models and estimates of the light attenuation by the suspended sediment, these results could be used to make predictions of the likely effects of dredging (i.e., at the EIA stage). By modelling different dredging scenarios (i.e., volume of material dredged, tidal phase, over flow options, etc.) the information could also be used to identify optimal dredging scenarios that minimise the likelihood and extent of impact. Benthic light availability should be considered over multiple different time periods (from days to weeks) allowing dredging proponents to be aware of, or alerted to, conditions that could potentially impact sponge physiology.

Methods

Sample collection. To facilitate a response comparison across nutritional modes, the study was conducted with the phototrophic sponges *Cymbastela coralliophila* (Hooper & Berquist 1992), *Carteriospongia foliascens* (Pallas, 1766) and *Cliona orientalis* (Thiele, 1900), and the heterotrophic sponges *Stylissa flabelliformis* (Hentschel, 1912) and *Ianthella basta* (Pallas, 1976)^{12,23,27,47,48}. All sponges were collected from 3–15 m depth from either the Palm Islands or Davies Reef, Great Barrier Reef (GBR) (see Supplementary Table S2). *C. orientalis* is an encrusting sponge that bioerodes coral, hence cores of sponge on top of dead coral substrate where chiselled from *Porites* sp. colonies. Sponges were cut into similar sized explants ($\sim 10 \times 10$ cm), and placed in natural light acclimation tanks with flow-through seawater for up to 6 weeks until they had completely healed.

Experimental Set up. All experiments were performed in the National Sea Simulator (SeaSim) at the Australian Institute of Marine Science (AIMS, Townsville). Tests were conducted in 50 L acrylic tanks supplied with a continuous inflow of 5 μm filtered seawater at a rate of 833 mL min^{-1} . The high inflow rates ensured one complete turnover of the tanks per hour of partially filtered seawater, which ensured that sponges received sufficient particulate food including microorganisms. Experiments were conducted in a constant environment room with water temperature set to 29 °C, representing the temperature at the time of sponge collection. Sponges were exposed to 5 different light treatments selected to represent different levels of light attenuation in a dredging plume^{19,49}. Tanks were illuminated on a 12:12 h L:D cycle, with a light regime designed to simulate daily conditions on the reef. Each day there was a 3 hour morning period (from 06:00–09:00) of gradually increasing light from darkness to a maximum instantaneous light level of 25, 100 and 250 μmol photons $m^{-2} s^{-1}$ for each of the 3 treatments, followed by a 3 h afternoon period (from 15:00–18:00) of gradually decreasing light until full darkness. A natural light control (~ 150 – $300 \mu mol$ photons $m^{-2} s^{-1}$ at noon) was also used, and the last treatment was complete darkness. Factoring in the increase and decrease in light levels and maximum instantaneous light level during the middle of the day, the daily light integrals (DLIs) were 0, 0.8, 3.2 and 8.1 mol photons $m^{-2} d^{-1}$ respectively, and 3.2–6.5 mol photons $m^{-2} d^{-1}$ for the natural light control, depending on weather conditions. The light attenuation experiment was conducted for a 28 d ‘experimental’ period, followed by a 14 d ‘observational’ (i.e., recovery) period under natural light. There were 3 tanks per treatment, each with 2 sponge replicates per species (i.e., 6 replicates of each species per treatment).

Studied parameters. The effect of the different light treatments on the sponge holobiont was determined using a suite of response variables, with a particular focus on changes in sponge photosymbionts and composition of the sponge microbial community. For each species, 3 extra individuals were collected as field controls, and immediately processed *in situ* (see below) in order to determine any potential effects of the handling and experimental enclosures. At the start of the experiment, 3 additional individuals per species were sampled ($t = 0$ controls) to obtain baseline data on sponge health. Unless otherwise stated, statistical analyses were performed using the software SigmaPlot v.11.0 (Systat Software Inc.).

Sponge growth. To obtain a proxy for sponge growth, initial and final weights were measured for all individuals using a buoyant weight scale (± 0.001 g) at a constant temperature of 29 °C. Among a selection of methods to measure growth, buoyant weights were used to prevent potential blockages from air exposure, to allow subsequent tissue sampling and because they are good estimators of sponge growth across environmental gradients⁵⁰. In the encrusting *C. orientalis*, buoyant weights indicate the net change between the weight of tissue (i.e., mostly spicules) and changes in the CaCO₃ substrate caused by its bioeroding activity. Hence, weights in *C. orientalis* are not comparable with other sponge species. The mass of excavated substrate per unit area was also calculated in *C. orientalis* using surface area based on images (see below). However, due to the irregularity in shape of some of the replicates, these values are an estimation rather than exact size values. The percentage weight change between day 0 and the end of the recovery phase was assessed for each species separately using one-way analysis of variance (ANOVA) with treatment as the fixed factor. The mass of excavated substrate per unit area between day 0 and the end of the experimental phase was also assessed for *C. orientalis* using one-way ANOVA and treatment as fixed factor.

A 2-dimensional proxy for partial mortality (tissue necrosis), size change (i.e., surface area), and colour was recorded weekly using a digital camera with underwater housing (Canon PowerShot SX50-HS) and image analysis software (Image J⁵¹). Images were always taken under maximum instantaneous light levels (9.00–15.00 h) to eliminate any possible diurnal variation in colour. Changes in percent surface area after the experimental and observational periods were studied for each species separately using one-way ANOVA with treatment as the fixed factor. In any instances where homogeneity of variances and normality were not evident, a Kruskal-Wallis one-way ANOVA on ranks was performed.

Pigment analyses. Pigment analyses were performed spectrophotometrically on the field controls, on the sponges collected at $t = 0$ and at the end of the experimental and observational periods. Two $1 \times 0.5 \times 0.5$ cm pieces of tissue incorporating pinacoderm and mesohyl regions were excised per individual, placed immediately in liquid nitrogen and stored at -80 °C until pigment and symbiont analysis. Pigments were extracted from a weighed piece of sponge using 95% ethanol and a Bead Beater (Bio Spec Products Inc., Bartlesville, USA)²⁷. Absorbance at 470, 632, 649, 665, 696 and 750 nm was measured using a Power Wave Microplate Scanning Spectrophotometer (BIO-TEK[®] Instruments Inc., Vermont USA). Chlorophyll a, b, c and d, and total carotenoids were calculated using the equations provided in refs 52,53 and standardized to sponge wet weight.

The concentration of chlorophyll a was used as a proxy for changes in photosymbiont health/activity (i.e., bleaching) due to light attenuation³. Changes in chlorophyll a concentration during the experimental period were assessed for each species separately using a one-way ANOVA with treatment as the fixed factor. In any instances where homogeneity of variances and normality were not evident, a Kruskal-Wallis one-way ANOVA on ranks was performed. Differences between chlorophyll a at the end of the experimental and observational periods were assessed with a t-test for each treatment and species, separately. Photopigments were additionally measured in a selection of samples (phototrophic species from the 0 and 0.8 mol photons $m^{-2} d^{-1}$ and natural light treatments, $n = 27$) by Ultra Performance Liquid Chromatography (UPLC) to determine the type and quantity of pigments present⁵⁴.

All pigments retrieved by spectrophotometry and UPLC were used to build resemblance matrices based on normalized data. Non-metric Multi-Dimensional Scaling (nMDS) plots were created for each method separately using Euclidean distances. Two factors were determined (species, light treatment) and examined by PERMANOVA (Permutational multivariate ANOVA based on distances). Analyses were performed using PRIMER 6 (Primer-E Ltd, UK).

Chlorophyll fluorescence. Changes in photosynthetic capacity (maximum quantum yield [Fv/Fm]) of the sponge's phototrophic symbionts were measured with a Diving-PAM (pulse amplitude modulation) chlorophyll fluorometer (Heinz Walz GmbH, Effeltrich, Germany). Chlorophyll fluorescence measurements were obtained 10 mm from the sponge tissue by placing a 6 mm fibre-optic probe perpendicular to the surface. Initial fluorescence was determined using a pulse-modulated red measuring light (655 nm, 0.15 μ mol photons $m^{-2} s^{-1}$ at 0.6 kHz). Three measures (maximum quantum yield) were obtained weekly on dark adapted samples (30 min) for the three phototrophic species (i.e., *C. coralliophila*, *C. foliascens* and *C. orientalis*) throughout the experimental and observational periods. One-way ANOVAs were performed to test whether treatment had any effect on chlorophyll fluorescence of the sponges at any given time. The effect of time within every treatment and species was also assessed with a one-way ANOVA.

Microbial community analysis. The composition of the sponges microbial community was assessed using Illumina amplicon sequencing of the 16S rRNA gene. Samples were collected at the end of the experimental and observation period, immediately frozen in liquid nitrogen and stored at -80 °C. Water samples were simultaneously collected from each tank to facilitate a direct comparison with microbes present in the surrounding environment. DNA was extracted from ~ 0.25 g of sponge tissue using the PowerSoil[®]-htp 96 Well Soil DNA Isolation Kit (MoBio Laboratories, Carlsbad, CA) according to standard protocols (<http://press.igsb.anl.gov/earthmicrobiome/emp-standard-protocols/dna-extraction-protocol/>). Microbial communities in seawater were collected by passing 1 L of seawater through 0.2 μ m Sterivex filters and DNA was extracted from the filters as previously described⁵⁵. Aliquots of the extracted DNA were shipped to the University of Colorado, (Boulder, Colorado, USA) for sequencing using standard Earth Microbiome Project (<http://www.earthmicrobiome.org/emp-standard-protocols/16s/>) protocols. Briefly, the V4 region of the 16S rRNA gene was amplified using the primer 515 f – 806r and sequenced using the HiSeq2500 platform (Illumina). Processed sequences and meta-data are available via the following portal (<http://qiita.microbio.me/>) under study number 10533.

Amplicon sequence data was processed in Mothur v.1.35.1⁵⁶. Firstly, quality-filtered, demultiplexed fastq sequences were trimmed according to quality and processed as per⁵⁷. Only sequences that aligned to the expected position were kept. Aligned reads were reduced to non-redundant sequences and chimeric sequences were detected using Uchime⁵⁸. Aligned sequences were phylogenetically classified based on the Ribosomal Database Project (RDP) reference file v.14⁵⁹, and all undersigned sequences removed (taxon = Chloroplast-Mitochondria-unknown-Eukaryota). Pairwise distances between aligned sequences were calculated and used for clustering. Operational taxonomic units (OTUs) were retrieved based on the distance among the clustered sequences and were further classified based on the Greengenes taxonomy⁶⁰.

Pivot tables were used to condense tables by phylum and class for graphical interpretation. OTU data was normalised to account for sampling depth and then square-root transformed to reduce the effect of abundant OTUs. Bray-Curtis distance matrices were constructed to examine additional patterns of community structure and visualised using non-metric multidimensional plots (nMDS) and principal coordinate analyses (PCO). Permutational analysis of variance (PERMANOVA, using 9,999 permutations) was used to determine significant differences in microbial communities based on source (sponge versus environmental control), time of sampling (field controls, t = 0, experimental and observational period), and all five light treatments. All multidimensional statistical analyses were performed in PRIMER 6. Similarity Percentage (SIMPER) analysis was used to determine the OTUs that contribute to the differences between the natural light, 0.8 and 0 mol photons m⁻² d⁻¹ treatments) for each phototrophic species, separately. The 100 OTUs with the most discriminating power from the SIMPER analysis were used to create networks on Cytoscape 3.2.0 (www.cytoscape.org)⁶¹.

References

- Bell, J. J. The functional roles of marine sponges. *Estuar. Coast. Shelf Sci.* **79**, 341–353 (2008).
- Peterson, B., Chester, C., Jochem, F. & Fourqurean, J. Potential role of sponge communities in controlling phytoplankton blooms in Florida Bay. *Mar. Ecol. Prog. Ser.* **328**, 93–103 (2006).
- Wilkinson, C. R. Net primary productivity in coral reef sponges. *Science*. **219**, 410–412 (1983).
- Webster, N. S. & Taylor, M. W. Marine sponges and their microbial symbionts: love and other relationships. *Environ. Microbiol.* **14**, 335–46 (2012).
- Wilkinson, C. R. Interocean differences in size and nutrition of coral reef sponge populations. *Science*. **236**, 1654–7 (1987).
- Erwin, P. & Thacker, R. Phototrophic nutrition and symbiont diversity of two Caribbean sponge–cyanobacteria symbioses. *Mar. Ecol. Prog. Ser.* **362**, 139–147 (2008).
- Arillo, A., Bavestrello, G., Burlando, B. & Sara, M. Metabolic integration between symbiotic cyanobacteria and sponges: a possible mechanism. *Mar. Biol.* **117**, 159–162 (1993).
- Freeman, C. J. & Thacker, R. W. Complex interactions between marine sponges and their symbiotic microbial communities. *Limnol. Oceanogr.* **56**, 1577–1586 (2011).
- Thacker, R. W. & Freeman, C. J. In *Adv. Mar. Biol.* (Becerro, M. A., Uriz, M. J., Maldonado, M. & Turon, X.) **62**, 57–111 (Elsevier Ltd, 2012).
- Usher, K. M. The ecology and phylogeny of cyanobacterial symbionts in sponges. *Mar. Ecol.* **29**, 178–192 (2008).
- Wilkinson, C. & Trott, L. Light as a factor determining the distribution of sponges across the central Great Barrier Reef. In *Proc. 5th Int Coral Reef Symp., Tahiti 5*, 125–130 (1985).
- Cheshire, A. C. A., Wilkinson, C. R. C., Seddon, S. & Westphalen, G. Bathymetric and seasonal changes in photosynthesis and respiration of the phototrophic sponge *Phyllospongia lamellosa* in comparison with respiration by the heterotrophic sponge *Ianthella basta* on Davies Reef, Great Barrier Reef. *Mar. Freshw. Res.* **48**, 589–599 (1997).
- de Goeij, J. M. *et al.* Surviving in a marine desert: the sponge loop retains resources within coral reefs. *Science* **342**, 108–110 (2013).
- Thacker, R. W. Impacts of shading on sponge–cyanobacteria symbioses: A comparison between host-specific and generalist associations. *Integr. Comp. Biol.* **45**, 369–376 (2005).
- Roberts, D., Davis, A. & Cummins, S. Experimental manipulation of shade, silt, nutrients and salinity on the temperate reef sponge *Cymbastela concentrica*. *Mar. Ecol. Prog. Ser.* **307**, 143–154 (2006).
- Bell, J. J. *et al.* Sediment impacts on marine sponges. *Mar. Pollut. Bull.* **94**, 5–13 (2015).
- Stubler, A. D., Duckworth, A. R. & Peterson, B. J. The effects of coastal development on sponge abundance, diversity, and community composition on Jamaican coral reefs. *Mar. Pollut. Bull.* **93**, 261–270 (2015).
- Morton, W. *Ecological effects of dredging and dredge spoil disposal: A literature review. United States Department of the Interior. Fish and Wildlife Service* (1977).
- Jones, R., Fisher, R., Stark, C. & Ridd, P. Temporal patterns in seawater quality from dredging in tropical environments. *PLoS One* **10**, e0137112 (2015).
- Jones, R., Bessell-Browne, P., Fisher, R., Klonowski, W. & Slivkoff, M. Assessing the impacts of sediments from dredging on corals. *Mar. Pollut. Bull.* **102**, 9–29 (2016).
- Fisher, R., Stark, C., Ridd, P. & Jones, R. Spatial patterns in water quality changes during dredging in tropical environments. *PLoS One* **10**, e0143309 (2015).
- Rützler, K. In *New Perspect. sponge Biol.* (Rützler, K.) 455–466 (Smithsonian Institution Press, 1990).
- Schönberg, C. H. L. & Loh, W. K. W. Molecular identity of the unique symbiotic dinoflagellates found in the bioeroding demosponge *Cliona orientalis*. *Mar. Ecol. Prog. Ser.* **299**, 157–166 (2005).
- Hill, M., Allenby, A., Ramsby, B., Schönberg, C. & Hill, A. *Symbiodinium* diversity among host clonoid sponges from Caribbean and Pacific reefs: Evidence of heteroplasmy and putative host-specific symbiont lineages. *Mol. Phylogenet. Evol.* **59**, 81–8 (2011).
- Taylor, M. W., Radax, R., Steger, D. & Wagner, M. Sponge-associated microorganisms: evolution, ecology, and biotechnological potential. *Microbiol. Mol. Biol. Rev.* **71**, 295–347 (2007).
- Lemloh, M.-L., Fromont, J., Brümmer, F. & Usher, K. M. Diversity and abundance of photosynthetic sponges in temperate Western Australia. *BMC Ecol.* **9**, 4 (2009).
- Pineda, M. C., Duckworth, A. & Webster, N. Appearance matters: sedimentation effects on different sponge morphologies. *J. Mar. Biol. Assoc. United Kingdom* **96**, 481–492 (2016).
- Fromont, J. Porifera (sponges) of the Dampier Archipelago, Western Australia: *Rec. West. Aust. Museum* **100**, 69–100 (2004).
- Rowan, K. S. *Photosynthetic pigments of algae*. (Cambridge University Press, 1989).
- Fromont, J. & Garson, M. Sponge bleaching on the West and East coasts of Australia. *Coral Reefs* **18**, 340 (1999).
- Riesgo, A. *et al.* Transcriptomic analysis of differential host gene expression upon uptake of symbionts: a case study with *Symbiodinium* and the major bioeroding sponge *Cliona varians*. *BMC Genomics* **15**, 376 (2014).
- Schönberg, C. H. L. & Suwa, R. In *Porifera Res. Biodiversity, Innov. Sustain.* (Custódio, M., Hajdu, E., Lôbo-Hajdu, G. & Muricy, G.) 569–580 (Publ Museu Nac Rio de Janeiro, 2007).
- Jeong, H. J. *et al.* Heterotrophic feeding as a newly identified survival strategy of the dinoflagellate *Symbiodinium*. *Proc. Natl. Acad. Sci. USA* **109**, 12604–9 (2012).

34. Bessell-Browne, P., Stat, M., Thomson, D. & Clode, P. L. *Coscinarinae marshallae* corals that have survived prolonged bleaching exhibit signs of increased heterotrophic feeding. *Coral Reefs* **33**, 795–804 (2014).
35. Abdul Wahab, M. A., Fromont, J., Whalan, S., Webster, N. & Andreakis, N. Combining morphometrics with molecular taxonomy: How different are similar foliose keratose sponges from the Australian tropics? *Mol. Phylogenet. Evol.* **73**, 23–39 (2014).
36. Webster, N. S. *et al.* Same, same but different: symbiotic bacterial associations in GBR sponges. *Front. Microbiol.* **3**, 444 (2013).
37. Erwin, P. M., Pita, L., López-Legentil, S. & Turon, X. Stability of sponge-associated bacteria over large seasonal shifts in temperature and irradiance. *Appl. Environ. Microbiol.* **78**, 7358–68 (2012).
38. Webster, N. S., Botté, E. S., Soo, R. M. & Whalan, S. The larval sponge holobiont exhibits high thermal tolerance. *Environ. Microbiol. Rep.* **3**, 756–762 (2011).
39. Luter, H. M., Whalan, S. & Webster, N. S. Thermal and sedimentation stress are unlikely causes of brown spot syndrome in the Coral Reef sponge, *Ianthella basta*. *PLoS One* **7**, 1–9 (2012).
40. Simister, R., Taylor, M. W., Tsai, P. & Webster, N. Sponge-microbe associations survive high nutrients and temperatures. *PLoS One* **7**, e52220 (2012).
41. Morrow, K. M. *et al.* Natural volcanic CO₂ seeps reveal future trajectories for host-microbial associations in corals and sponges. *ISME J.* **9**, 894–908 (2015).
42. Webster, N. S. *et al.* Bacterial community dynamics in the marine sponge *Rhopaloeides odorabile* under *in situ* and *ex situ* cultivation. *Mar. Biotechnol. (NY)*. **13**, 296–304 (2011).
43. Simister, R. *et al.* Thermal stress responses in the bacterial biosphere of the Great Barrier Reef sponge, *Rhopaloeides odorabile*. *Environ. Microbiol.* **14**, 3232–46 (2012).
44. Webster, N. S., Cobb, R. E. & Negri, A. P. Temperature thresholds for bacterial symbiosis with a sponge. *ISME J.* **2**, 830–42 (2008).
45. Fan, L., Liu, M., Simister, R., Webster, N. S. & Thomas, T. Marine microbial symbiosis heats up: the phylogenetic and functional response of a sponge holobiont to thermal stress. *ISME J.* **7**, 991–1002 (2013).
46. Harris, C. A. *et al.* Principles of sound ecotoxicology. *Environ. Sci. Technol.* **48**, 3100–3111 (2014).
47. Cheshire, A. *et al.* Preliminary study of the distribution and photophysiology of the temperate phototrophic sponge *Cymbastela* sp. from South Australia. *Mar. Freshw. Res.* **46**, 1211–1216 (1995).
48. Ridley, C. P., Faulkner, D. & Haygood, M. G. Investigation of *Oscillatoria spongelliae*-dominated bacterial communities in four didymoceratid sponges. *Appl. Environ. Microbiol.* **71**, 7366–75 (2005).
49. Anthony, K. R. N., Ridd, P. V., Orpin, A. R., Larcombe, P. & Lough, J. Temporal variation of light availability in coastal benthic habitats: Effects of clouds, turbidity and tides. *Limnol. Oceanogr.* **49**, 2201–2211 (2004).
50. Trussell, G. C., Lesser, M. P., Patterson, M. R. & Genovese, S. J. Depth-specific differences in growth of the reef sponge, *Callyspongia vaginalis*: role of bottom-up effects. **323**, 149–158 (2006).
51. Schneider, C. A., Rasband, W. S. & Eliceiri, K. W. NIH Image to ImageJ: 25 years of image analysis. *Nat. Methods* **9**, 671–675 (2012).
52. Lichtenthaler, H. Chlorophylls and Carotenoids—Pigments of photosynthetic biomembranes. *Methods Enzymol.* **148**, 350–382 (1987).
53. Ritchie, R. Universal chlorophyll equations for estimating chlorophylls a, b, c, and d and total chlorophylls in natural assemblages of photosynthetic organisms using acetone, methanol, or ethanol solvents. *Photosynthetica* **46**, 115–126 (2008).
54. Uthicke, S., Vogel, N., Doyle, J., Schmidt, C. & Humphrey, C. Interactive effects of climate change and eutrophication on the dinoflagellate-bearing benthic foraminifer *Marginopora vertebralis*. *Coral Reefs* **31**, 401–414 (2012).
55. Webster, N. S. *et al.* Deep sequencing reveals exceptional diversity and modes of transmission for bacterial sponge symbionts. *Environ. Microbiol.* **12**, 2070–82 (2010).
56. Schloss, P. D. *et al.* Introducing mothur: Open-Source, Platform-Independent, Community-Supported Software for Describing and Comparing Microbial Communities. *Appl. Environ. Microbiol.* **75**, 7537–7541 (2009).
57. Luter, H. M. *et al.* Biogeographic variation in the microbiome of the ecologically important sponge, *Carteriospongia foliascens*. *PeerJ* **3**, e1435 (2015).
58. Edgar, R. C., Haas, B. J., Clemente, J. C., Quince, C. & Knight, R. UCHIME improves sensitivity and speed of chimera detection. *Bioinformatics* **27**, 2194–2200 (2011).
59. Cole, J. R. *et al.* Ribosomal Database Project: data and tools for high throughput rRNA analysis. *Nucleic Acids Res.* **42**, D633–D642 (2014).
60. DeSantis, T. Z. *et al.* Greengenes, a Chimera-Checked 16S rRNA Gene Database and Workbench Compatible with ARB. *Appl. Environ. Microbiol.* **72**, 5069–5072 (2006).
61. Shannon, P. *et al.* Cytoscape: A Software Environment for Integrated Models of Biomolecular Interaction Networks. *Genome Res.* **13**, 2498–2504 (2003).

Acknowledgements

This research was funded by the Western Australian Marine Science Institution (WAMSI) as part of the WAMSI Dredging Science Node, and made possible through investment from Chevron Australia, Woodside Energy Limited, BHP Billiton as environmental offsets and by co-investment from the WAMSI Joint Venture partners. The commercial entities had no role in data analysis, decision to publish, or preparation of the manuscript. NSW was funded through an Australian Research Council Future Fellowship FT120100480. The views expressed herein are those of the authors and not necessarily those of WAMSI. All collections were performed under Great Barrier Reef Marine Park Regulations 1983 (Commonwealth) and Marine Parks regulations 2006 (Queensland) Permit G12/35236.1 and Permit G13/35758.1. We are thankful to staff at the AIMS National Sea Simulator for their help during experiment set up. Dr. C. Schönberg and Dr. J. Fromont contributed to the species identification. Dr. M. Abdul Wahab commented on a previous version of the manuscript. Sequence data was obtained through support from the Earth Microbiome Project and Dr. H. Luter, Dr. L. Moitinho-Silva, Dr. P. Laffy, C. Astudillo and G. Millar provided useful advice on the microbial community data analyses and use of the HPC.

Author Contributions

M.C.P., B.S., A.D., R.J. and N.S.W. designed the experiment. M.C.P. and B.S. undertook the experiment. M.C.P., B.S. and J.D. undertook laboratory analyses. M.C.P. and B.S. analysed the data. M.C.P., B.S., A.D., R.J. and N.S.W. wrote the manuscript. All authors reviewed the manuscript.

Additional Information

Supplementary information accompanies this paper at <http://www.nature.com/srep>

Competing financial interests: The authors declare no competing financial interests.

How to cite this article: Pineda, M.-C. *et al.* Effects of light attenuation on the sponge holobiont- implications for dredging management. *Sci. Rep.* **6**, 39038; doi: 10.1038/srep39038 (2016).

Publisher's note: Springer Nature remains neutral with regard to jurisdictional claims in published maps and institutional affiliations.



This work is licensed under a Creative Commons Attribution 4.0 International License. The images or other third party material in this article are included in the article's Creative Commons license, unless indicated otherwise in the credit line; if the material is not included under the Creative Commons license, users will need to obtain permission from the license holder to reproduce the material. To view a copy of this license, visit <http://creativecommons.org/licenses/by/4.0/>

© The Author(s) 2016

Supporting Online Material

Effects of light attenuation on the sponge holobiont- implications for dredging management

Mari-Carmen Pineda^{1,2*}, Brian Strehlow^{1,2,3}, Alan Duckworth^{1,2}, Jason Doyle¹, Ross Jones^{1,2} and Nicole S. Webster^{1,2}

¹*Australian Institute of Marine Science, Townsville, QLD, and Perth, WA, Australia*

²*Western Australian Marine Science Institution, Perth, WA, Australia*

³*School of Plant Biology and Centre for Microscopy Characterisation and Analysis: University of Western Australia, Perth, WA, Australia*

*Corresponding author:

Mari-Carmen Pineda

Australian Institute of Marine Science, PMB3, Townsville, QLD, 4810, Australia

E-mail: mcarmen.pineda@gmail.com.

Tel.: +61 7 4753 4522, fax: +61 7 4772 5852

Figure S1. Sponges under different light treatments. Sponge health at the end of the 28 d exposure period, in the phototrophic species (A) *C. orientalis*, (B) *C. foliascens* and (C) *C. coralliophila*, and in the heterotrophic species (D) *S. flabelliformis* and (E) *I. basta*. From left to right, representative sponges exposed to the 0, 0.8, 3.2, 8.1 mol photons $m^{-2} d^{-1}$ treatments and natural light (NL, 3.2–6.5 mol photons $m^{-2} d^{-1}$).



Figure S2. Area change of all sponges. Percentage of area change (mean \pm SE) for all species and treatments (0, 0.8, 3.2, 8.1 mol photons $m^{-2} d^{-1}$ and natural light (3.2–6.5 mol photons $m^{-2} d^{-1}$)) during the 28 d exposure period and 14 d observational period.

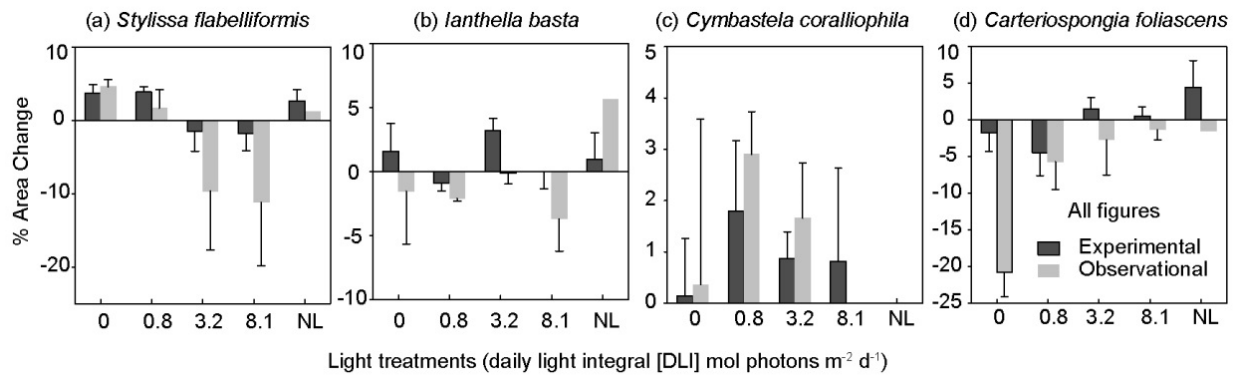


Figure S3. Non-metric Multi-Dimensional Scaling plots on pigments data. nMDS of all photopigments retrieved by A) Spectrophotometry (Chl a, Chl b, Chl c, Chl d, Total Chl and Carotenoids) and B) UPLC (Total Chl a, Total Chl, Total Xanthophylls, Total Carotenoids, Chl c2, Peridinin, Neoxanthin, Violaxanthin, Diadinoxanthin, Dinoxanthin, Zeaxanthin, Chl b, Chl a, Chl a epimer, Pheophytin a, α -carotene and β -carotene). Symbols correspond to species: triangles for *C. coralliophila*, inverted triangles for *C. foliascens*, and squares for *C. orientalis*. Colours represent light treatments: grey for low light intensity treatment (0.8 mol photons $m^{-2} d^{-1}$), black for 0 mol photons $m^{-2} d^{-1}$ and white for natural light control.



Figure S4. Non-metric Multi-Dimensional Scaling plots on microbial OTU data. nMDS of microbial communities for all 5 sponge species and the environmental control (seawater).

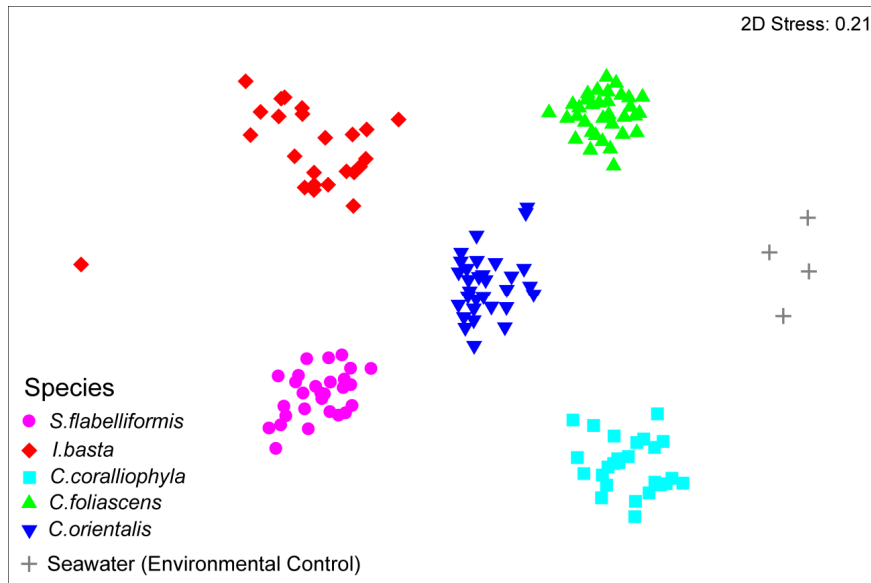


Table S1. SIMPER results on *C. foliascens* and *C. orientalis*. Similarity Percentage Analysis (SIMPER) for 30 most significant OTUs driving differences between Natural Light and the 0 mol photons m⁻² d⁻¹ light treatment at 28d and on the species that showed significant differences according to the PERMANOVA analysis (Table 3C).

OTU	Average relative abundance (%)		Contribution (%)	Taxonomic ID
	Natural Light	0		
<i>C. foliascens</i>				
Otu000006	5.39	0.04	6.62	Cyanobacteria
Otu000013	3.7	1.76	2.4	Gammaproteobacteria
Otu000033	0	1.33	1.66	Alphaproteobacteria
Otu000015	1.7	3	1.61	Gammaproteobacteria
Otu000023	1.01	2.05	1.38	Bacteroidetes
Otu000019	2.12	1.84	1.36	Alphaproteobacteria
Otu000034	1.25	1.84	1.34	Gammaproteobacteria
Otu000032	0.96	2.01	1.32	Gammaproteobacteria
Otu000016	1.29	2.04	1.09	Bacteroidetes
Otu000026	1.58	2.37	1.09	Bacteroidetes
Otu000017	2.06	2.86	1.01	Alphaproteobacteria
Otu000059	0.29	0.75	0.81	Alphaproteobacteria
Otu000007	4.28	4.36	0.76	Bacteroidetes
Otu000050	0.57	0.75	0.74	Gammaproteobacteria
Otu000064	0.81	1.25	0.66	Alphaproteobacteria
Otu000048	0.68	0.82	0.63	Gammaproteobacteria
Otu000070	0	0.51	0.63	Alphaproteobacteria
Otu000029	1.65	2.14	0.61	Gammaproteobacteria
Otu000204	0.04	0.53	0.61	Gammaproteobacteria
Otu000073	0.37	0.36	0.6	Gammaproteobacteria
Otu000185	0.04	0.51	0.58	Deltaproteobacteria
Otu000173	0.44	0	0.55	Cyanobacteria
Otu000113	0.17	0.59	0.51	Chloroflexi
Otu000047	0	0.41	0.51	Bacteroidetes
Otu000156	0.11	0.43	0.49	Gammaproteobacteria
Otu000170	0.39	0	0.48	Gammaproteobacteria
Otu000209	0.07	0.45	0.47	Gammaproteobacteria
Otu000077	0.24	0.28	0.44	Alphaproteobacteria
Otu000176	0.18	0.5	0.4	Gammaproteobacteria
Otu000090	0.78	0.47	0.4	Gammaproteobacteria
<i>C. orientalis</i>				
Otu000070	0.08	1.24	1.28	Alphaproteobacteria
Otu000061	1.04	0	1.07	Cyanobacteria
Otu000075	0.14	1.12	1.03	Gammaproteobacteria
Otu000088	1.06	0.11	1.02	Bacteroidetes
Otu000078	0.18	0.99	0.87	Gammaproteobacteria
Otu000083	0.1	0.88	0.84	Gammaproteobacteria
Otu000058	0.57	1.33	0.81	Unclassified Bacteria
Otu000001	9.08	8.42	0.78	Alphaproteobacteria
Otu000104	0.7	0	0.76	Bacteroidetes
Otu000285	0.69	0	0.74	SBR1093
Otu000067	0.11	0.65	0.65	Alphaproteobacteria
Otu000107	0.07	0.56	0.65	Alphaproteobacteria
Otu000124	0	0.58	0.62	Alphaproteobacteria
Otu000253	0.57	0	0.57	Alphaproteobacteria
Otu000110	0.59	0.18	0.57	Cyanobacteria

Otu000141	0.5	0	0.52	SBR1093
Otu000335	0.49	0	0.5	Gammaproteobacteria
Otu000123	0.04	0.47	0.45	Alphaproteobacteria
Otu000091	0.17	0.57	0.43	Gammaproteobacteria
Otu000159	0.45	0.04	0.42	Alphaproteobacteria
Otu000339	0.06	0.39	0.38	Gammaproteobacteria
Otu000286	0	0.41	0.37	Crenarchaeota
Otu000259	0.35	0	0.37	Alphaproteobacteria
Otu000261	0	0.36	0.37	Chlamydiae
Otu000276	0.35	0	0.37	Alphaproteobacteria
Otu000445	0.33	0.1	0.37	Chloroflexi
Otu000273	0.04	0.37	0.36	Chloroflexi
Otu000115	0.06	0.38	0.36	Alphaproteobacteria
Otu000593	0.27	0.19	0.36	Deltaproteobacteria
Otu000079	0.36	0.04	0.35	Alphaproteobacteria

Table S2. Sponge sampling details. List of species, morphologies, nutritional mode and sampling location.

Species Name (Author)	Functional Morphology	Primary Nutritional Mode	Sampling Location
<i>Cymbastela coralliophila</i> (Hooper & Bergquist, 1992)	Encrusting (thick) Cup (table)	Phototrophic ¹	Davies Reef (central Offshore GBR) S 18°49.354', E 147°38.253'
<i>Carteriospongia foliascens</i> (Pallas, 1766)	Cup (wide cup)	Phototrophic ²	Fantome Island (Palm Islands) S 18°41.028', E 146° 30.706'
<i>Cliona orientalis</i> (Thiele, 1900)	Encrusting (bioeroding)	Phototrophic ³	Pelorus Island (Palm Islands) S 18°32.903', E 146° 29.172'
<i>Stylissa flabelliformis</i> (Hentschel, 1912)	Erect (laminar)	Heterotrophic ⁴	Pelorus Island (Palm Islands) S 18°32.903' E 146°9.172'
<i>Ianthella basta</i> (Pallas, 1976)	Erect (laminar)	Heterotrophic ⁵	Davies Reef S 18°49.354' 147°38.253'

References

- Cheshire, A. *et al.* Preliminary study of the distribution and photophysiology of the temperate phototrophic sponge *Cymbastela* sp. from South Australia. *Mar. Freshw. Res.* **46**, 1211–1216 (1995).
- Ridley, C. P., Faulkner, D. & Haygood, M. G. Investigation of Oscillatoria spongeliae-dominated bacterial communities in four dictyoceratid sponges. *Appl. Environ. Microbiol.* **71**, 7366–75 (2005).
- Schönberg, C. H. L. & Loh, W. K. W. Molecular identity of the unique symbiotic dinoflagellates found in the bioeroding demosponge *Cliona orientalis*. *Mar. Ecol. Prog. Ser.* **299**, 157–166 (2005).
- Pineda, M. C., Duckworth, A. & Webster, N. Appearance matters: sedimentation effects on different sponge morphologies. *J. Mar. Biol. Assoc. United Kingdom* **96**, 481–492 (2016).
- Cheshire, A. C. A., Wilkinson, C. R. C., Seddon, S. & Westphalen, G. Bathymetric and seasonal changes in photosynthesis and respiration of the phototrophic sponge *Phyllospongia lamellosa* in comparison with respiration by the heterotrophic sponge *Ianthella basta* on Davies Reef, Great Barrier Reef. *Mar. Freshw. Res.* **48**, 589–599 (1997).

SCIENTIFIC REPORTS

OPEN

Effects of suspended sediments on the sponge holobiont with implications for dredging management

Mari-Carmen Pineda^{1,2}, Brian Strehlow^{1,2,3}, Miriam Sternel⁴, Alan Duckworth^{1,2}, Ross Jones^{1,2} & Nicole S. Webster^{1,2}

Dredging can cause high suspended sediment concentrations (SSC) in the water column, posing a hazard to filter feeding organisms like sponges as sediment may clog their aquiferous systems and reduce feeding. In order to provide pressure–response values for sponges to SSC and tease apart the cause:effect pathways of dredging pressures, five heterotrophic and phototrophic species were experimentally exposed to a range of dredging-relevant SSC of up to 100 mg L⁻¹, with light compensation across treatments to ensure that SSC was the primary physical parameter. This study shows that some sponge species exposed to high SSC (≥ 23 mg L⁻¹) for extended periods (28 d) have lower survival, increased necrosis and depletion of energy reserves. In contrast, SSC of ≤ 10 mg L⁻¹ caused few, if any, negative effects and is thus suggested as a prudent sub-lethal threshold for sponges. Microbial communities did not change significantly among SSC treatments, although a nutritional shift from mixotrophy towards increased phototrophy was detected for some sponge species exposed to high SSC. Importantly however, it is expected that the combined effect of SSC with low light availability and sediment smothering as occurs during dredging operations will increase the negative effects on sponges.

Dredging is an essential part of all port operations and the need for dredging is likely to increase with the current trend towards larger ships with deeper draft requirements¹. World population growth and the related energy demands have also resulted in a new market for dredging associated with expanding port infrastructure to exploit remotely located fossil fuels deposits (CEDA 2013). In recent years there has been a very high demand for this type of dredging in tropical NW Australia associated with a resources boom and a burgeoning liquefied natural gas (LNG) industry^{2,3}.

Capital and maintenance dredging, and a suite of dredging-related activities such as bed levelling, trench digging for gas pipe lines, and especially dredge material placement, releases sediment into the water column. The cloudy (turbid) plumes that are generated can drift onto nearby benthic habitats, posing risks to ecologically important marine ecosystems such as coral reefs, seagrass meadows and sponge gardens^{4–8}. The effect of suspended sediment on sponges in NW Australia is particularly interesting, because macrobenthic filter feeders can dominate in many locations^{9,10}. The response of sponges to the increased turbidity is not well known¹¹, and this is a significant challenge to their effective management¹².

Sponges are sessile filter-feeding organisms playing important roles in many marine ecosystems, including substrate consolidation, habitat provision, seawater filtration, and benthic-pelagic energy transfer^{11,13}. They obtain energy heterotrophically by filtering seawater through an aquiferous system or internal canal network^{14,15}. Many sponges also obtain energy autotrophically from photosymbionts, of which *Cyanobacteria* are the most ubiquitous^{16–20}, encompassing sponge-specific groups such as ‘*Candidatus Synechococcus spongiarium*’ and *Oscillatoria spongeliae*^{21–24}. Dinoflagellates of the genus *Symbiodinium* are also known to be photosymbionts of sponges,

¹Australian Institute of Marine Science (AIMS), Townsville, QLD and Perth, WA, Australia. ²Western Australian Marine Science Institution, Perth, WA, Australia. ³Centre for Microscopy Characterisation and Analysis, School of Plant Biology and Oceans Institute, University of Western Australia, Crawley, WA, Australia. ⁴University of Bremen, Bremen, Germany. Correspondence and requests for materials should be addressed to M.-C.P. (email: mcarmen.pineda@gmail.com)

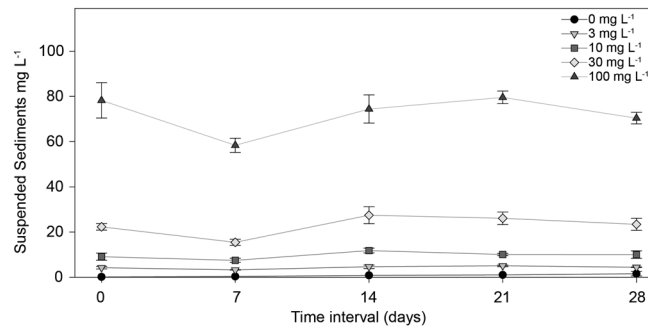


Figure 1. SSC during the experiment. (a) Means (\pm SE) SSCs (mg L^{-1}) at each treatment, according to gravimetric measures.

especially in bioeroding sponge species^{19, 25, 26}. In some tropical sponge species the photosymbionts can provide >50% of the energy requirements of the host^{18, 27}, and the diverse symbiotic consortia can comprise up to 40% of the sponge volume²⁸. Sponge symbionts tend to be highly host specific, but are generally stable across broad geographic and environmental gradients²⁹, with the stable host-microbe consortium often referred to as the ‘sponge holobiont’²⁸.

Depending on their degree of nutritional dependence from symbiont primary production, the sponge holobiont can be described as either ‘phototrophic’, ‘mixotrophic’ or ‘heterotrophic’. Some species exhibit considerable flexibility in their feeding strategy and are able to alter their nutritional mode depending on prevailing conditions^{27, 30, 31}. The different modes of nutrition have important implications for understanding the environmental effects of dredging activities on sponges. Due to their filter feeding activity, sponges may be affected by elevated suspended sediment concentrations (SSCs) and long term exposure to high SSCs can lead to clogging of their aquiferous systems, reducing the flow of oxygenated seawater to the sponge mesohyl and compromising heterotrophic feeding³². Some sponges exhibit short term responses to high turbidity such as temporarily closing or reducing the size of their incurrent openings (ostia) and arresting pumping (filtering) activity^{33–36}. However, reduced pumping activity has flow-on consequences for host energetics, health and reproductive output^{32, 37–39}. Since some sponges also rely on photoautotrophy for nutrition, they may be affected by the pronounced reduction in benthic light availability that occurs in dredging plumes^{4, 40, 41}. Periods of low light levels associated with dredging can cause photoacclimation of the photosymbionts^{32, 42, 43}, but extended periods of low light can also result in dissociation of the holobiont (bleaching) and subsequent mortality in some phototrophic species⁴⁴.

Understanding the effects of turbidity on sponges would facilitate development of water quality thresholds (or trigger values) that could be used to alert dredging proponents of conditions that could, if continued, cause environmental harm. Depending upon permit requirements, the option could then be to modify the dredging operations i.e. changing the rate or location of dredging, and hence avoid or minimize impacts. Developing thresholds is predicated upon identifying key cause-effect pathways and determination of dose–response relationships which is technically challenging. Close to dredging activities, sponges will be exposed to both high SSCs in combination with low light conditions (caused by the water turbidity), and may also be simultaneously exposed to high levels of sedimentation and possibly smothering. There are, therefore, many potential cause-effect pathways. In order to avoid conflation of these in a single experiment (see ref. 4), in this study we examine the response of sponges to a range of suspended sediments but kept light uniform across treatments. Experiments were conducted over 28 d, with a similar suite of 3 heterotrophic and 2 phototrophic sponges as used in previous studies assessing the effects of sedimentation³⁸ and light⁴⁴.

Results

Physical parameters. The nominal SSCs (0, 3, 10, 30 and 100 mg L^{-1}) were largely constant over time and varied significantly among treatments (ANOVA: $P < 0.001$; Fig. 1). Gravimetric analysis of SSCs indicated the tanks containing sediment ($0.4 \pm 0.04 \text{ mg L}^{-1}$, $4.3 \pm 0.2 \text{ mg L}^{-1}$, $9.7 \pm 0.6 \text{ mg L}^{-1}$, $23 \pm 1.2 \text{ mg L}^{-1}$, $73 \pm 2.8 \text{ mg L}^{-1}$, mean \pm SE) were generally slightly lower than the desired concentrations, especially for the two highest treatments (Fig. 1). For simplicity, we refer to the nominal SSCs throughout the manuscript.

Sponge growth, necrosis and mortality. Most sponges appeared visibly healthy at the end of the experiment, with the exception of all *Carteriospongia foliascens*, a few individuals of *Coscinoderma matthewsi*, and *Cliona orientalis* exposed to 100 mg L^{-1} . No visible effects were observed in *Cymbastela coralliophila* and *Stylissa flabelliformis* in any treatment. Percentage growth and relative growth rates based on thickness measurements before and after the 28 d sediment exposure and observational period, were negative for most sponges exposed to SSC of $\geq 30 \text{ mg L}^{-1}$; however with the exception of *Cliona orientalis*, these negative growth rates were not significantly different from control groups (Fig. 2a, Table 1a). The bioeroding sponge *Cliona orientalis* grew during the sediment exposure and recovery periods in all treatments except at the highest SSC of 100 mg L^{-1} (Fig. 2a, Table 1a). The massive sponge *Coscinoderma matthewsi* shrank when exposed to suspended sediments (3–100 mg L^{-1}) and only grew in the control treatment, although this growth was not statistically significant. The erect sponge *Stylissa flabelliformis* shrank in all treatments with tissue regression increasing with increasing SSC and no growth evident during the observational period (Fig. 2a, Table 1a). Sponge growth based on surface area

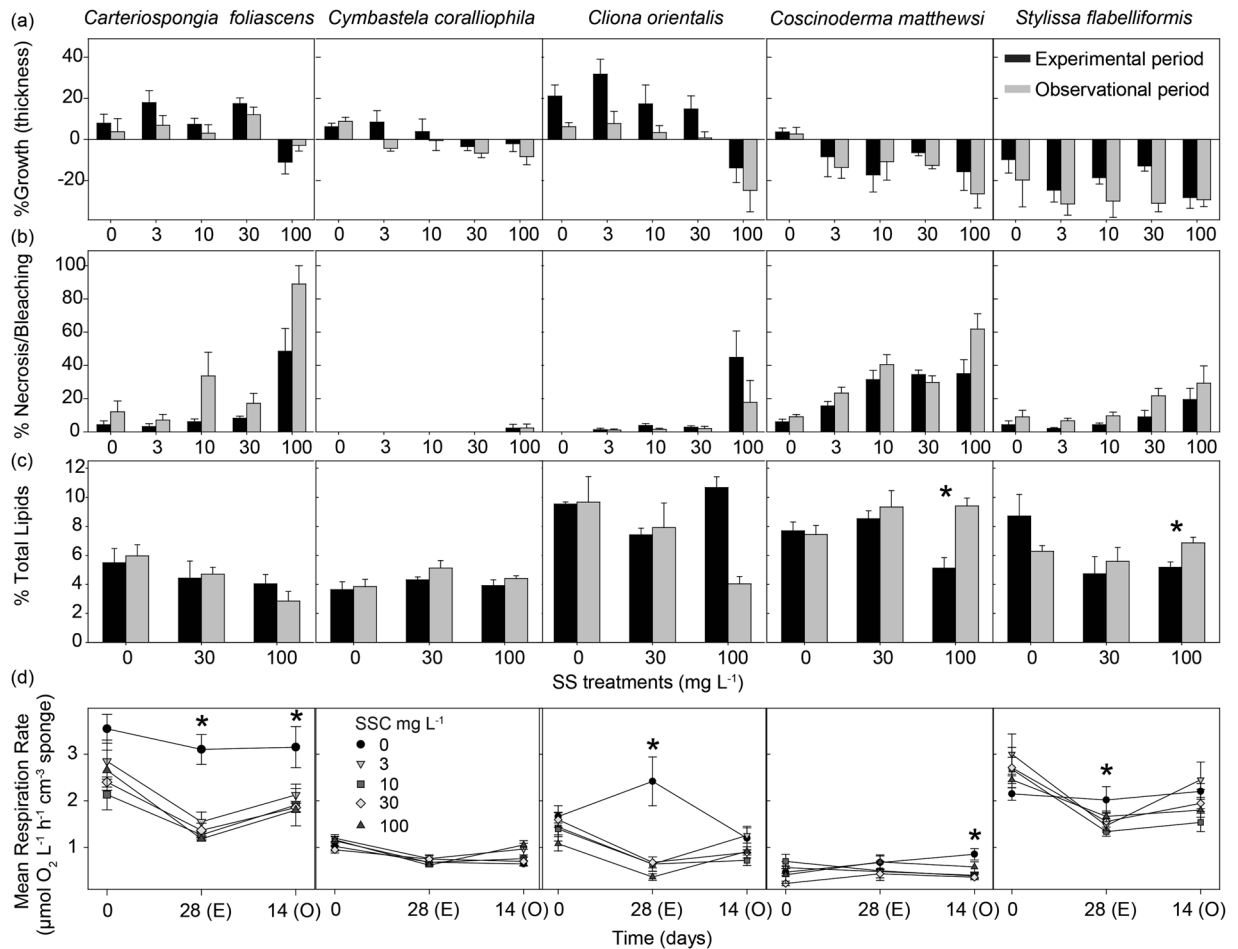


Figure 2. Physiological responses of sponges to elevated SSCs. **(a)** Percentage of growth (mean \pm SE) (based on sponge tissue thickness), **(b)** Percentage of necrotic or bleached tissue, **(c)** Percentage of sponge biomass comprised of lipids, and **(d)** Mean respiration rates ($\mu\text{mol O}_2 \text{ L}^{-1} \text{ h}^{-1} \text{ cm}^{-3}$ sponge), for all species and SSCs (0, 3, 10, 30 and 100 mg L^{-1}) after the 28 d experimental period (E), and 14 d observational period (O) (mean \pm SE). Asterisks show statistically significant differences between the experimental and observational phase in a–c and between treatments in d (t-tests: $P < 0.05$).

(SA) for all species showed similar results, generally shrinking in the higher SSC treatments (Supplementary Fig. S1, Table S1).

The percentage of dead (i.e. partial mortality or necrosis) and bleached (discoloured) tissue also increased significantly with higher SSC in all species except for *Cymbastela coralliophila* and *Stylissa flabelliformis* (Fig. 2b, Table 1b). The highest percentages of necrosed tissue were observed among individuals of *Carteriospongia foliascens* and *Coscinoderma matthewsi* exposed to the highest SSC, reaching 80 and 60% of sponge tissue respectively by the end of the observational period. *Carteriospongia foliascens* showed signs of necrosis from the second week of sediment exposure to 100 mg L^{-1} , although some necrosis was also observed in lower treatments by the end of the experiment (Fig. 2b). In terms of total mortality, 90% of *Carteriospongia foliascens* died in the 100 mg L^{-1} treatment by the end of the observational period and 20% had died in each of the 30 and 10 mg L^{-1} treatments (Supplementary Fig. S2). The bioeroding sponge *Cliona orientalis* also showed signs of stress, as evidenced by significant bleaching, within the 100 mg L^{-1} treatment, although significant recovery of pigmentation occurred during the observational phase (ANOVA: $P < 0.05$). *Coscinoderma matthewsi* also exhibited considerable necrosis at high SSC including 20% total mortality in the 100 mg L^{-1} treatment by the end of the observational period (Supplementary Fig. S2). No mortality occurred in *Cymbastela coralliophila*, *Cliona orientalis* and *Stylissa flabelliformis*.

Mortality data for *Carteriospongia foliascens* was fitted to nonlinear regression curves to calculate the lethal concentration (LC) at which 50% (LC_{50}) and 10% (LC_{10}) of the population died. Nonlinear regression of the dose–response curve ($R^2 = 0.8675$, $\text{AICc} = 85.23$) met assumptions of normality and homoscedasticity and there was no evidence for a lack of fit in the replicates test ($P = 0.694$). After the 28 d exposure period, the LC_{50} (and 95% confidence intervals range) for mortality in *Carteriospongia foliascens* was 40.6 mg L^{-1} (range: $28.9\text{--}57.0 \text{ mg L}^{-1}$) and the LC_{10} was 21.5 mg L^{-1} (range: $13.1\text{--}35.2 \text{ mg L}^{-1}$). Mortality data from *Coscinoderma matthewsi* did not meet model assumptions and LC values could not be calculated.

Source	df	<i>Carteriospongia foliascens</i>		<i>Cymbastela coralliophila</i>		<i>Cliona orientalis</i>		<i>Coscinoderma matthewsi</i>		<i>Stylissa flabelliformis</i>	
		F	P	F	P	F	P	F	P	F	P
(A) Relative growth rate (thickness)											
Experimental phase											
Treatment	4	3.337	0.109	1.47	0.337	5.81	0.04	0.767	0.589	1.752	0.275
Error	20										
Tukey						0,3,10,30 > 100					
Observational phase											
Treatment	4	2.761	0.148	4.319	0.07	3.94	0.08	1.887	0.251	0.251	0.898
Error	20										
(B) Percentage of necrosis and bleaching											
Experimental phase											
Treatment	4	9.12	<0.0001	0.8	0.574	7.25	0.02	7.07	0.02	3.64	0.09
Error	20										
Tukey		0,3,10,30 < 100				0,3,10,30 < 100		0 < 3,10,30,100			
Observational phase											
Treatment	4	9.80	0.01	0.8	0.573	1.598	0.306	12.9	<0.0001	3.14	0.12
Error	20										
Tukey		0,3,10,30 < 100						0,3 < 10,100			
(C) Percentage of sponge biomass comprised of lipids											
Experimental phase											
Treatment	2	0.612	0.598	0.733	0.550	10.95	0.04	4.837	0.115	3.783	0.151
Error	12										
Tukey						0,100 > 30					
Observational phase											
Treatment	2	5.255	0.105	2.220	0.256	7.212	0.071	1.951	0.287	0.998	0.465
Error	12										
(D) Respiration Rates											
Treatment	4	6.920	0.0285	1.832	0.2605	2.076	0.2218	1.344	0.3701	0.7203	0.613
Time	2	17.177	<0.001	63.407	<0.001	16.51	<0.001	1.477	0.2406	38.153	<0.001
Treatm. x Time	8	0.6266	0.7494	3.581	0.00323	8.490	<0.001	4.118	0.0012	3.165	0.007
Error	40										
Tukey											
Treatment		0 > 10,30									
Time				T0 > E; T0 > O		T0 > E < O					
Treatm. within E						0 > 3,10,30,100					
Time within 0				T0 > E,O		T0 < E > O		T0 < O			
Time within 3				T0 > O > E		T0 > E,O				T0 > E < O	
Time within 10				T0 > E,O		T0 > E,O		T0 > O		T0 > E,O	
Time within 30				T0 > E,O		T0 > E,O				T0 > E,O	
Time within 100				T0 > E < O		T0 > E,O		T0 < E		T0 > E,O	

Table 1. ANOVA tables and summaries of linear mixed models testing the effects of different SSCs on the physiological responses of sponges. (A) Growth rate based on thickness measures, (B) Percentage of necrotic and bleached tissue, (C) Percentage of sponge biomass comprised of lipids, (D) Mean respiration rates, for each species separately, at the end of experimental phase (E) and observational phase (O). Tukey tests were performed for significant pairwise multiple comparisons. (SSC: 0, 3, 10, 30 and 100 mg L⁻¹).

Lipids. For all species, total lipid content was similar between time of sample collection and the start of the sediment dosing, as well as during the experiment for sponges exposed to no suspended sediment (ANOVA: $P > 0.05$). With the exception of *Cymbastela coralliophila*, all species had lower lipid content when exposed to SSCs ≥ 30 mg L⁻¹, although this was only statistically significant for *Cliona orientalis* at the end of the 28 d sediment exposure (Fig. 2c, Table 1c). Unexpectedly, *Cliona orientalis* had a higher lipid content in the 100 mg L⁻¹ treatment than in the 30 mg L⁻¹ treatment and while lipid content appeared to decrease in samples from the 100 mg L⁻¹ treatment during the observational phase, this decrease was not significant. *Coscinoderma matthewsi* and *Stylissa flabelliformis* increased their lipid content during the observational period (Fig. 2c).

Respiration rates. Respiration rates did not significantly differ among treatments at day = 0 for any species (Fig. 2d, Table 1d). However, after 28 days, respiration rates were significantly lower for *Carteriospongia*

Source	df	<i>Carteriospongia foliascens</i>		<i>Cymbastela coralliophila</i>		<i>Cliona orientalis</i>	
		F	P	F	P	F	P
(A) Maximum quantum yield							
Treatment	4	1.238	0.4016	0.380	0.8154	2.912	0.1356
Time	6	3.410	0.0040	2.949	0.0101	2.523	0.0247
Treatm. × Time	18	1.468	0.0646	1.451	0.0985	2.582	<0.001
Error	96						
Tukey							
Time						Day 0 ≠ Day 14; O7 ≠ Day 7	
Time within 10 mg L ⁻¹						Day 0 ≠ Day 21	
Time within 100 mg L ⁻¹						Day 7 ≠ Day 0, 21, 28	
Treatment within Day 21(E)						0, 10 ≠ 100	
Treatment within Day 14(O)						0 ≠ 100	
(B) Chl a							
Experimental phase							
Treatment	4	5.400	0.0464	0.8582	0.5462	2.473	0.1738
Error	20						
Tukey		3, 10 > 100					
Observational phase							
Treatment	4	2.225	0.2018	2.238	0.2002	0.5241	0.7245
Error	20						
(C) PERMANOVA of all pigment data							
Treatment	4	4.738	0.001	1.698	0.078	2.383	0.021
Time(Treatment)	5	2.235	0.019	1.305	0.207	1.789	0.082
Error	40						
Pair-wise Tests		0 ≠ 3, 10, 30 ≠ 100				3 ≠ 10, 30, 100	

Table 2. ANOVA tables and summaries of linear mixed models on the effects of elevated SSCs on photosymbionts. (A) Effects of treatment and time on maximum quantum yield throughout the experiment (B) Effects of treatment on Chl a concentrations at the end of the experimental (E) and observational (O) periods, and (C) Two-way PERMANOVA of all pigment data (Chl a, b, c, d, Total Chlorophyll and Carotenoids) with SSC and Time as factors, for the three phototrophic species (SSC: 0, 3, 10, 30 and 100 mg L⁻¹). In a-c, Tukey tests were performed for significant pairwise multiple comparisons.

foliascens and *Cliona orientalis* exposed to suspended sediment than conspecifics in the 0 mg L⁻¹ treatment (ANOVA, $P < 0.05$; Fig. 2d). In *Carteriospongia foliascens*, respiration rates were lower than controls in the 10 and 30 mg L⁻¹ treatments and the absence of a significant difference at 100 mg L⁻¹ is likely due to the high mortality of *Carteriospongia foliascens* in this treatment (which precluded *post hoc* analysis, Table 1d). No interactive effect of time and treatment was observed for *Carteriospongia foliascens*. Respiration in *Cliona orientalis* in the 0 mg L⁻¹ treatment increased significantly between day 0 and the end of the experimental phase, returning to pre-treatment levels in the observational period. Although this response in control sponges was unexpected, respiration rates were still observed to decrease for *Cliona orientalis* in all sediment treatments over time. Furthermore, respiration rates were significantly lower at the end of the observational phase than at day 0 within each sediment treatment, indicating that a longer recovery period was required for *Cliona orientalis* to return to pre-exposure respiration rates (Fig. 2d, Table 1d). A similar recovery capacity was observed in *Cymbastela coralliophila*, although increased respiration during the observational phase was only detected in the 3 mg L⁻¹ treatment. Respiration rates in the massive species *Coscinoderma matthewsi* were significantly increased in sponges in the 100 mg L⁻¹ treatment. *Coscinoderma matthewsi* was the only species to exhibit an increased respiration rate on exposure to SSC. Finally, respiration rates in *Stylissa flabelliformis* were not significantly different among treatments, although when looking within each sampling time individually, a significant decrease at the end of the 28 d was detected for all treatments exposed to sediments, with recovery only evident in the sponges exposed to the 3 mg L⁻¹ treatment (Fig. 2d, Table 2d).

Histology. Choanocyte chambers could only be accurately quantified in *Cliona orientalis*. While the number of choanocyte chambers at the end of the experimental period was 37.3 ± 11.6 and 9.7 ± 2.7 , (mean \pm SD) in sponges from the 0 mg L⁻¹ and 100 mg L⁻¹ treatments respectively, this difference was not statistically significant (t test: $P = 0.103$) (Supplementary Fig. S3).

Chlorophyll fluorescence. Overall, no significant differences in maximum quantum yield were observed between treatments for any of the phototrophic species hosting cyanobacterial symbionts, with minor fluctuations throughout the experiment and observational periods (Fig. 3a, Table 2a). For instance, lower quantum yields were measured from bleached *Carteriospongia foliascens* individuals on days 14 and 21, before they died,

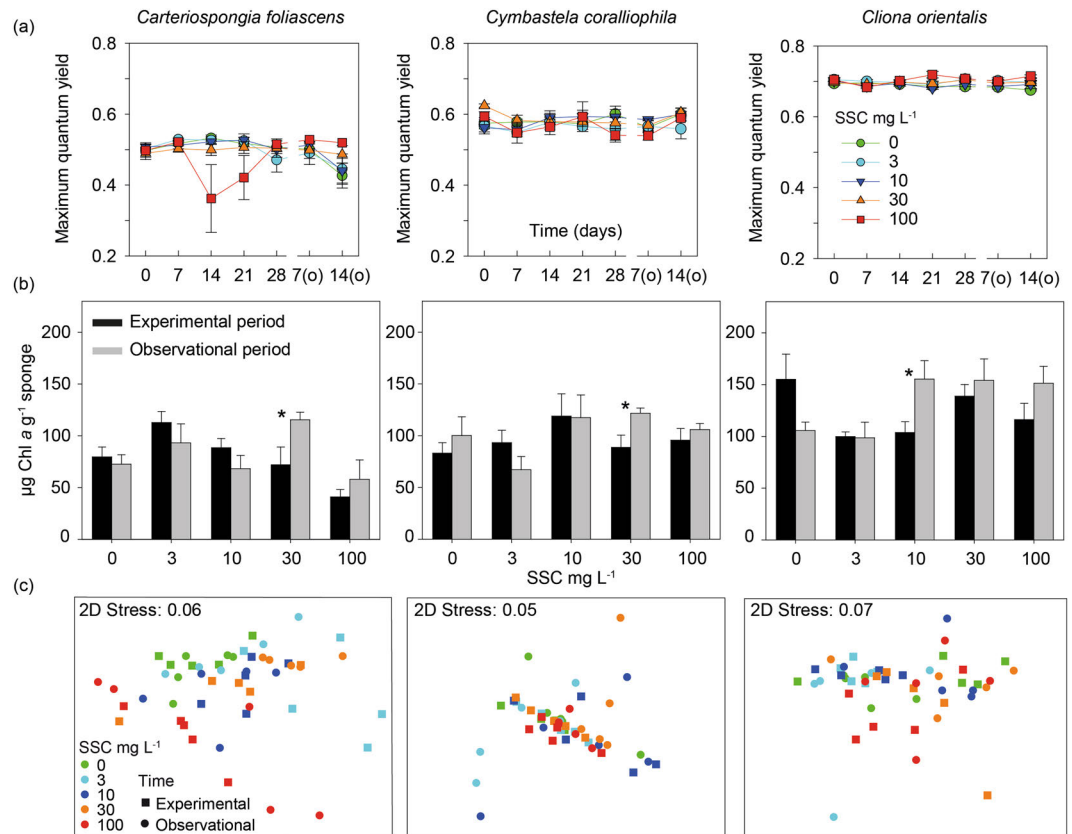


Figure 3. Response of the photosymbionts to elevated SSCs. **(a)** Mean values (\pm SE) of maximum quantum yield, **(b)** Mean values (\pm SE) of Chl *a*, and **(c)** Non-metric Multi-Dimensional Scaling (nMDS) of all photopigments retrieved by spectrophotometry, for the three phototrophic species and for all SSCs through the experimental phase and observational phase. Asterisks show statistically significant differences between the experimental and observational phase on b (t-tests: $P < 0.05$).

but while the decrease with time was significant, the interaction of time and treatment was not (Fig. 3a). In contrast, for *Cliona orientalis* which hosts *Symbiodinium* symbionts, the interaction term (treatment*time) was significant. Within the 10 mg L⁻¹ treatment, quantum yields decreased significantly on day 14 and were also lower on observation day 7 than on day 7 of the exposure (Fig. 3a, Table 2a). Within the 100 mg L⁻¹ treatment, quantum yields decreased after 7 days and then significantly increased after 21 days. After 21 days exposure, quantum yields in sponges from 0 and 10 mg L⁻¹ treatments were significantly different from sponges in the 100 mg L⁻¹ treatment. After 14 days of the observational period, quantum yields were significantly greater than in sponges exposed to 100 mg L⁻¹ for 21 days.

Pigment analysis. Chl *a*, was highly correlated with Total chlorophyll for *Carteriospongia foliascens*, *Cymbastela coralliophila* and *Cliona orientalis* ($R^2 > 0.85$, $P < 0.001$), so Chl *a* concentration was used as a proxy for total photosymbiont health (i.e. bleaching). Overall, concentrations of Chl *a* were stable throughout the experiment (Fig. 3b). Significant differences in Chl *a* among SSC treatments were only observed for *Carteriospongia foliascens* at the end of the 28 d sediment exposure period, with lower concentrations in individuals exposed to 100 mg L⁻¹ (Table 2b). However, a negative and significant correlation between Chl *a* and Chl *d* in both *Carteriospongia foliascens* and *Cymbastela coralliophila* ($R^2 = -0.254$, -0.265 , and $P = 0.046$, 0.037 , respectively), and an increase in Chl *d* in samples exposed to 100 mg L⁻¹ in both species (Supplementary Fig. S4), suggests an increase in some Chl *d*-containing Cyanobacteria under high SSCs. Chl *a* concentration in samples exposed to high SSCs returned to control levels following the observational period for all three species (Fig. 3b).

Non-metric Multi-Dimensional Scaling (nMDS) analysis of normalized data for all pigments retrieved by spectrophotometry (Chl *a*, Chl *b*, Chl *c*, Chl *d*, Total Chlorophyll and Carotenoids) showed no grouping according to SSC treatment (Fig. 3c). The only exception was *Carteriospongia foliascens* exposed to 100 mg L⁻¹, which grouped closer together, consistent with patterns observed for Chl *a*. PERMANOVA analysis confirmed significant differences between treatments in *Carteriospongia foliascens*, but also in *Cliona orientalis*, with subsequent pair-wise testing showing main differences between low and high SSCs (Table 2c).

Microbial community analysis. A total of 9,530,650 high quality 16S rRNA gene amplicon sequences were recovered from the 5 sponge species ($n = 200$ individual samples) and 9 seawater samples. Each sponge species maintained a unique microbial community (Table 3a, Fig. 4, see also Supplementary Fig. S5 and Table S2) that

Source	df	MS	Pseudo-F	P (perm)
A)				
Species	4	73421	34.606	0.0001
Time	3	4680	2.2062	0.0001
Species × Time	1	3344	1.5765	0.0001
Residuals	1	2121		
Pair-wise Tests				
CAR: F ≠ E (P < 0.005); CYM: F ≠ E, O (P < 0.005); CLI: F, T0 ≠ E ≠ O (P < 0.005); COS: F, T0 ≠ E, O (P < 0.05); STY: F, T0 ≠ E, O (P < 0.05)				
B)				
Source	1	26923	6.3132	0.0001
Residuals	1	4269		
C)				
<i>Carteriospongia foliascens</i>				
SS	2	3447	1.54	0.1604
Time (SS)	3	2239	1.0156	0.3855
Residuals	2	2204		
<i>Cymbastela coralliophila</i>				
SS	2	1474	1.0237	0.4304
Time (SS)	2	1427	1.1049	0.199
Residuals	1	1291		
<i>Cliona orientalis</i>				
SS	2	4458	1.0368	0.3809
Time (SS)	3	4302	1.7738	0.0001
Residuals	2	2425		
<i>Coscinoderma matthewsi</i>				
SS	2	3362	1.2413	0.0682
Time (SS)	3	2709	1.0787	0.1323
Residuals	2	2511		
<i>Stylissa flabelliformis</i>				
SS	2	1984	1.1119	0.2005
Time (SS)	3	1784	1.0984	0.1205
Residuals	2	1624		

Table 3. PERMANOVA analyses of the sponge-associated microbiome with (A) species and time as factors, (B) source as factor (sponge host vs. seawater) and, (C) SSC and time (nested to SSC) as fixed factors for all five sponge species. In pair-wise tests, F: field control, T0: time 0 control, E: sampling after the 28 d experimental period, O: sampling after the 14 d observational period; CAR for *Carteriospongia foliascens*, CYM for *Cymbastela coralliophila*, CLI for *Cliona orientalis*, COS for *Coscinoderma matthewsi* and STY for *Stylissa flabelliformis*; 0, 30 and 100 mg L⁻¹ within SSC.

was distinct from the seawater microbiome (Table 3b, Supplementary Figs S5 and S6). Aquarium acclimation (for 4 weeks) did not affect the sponge-associated microbial community of any species (Table 3a) as field controls were not significantly different from Time 0 controls (i.e. samples collected after the acclimation period, right before starting the exposure to sediments) (Table 3a). However, both field/time 0 controls showed significant differences with samples at the end of the experimental/observational period in all species (Table 3a). Elevated SSC did not have a major impact on the overall composition of the sponge microbiome at the phyla level (Fig. 4b) and no significant differences were detected at the OTU level (97% sequence similarity) for any species (Table 3c). In addition, no clear groupings were observed in the ordination (Fig. 4a). The only exception to this microbial stability was in *Carteriospongia foliascens*, where samples exposed to 100 mg L⁻¹ exhibited greater dispersion across the ordination (Fig. 4a). *Cliona orientalis* also showed greater separation between samples at the end of the experimental and observational periods, particularly in the 30 and 100 mg L⁻¹ treatments (Table 3c, Fig. 4a).

Network analyses of the 30 most discriminatory operational taxonomic units (OTUs) for the control (0 mg L⁻¹) and highest SSC (100 mg L⁻¹) in each species revealed phylogenetically diverse and stable core microbiomes (i.e. the component shared between all samples) as well as treatment specific OTUs (Fig. 4c, Supplementary Table S2). In each species, the number and taxonomy of OTUs observed exclusively in control samples was generally balanced by the number and taxonomy of new OTUs that were observed only in sediment treated samples. A notable exception however was the recruitment of 3 novel *Cyanobacteria* OTUs in *Carteriospongia foliascens* within samples from the high SSC. Also of interest was the finding that core *Cyanobacteria* OTUs in the two photosynthetic species *Carteriospongia foliascens* and *Cymbastela coralliophila* are not disrupted by sediments, even at the highest SSC.

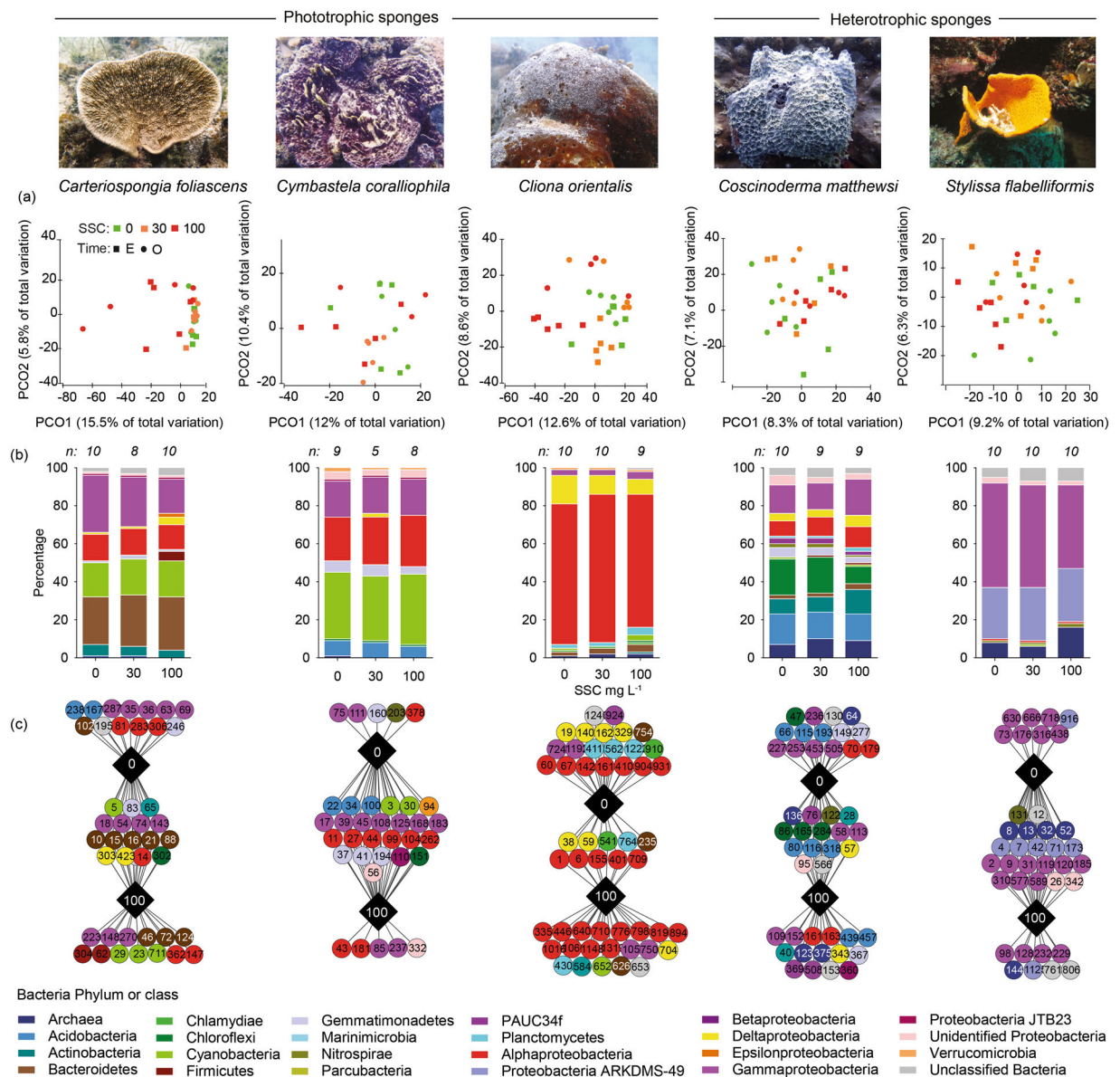


Figure 4. Microbial responses to SSCs. (a) Principal coordinate analysis plots for all species and treatments after the 28 d experimental period (E) and 14 d observational period (O), (b) Average relative abundance of each bacteria phylum (and class for *Proteobacteria*) using OTUs representing greater than 1% of the community for each treatment across both sampling times, (c) Cytoscape networks of the microbiome community in all species at 0 and 100 mg L⁻¹ of SSC across both sampling times. Circles correspond to different OTUs (with OTU numbers) and colours relate to their phylum or class level in the case of *Proteobacteria*.

Discussion

Establishing dose-response relationships relies on identifying the significance and relative importance of different cause-effect pathways. As part of a sequence of experiments, and a wider investigation into the effects of sediment deposition, light attenuation and elevated SSC (alone and in combination)^{38, 44}, we exposed five sponge species spanning a range of morphologies and nutritional modes to elevated SSCs for a chronic (28 d) period. Light levels were kept constant across the different treatments to isolate SSC as the primary variable. The SSCs used in this study (range 0–100 mg L⁻¹) were designed to bracket SSCs measured during a recent large scale capital dredging project in NW Australia (the Barrow Island project, see ref. 4). During this project, at 4 shallow water sites (~5–11 m depth) located <~0.5 km from the dredging, the 95th percentile (P_{95}) of SSCs over a 30 d running mean period was 16.0 mg L⁻¹ (range: 12.9–20.9) during the dredging phase as compared to 2.0 mg L⁻¹ (range: 1.5–3.1) before dredging. Exposure of the sponges to SSCs ≥ 23 mg L⁻¹ which corresponded to the 30 and 100 mg L⁻¹ nominal treatments, for 28 d had an overall negative effect on sponge physiology, including decreases in lipid content, suggesting that sponge feeding behaviour may be compromised. High levels of SSC also resulted in negative growth, decreased respiration rates and caused significant necrosis and mortality within the cup sponge *Carteriospongia foliascens* and, to a lesser extent, the massive sponge *Coscinoderma matthewsi*. The high levels

of *Carteriospongia foliascens* mortality in response to elevated SSCs supports previous research proposing this species as a sensitive bioindicator for assessing impacts from the dredging related pressure of light attenuation⁴⁴. *Cliona orientalis* was also negatively affected by high SSC, although it demonstrated a capacity for rapid recovery. LC₅₀ and LC₁₀ levels could only be calculated for *Carteriospongia foliascens* and were 40.61 and 21.51 mg L⁻¹, respectively. On the other hand, exposure to SSCs ≤ 10 mg L⁻¹ was tolerated by most species over the experimental period. These water quality values cannot be used for impact prediction and management purposes in isolation, as the SSCs are likely to have profound effects on light attenuation (see refs 4, 40 and 41) which is also known to significantly affect some sponge species used in this study⁴⁴.

In general, respiration rates decreased with elevated SSC, consistent with responses reported for the deep sea sponge *Geodia barretti* following sediment exposure^{45,46}. *Cliona orientalis*, *Cymbastela coralliophila* and *Stylissa flabelliformis* were able to metabolically recover within two weeks when exposed to the lowest sediment treatment (3 mg L⁻¹); however, a greater recovery time is likely required at higher SSC. In contrast to the other species, respiration rates in the massive species *Coscinoderma matthewsi* increased significantly at 100 mg L⁻¹, a trend that has also been reported in other heterotrophic massive species following short term exposure to elevated SSC⁴⁷. However, the higher respiration rates in *Coscinoderma matthewsi* may also be a result of stress associated with oxygen depletion within the experimental respiration chambers⁴⁸. Hence, due to the wide range of species-specific responses, it is difficult to generalise about how sponge respiration rates will respond to elevated SSCs.

Sponges are highly efficient filter-feeders, processing large amounts of water from which they efficiently remove bacteria and nutrients^{13,14}. Elevated SSCs from natural events or anthropogenic activities such as dredging are a natural hazard to the filter feeding mode of nutrition^{49,50}. Different sponge species have evolved different strategies to avoid excessive sediment intake and prevent clogging of their aquiferous systems. Sponges can slow their pumping activity^{33,34,46} and accumulate sediments in pockets that can be subsequently expelled with mucus secretions (reviewed in refs 32 and 39). Some sponges such as *Cliona orientalis*, are also capable of entirely closing their oscula (excurrent opening) in response to sediment deposition³⁶. Oscular closure can decrease and entirely arrest sponge pumping within hours³⁶ which would result in decreased respiration rates over very short time scales^{46,51}.

Different sediment removal mechanisms are likely to have very different energetic demands. However, all strategies are thought to contribute to a reduction in the food-retention efficiency of the sponges' aquiferous system^{47,52} which may compromise energy stores in the long term. Lipids are essential to an organism's physiological processes as they are a major source of metabolic energy and are often considered the most effective energy store in marine ecosystems^{53,54}. Lipids can be broadly grouped into storage and structural functions, with storage lipids predominantly being used as energy reserves and both categories playing a significant role in stress tolerance⁵⁵⁻⁵⁷. A decrease in lipids has previously been associated with lower levels of energy storage and lower survival rates in corals^{58,59} and sponges¹⁶. However, in this study, no significant decreases in total lipid reserves were observed in sponges exposed to high SSC. Phototrophic sponges may have the potential to compensate their energy intake through photosymbiosis. For instance, the variable lipid content in the phototrophic *Cliona orientalis* across treatments likely reflects the flexible feeding strategy of this species including an ability to switch to heterotrophic feeding, as evidenced by its survival during extended periods of darkness⁴⁴ and consistent with results for other species of the same genera⁶⁰. The increase in total lipids in *Cliona orientalis* in the 100 mg L⁻¹ treatment may result from an increase of the photosynthetic dinoflagellates *Symbiodinium* sp. in an attempt to increase phototrophic feeding, as corroborated by histological results. In a similar way, *Symbiodinium* sp. living in shallow water corals have been reported to supply host polyps with an excess of energy-rich lipids^{61,62}. In *Cliona orientalis* these energy stores were likely used during the observational period to aid recovery from bleaching and tissue regression and to increase choanocyte chamber density; although a longer recovery time may be necessary to return total lipids to control levels.

As light was compensated across treatments to maintain equivalent daily light integrals and intensities irrespective of SSC, no direct effects were detected of SSC on maximum quantum yields or Chl a concentrations, until disruption of the holobiont due to temporary (e.g. *Cliona orientalis*) or permanent bleaching (e.g. *Carteriospongia foliascens*). Hence, our results suggest that the health and photosynthetic efficiency of the photosymbionts is unaffected by high SSC in the absence of light attenuation. Interestingly though, increased chlorophyll d in samples of *Carteriospongia foliascens* and *Cymbastela coralliophila* exposed to 100 mg L⁻¹ suggested an increase in some Chl d-containing Cyanobacteria⁶³, providing further support for increased reliance on phototrophic feeding under high SSC. Previous research has also shown that the presence of photosymbionts often influences the composition of the host associated microbiome⁶⁴ hence any SSC induced change in photosymbiosis may have flow-on effects for the entire sponge microbiome.

Overall, sponge associated microbiomes were not significantly affected by SSC in any species, although minor differences were observed in *Carteriospongia foliascens* and *Cymbastela coralliophila*. In particular, under high SSC (100 mg L⁻¹) an increase in *Firmicutes*, *Deltaproteobacteria* and *Epsilonproteobacteria* was evident which is consistent with numerous reports of microbial shifts associated with stressed and diseased sponges⁶⁵⁻⁶⁷. Interestingly, novel *Cyanobacteria* OTUs inhabited *Carteriospongia foliascens* and *Cliona orientalis* exposed to high SSC, indicating a potential mechanism for acclimation to a high SSC environment. However, while some species may have the ability to successfully alter the composition of their microbial community under different environmental conditions^{44,68,69}, species with intimate and/or potentially obligate symbioses can be adversely impacted by disruption of their microbiome^{66,67} or loss of symbiotic function⁷⁰. The rapid deterioration in health of *Carteriospongia foliascens* under conditions of high SSC following the microbiome shift is consistent with its documented intimate reliance on a highly specialised microbial community⁴⁴.

Our results and previous studies suggest that most sponges have well developed mechanisms to survive periods of elevated SSC, however extended exposure to high SSC has significant adverse effects on sponge metabolism^{34,45,47}. Some species appear to have plasticity in modifying their aquiferous system^{71,72}, including the density

of their choanocyte chambers⁷³ depending on environmental conditions. Shifts from phototrophy to heterotrophy depending on irradiance have been also described in numerous sponge species^{16, 27, 74}. Alternatively, mixotrophic sponges may increase their reliance on phototrophic nutrition as observed in the current study. Our results also suggest that discolouration (i.e. bleaching) and necrosis of sponge tissue are effective bioindicators for dredging related stress.

In this study, the isolation of SSC from other dredging-related factors (i.e. sedimentation and light attenuation) allowed us to identify a specific cause:effect pathway and determine lethal and sub-lethal SSC for sponges⁴, including LC₅₀ and LC₁₀ levels for *Carteriospongia foliascens* (i.e. 40.61 and 21.51 mg L⁻¹, respectively). In conjunction with previous research on the impacts of light attenuation⁴⁴, these thresholds can now be used in water quality monitoring programs to alert dredging proponents to levels of light reduction and SSC that, if continued, could detrimentally impact sponge populations. In combination with sediment plume and light attenuation models, these results can be used to predict the likely effects of dredging (i.e. at the EIA stage) and to establish impact zones. By modelling different dredging scenarios (i.e. volume of material dredged, tidal phase, over flow options, etc.) the information could also be used to identify optimal dredging scenarios that minimise the likelihood and extent of impact.

Here we show that exposure to high SSC (≥ 23 mg L⁻¹) for extended periods (28 d) has a negative effect on sponge feeding behaviour with associated depletion of energy reserves. However, while ≤ 10 mg L⁻¹ for <28 d seems tolerable by most species and could be established as a prudent sub-lethal threshold in adult sponges, it is expected that the combined effect of SSC with low light availability and sediment smothering will increase the negative effects on sponges under realistic field conditions. These experimental results will assist regulators and environmental managers in reducing risks from dredging development although experimental research combining sedimentation, SSC and light attenuation is required before final thresholds can be derived for dredging impacts on sponges.

Methods

Sample collection. To assess impacts across nutritional modes, this study used the phototrophic sponges *Carteriospongia foliascens* (Pallas, 1766), *Cymbastela coralliophila* (Hooper & Berquist, 1992) and *Cliona orientalis* (Thiele, 1900) and the heterotrophic sponges *Coscinoderma matthewsi* (Lendenfeld, 1886) and *Stylissa flabelliformis* (Hentschel, 1912)^{18, 23, 25, 38, 75}. All species are common throughout the Indo-Pacific, including the east and west coasts of tropical Australia. Sponges were collected from 3–15 m depth from the Palm Islands, Great Barrier Reef (GBR) (Supplementary Table S3). *Cliona orientalis* is an encrusting sponge that bioerodes coral, so cores of *Cliona orientalis* were air-drilled from dead colonies of *Porites* sp. ensuring >2 cm of coral substrate below the sponge. For all species, sponges were cut into similar sized explants (~5 × 5 cm), and acclimated under natural light in flow-through seawater for 4 weeks until fully healed.

Experimental set up. The SSC exposure was performed in the National Sea Simulator (SeaSim) at the Australian Institute of Marine Science (AIMS, Townsville) using square 115L clear PVC acrylic tanks with an inverted pyramid at the base. Water within the tanks was circulated by a magnetic drive centrifugal pump that collected water from the top of the tank and forced flow up from the centre point of the inverted pyramid at the base. Sponges were placed on a gridded, false bottom floor 20 cm from the top of the tank and a second pump (VorTech™ MP10, EcoTech Marine, PA, US) was placed in the tank at the same height as the sponges to aid in water circulation. The seawater in experimental tanks was set to 27 °C, representing the temperature at the time of sponge collection.

Sponge explants were exposed to 5 nominal SSCs of 0 (i.e. experimental control), 3, 10, 30 and 100 mg L⁻¹ and the tanks were supplied with a continuous inflow of 5 µm filtered seawater at a rate of 400 mL min⁻¹, providing ~6 complete turnovers of seawater in each tank per day. Each treatment level had 3 replicate tanks containing 3–4 sponge replicates per species. To replace sediment lost from the tanks because of the continuous flow through of filtered seawater, new sediment was periodically introduced by small volumes of sediment slurry (~8 g L⁻¹) from an adjacent 500 L stock suspension. SSCs within each tank were monitored and controlled from turbidity readings (as nephelometric turbidity units, NTUs) using Turbimax CUS31 (Endress and Hauser, Germany) nephelometers connected to a programmable logic controller (PLC) system (see below). NTUs were converted to SSCs (as mg L⁻¹) by applying sediment specific algorithms determined gravimetrically (filtration of SSCs through 0.4 µm (nominal pore size) polycarbonate filters and calculating dry weight of the filters). The PLC system monitored NTU in each tank and controlled the SSCs by episodically opening and closing solenoid valves connected to the stock tank. Triplicate 250 mL water samples were collected from each tank weekly and the SSCs determined gravimetrically. Differences in SSC between treatments throughout the experiment were studied at each sampling day separately with a one-way analysis of variance (ANOVA) using treatment as the fixed factor. Data was log-transformed to achieve homogeneity of variances and normality when required.

The sediment used in this experiment was selected after an initial comparison between inshore sediments (siliclastic sediment collected subtidally from Onslow, Western Australia)³⁸ and offshore sediments (calcareous sediment collected from the lagoon of Davies Reef, a mid-shelf reef centrally located in the GBR, Queensland; S 18° 49.354' E 147° 38.253'). Similar responses were observed in sponges from comparative dosing for both sediments. For comparative purposes with other experiments, the calcareous sediment from Davies Reef was selected. Most importantly, all sediments were ground to ~30 µm (with 80% of the sediment 3–65 µm) with a rod mill grinder and measured using laser diffraction techniques (Mastersizer 2000, Malvern instruments Ltd, UK). Hence, the sediments used were predominantly silt-sized, typical for dredge plumes, to ensure environmental relevance. Tanks were illuminated by AI Hydra FiftyTwo™ HD LED lights (Aquaria Illumination, IA, US) on a 13:11 h L:D cycle. The light regime was designed to simulate daily conditions on the reef^{41, 76}, and made up of a 6 h period of gradually increasing light in the morning (06:00–12:00 h), an hour of constant illumination at 200 µmol

photons $\text{m}^{-2} \text{s}^{-1}$, and a 6 h period of gradually decreasing light in the afternoon (13:00–19:00 h). Over the course of the day the sponges experienced a daily light integral (DLI) of 5 mol photons m^{-2} .

In order to isolate the effect of SSC from the associated light attenuation that would occur under different SSCs, light intensities were adjusted between the tanks using a Li-250A light meter (LI-COR Biosciences, NE, US) at the grid level and adjusting the light intensity provided by the LED lights accordingly to ensure that all sponges received the same DLI regardless of SSC treatment. The surface of all sponges was also gently brushed each day to remove any deposited sediment that could negatively affect the sponges. The SSC experiment was conducted for a 28 d ‘experimental’ period, followed by a 14 d ‘observational’ period in clear water (0 mg L^{-1}). The length of the experiment was selected to simulate chronic conditions and to facilitate comparison with the 30-days running means for dredging-related turbidity events from 3 major capital dredging programs in North Western Australia⁴¹.

Studied parameters and statistical analyses. The effect of SSC on the sponge holobiont was determined using a suite of response variables, with a particular focus on changes in sponge feeding strategies, including changes in sponge photosymbionts, composition of the sponge microbial community and growth. To obtain baseline data on sponge health, 6 extra individuals were processed for each species immediately after collection (field controls) and after aquarium acclimation ($t = 0$ controls). From the initial 10 individuals stocked per species and treatment, 5 individuals were sampled (and removed from the experiment) for ‘destructive’ response variables (i.e. pigments, lipids and microbial community analyses) at the end of the experimental period and the remaining 5 individuals were sampled at the end of the observational period, in order to avoid negative effects on sponge health due to sub-sampling of the same individuals. Unless otherwise stated, statistical analyses were performed and graphs prepared using the software R v. 3.1.0 and SigmaPlot v.11.0 (Systat Software Inc.).

Linear mixed models using tank as a random factor and treatment as a fixed factor were fitted by residual maximum likelihood (REML) for data pertaining to relative growth rates, necrosis, lipid content, respiration, histology, chlorophyll fluorescence and total pigments at the end of the exposure and observational periods for each species, separately. An analysis of variance (ANOVA) table was generated for each model and Tukey’s post-hoc multiple comparisons were performed to compare treatment levels for each model⁷⁷.

Growth and necrosis. Initial and final thickness (in *Carteriospongia foliascens*, *Cymbastela coralliophila* and *Stylissa flabelliformis*), height (in *Coscinoderma matthewsi*), or sponge tissue depth inside coral cores (in *Cliona orientalis*), of each sponge ($\pm 0.1 \text{ mm}$) was measured with callipers as a 2-dimensional proxy for growth. Three measurements per sponge were averaged to calculate percentage change throughout the experimental and subsequent observational period. Changes in size, partial mortality (i.e. necrosis, assessed through species-specific changes in tissue characteristics, such as changes towards brown/black colour, absence of a healthy pinacoderm and exposure of fibres and skeleton) and loss of photosynthetic symbionts (bleaching) was recorded weekly using a digital camera (Canon S120) with underwater housing and analysed using image analysis software (ImageJ⁷⁸). Relative growth rates were calculated as the logarithm of the final measure divided by the initial measure, based on both thickness of sponges and their surface area. Percent mortality per tank ($n = 3$ per treatment) was fitted to nonlinear regression curves using the program Prism v7.01 (GraphPad Software Inc, CA, US). Regression curves were used to calculate the lethal concentrations (LC) of SSC at which 50% (LC_{50}) and 10% (LC_{10}) of the population died. The models were constrained between 0 and 100 with F values set at 50 and 10, for LC_{50} and LC_{10} , respectively. The curve was tested for normality of the residuals and a replicate test was applied to assess goodness of fit. Symmetric, asymptotic confidence intervals were calculated for the LC values.

Lipid analysis. The concentration of total lipids in sponge tissue was measured over time to assess whether SSC interferes with sponge feeding capability. Samples were analysed from the field controls and at the start of the experiment and at the end of the experimental and observational periods for samples exposed to the 0, 30 and 100 mg L^{-1} SSCs. Approximately 3 cm^3 of sponge tissue was excised, wrapped in aluminium foil to prevent plasticizer contamination and immediately frozen in liquid nitrogen. Lipids were extracted from approximately 100 mg of freeze-dried ground sample as described in ref. 79 and following modifications in ref. 80, with total lipid content reported as percentage biomass based on a dry weight conversion factor.

Respiration rates. Changes in sponge respiration rates were measured throughout the experimental and observational period. Samples were dark adapted for a minimum of 30 min before being transferred to 600 mL respiration chambers where they were incubated for 30 min at 27°C . Constant mixing within the chamber was achieved using a magnetic stir bar and a submersible battery-operated platform. An HDQ30D flexi meter (HACH LDO™, CA, US) was used to take three initial readings (i.e. initial O_2) and to measure the mg L^{-1} of O_2 and the % O_2 in each chamber at the end of the incubation. The final oxygen concentration inside the chamber did not drop below 85% saturation in most cases. To control for microbial community respiration, a chamber containing only environmental water (blank) was incubated under identical conditions.

Histology. Changes in the structure of the aquiferous system, in particular the number of choanocyte chambers, was examined from histological sections of samples collected at the end of the 28 d experimental period for the 0 and 100 mg L^{-1} treatments. Samples were fixed for 6 weeks in FAACC fixative (10 mL 40% formaldehyde, 5 mL glacial acetic acid, 1.3 g calcium chloride dehydrate, 85 mL water), and then transferred to 70% ethanol and stored at room temperature. Samples were dehydrated through a graded series of ethanol, embedded in paraffin, sectioned to $5 \mu\text{m}$ and stained using Mayer’s Haematoxylin, and Young’s Eosin Erythrosine. Samples were visualized and photographed using an Axioskop 2 plus Microscope and AxioCam MRC5 Digital Camera (Carl Zeiss Microscopy, LLC, US). Choanocyte chambers were only quantified for *Cliona orientalis* as the presence of spicules in all other species resulted in poor quality sections that precluded accurate choanocyte chamber quantification.

In *Cliona orientalis*, five fields of view (FOV) per section were examined to quantify the total number of choanocyte chambers at 200 \times . Choanocyte chambers were identified as circular rings of cells⁷³ and chamber density was averaged across the 5 FOVs to provide a mean choanocyte chamber density per sponge.

Chlorophyll fluorescence. Changes in photosynthetic capacity (maximum quantum yield) of the sponge's phototrophic symbionts were measured with a Diving-PAM (pulse amplitude modulation) chlorophyll fluorometer (Heinz Walz GmbH, Effeltrich, Germany) for *Carteriospongia foliascens*, *Cymbastela coralliophila* and *Cliona orientalis* as described in ref. 44. Briefly, maximum quantum yield (F_v/F_m)⁸¹ measurements were obtained from dark-adapted sponges at weekly intervals throughout the experimental and observational periods.

Pigment analysis. Pigment analyses were performed on ~0.2 g of tissue from all phototrophic sponges (*Carteriospongia foliascens*, *Cymbastela coralliophila* and *Cliona orientalis*) at the end of the experimental and recovery periods. Pigments from samples incorporating pinacoderm and mesohyl regions were extracted and analysed as described in ref. 44 and standardized to sponge wet weight. The concentration of Chlorophyll *a* (hereafter Chl *a*) was used as a proxy for changes in photosymbiont health/activity (i.e. bleaching)¹⁸. Differences between Chl *a* at the end of the 28 d experiment and after the 14 d recovery phase were assessed with a t-test for every treatment and species, separately. Pearson correlations were performed between all the studied pigments. All pigments retrieved by spectrophotometry (i.e. chlorophylls *a*, *b*, *c*, *d*, Total chlorophylls and carotenoids) were used to build resemblance matrices based on normalized data for each species, separately. Non-metric Multi-Dimensional Scaling (nMDS) plots were created using Euclidean distances. Two factors were determined (i.e. SSC and sampling time, nested to SSC) and examined by PERMANOVA (Permutational multivariate ANOVA based on distances). All multivariate analyses were performed using Primer 6 (Primer-E Ltd, UK).

Microbial community analysis. Microbial community composition was assessed using Illumina amplicon sequencing of the 16S rRNA taxonomic marker gene, for field controls, $t = 0$ controls and at the end of the experimental and observational periods for sponges exposed to 0, 30 and 100 mg L⁻¹ SSC. All samples were immediately frozen in liquid nitrogen and subsequently stored at -80 °C. Water was also collected from each tank at the time of sampling to facilitate a direct comparison with microbes present in the surrounding environment. DNA was extracted from ~0.2 g of sponge tissue using the PowerPlant[®] Pro DNA Isolation Kit (MoBio Laboratories, CA, US) according to the Manufacturer's protocol. Microbial communities in seawater were filtered and DNA was extracted as previously described⁸². Sequencing of the 16S rRNA gene was performed at the Australian Centre for Ecogenomics using primers 515f and 806r and the Illumina HiSeq2500 platform. Sequence data was deposited at the NCBI under the accession number SRP080228.

Amplicon sequence data was processed in Mothur v.1.35.1⁸³ according to the MiSeq standard operating procedure⁸⁴. Briefly, demultiplexed fastq paired-end reads were first quality-filtered and assembled into contigs (make.contigs and screen.seqs: maxambig = 0, maxhomop = 8, minlength = 100, maxlength = 292). Aligned reads were reduced to non-redundant sequences and chimeric sequences were detected using Uchime⁸⁵. Aligned sequences were phylogenetically classified based on the Silva reference file v.123, and all unassigned sequences removed (taxon = Chloroplast-Mitochondria-unknown-Eukaryota). Samples with low read numbers were eliminated from the dataset and remaining samples were sub-sampled to 10385 sequences. Pairwise distances were calculated and used for clustering and OTU assignment and OTUs were further classified based on the SILVA v.123 taxonomy.

OTU data was normalised to account for sampling depth and then square-root transformed to reduce the effect of abundant OTUs. Bray-Curtis distance matrices were constructed and visualised using non-metric multidimensional ordinations (nMDS) and principal coordinates analyses (PCO). Permutational analysis of variance (PERMANOVA, using 9999 permutations) was used to determine significant differences in microbial communities. All multidimensional statistical analyses were performed in Primer 6/PERMANOVA. Similarity Percentage (SIMPER) analysis was used to determine the OTUs that contribute to the differences between 2 SSC (0 and 100 mg L⁻¹) for each phototrophic species, separately. The 30 OTUs with the most discriminating power from the SIMPER analysis were used to create networks on Cytoscape 3.2.0⁸⁶.

References

1. Ports_Australia. Dredging and Australian Ports. Subtropical and Tropical Ports. (2014).
2. McCook, L. J. *et al.* Synthesis of current knowledge of the biophysical impacts of dredging and disposal on the Great Barrier Reef: Report of an Independent Panel of Experts. (2015).
3. Hanley, J. Environmental monitoring programs on recent capital dredging projects in the Pilbara (2003–10): a Review. *Aust. Pet. Prod. Explor. Assoc.* **51**, 273–294 (2011).
4. Jones, R., Bessell-Browne, P., Fisher, R., Klonowski, W. & Slivkoff, M. Assessing the impacts of sediments from dredging on corals. *Mar. Pollut. Bull.* **102**, 9–29 (2016).
5. Schönberg, C. H. L. & Fromont, J. Sponge gardens of Ningaloo Reef (Carnarvon Shelf, Western Australia) are biodiversity hotspots. *Hydrobiologia* **687**, 143–161 (2011).
6. Jones, R., Ricardo, G. F. & Negri, A. P. Effects of sediments on the reproductive cycle of corals. *Mar. Pollut. Bull.* **100**, 13–33 (2015).
7. Erfemeijer, P. L. A. & Lewis, R. R. Environmental impacts of dredging on seagrasses: a review. *Mar. Pollut. Bull.* **52**, 1553–72 (2006).
8. Flores, F. *et al.* Chronic exposure of corals to fine sediments: lethal and sub-lethal impacts. *PLoS One* **7**, e37795 (2012).
9. Heyward, A. *et al.* The sponge gardens of Ningaloo Reef, Western Australia. *Open Mar. Biol. J.* **4**, 3–11 (2010).
10. Przeslawski, R., Alvarez, B., Battershill, C. & Smith, T. Sponge biodiversity and ecology of the Van Diemen Rise and eastern Joseph Bonaparte Gulf, northern Australia. *Hydrobiologia* **730**, 1–16 (2014).
11. Bell, J. J. The functional roles of marine sponges. *Estuar. Coast. Shelf Sci.* **79**, 341–353 (2008).
12. Environmental Protection Authority WA. Environmental Assessment Guidelines. (2013).
13. Goeij, J. M. D. *et al.* Surviving in a marine desert: the sponge loop retains resources within coral reefs. *Science* (80-). **342**, 108–110 (2013).
14. Reiswig, H. Particle feeding in natural populations of three marine demosponges. *Biol. Bull.* **141**, 568–591 (1971).

15. Wilkinson, C. R., Garrone, R. & Vacelet, J. Marine Sponges Discriminate between Food Bacteria and Bacterial Symbionts: Electron Microscope Radioautography and *in situ* Evidence. *Proc. R. Soc. London. Ser. B. Biol. Sci.* **220**, 519 LP–528 (1984).
16. Arillo, A., Bavestrello, G., Burlando, B. & Sara, M. Metabolic integration between symbiotic cyanobacteria and sponges: a possible mechanism. *Mar. Biol.* **117**, 159–162 (1993).
17. Freeman, C. J. & Thacker, R. W. Complex interactions between marine sponges and their symbiotic microbial communities. *Limnol. Oceanogr.* **56**, 1577–1586 (2011).
18. Wilkinson, C. R. Net primary productivity in coral reef sponges. *Science (80-)*. **219**, 410–412 (1983).
19. Hill, M., Allenby, A., Ramsby, B., Schönberg, C. & Hill, A. Symbiodinium diversity among host clonoid sponges from Caribbean and Pacific reefs: Evidence of heteroplasmy and putative host-specific symbiont lineages. *Mol. Phylogenet. Evol.* **59**, 81–8 (2011).
20. Thacker, R. W. & Freeman, C. J. In *Advances in Marine Biology* (eds Becerro, M. A., Uriz, M. J., Maldonado, M. & Turon, X.) **62**, 57–111 (Elsevier Ltd, 2012).
21. Usher, K. M. The ecology and phylogeny of cyanobacterial symbionts in sponges. *Mar. Ecol.* **29**, 178–192 (2008).
22. Thacker, R. W. Impacts of Shading on Sponge-Cyanobacteria Symbioses: A Comparison between Host-Specific and Generalist Associations. *Integr. Comp. Biol.* **45**, 369–376 (2005).
23. Ridley, C. P., Faulkner, D. & Haygood, M. G. Investigation of Oscillatoria spongelliae-dominated bacterial communities in four dictyoceratid sponges. *Appl. Environ. Microbiol.* **71**, 7366–75 (2005).
24. Taylor, M. W., Radax, R., Steger, D. & Wagner, M. Sponge-associated microorganisms: evolution, ecology, and biotechnological potential. *Microbiol. Mol. Biol. Rev.* **71**, 295–347 (2007).
25. Schönberg, C. H. L. & Loh, W. K. W. Molecular identity of the unique symbiotic dinoflagellates found in the bioeroding demersal sponge *Cliona orientalis*. *Mar. Ecol. Prog. Ser.* **299**, 157–166 (2005).
26. Carlos, A. A., Baillie, B. K., Kawachi, M. & Maruyama, T. Phylogenetic position of Symbiodinium (Dinophyceae) isolates from Tridacnids (Bivalvia), Cardiids (Bivalvia), a sponge (Porifera), a soft Coral (Anthozoa), and a free-living strain. *J. Phycol.* **35**, 1054–1062 (1999).
27. Erwin, P. & Thacker, R. Phototrophic nutrition and symbiont diversity of two Caribbean sponge–cyanobacteria symbioses. *Mar. Ecol. Prog. Ser.* **362**, 139–147 (2008).
28. Webster, N. S. & Thomas, T. The Sponge Hologenome. *MBio* **7**, e00135–16 (2016).
29. Thomas, T. *et al.* Diversity, structure and convergent evolution of the global sponge microbiome. *Nat. Commun.* **7**, 11870 (2016).
30. Wilkinson, C. & Trott, L. Light as a factor determining the distribution of sponges across the central Great Barrier Reef. *Proc. 5th int Coral Reef Symp., Tahiti* **5**, 125–130 (1985).
31. Cheshire, A. C. & Wilkinson, C. R. Modelling the photosynthetic production by sponges on Davies Reef, Great Barrier Reef. *Mar. Biol.* **109**, 13–18 (1991).
32. Bell, J. J. *et al.* Sediment impacts on marine sponges. *Mar. Pollut. Bull.* **94**, 5–13 (2015).
33. Gerrodette, T. & Flechsig, A. Sediment-induced reduction in the pumping rate of the tropical sponge *Verongia lacunosa*. *Mar. Biol.* **55**, 103–110 (1979).
34. Tompkins-MacDonald, G. J. & Leys, S. P. Glass sponges arrest pumping in response to sediment: implications for the physiology of the hexactinellid conduction system. *Mar. Biol.* **154**, 973–984 (2008).
35. Ilan, M. & Abelson, A. The Life of a Sponge in a Sandy Lagoon. *Biol. Bull.* **189**, 363 (1995).
36. Strehlow, B. W., Jorgensen, D., Webster, N. S., Pineda, M.-C. & Duckworth, A. Using a thermistor flowmeter with attached video camera for monitoring sponge excurrent speed and oscular behaviour. *PeerJ* **4**, e2761 (2016).
37. Stubler, A. D., Duckworth, A. R. & Peterson, B. J. The effects of coastal development on sponge abundance, diversity, and community composition on Jamaican coral reefs. *Mar. Pollut. Bull.* **93**, 261–270 (2015).
38. Pineda, M. C., Duckworth, A. & Webster, N. Appearance matters: sedimentation effects on different sponge morphologies. *J. Mar. Biol. Assoc. United Kingdom* **96**, 481–492 (2016).
39. Schönberg, C. Literature review: effects of dredging on filter feeder communities, with a focus on sponges. Final Report of Theme 6 Project 6.1 of the Western Australian Marine Science Institution (WAMSI) Dredging Science Node. (2015).
40. Fisher, R., Stark, C., Ridd, P. & Jones, R. Spatial patterns in water quality changes during dredging in tropical environments. *PLoS One* **10**, e0143309 (2015).
41. Jones, R., Fisher, R., Stark, C. & Ridd, P. Temporal patterns in seawater quality from dredging in tropical environments. *PLoS One* **10**, e0137112 (2015).
42. Roberts, D. E., Davis, A. R. & Cummins, S. P. Experimental manipulation of shade, silt, nutrients and salinity on the temperate reef sponge *Cymbastela concentrica*. **307**, 143–154 (2006).
43. Biggerstaff, A., Smith, D. J., Jompa, J. & Bell, J. J. Photoacclimation supports environmental tolerance of a sponge to turbid low-light conditions. *Coral Reefs* **34**, 1049–1061 (2015).
44. Pineda, M. C. *et al.* Effects of light attenuation on the sponge holobiont- implications for dredging management. *Sci. Rep.* **6**, 39038 (2016).
45. Kutti, T. *et al.* Metabolic responses of the deep-water sponge *Geodia barretti* to suspended bottom sediment, simulated mine tailings and drill cuttings. *J. Exp. Mar. Bio. Ecol.* **473**, 64–72 (2015).
46. Tjensvoll, I., Kutti, T., Fosså, J. H. & Bannister, R. J. Rapid respiratory responses of the deep-water sponge *Geodia barretti* exposed to suspended sediments. *Aquat. Biol.* **19**, 65–73 (2013).
47. Bannister, R. J., Battershill, C. N. & de Nys, R. Suspended sediment grain size and mineralogy across the continental shelf of the Great Barrier Reef: Impacts on the physiology of a coral reef sponge. *Cont. Shelf Res.* **32**, 86–95 (2012).
48. Coma, R. & Ribes, M. Seasonal energetic constraints in Mediterranean benthic suspension feeders: effects at different levels of ecological organization. *Oikos* **1**, 205–215 (2003).
49. Larcombe, P., Costen, A. & Woolfe, K. J. The hydrodynamic and sedimentary setting of nearshore coral reefs, central Great Barrier Reef shelf, Australia: Paluma Shoals, a case study. *Sedimentology* **48**, 811–835 (2001).
50. Foster, T. *et al.* Dredging and port construction around coral reefs. (2010).
51. Hadas, E., Ilan, M. & Shpigel, M. Oxygen consumption by a coral reef sponge. *J. Exp. Biol.* **211**, 2185–2190 (2008).
52. Kowalke, J. Ecology and energetics of two Antarctic sponges. **247**, 85–97 (2000).
53. Parrish, C. C. Lipids in Marine Ecosystems. *ISRN Oceanogr.* **2013**, 1–16 (2013).
54. Bergé, J.-P. & Barnathan, G. In *Marine Biotechnology I* (eds Ulber, R. & Le Gal, Y.) 49–125, doi:10.1007/b135782 (Springer Berlin Heidelberg, 2005).
55. Hazel, J. R. Thermal Adaptation in Biological Membranes: Is Homeoviscous Adaptation the Explanation? *Annu. Rev. Physiol.* **57**, 19–42 (1995).
56. Rod'kina, S. A. Fatty Acids and Other Lipids of Marine Sponges. *Russ. J. Mar. Biol.* **31**, S49–S60 (2005).
57. van Meer, G., Voelker, D. R. & Feigenson, G. W. Membrane lipids: where they are and how they behave. *Nat. Rev. Mol. Cell Biol.* **9**, 112–124 (2008).
58. Anthony, K. R. N., Hoogenboom, M. O., Maynard, J. A., Grotto, A. G. & Middlebrook, R. Energetics approach to predicting mortality risk from environmental stress: a case study of coral bleaching. *Funct. Ecol.* **23**, 539–550 (2009).
59. Strahl, J., Francis, D. S., Doyle, J., Humphrey, C. & Fabricius, K. E. Biochemical responses to ocean acidification contrast between tropical corals with high and low abundances at volcanic carbon dioxide seeps. *ICES J. Mar. Sci. J. du Cons.*, doi:10.1093/icesjms/fsv194 (2015).

60. Riesgo, A. *et al.* Transcriptomic analysis of differential host gene expression upon uptake of symbionts: a case study with Symbiodinium and the major bioeroding sponge *Cliona varians*. *BMC Genomics* **15**, 376 (2014).
61. Stimson, J. S. Location, quantity and rate of change in quantity of lipids in tissue of Hawaiian hermatypic corals. *Bull. Mar. Sci.* **41**, 889–904 (1987).
62. Patton, J. S., Abraham, S. & Benson, A. A. Lipogenesis in the intact coral *Pocillopora cap tata* and its isolated zooxanthellae: Evidence for a light-driven carbon cycle between symbiont and host. *Mar. Biol.* **44**, 235–247 (1977).
63. Alex, A., Vasconcelos, V., Tamagnini, P., Santos, A. & Antunes, A. Unusual symbiotic Cyanobacteria association in the genetically diverse intertidal marine sponge *Hymeniacidon perlevis* (Demospongiae, Halichondrida). *PLoS One* **7**, e51834 (2012).
64. Bourne, D. G. *et al.* Coral reef invertebrate microbiomes correlate with the presence of photosymbionts. *ISME J.* **7**, 1452–1458 (2013).
65. Webster, N. S., Xavier, J. R., Freckelton, M., Motti, C. A. & Cobb, R. Shifts in microbial and chemical patterns within the marine sponge *Aplysina aerophoba* during a disease outbreak. *Environ. Microbiol.* **10**, 3366–3376 (2008).
66. Webster, N. S., Cobb, R. E. & Negri, A. P. Temperature thresholds for bacterial symbiosis with a sponge. *ISME J.* **2**, 830–842 (2008).
67. Simister, R. *et al.* Thermal stress responses in the bacterial biosphere of the Great Barrier Reef sponge, *Rhopaloeides odorabile*. *Environ. Microbiol.* **14**, 3232–46 (2012).
68. Webster, N. S. *et al.* Bacterial community dynamics in the marine sponge *Rhopaloeides odorabile* under *in situ* and *ex situ* cultivation. *Mar. Biotechnol. (NY)*. **13**, 296–304 (2011).
69. Morrow, K. M. *et al.* Natural volcanic CO₂ seeps reveal future trajectories for host-microbial associations in corals and sponges. *ISME J.* **9**, 894–908 (2015).
70. Fan, L., Liu, M., Simister, R., Webster, N. S. & Thomas, T. Marine microbial symbiosis heats up: the phylogenetic and functional response of a sponge holobiont to thermal stress. *ISME J.* **7**, 991–1002 (2013).
71. Palumbi, S. R. How body plans limit acclimation: responses of a Demosponge to wave force. *Ecology* **67**, 208–214 (1986).
72. Goeij, J. M. D. *et al.* Cell kinetics of the marine sponge *Halisarca caerulea* reveal rapid cell turnover and shedding. 3892–3900, doi:10.1242/jeb.034561 (2009).
73. Luter, H. M., Whalan, S. & Webster, N. S. The marine sponge *Ianthella basta* can recover from stress-induced tissue regression. *Hydrobiologia* **687**, 227–235 (2011).
74. Weisz, J. B., Massaro, A. J., Ramsby, B. D. & Hill, M. S. Zooxanthellar symbionts shape host sponge trophic status through translocation of carbon. *Biol. Bull.* **219**, 189–197 (2010).
75. Cheshire, A. *et al.* Preliminary study of the distribution and photophysiology of the temperate phototrophic sponge *Cymbastela* sp. from South Australia. *Mar. Freshw. Res.* **46**, 1211–1216 (1995).
76. Anthony, K. R. N., Ridd, P. V., Orpin, A. R., Larcombe, P. & Lough, J. Temporal variation of light availability in coastal benthic habitats: Effects of clouds, turbidity and tides. *Limnol. Oceanogr.* **49**, 2201–2211 (2004).
77. Logan, M. *Biostatistical design and analysis using R: a practical guide.* (John Wiley & Sons, Ltd, 2010).
78. Schneider, C. A., Rasband, W. S. & Eliceiri, K. W. NIH Image to ImageJ: 25 years of image analysis. *Nat. Methods* **9**, 671–675 (2012).
79. Folch, J., Lees, M. & Sloane-Stanley, G. A simple method for the isolation and purification of total lipids from animal tissues. *J. Biol. Chem.* **226**, 497–509 (1957).
80. Conlan, J., Jones, P., Turchini, G., Hall, M. & Francis, D. Changes in the nutritional composition of captive early-mid stage *Panulirus ornatus* phyllosoma over ecdysis and larval development. *Aquaculture* **434**, 159–170 (2014).
81. Genty, B., Briantais, J. & Baker, N. The relationship between the quantum yield of photosynthetic electron-transport and quenching of Chlorophyll fluorescence. *Biochim. Biophys. Acta* **990**, 87–92 (1989).
82. Webster, N. S. *et al.* Deep sequencing reveals exceptional diversity and modes of transmission for bacterial sponge symbionts. *Environ. Microbiol.* **12**, 2070–82 (2010).
83. Schloss, P. D. *et al.* Introducing mothur: Open-Source, Platform-Independent, Community-Supported Software for Describing and Comparing Microbial Communities. *Appl. Environ. Microbiol.* **75**, 7537–7541 (2009).
84. Kozich, J. J., Westcott, S. L., Baxter, N. T., Highlander, S. K. & Schloss, P. D. Development of a dual-index sequencing strategy and curation pipeline for analyzing amplicon sequence data on the miseq illumina sequencing platform. *Appl. Environ. Microbiol.* **79**, 5112–5120 (2013).
85. Edgar, R. C., Haas, B. J., Clemente, J. C., Quince, C. & Knight, R. UCHIME improves sensitivity and speed of chimera detection. *Bioinformatics* **27**, 2194–2200 (2011).
86. Shannon, P. *et al.* Cytoscape: A Software Environment for Integrated Models of Biomolecular Interaction Networks. *Genome Res.* **13**, 2498–2504 (2003).

Acknowledgements

This research was funded by the Western Australian Marine Science Institution (WAMSI) as part of the WAMSI Dredging Science Node, and made possible through investment from Chevron Australia, Woodside Energy Limited, BHP Billiton as environmental offsets and by co-investment from the WAMSI Joint Venture partners. The commercial entities had no role in data analysis, decision to publish, or preparation of the manuscript. The views expressed herein are those of the authors and not necessarily those of WAMSI. All collections were performed under Great Barrier Reef Marine Park Regulations 1983 (Commonwealth) and Marine Parks regulations 2006 (Queensland) Permit G12/35236.1 and Permit G13/35758.1. We are thankful to P Bessell-Browne and staff at the AIMS National Sea Simulator for their time and efforts on the WAMSI tank prototyping and sediment delivery system. S Reilly processed the samples for histology analyses. Dr P Menendez provided valuable advice on statistical analyses. Thanks are also due to E Arias for his valuable help in the field and while running the experiment. N.S.W was funded by an Australian Research Council Future Fellowship FT120100480.

Author Contributions

M.C.P., B.S., A.D., R.J. and N.S.W. designed the experiment. M.C.P. and B.S. undertook the experiment. M.C.P., B.S. and M.S. undertook laboratory analyses. M.C.P. and B.S. analysed the data. M.C.P., B.S., A.D., R.J. and N.S.W. wrote the manuscript. All authors reviewed the manuscript.

Additional Information

Supplementary information accompanies this paper at doi:10.1038/s41598-017-05241-z

Competing Interests: The authors declare that they have no competing interests.

Publisher's note: Springer Nature remains neutral with regard to jurisdictional claims in published maps and institutional affiliations.



Open Access This article is licensed under a Creative Commons Attribution 4.0 International License, which permits use, sharing, adaptation, distribution and reproduction in any medium or format, as long as you give appropriate credit to the original author(s) and the source, provide a link to the Creative Commons license, and indicate if changes were made. The images or other third party material in this article are included in the article's Creative Commons license, unless indicated otherwise in a credit line to the material. If material is not included in the article's Creative Commons license and your intended use is not permitted by statutory regulation or exceeds the permitted use, you will need to obtain permission directly from the copyright holder. To view a copy of this license, visit <http://creativecommons.org/licenses/by/4.0/>.

© The Author(s) 2017

Supporting Online Material

Effect of suspended sediments on the sponge holobiont with implications for dredging management

Mari-Carmen Pineda^{1,2*}, Brian Strehlow^{1,2,3}, Miriam Sternel⁴, Alan Duckworth^{1,2}, Ross Jones^{1,2} and Nicole S. Webster^{1,2}

¹ *Australian Institute of Marine Science (AIMS), Townsville, QLD and Perth, WA, Australia*

² *Western Australian Marine Science Institution, Perth, WA, Australia*

³ *School of Plant Biology and Centre for Microscopy Characterisation and Analysis: University of Western Australia, Perth, WA, Australia*

⁴ *University of Bremen, Bremen, Germany*

*Corresponding author:

Mari-Carmen Pineda

Australian Institute of Marine Science, PMB3, Townsville, QLD, 4810, Australia

E-mail: mcarmen.pineda@gmail.com.

Tel.: +61 7 4753 4522, fax: +61 7 4772 5852

Table S1. ANOVA tables and summaries of linear mixed models examining the effects of treatment on relative growth rate based on surface area (not relevant for *Cliona orientalis*), for each species separately, at the end of the experimental and observational periods. Tukey tests have been performed for significant pairwise multiple comparisons.

		<i>Carteriospongia foliascens</i>		<i>Cymbastela coralliophila</i>		<i>Coscinoderma matthewsi</i>		<i>Stylissa flabelliformis</i>	
Source	df	F	P	F	P	F	P	F	P
Experimental phase									
Treatment	4	14.315	0.060	5.795	0.04	6.741	0.03	2.865	0.1394
Error	20								
Tukey		0>3,10,30>100		0,3,>30,100		0>3,10,100			
Observational phase									
Treatment	4	11.646	0.01	8.20	0.020	4.65	0.061	3.704	0.092
Error	20								
Tukey		0,3>10,30,100		0,3>30,100					

Table S2. Similarity Percentage Analysis (SIMPER) for 30 most significant OTUs driving differences between 0 and 100 mg L⁻¹ SSC.

OTU	Average relative abundance (%)		Contribution (%)	Taxonomic ID
	0 mg L ⁻¹	100 mg L ⁻¹		
<i>Carteriospongia foliascens</i>				
Otu000005	2.53	2.82	1.04	Cyanobacteria
Otu000010	1.76	1.4	0.82	Bacteroidetes
Otu000015	1.35	0.91	0.68	Bacteroidetes
Otu000062	0	1.16	0.64	Firmicutes
Otu000035	1.3	0.52	0.62	Gammaproteobacteria
Otu000023	0.8	0.9	0.6	Cyanobacteria
Otu000029	0.68	0.95	0.59	Cyanobacteria
Otu000025	0.97	0.5	0.56	Alphaproteobacteria
Otu000036	1.11	0.44	0.54	Gammaproteobacteria
Otu000018	1.44	0.74	0.53	Gammaproteobacteria
Otu000014	1.69	1.17	0.53	Alphaproteobacteria
Otu000016	1.63	1.45	0.5	Bacteroidetes
Otu000021	1.26	1.42	0.46	Bacteroidetes
Otu000063	0.88	0.6	0.42	Gammaproteobacteria
Otu000065	1.05	0.71	0.41	Actinobacteria
Otu000046	0.32	0.88	0.41	Bacteroidetes
Otu000069	0.82	0.25	0.41	Gammaproteobacteria
Otu000050	0.75	0.37	0.4	Cyanobacteria
Otu000103	0	0.68	0.39	Bacteroidetes
Otu000081	0.85	0.59	0.39	Alphaproteobacteria
Otu000102	0.79	0.27	0.37	Bacteroidetes
Otu000304	0	0.66	0.37	Firmicutes
Otu000096	0.43	0.46	0.36	Gammaproteobacteria
Otu000072	0.79	0.74	0.35	Bacteroidetes
Otu000084	0.61	0.41	0.35	Alphaproteobacteria
Otu000082	0.48	0.39	0.35	Bacteroidetes
Otu000148	0.35	0.78	0.34	Gammaproteobacteria
Otu000054	0.87	0.73	0.33	Gammaproteobacteria
Otu000074	1.02	0.56	0.32	Gammaproteobacteria
Otu000362	0	0.62	0.32	Alphaproteobacteria
<i>Cymbastela coralliophila</i>				
Otu000022	1.97	0.8	1.48	Acidobacteria
Otu000030	1.1	1.26	1.47	Cyanobacteria

Otu000011	2.33	2.93	1.42	Alphaproteobacteria
Otu000044	1.49	0.62	1.2	Alphaproteobacteria
Otu000043	0.6	0.97	1.16	Alphaproteobacteria
Otu000041	1.1	0.63	1.11	Gemmatimonadetes
Otu000033	0.92	0.63	1.08	Cyanobacteria
Otu000017	1.89	1.6	1.08	Gammaproteobacteria
Otu000092	0.82	0.84	1	Cyanobacteria
Otu000068	0.91	0.52	0.98	Alphaproteobacteria
Otu000003	5.1	5.31	0.97	Cyanobacteria
Otu000056	0.93	1.22	0.93	Unidentified Proteobacteria
Otu000037	1.11	1.24	0.93	Gemmatimonadetes
Otu000202	0.24	0.66	0.83	Alphaproteobacteria
Otu000075	1.07	0.68	0.8	Gammaproteobacteria
Otu000027	1.63	1.6	0.8	Alphaproteobacteria
Otu000184	0.3	0.57	0.78	Alphaproteobacteria
Otu000034	0.94	1.38	0.76	Acidobacteria
Otu000207	0.68	0.48	0.74	Alphaproteobacteria
Otu000160	0.77	0.41	0.72	Gemmatimonadetes
Otu000111	0.93	0.64	0.72	Gammaproteobacteria
Otu000045	0.96	1.17	0.72	Alphaproteobacteria
Otu000097	0.47	0.61	0.71	Alphaproteobacteria
Otu000094	0.93	0.78	0.69	Verrucomicrobia
Otu000087	0.4	0.49	0.68	Gammaproteobacteria
Otu000104	0.81	0.93	0.67	Alphaproteobacteria
Otu000125	0.73	0.83	0.66	Gammaproteobacteria
Otu000039	1.28	1.17	0.65	Gammaproteobacteria
Otu000181	0.38	0.7	0.64	Alphaproteobacteria
Otu000201	0.57	0.34	0.63	Unidentified Proteobacteria

Cliona orientalis

Otu000019	1.62	0.41	0.9	Deltaproteobacteria
Otu000060	1.22	0.34	0.59	Alphaproteobacteria
Otu000001	6.67	6.47	0.51	Alphaproteobacteria
Otu000038	1.09	0.67	0.48	Deltaproteobacteria
Otu000006	3.1	2.39	0.48	Alphaproteobacteria
Otu000059	0.68	0.87	0.39	Deltaproteobacteria
Otu000091	0.35	0.52	0.39	Alphaproteobacteria
Otu000067	0.77	0.18	0.36	Alphaproteobacteria
Otu000162	0.58	0.23	0.35	Deltaproteobacteria
Otu000248	0.09	0.6	0.31	Deltaproteobacteria
Otu000140	0.63	0.11	0.28	Deltaproteobacteria
Otu000142	0.6	0.12	0.28	Alphaproteobacteria
Otu000118	0.36	0.28	0.26	Alphaproteobacteria
Otu000329	0.47	0.08	0.22	Deltaproteobacteria
Otu000394	0.28	0.33	0.22	Gammaproteobacteria
Otu000255	0.02	0.43	0.21	Alphaproteobacteria
Otu000221	0.44	0	0.21	Alphaproteobacteria
Otu000410	0.43	0.09	0.21	Alphaproteobacteria
Otu000381	0.12	0.45	0.21	Cyanobacteria
Otu000254	0.38	0.06	0.2	Alphaproteobacteria
Otu000186	0.26	0.38	0.19	Plantomycetes
Otu000652	0.08	0.42	0.19	Cyanobacteria
Otu000077	0.3	0.25	0.19	Archaea
Otu000622	0.04	0.28	0.18	Alphaproteobacteria
Otu000182	0.29	0.15	0.18	Alphaproteobacteria
Otu000419	0.23	0.27	0.17	Verrucomicrobia
Otu000256	0.2	0.26	0.17	Archaea
Otu000475	0.17	0.32	0.17	Alphaproteobacteria
Otu000335	0.17	0.43	0.17	Alphaproteobacteria
Otu000420	0.23	0.21	0.16	Alphaproteobacteria

Coscinoderma matthewsi

Otu000040	0.5	1.48	0.45	Actinobacteria
-----------	-----	------	------	----------------

Otu000028	0.95	1.42	0.34	Actinobacteria
Otu000047	1.01	0.42	0.31	Chloroflexi
Otu000078	0.92	0.18	0.3	Chloroflexi
Otu000061	0.74	0.72	0.3	Gammaproteobacteria
Otu000106	0.78	0.47	0.27	Acidobacteria
Otu000066	0.93	0.45	0.26	Acidobacteria
Otu000057	0.84	1.2	0.23	Deltaproteobacteria
Otu000079	0.51	0.41	0.23	Gammaproteobacteria
Otu000132	0.65	0.49	0.22	Unidentified Proteobacteria
Otu000064	0.56	0.51	0.22	Archaea
Otu000053	0.43	0.46	0.21	Chloroflexi
Otu000130	0.75	0.35	0.2	Unclassified Bacteria
Otu000127	0.62	0.07	0.2	Chloroflexi
Otu000150	0.65	0.41	0.2	Actinobacteria
Otu000117	0.49	0.46	0.2	Acidobacteria
Otu000152	0.46	0.7	0.2	Gammaproteobacteria
Otu000070	0.67	0.4	0.2	Alphaproteobacteria
Otu000224	0.57	0.24	0.2	Chloroflexi
Otu000159	0.37	0.63	0.19	Alphaproteobacteria
Otu000049	0.2	0.65	0.19	Archaea
Otu000193	0.68	0.4	0.19	Acidobacteria
Otu000109	0.48	0.64	0.19	Gammaproteobacteria
Otu000174	0.39	0.42	0.18	Chloroflexi
Otu000218	0.42	0.57	0.18	Gammaproteobacteria
Otu000154	0.5	0.53	0.18	Acidobacteria
Otu000245	0.54	0.31	0.17	Chloroflexi
Otu000051	0.35	0.54	0.17	Chloroflexi
Otu000153	0.37	0.77	0.17	Unclassified Bacteria
Otu000086	0.89	0.57	0.17	Chloroflexi

Stylissa flabelliformis

Otu000008	1.43	1.74	2.06	Archaea
Otu000013	0.65	1.68	1.63	Archaea
Otu000012	1.85	1.89	0.99	Unclassified Bacteria
Otu000032	0.67	1.03	0.88	Archaea
Otu000002	5.77	5.19	0.86	Gammaproteobacteria
Otu000071	0.44	0.75	0.84	Proteobacteria ARKDMS-49
Otu000052	0.55	0.99	0.8	Archaea
Otu000073	0.82	0.47	0.8	Gammaproteobacteria
Otu000004	3.65	3.54	0.77	Proteobacteria ARKDMS-49
Otu000031	0.83	0.94	0.69	Gammaproteobacteria
Otu000009	2.44	2.23	0.69	Gammaproteobacteria
Otu000120	0.63	0.54	0.67	Gammaproteobacteria
Otu000176	0.62	0.35	0.67	Gammaproteobacteria
Otu000026	1.39	1.21	0.66	Unidentified Proteobacteria
Otu000119	0.66	0.45	0.65	Gammaproteobacteria
Otu000098	0.52	0.54	0.65	Gammaproteobacteria
Otu000007	2.81	2.86	0.56	Proteobacteria ARKDMS-49
Otu000131	0.51	0.75	0.56	Nitrospirae
Otu000093	0.26	0.41	0.56	Nitrospirae
Otu000232	0.12	0.52	0.53	Gammaproteobacteria
Otu000128	0.37	0.41	0.5	Gammaproteobacteria
Otu000121	0.23	0.32	0.5	Gammaproteobacteria
Otu000144	0.32	0.58	0.49	Archaea
Otu000260	0.22	0.43	0.47	Gammaproteobacteria
Otu000315	0.05	0.44	0.46	Archaea
Otu000264	0.27	0.43	0.45	Unclassified Bacteria
Otu000175	0.14	0.34	0.45	Unclassified Bacteria
Otu000145	0.06	0.39	0.42	Proteobacteria ARKDMS-49
Otu000135	0.26	0.21	0.41	Archaea
Otu000173	0.54	0.41	0.41	Proteobacteria ARKDMS-49

Table S3. Sponge sampling details. List of species, morphologies, nutritional mode and sampling location.

Species Name (Author)	Functional Morphology	Primary Nutritional Mode	Sampling Location
<i>Carteriospongia foliascens</i> (Pallas, 1766)	Cup (wide cup)	Phototrophic ¹	Fantome Is. (Palm Is.) S 18°41.028' E 146° 30.706'
<i>Cymbastela coralliophila</i> Hooper & Bergquist, 1992	Encrusting (thick) Cup (table)	Phototrophic ²	Pelorus Is. (Palm Is.) S 18°32.903' E 146° 29.172'
<i>Cliona orientalis</i> Thiele, 1900	Encrusting (bioeroding)	Phototrophic ³	Pelorus Is. (Palm Is.) S 18°32.903' E 146° 29.172'
<i>Coscinoderma matthewsi</i> (Lendenfeld, 1886)	Massive	Heterotrophic ⁴	Pelorus Is. (Palm Is.) S 18°32.903', E 146° 29.172'
<i>Stylissa flabelliformis</i> (Hentschel, 1912)	Erect (laminar)	Heterotrophic ⁵	Pelorus Is. (Palm Is.) S 18°32.903' E 146° 29.172'

1. Ridley, C. P., Faulkner, D. & Haygood, M. G. Investigation of Oscillatoria spongeliae-dominated bacterial communities in four dictyoceratid sponges. *Appl. Environ. Microbiol.* **71**, 7366–75 (2005).
2. Cheshire, A. *et al.* Preliminary study of the distribution and photophysiology of the temperate phototrophic sponge *Cymbastela* sp. from South Australia. *Mar. Freshw. Res.* **46**, 1211–1216 (1995).
3. Schönberg, C. H. L. & Loh, W. K. W. Molecular identity of the unique symbiotic dinoflagellates found in the bioeroding demosponge *Cliona orientalis*. *Mar. Ecol. Prog. Ser.* **299**, 157–166 (2005).
4. Wilkinson, C. R. Net primary productivity in coral reef sponges. *Science (80-.)*. **219**, 410–412 (1983).
5. Pineda, M. C., Duckworth, A. & Webster, N. Appearance matters: sedimentation effects on different sponge morphologies. *J. Mar. Biol. Assoc. United Kingdom* **96**, 481–492 (2016).

Figure S1. Percentage of growth (mean \pm SE) (based on sponge surface area) for all species (except for *Cliona orientalis*) and targeted treatments (SSC: 0, 3, 10, 30 and 100 mg L⁻¹) at the end of the experimental (black) and observational periods (grey).

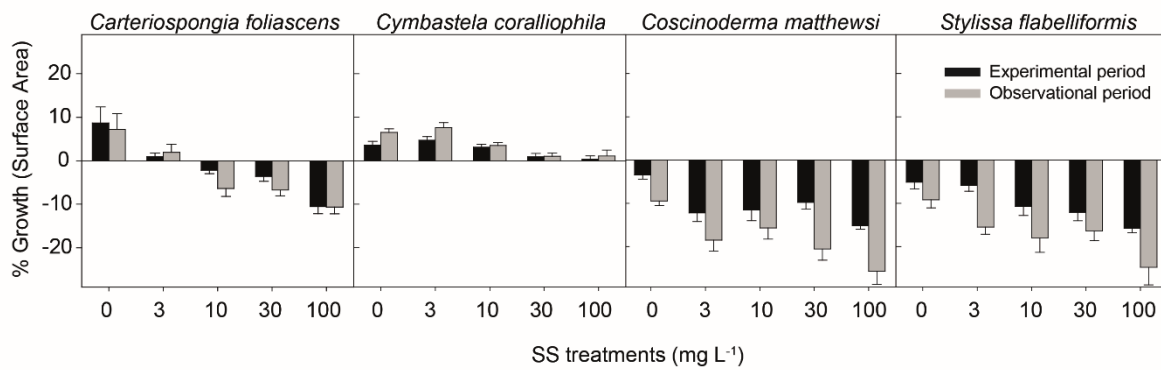


Figure S2. Percentage of mortality for each treatment across the experiment in *Carteriospongia foliascens* and *Coscinoderma matthewsi*.

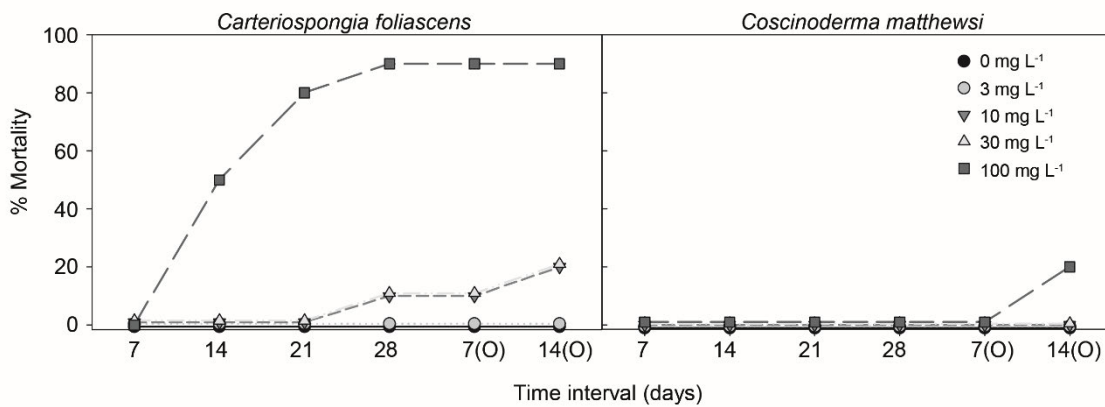


Figure S3. Histological image at 200x of *Cliona orientalis* grown in SSC of a) 0 mg L⁻¹ and b) 100 mg L⁻¹ for 28 days. Arrows indicate photosymbionts (pink cells) while cc refers to choanocyte chambers.

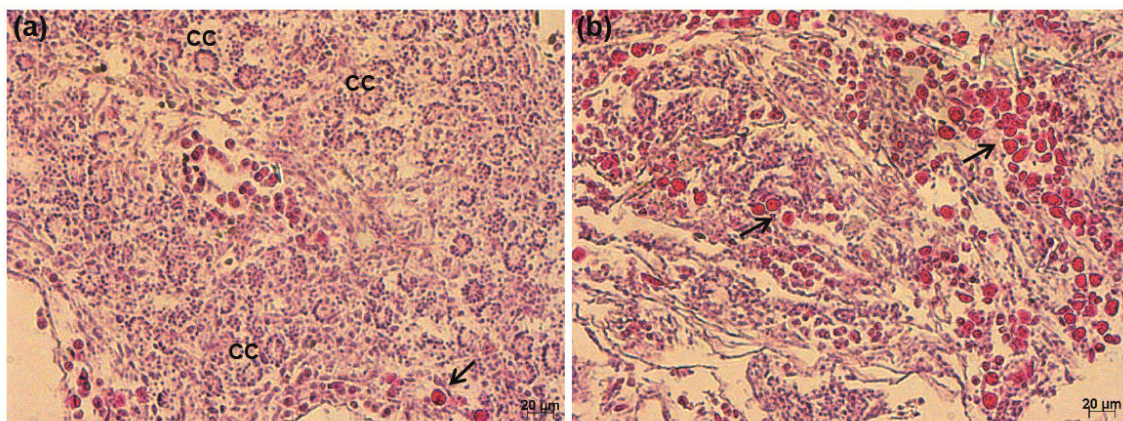


Figure S4. Mean values (\pm SE) of Chl d, for each phototrophic species at all SSC mg L⁻¹ after the experimental and observational periods.

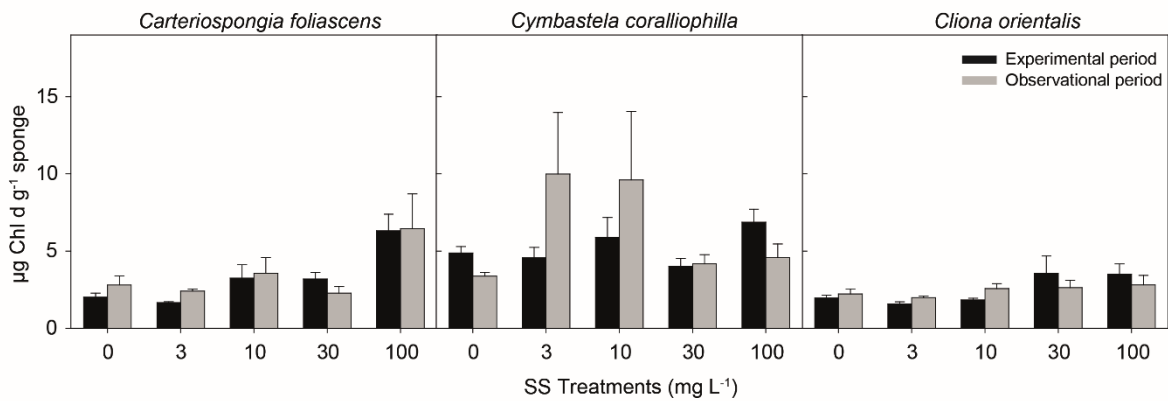


Figure S5. Non-metric Multi-Dimensional Scaling plots on microbial OTU data. nMDS of microbial communities for all 5 sponge species and the environmental control (seawater).

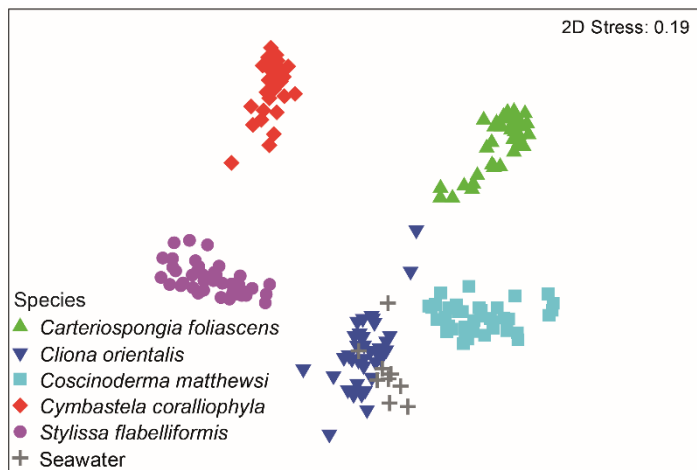
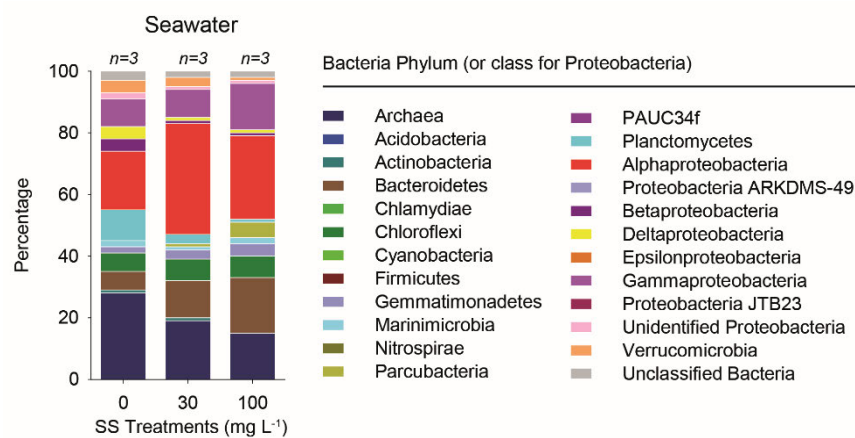



Figure S6. Phylum level bar chart for Seawater (Environmental control). Average relative abundance of each bacteria phylum (and class for Proteobacteria) for 3 replicate seawater samples within each targeted SSC (0, 30 and 100 mg L⁻¹). Only OTUs representing greater than 1% of the overall community were included.



SCIENTIFIC REPORTS



OPEN

Effects of sediment smothering on the sponge holobiont with implications for dredging management

Mari-Carmen Pineda^{1,2}, Brian Strehlow^{1,2,3}, Miriam Sternel⁴, Alan Duckworth^{1,2}, Joost den Haan⁵, Ross Jones^{1,2} & Nicole S. Webster^{1,2}

One of the ways dredging can affect benthic habitats is through high levels of sediment deposition, which has the potential to smother sessile organisms such as sponges. In order to provide pressure-response values to sedimentation and tease apart the different cause-effect pathways of high turbidity, 5 sponge species, including heterotrophic and phototrophic nutritional modes, were exposed for up to 30 d to multiple sediment deposition events, each of which resulted in an initial covering of 80–100% of the surface of the sponges in a layer ~0.5 mm thick. The response of the sponges was examined using a suite of different response variables including growth, respiration, lipid content, community composition of the microbial symbionts, and maximum quantum yield and chlorophyll content of the phototrophic symbionts. Different species showed different mechanisms of sediment rejection and different patterns of sediment clearance. All species survived the treatments, were able to tolerate high levels of partial covering of their surfaces, and for most species the treatment did not alter the health of the sponge holobiont. Results from this study will guide interpretation of experiments examining the combined effects of all three dredging-related pressures, and aid the development of water quality thresholds for impact prediction purposes.

The growing natural resource industry and global expansion of maritime transport have increased the need for capital and maintenance dredging over the past decades, with millions of cubic metres of sediments being displaced annually around the world^{1–4}. The release of sediments into the water column by dredging and dredging activities such as spoil disposal, temporarily increases water turbidity (cloudiness)^{5,6}. The increased suspended sediment concentrations (SSCs) can clog the feeding apparatus of sessile filter feeders⁷ as well as reduce the quantity and quality of benthic light for phototrophs^{3,5–9}. Sediments can remain in suspension for many hours, depending on their particle size and the local hydrodynamic conditions, but will ultimately fall back out of suspension. High sediment deposition rates occur during dredging programs as high SSCs are created in sea-states where ambient hydrodynamics cannot support the load. When sediments deposition rates become too high, sediments can begin to smother benthic organisms and there are many *in situ* observations of this occurring in dredging projects (see photographs in refs 6, 10 and 11). In order to improve the ability to predict and manage the impacts of dredging it is necessary to understand the tolerance of ecologically important habitat-forming species to all potential hazards associated with dredging. In this study, we examine the response of five sponge species (including heterotrophic and phototrophic nutritional modes), to repeated smothering by sediments, complementing earlier studies of the effects of suspended sediments⁷ and light attenuation⁸ on the same species.

Sponges (Porifera) are sessile filter-feeding organisms that play important roles in marine ecosystems, including substrate consolidation, habitat provision, seawater filtration, and linking the benthic and pelagic environments via energy transfer^{12,13}. Sponges are abundant and highly diverse, being the dominant fauna in many regions including some coral reefs, inter-reefal habitats and deep water environments (e.g. refs 14–18). However,

¹Australian Institute of Marine Science (AIMS), Townsville, QLD and Perth, WA, Australia. ²Western Australian Marine Science Institution, Perth, WA, Australia. ³Centre for Microscopy Characterisation and Analysis, School of Plant Biology, and Oceans Institute, University of Western Australia, Crawley, WA, Australia. ⁴University of Bremen, Bremen, Germany. ⁵Max Plank Institute for Marine Microbiology, Bremen, Germany. Correspondence and requests for materials should be addressed to M.-C.P. (email: mcarmen.pineda@gmail.com)

sponge assemblages can also be sensitive to global and local pressures including dredging-associated increases in sediment suspension and deposition^{7, 19–22}. Sponges harbour dense and diverse symbiotic microorganisms which are known to contribute to the health, fitness and nutrition of their hosts²³. In some species, these symbiotic microbes can comprise 40% of the sponge volume and due to their functional importance, we do not consider the symbionts independently, but rather consider the sponge as a stable host-microbe consortium termed the ‘sponge holobiont’²³. Sponge symbionts tend to be highly host specific and are generally stable across broad geographic and environmental gradients²⁴, although loss of symbiont function and holobiont destabilisation has been reported following acute environmental stress²⁵. Importantly, most sponge species are unable to survive environmentally induced symbiont disruption^{8, 26, 27}.

Whilst most sponge species obtain food by filtering particles from the surrounding seawater, >100 different sponge species also supplement their heterotrophic feeding with the autotrophic metabolism of dinoflagellates or microbial photosymbionts^{28–32}. Depending on their degree of nutritional dependence on symbiont primary production, sponges are described as either ‘phototrophic’, ‘mixotrophic’ or ‘heterotrophic’. Notably, some species exhibit considerable flexibility in their feeding strategy and are able to alter their nutritional mode depending on prevailing environmental conditions^{7, 8, 33–35}.

Sediment deposition may differentially affect sponges depending on their morphology, their dependence on heterotrophic versus phototrophic feeding, the stability of their microbiomes as well as other physiological traits²⁰. Sponges known to tolerate sediment stress include endosymbiotic species (living partially buried within sediments), fast growing species with morphological plasticity and species with growth forms that have exhalant openings on apical body parts^{20, 36, 37}. Sponge morphology is a particularly important factor in sediment tolerance, with erect and upright species generally less prone to sediment smothering than encrusting, massive, cups and plate-like morphologies^{19, 20}. Sediment smothering may also block light from reaching the sponge surface, thereby adversely affecting the photosynthetic ability of microbial symbionts. Sediments could also cause temporary closure of the incurrent openings (ostia), affecting water pumping and nutrient uptake by the sponge^{7, 20}. These effects can compromise both phototrophic and heterotrophic feeding, reducing flow of oxygenated seawater to the sponge mesohyl and having flow on consequences for host energetics, health and reproductive output^{7, 19–22, 38}. In addition, while some species may experience a sediment induced shift in the microbiome which enables them to acclimate to the new environmental conditions, other species may undergo microbial changes that destabilise the holobiont and trigger high levels of bleaching and mortality^{7, 8}.

Sponges have a number of cleaning mechanisms to remove sediments from their surfaces and reduce the risk of clogging of the internal canal system. These include mucus production, tissue sloughing, self-cleaning surfaces, sediment removal by epibionts, selective rejection of inhaled particles and the use of water jets to unblock inhalant areas^{20, 39–41}. Some of these self-cleaning strategies are energy-depleting processes which may not be sustainable in the longer term^{19, 20}. Once the capacity to remove sediments becomes overwhelmed, sediments will remain on the sponges’ surface and accumulate. While hard corals are known to be very susceptible to accumulation and smothering, with effects occurring within a few days⁴², the sensitivity of sponges to sediment smothering is not well known. Close to dredging operations, sponges will be exposed to high sediment deposition levels, but this will invariably occur in combination with elevated SSCs and the associated high levels of light attenuation⁶. Simultaneous testing of all dredging-related pressures in combination prevents isolation of the specific effects of sediment deposition alone, precluding identification of cause-effect pathways (mechanisms) and hindering the establishment of potential bio-indicators. The effects of elevated SSCs and low light on 5 sponge species (spanning heterotrophic and phototrophic nutritional modes) has recently been described using a suite of physiological and molecular assays^{7, 8}. In this study, we use the same assays to examine the response of the same species to repeated sediment deposition (i.e. smothering events) over an extended (up to 30 d) period.

Results

Physical parameters. In order to keep a continuous layer of sediment over sponges within the smothered treatment, sediment deposition events ranging from 29 ± 2 to $44.5 \pm 1.9 \text{ mg cm}^{-2}$, were created on days 0, 4, 8, 12, 16, 21 and 24 (mean \pm SE, Fig. 1a). Sedimentation in control tanks ranged between 0.1 – 0.2 mg cm^{-2} . No significant differences occurred between replicate tanks within either the control or smothered treatment at each monitoring time separately (ANOVA: $P > 0.1$). However, significantly higher sedimentation levels were obtained after the initial pulse (Day 0, Fig. 1a, ANOVA: $P < 0.001$), due to the resuspension of previously settled sediments once pumps were turned on to ensure homogenous turbidity after each pulse.

Turbidity values in the tanks during the injection of the sediment (to create the sedimentation events) reached ~430 NTUs, although turbidity rapidly decreased to <10 NTUs within 6 h, and for ~95% of the time turbidity levels were <1 NTU in both the smothered and control treatments (Fig. 1a). Hence, despite the high turbidity levels observed immediately after the sediment pulse, sedimentation/smothering remained the primary dredging-related pressure being applied to sponges in this study. No significant differences in turbidity levels were found between replicate tanks within a treatment (ANOVA: $P > 0.999$).

Sediment clearance rates and removal mechanisms. The sedimentation events typically resulted in an initial coverage of 80–100% of the sponge surfaces across all species in a layer of sediment ~0.5 mm thick. The percentage of sponge surface covered by sediments often decreased on the days following the events (Fig. 1b). The pattern of sediment clearance differed among species, with an overall significant decrease in surface sediments after the initial event, but the ability to clear the sediment decreased after subsequent events in *Carteriospongia foliascens*, *Cymbastela coralliophila* and *Coscinoderma matthewsi* ($P < 0.0001$, < 0.001 and < 0.001 , respectively) (Fig. 1b). In contrast, *Cliona orientalis* and *Stylissa flabelliformis* maintained similar clearance rates throughout the experiment. *C. orientalis* was more effective at removing sediment than *S. flabelliformis*, with sediment cover significantly decreasing from 80 to 20–40% at 3 d post-deposition, while the latter species showed higher

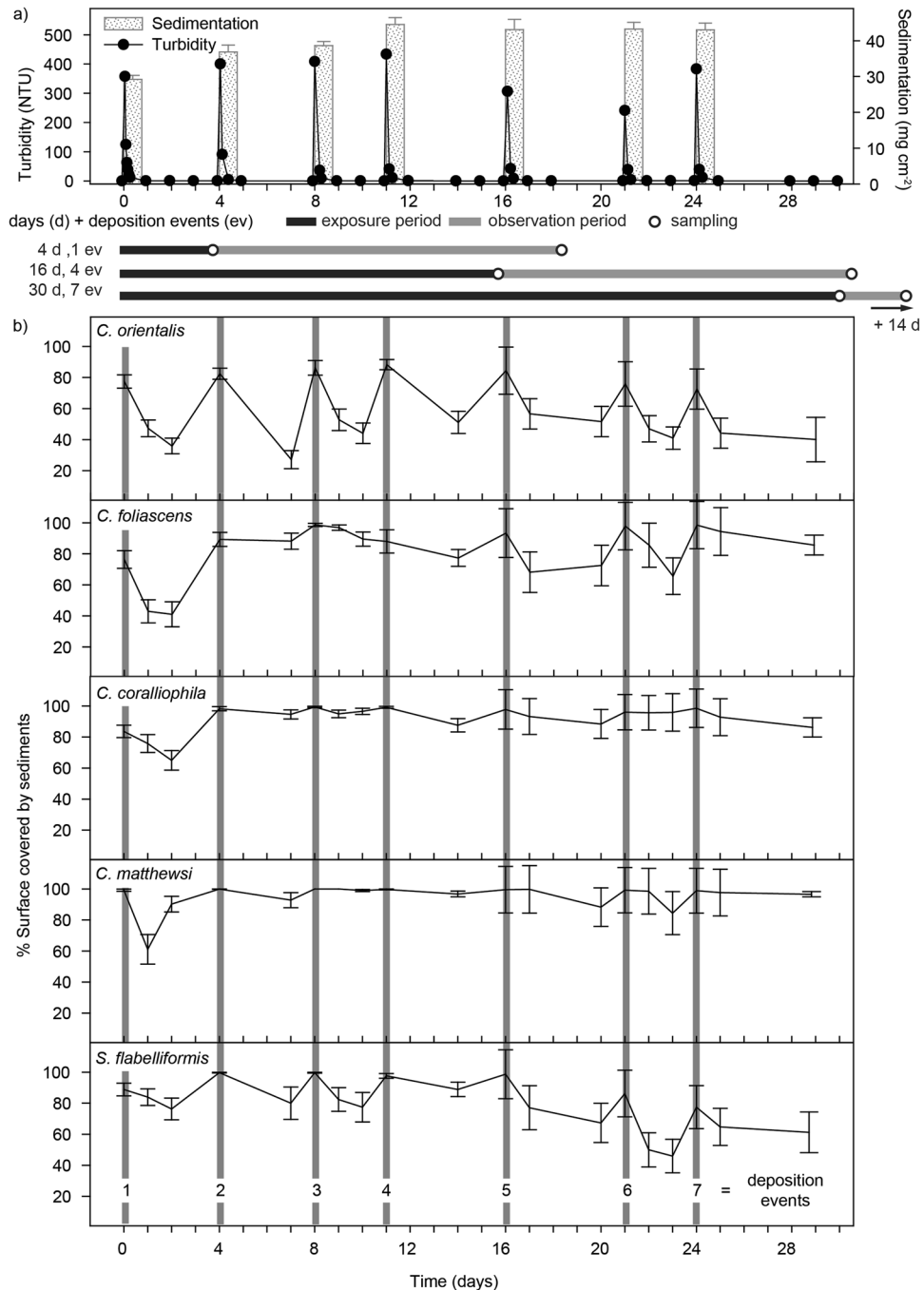


Figure 1. Sediment behaviour across the experiment. Mean values (\pm SE) of (a) sedimentation and turbidity levels in the smothering treatments. Deposition events occurred every ~4 d with sponges being exposed to either 1, 4 or 7 deposition events and then transferred to clean seawater (for a 14 d observation period), and (b) percentage of sponge surface covered by sediments for each species, throughout the experiment.

variability and >50% of its surface remained covered throughout the experiment ($P < 0.0001$ and < 0.0001 , respectively) (Fig. 1b). Sponges demonstrated an array of different mechanisms for coping with sedimentation, such as sediment sloughing via spicule hispidity and removal of surface sediment by infauna such as brittle stars (Supplementary Fig. S1). Mucus production was also observed in *S. flabelliformis* and *C. foliascens* and the peeling of the sediment-impregnated mucus resulted in a comparatively sediment-free surface in these species (see Supplementary Fig. S1).

Sponge health, growth and necrosis. All sponges survived the 4, 16 and 30 d treatments and subsequent observational phase, and necrosis was not observed in any species. The partial sediment covering caused no visible signs of stress in most sponges, with the exception of some (~7%) partial bleaching in the phototrophic

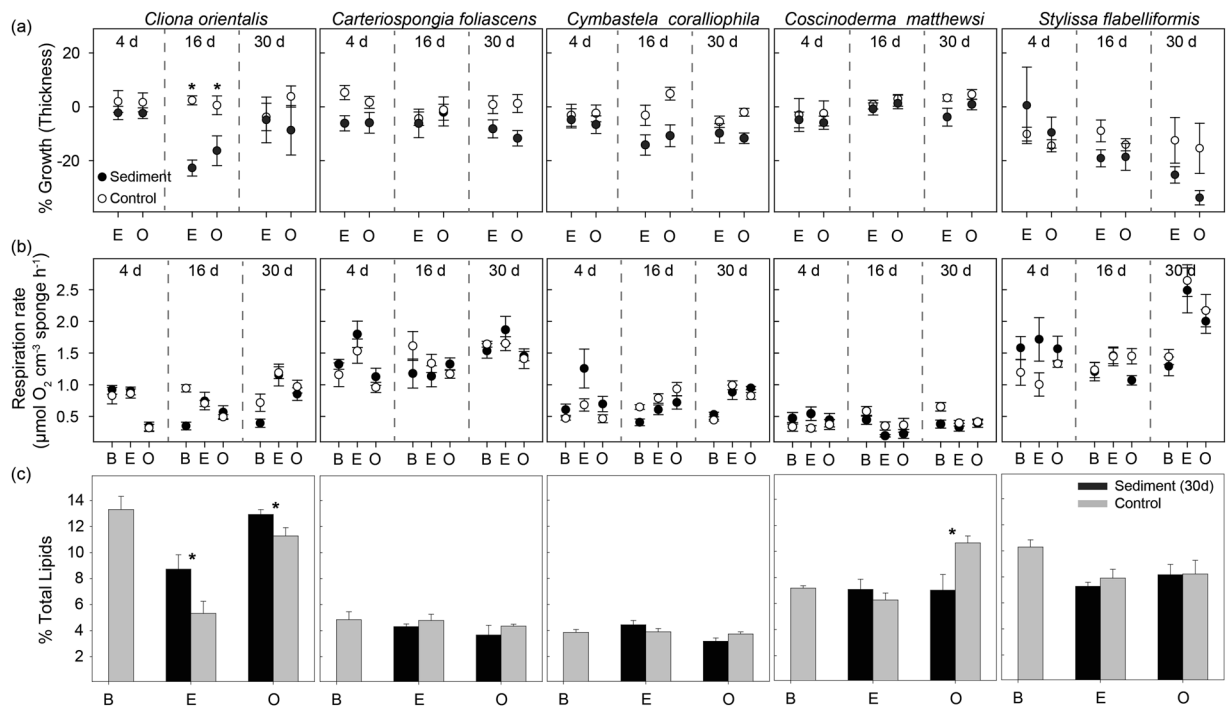


Figure 2. Physiological responses of sponges to sediment smothering. **(a)** Percentage of growth (based on sponge thickness), **(b)** Mean respiration rates ($\mu\text{mol O}_2 \text{ cm}^{-3} \text{ sponge h}^{-1}$) for all species and treatments (control vs. smothered for 4, 16 or 30 d), **(c)** Percentage of sponge biomass comprised of lipids, for all species exposed for 30 d, where 'B' is before sediment addition, 'E' is after the exposure period and 'O' is at the end of the observational phase. All data are mean \pm SE and asterisks show statistically significant differences between smothered and control sponges (t -tests: $P < 0.05$).

species *C. orientalis* in the 16 d and 30 d treatments, although this species recovered its initial appearance by the end of the observational phase. No visible effects of sediment covering were observed in any of the other species at the end of the experiment.

Analysis of growth rates based on tissue thickness measurements showed negative growth in most sponges covered by sediments for 16 and 30 d, although the response was species-specific and significant differences between controls and smothered sponges were only observed in the phototrophic species *C. orientalis* (Fig. 2a).

Respiration Rates. Overall sponge respiration rates were not significantly different between treatments (control vs. smothered) before the deposition events ($t=0$), with species-specific responses following sediment exposure (Fig. 2b). In general, a rapid increase in respiration rates was observed in the sponges covered and partially covered for 4 d, although this was not significantly different to the controls (Fig. 2b). Respiration rates in *C. foliascens* and *C. coralliophila* smothered for 4 d were significantly higher than before exposure (Fig. 2b, Table 1B). A similar response was observed in *C. orientalis* and *C. coralliophila* after 16 d and in *S. flabelliformis* after 30 d (Table 1B). However, similar respiration rates between controls and smothered samples were observed under the longer term treatments (16 and 30 d) (Fig. 2b).

Lipids. Total lipid content (representing 2–16% of total sponge biomass) was highly stable in all studied species across the 30 d exposure period and subsequent 14 d observational period (Fig. 2c). Overall, smothered sponges did not have lower lipid concentrations. In contrast, *C. orientalis* had a higher percentage of lipids per biomass in the sediment treatment (Fig. 2c, Table 1C). In addition, significantly lower lipid content was detected in sediment-exposed samples of *C. coralliophila* after the observational phase, in comparison with samples at the end of the exposure time (Table 1C). *C. matthewsi* had significantly higher lipid content in control samples during the observational period. *C. foliascens* and *S. flabelliformis* did not show any significant change in lipid content throughout the experiment (Fig. 2c, Table 1C).

Hyperspectral imaging. Hyperspectral imaging revealed that the relative chlorophyll content derived from reflectance spectra over the surface of the specimens differed significantly between species, with higher chlorophyll in *C. orientalis*, followed by *C. coralliophila* and *C. foliascens* (ANOVA: $P < 0.001$). Hyperspectral scans of smothered sponges yielded negligible relative chlorophyll contents (0.34 ± 0.1 , 0.08 ± 0.08 and 0.04 ± 0.01 in *C. orientalis*, *C. foliascens* and *C. coralliophila*, respectively, mean \pm SE). However, the chlorophyll signal became clear once sediment was removed and significantly lower chlorophyll content was detected in smothered sponges than in control individuals for all species (ANOVA: $P < 0.05$, Fig. 3a, Supplementary Table S1). However, after

Source	df	<i>C. orientalis</i>		<i>C. foliascens</i>		<i>C. coralliophila</i>		<i>C. matthewsi</i>		<i>S. flabelliformis</i>	
		F	P	F	P	F	P	F	P	F	P
(A) Growth											
Treatment	5	5.46	0.008	1.735	0.201	2.556	0.085	1.666	0.2171	1.797	0.188
Time	1	0.215	0.645	0.001	0.974	1.398	0.243	0.945	0.336	2.600	0.114
Treat. × Time	5	0.442	0.817	0.588	0.709	0.964	0.449	0.226	0.950	0.244	0.941
Error	48										
Significant Pairwise Multiple Comparisons (Tukey)											
Treatment		16 d-C > 16 d-S 4 d-S > 16 d-S									
(B) Respiration Rates											
Treatment	5	2.154	0.12	2.558	0.084	2.465	0.093	2.056	0.144	6.530	<0.01
Ind.(Treatment)	30										
Time	2	32.269	<0.001	8.345	<0.001	64.397	<0.001	8.885	<0.001	8.208	<0.001
Treat. × Time	60	11.453	<0.001	2.097	0.039	6.447	<0.001	2.168	0.033	2.823	<0.01
Error	107										
Significant Pairwise Multiple Comparisons (Tukey)											
Time				B > O		B < O		B > E, O			
Time within 4 d-S		B, E > O		B < E > O		B, O < E					
Time within 16 d-S		B < E				B < E, O		B > E, O			
Time within 30 d-S		B < E > O				B < E, O				B < E, O	
Treatments within E				16 d-S < 30 d-S		4 d-S > 16 d-S		4 d-S > 16 d-S			
Treatments within O										16 d-S < 30 d-S	
(C) Percentage of sponge biomass comprised of lipids											
Time	1	39.043	<0.001	1.448	0.295	7.882	0.047	8.4428	0.010	0.692	0.418
Treatment	1	9.888	0.034	1.444	0.247	0.004	0.951	1.887	0.242	0.144	0.724
Treat. × Time	20	1.187	0.292	0.039	0.846	4.642	0.013	8.836	0.009	0.154	0.700
Error	23										
Significant Pairwise Multiple Comparisons (Tukey)											
Time		E < O						E < O			
Treatment		C < S									
Treat. × Time						[S] E > O		[C] E < O; [O] C > S			

Table 1. ANOVA tables and summaries of linear mixed models testing the effects of smothering on the physiological responses of sponges. (A) Percent growth rate based on thickness measures, (B) Respiration rates and (C) Percentage of sponge biomass comprised of lipids. Tukey tests have been performed for significant pairwise multiple comparisons. Abbreviations: ‘B’ for before sediment pulse (T = 0), ‘E’ for end of experimental phase, ‘O’ for end of observational period, ‘C’ for controls, ‘S’ for smothered, and ‘4 d’, ‘16 d’ and ‘30 d’ for time smothered.

24 h recovery from sediment exposure, the relative chlorophyll content was not significantly different from the control group for any species, indicating rapid recovery potential (Fig. 3a).

The recovery response was observed in greater detail for *C. orientalis* (Fig. 3b,c). This species appeared to be capable of manipulating and consolidating the settled sediments into discrete patches which were typically observed in the central areas and usually in surface troughs or depressions (Fig. 3b-2, see also Supplementary Fig. S1). Following sediment removal, the areas under the sediment appeared bleached (Fig. 3b-3). Time-lapse photography revealed near full recovery of the bleached patches within 52 h (Fig. 3c), and full recovery after 6 d (Fig. 3b-4). The bleached area recovered from the centre outwards as well as from the borders inwards, indicating that *Symbiodinium* sp. cells are migrating not only from the unbleached tissue but also possibly from a population residing deeper within the sponge where the substrate has been excavated.

Chlorophyll fluorescence. The photosynthetic efficiency of sponge symbionts was only affected by sediment in *C. orientalis*, with significantly lower quantum yields from smothered samples at the end of the 16 and 30 d experimental period (Fig. 4a, Table 2A). This result is consistent with the observed bleaching in this species. Maximum quantum yield values returned to control levels after the 14 d observational period and colouration also recovered during this period (Fig. 4a). Increased yield values after only 4 d of smothering indicates an initial photoacclimation response in this species, although longer term sediment exposure appears to damage the photosystems (Fig. 4a). There were few significant changes in yield values among the other two phototrophic species, *C. foliascens* and *C. coralliophila*, with only minor fluctuations through the experiment and observational periods (Fig. 4a, Table 2A).

Pigment analysis. Total chlorophyll was found to be highly correlated to Chl a in all 3 phototrophic species ($R^2 = 0.999, 0.998, 0.952$ and $P < 0.001$; for *C. orientalis*, *C. foliascens* and *C. coralliophila*, respectively) and

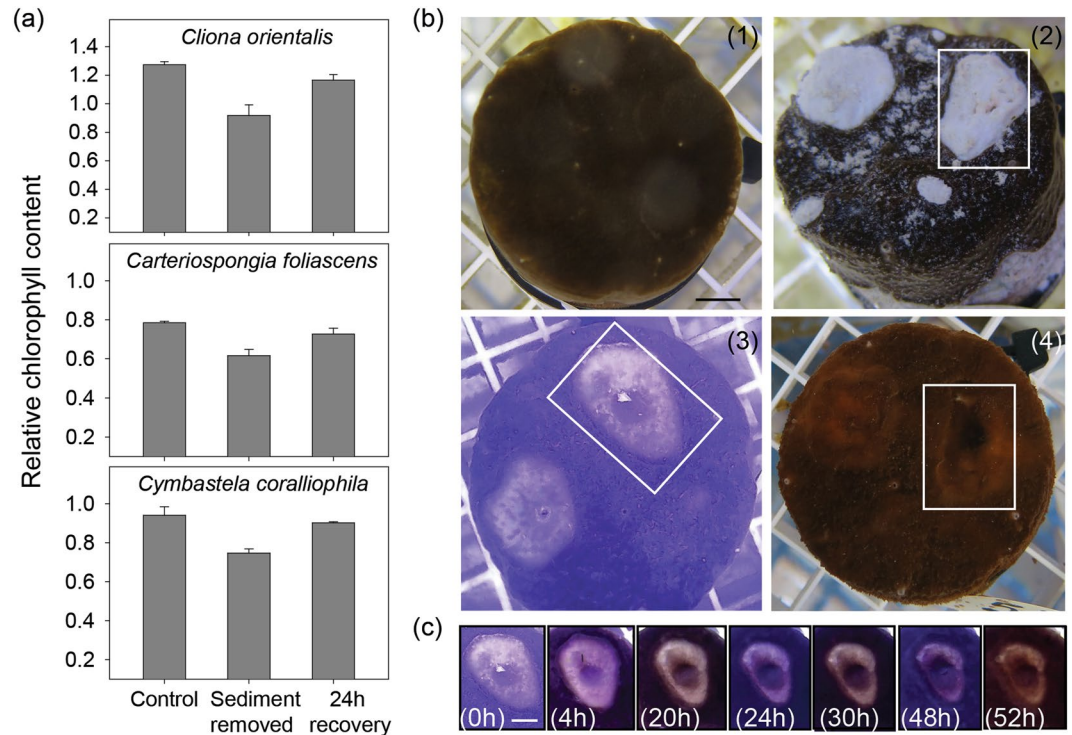


Figure 3. *In-situ* chlorophyll assessment using hyperspectral and time-lapse imaging. **(a)** Relative chlorophyll content of the three phototrophic sponge species smothered with sediments for 8 d (mean \pm SE); **(b)** Bleaching recovery in *C. orientalis* following treatment with sediments for 30 d: (1) Before exposure to sediments (T = 0), (2) During smothering, (3) Bleached area (note white rectangle) evident following sediment removal, (4) Colouration after 6 d recovery; **(c)** Time-lapse recovery following sediment clearance (0 h) until 52 h later (scale = 1 cm).

overall, concentrations of Chl a were stable in the 3 phototrophic species throughout the experiment (Fig. 4b). Lower concentrations of Chl a were only detected in *C. orientalis* smothered by sediment for 30 d and *C. coralliophila* for 16 d, although this was not significantly different to the respective controls (Fig. 4b, Table 2B). Non-metric Multi-Dimensional Scaling (nMDS) analysis of normalized data for all pigments retrieved by spectrophotometry (Chl a, Chl b, Chl c, Chl d, total chlorophylls and carotenoids) showed no grouping according to smothering time (Fig. 4c). PERMANOVA analysis detected marginally significant differences between smothering times in *C. foliascens* (Table 2C).

Microbial community analysis. A total of 9,136,254 high quality 16S rRNA gene amplicon sequences were recovered from the 5 sponge species (n = 169 individual samples) and 6 seawater samples. Each sponge species maintained a unique microbial community (Table 3A, Fig. 5, see also Supplementary Fig. S2) that was distinct from the microbial community of the seawater (Table 3B, Supplementary Figs S2, S3). Aquarium acclimation (for 4 weeks) did not affect the sponge-associated microbial community of any species (Table 3A), although significant differences were observed between field/time 0 and experimental/observational samples in all species (Table 3A). The 30 d smothering treatment did not have a major impact on the overall composition of the sponge microbiome at the phyla level (Fig. 5b), and no significant differences were detected at the OTU level (97% sequence similarity) for any species (Table 3C). In addition, no clear groupings were observed in the ordination (Fig. 5a). For all species, network analyses of the 30 most discriminatory operational taxonomic units (OTUs) for the control sponges and sponges smothered for 30 d, revealed phylogenetically diverse and stable core microbiomes (i.e. the component shared between all samples), as well as treatment-specific OTUs (Fig. 4c, Supplementary Table S2). In each species, the number and taxonomy of OTUs observed exclusively in control samples was generally balanced by the number and taxonomy of new OTUs that were observed only in sediment-exposed samples. Also of note was the finding that core *Cyanobacteria* OTUs in the two photosynthetic species *C. foliascens* and *C. coralliophila* were not disrupted by the sediment exposure.

Discussion

All sponges survived the repeated deposition events and subsequent sediment covering, with no partial mortality and few observable physiological effects. To separate cause-effect pathways for dredging related pressures, this experiment focussed on the effects of sediment deposition (i.e. smothering). The SSCs in the experimental tanks were very low once sediments had settled out of suspension, and were typically $<1-2 \text{ mg L}^{-1}$ for 95% of the exposure periods. All species showed the ability to clear some of the sediment from their surfaces although the self-cleaning capacity varied considerably between species. The highest self-clearance was observed in *C.*

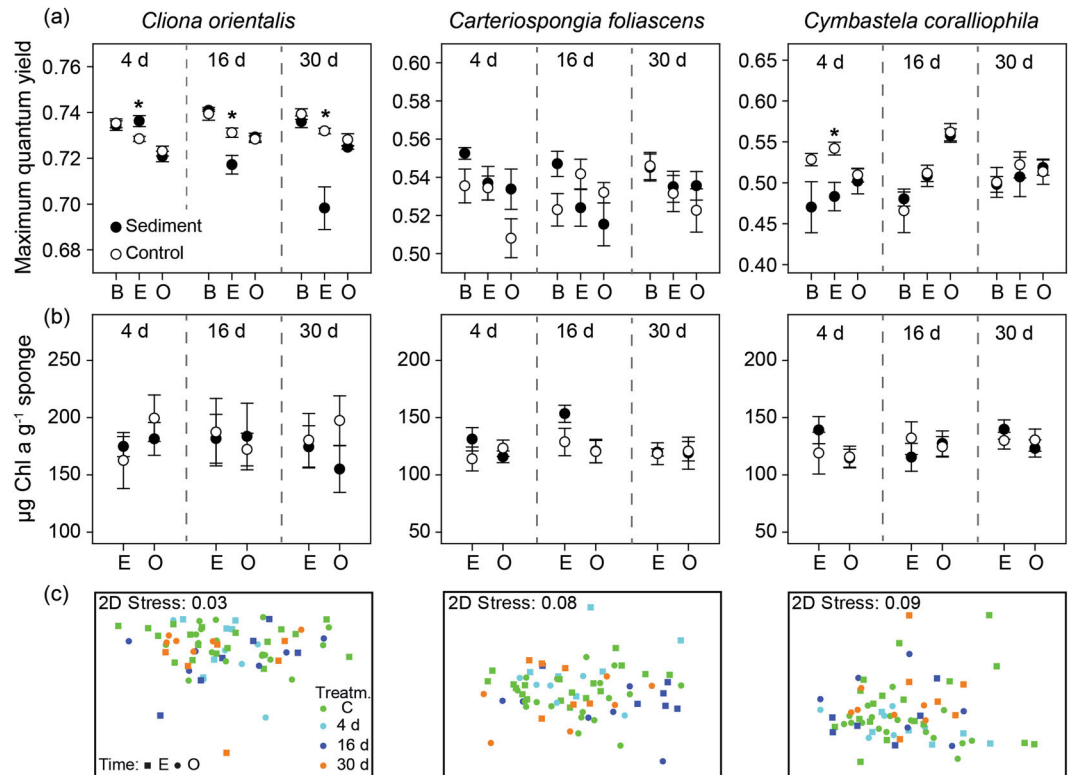


Figure 4. Responses of photosymbionts to smothering treatments. **(a)** Mean values (\pm SE) of maximum quantum yield, **(b)** Mean values (\pm SE) of Chl a, and **(c)** Non-metric Multi-Dimensional Scaling (nMDS) of all photopigments retrieved by spectrophotometry, for the 3 phototrophic species and for all smothering treatments (4, 16 and 30 d smothered vs. controls), before exposure **(b)** and through the experimental (E) and observational periods (O). Asterisks show statistically significant differences between controls and smothered samples (Table 2) (t-tests: $P < 0.05$).

orientalis followed by *S. flabelliformis* and *C. foliascens*. Both *C. coralliophila* and *C. matthewsi* were less effective and remained with $>85\%$ of their surface covered with sediment for the most of the study.

Sponge morphology provided a passive mechanism for sediment rejection. Erect growth forms are expected to be less affected by sedimentation^{20,22}, and in this experiment, the erect sponge *S. flabelliformis* had some of the highest sediment removal rates. Massive and cup shaped sponge species are prone to sedimentation^{19,20,22,43,44} consistent with the high sediment covering ($>70\text{--}80\%$ of their surface) observed here in the massive species *C. matthewsi* and cup morphologies *C. foliascens* and *C. coralliophila*. Other strategies used by sponges to cope with heavy sedimentation rates include sediment sloughing via mucus production (reviewed in ref. 20) and the production of a mucus-like substance was particularly prominent in *C. foliascens* and *S. flabelliformis* (see Supplementary Fig. S1). For vertically oriented planes of tissue, the production and subsequent sloughing of the sediment-impregnated substances resulted in clean underlying tissue surfaces (see Supplementary Fig. S1). The term mucus is used here in a broad sense (see ref. 45) as no attempt was made to identify the nature of the mucus-like layers. The production of similar mucus-like layers (also referred to as sheets, envelopes, webs, films, mats and tunics) which collect sediment and then peel from the surfaces have been described in scleractinian corals (principally *Porites* spp., ref. 46), and appear to play a similar self-cleaning role^{10,47}.

The phototropic, bioeroding sponge *C. orientalis* manipulated and cleaned its surfaces of sediments differently to the other experimental species. *C. orientalis* showed the highest clearance rate, was capable of removing 60–80% of the sediment covering its surface within a few days, and did not lose this ability despite multiple deposition events. *C. orientalis* appears to be able to manipulate settled sediment as evidenced by the discrete sediment patches with well-defined edges, located on otherwise sediment-free tissue. The sediment patches were rarely seen on the sponge periphery and were often located in central hollows or concave areas. These observations suggest that some species are capable of moving and shedding sediment from the edges, as long as the sediment doesn't become trapped in local depressions (see below). Similar sediment-shedding has been seen in encrusting scleractinian corals associated with muco-ciliary transport⁴⁸, although the mechanism of sediment manipulation in *C. orientalis* is still unclear. Clionaid species have a microhispid surface where spicules protrude from the surface for 0.1–2 mm, and it has been suggested that this creates surface roughness that prevents adherence of dirt and induces passive self-cleaning, repelling debris^{20,40}. For clay and fine silt sized particles ($<30\mu\text{m}$) as used in these experiments (and typically encountered in dredging plumes⁶), this bristly surface is more likely to trap and prevent the movement of sediments, rather than repelling them. In scleractinian corals, pulsed tissue contraction is an additional mechanism to mobilize settled sediments and a parallel mechanism may exist for *C. orientalis*.

Source	df	<i>Cliona orientalis</i>		<i>Carteriospongia foliascens</i>		<i>Cymbastela coralliophila</i>	
		F	P	F	P	F	P
(A) Maximum quantum yield							
Treatment	5	5.10	0.01	0.850	0.542	1.777	0.192
Time	2	46.00	<0.001	8.860	<0.001	11.832	<0.001
Treatm. × Time	10	10.10	<0.001	1.780	0.084	2.430	0.017
Error	60						
Tukey							
Time		O < B				B < O; E < O	
Time within 4 d-S		B, E > O				B < O	
Time within 16 d-S		B > E, O; E < O		B > O		B < O	
Time within 30 d-S		B > O					
Treatment within E		4 d-S > 16 d-S, 30 d-S 30 d-C > 30 d-S					
(B) Chl a							
Treatment	5	0.250	0.932	0.847	0.543	0.450	0.778
Time	1	0.149	0.701	2.114	0.153	1.074	0.305
Treatm. × Time	5	0.496	0.777	1.373	0.2511	0.684	0.638
Error	60						
(C) PERMANOVA of all pigment data							
Treatment	5	0.53843	0.8182	2.2158	0.0332	0.4343	0.1679
Time (Treatment)	6	0.6232	0.7694	1.199	0.299	1.6895	0.078
Error	60						
Pair-wise Tests				4 d-C, 16 d-C, 4 d-S ≠ 16 d-S ≠ 30 d-S			

Table 2. ANOVA tables and summaries of linear mixed models of the effects of smothering on the photosymbionts. (A) The effects of treatment and time on maximum quantum yield throughout the experiment with Tukey tests performed for significant pairwise multiple comparisons, (B) The effects of treatment on Chl a concentrations across time (at the end of the experimental (E) and observational (O) periods) and treatment, with Tukey tests performed for significant pairwise multiple comparisons, and (C) Two-way PERMANOVA of all pigment data (Chl a, b, c, d, total Chl and carotenoids) with sediment treatment and time as factors, for the 3 phototrophic species (sediment treatments: 4, 16 and 30 d smothered vs. controls).

Sponge respiration rates have been reported to fluctuate greatly in response to elevated suspended sediments^{7,49–51}, but sediment smothering for 30 d did not impact sponge respiration. The lack of significant effects on respiration is consistent with the absence of sponge necrosis or mortality, as opposed to the high mortality rates and bleaching observed in response to high SSC in previous experiments⁷. However, the slight increase in respiration rates observed after 4 d of sediment smothering in most species was concomitant with higher clearance rates and increased mucus production indicating an initial short-term response as sponges activate their cleaning mechanisms to remove sediments. Respiration rates were nevertheless consistent after 16 and 30 d exposure, suggesting a longer term acclimation to sedimentation. Increased respiration rates after short-term acute sediment exposure have been reported in the massive sponge species *Rhopaloeides odorabile*⁵¹ and *Coscinoderma matthewsi*⁷, although decreased respiration rates have been described in other species exposed to chronic levels of high suspended sediments^{7,49,50}, likely in an attempt to reduce clogging of their aquiferous systems.

Previous research has suggested that whilst sponges with high clearance rates may perform better in environments where there is high sedimentation, this cleaning strategy is likely to be energetically taxing, with longer term implications for energy reserves²⁰. In this study there was no clear effect of sediment smothering on total lipid content in any species. However, significantly higher lipid content in smothered versus control *C. orientalis* samples was observed, which may relate to an increase in *Symbiodinium* populations in an attempt to elevate phototrophy, as has been observed in response to high SSC⁷. These results clearly demonstrate that repetitive smothering events for up to 30 d do not cause a decrease in nutritional reserves. This contrasts with previous research assessing the impact of elevated SSCs, where an overall decrease in lipid content, especially among the heterotrophic species was observed⁷. Negative growth rates were observed in most sponges exposed to 16 and 30 d of smothering; however, 30 d of sediment smothering did not cause any total or partial mortality, visible signs of host stress (e.g. bleaching or necrosis), lipid depletion, changes in sponge respiration rates or effects on the microbial composition of any species.

The primary exception to the lack of visible signs of stress was partial discolouration (bleaching) in the phototrophic species *C. orientalis*. As discussed earlier, *C. orientalis* appears capable of clearing sediments from its surface although small patches of sediments were observed in local surface depressions and remained there for extended periods. Significantly higher photosynthetic yields in *C. orientalis* after the 4 d treatment suggested some initial photoacclimation, as reported for other sponges under low light or sediment exposure^{8,19,52}. However, in *C. orientalis* this photoacclimation could not be maintained in the long term. Lower photosynthetic yields and Chl a concentrations and bleaching were seen in the 16 d and 30 d treatments, and in areas where sediments had

Source	df	MS	Pseudo-F	P (perm)
(A)				
Species	4	73933	36.478	0.0001
Time	3	4040.6	1.9936	0.0001
Species × Time	12	2978.2	1.4694	0.0001
Residuals	145	2026.8		
Pair-wise Tests CLI:F ≠ E,O; CAR:F ≠ E ≠ O; CYM: T0 ≠ O; COS: F,T0 ≠ E,O; STY: F ≠ E,O				
(B)				
Source	1	23050	5.3963	0.0001
Residuals	169	4271.5		
(C)				
<i>C. orientalis</i>				
Treatment	1	3316.9	1.23335	0.1431
Time (treatm.)	2	2872.8	1.0684	0.2923
Residuals	18	2689		
<i>C. foliascens</i>				
Treatment	1	1989.6	1.0912	0.2612
Time (treatm.)	2	2020.2	1.108	0.1326
Residuals	20	1823.3		
<i>C. coralliophila</i>				
Treatment	1	2048.2	1.0691	0.3399
Time (treatm.)	2	1619.3	0.84523	0.854
Residuals	20	1915.8		
<i>C. matthewsi</i>				
Treatment	1	2558.5	1.18888	0.1192
Time (treatm.)	2	2774.7	1.2892	0.0205
Residuals	20	2152.2		
<i>S. flabelliformis</i>				
Treatment	1	1485.4	0.95496	0.5617
Time (treatm.)	2	1889.1	1.2145	0.0728
Residuals	22	1555.4		

Table 3. PERMANOVA analyses of the microbiome community. PERMANOVA with (A) species and time as factors, (B) source as factor (sponge host vs. seawater) and, (C) sediment treatment and time (nested to treatment) as fixed factors for all 5 sponge species. In pair-wise tests, F: field control, T0: time 0 control, E: sampling at the end of the exposure time (i.e. 30 d), O: sampling after the 14 d observational period; CAR for *C. foliascens*, CYM for *C. coralliophila*, CLI for *C. orientalis*, COS for *C. matthewsi* and STY for *S. flabelliformis*; Control (C) and smothered (S) within treatments.

overlain the tissues for at least 8 consecutive days. The light attenuating properties of sediment are well known, and light transmission through a 66 mg (dry weight) layer of silt-sized sediments (similar to the exposure conditions used here) is reduced to 0.2–7.7%⁴². Partial sponge bleaching was likely a response to light deprivation under the sediment layer, but once removed there was full recovery of colour in the observational phase. In fact, all phototrophic species experienced total recovery of Chl a in less than 2 d once sediments were removed, as evidenced by hyperspectral and time-lapse imaging. The recovery of bleached areas of *C. orientalis* within ~6 d was facilitated by symbionts rapidly repopulating from unbleached areas, consistent with symbiont translocation patterns previously described in this species⁵³.

In addition to changes in photosymbionts, the composition of the sponge microbiome at both the phyla and OTU levels was unaffected by 30 d of sediment smothering, with cyanobacterial OTUs maintained in all sediment-smothered sponges. The only exception to the microbiome stability was a small increase in Archaea in smothered samples of *S. flabelliformis*, and also in water samples from tanks where the sediment-exposures occurred. This result contrasts with previous experiments where the microbial community rapidly shifted in response to other dredging related pressures (i.e. light attenuation). Microbiome shifts are known to destabilise the sponge holobiont and cause subsequent mortality of some species (e.g. *C. foliascens*)^{7,8}. Hence, although sediment smothering does not appear to impact symbiont health and composition, continuous and complete smothering which results in prolonged light attenuation may affect holobiont health in the longer term.

Different sponges have different strategies to cope with sediments and in some cases these can be beneficial, with some species incorporating sediments into their tissues to reinforce outer layers and provide shade³⁶, and others living partially embedded in sediments (psammobiosis) to reduce the risk of spongivory³⁶. However, sediments can also be detrimental, and previously we have shown that high SSCs alone (in the absence of light attenuation or sediment smothering) resulted in negative sponge growth and decreased respiration rates in most

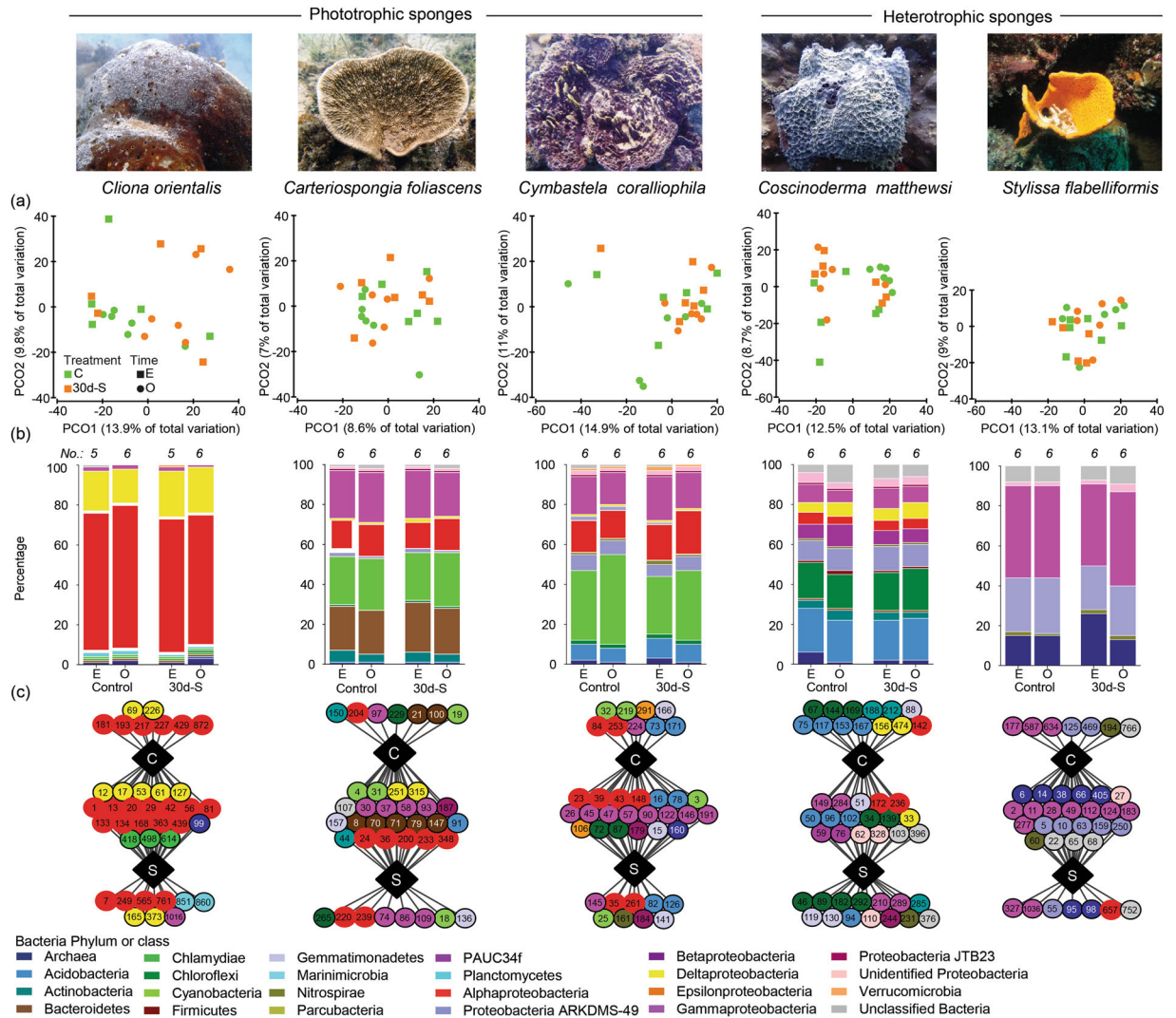


Figure 5. Microbial responses to smothering. (a) Principal coordinate analysis plots for control and samples smothered for 30 d (30d-S) at the end of the experimental period (E) and 14 d observational period (O), (b) Average relative abundance of each bacterial phylum (and class for *Proteobacteria*) using OTUs representing greater than 1% of the community for 30d-S vs. control samples across both sampling times, (c) Cytoscape networks of the microbial community in all species for controls (C) versus 30d-S samples (S) across both sampling times.

species, and necrosis and mortality within the cup sponge *C. foliascens*, and to a lesser extent in the massive sponge *C. matthewsi*⁷. In another study, light attenuation (in the absence of elevated SSCs or sediment smothering) impacted the phototrophic species *C. orientalis* and *C. foliascens*⁸, resulting in tissue bleaching. Although *C. orientalis* exhibited full recovery under normal light conditions, *C. foliascens* did not, showing high levels of mortality⁸. Results from this study, where sediment deposition was isolated as the primary variable, showed that repeated deposition events and near continual covering of the sponges in a sediment layer for an extended period did not cause sponge mortality. Some species seem capable of existing partially or fully covered in sediment i.e. *C. coralliophila* and *C. matthewsi*, while other species possess an ability to self-clean, i.e. they have active sediment-rejection mechanisms. However, when these mechanisms become overwhelmed and sediments build-up, localized reductions in Chl a concentrations or partial bleaching can occur, e.g. *C. orientalis*. The cause-effect pathway is likely to involve light limitation, and the effect is rapidly reversible upon removal of the sediment. In conjunction with previous research on the impacts of light attenuation⁸ and SSC⁷, thresholds can now be used in water quality monitoring programs to alert dredging proponents to levels of light reduction, SSC and sedimentation that, if continued, could detrimentally impact sponge populations.

Relating these findings to conditions that can occur *in situ* during dredging programs, or natural wind and wave induced sedimentation events is difficult because of the problems associated with accurately measuring sediment deposition rates in shallow benthic environments at the appropriate sensitivity and temporal scale (i.e. mg cm⁻² over hours or days, reviewed in ref. 54). Sediment traps have been used extensively to estimate ‘sedimentation’ rates on reefs but are more apt to record information on suspended-sediment dynamics than to

provide any useful data on sedimentation *per se*⁵⁵. Two recent studies have measured sediment deposition rates at a highly turbid site in the inshore zone of the Great Barrier Reef. The techniques used which involved shallow trays⁵⁶ and a newly configured sediment deposition sensor⁵⁷, do not suffer from the resuspension-limitation and deposition-bias associated with traps. Estimates of net sedimentation were 3–7 mg cm⁻² d⁻¹ (over the course of a year)⁵⁶ and ~8 mg cm⁻² d⁻¹ (during typical conditions where SSCs ranged from 1–28 mg L⁻¹)⁵⁷. The deposition rates in this experiment (30–45 mg cm⁻² d⁻¹) were up to 6× higher than levels found in the highly turbid inshore reef system. Experimental deposition events initially resulted in 80–100% of the sponges surface being covered with a 0.5 mm thick layer of sediment and sponges in some treatments were exposed to up to 7 such deposition events over an extended 30 d period. We consider the exposure regimes in terms of intensity, duration and frequency to be extreme compared to what can occur naturally *in situ* and the resulting smothering of the sponges is consistent with *in situ* observations of smothering of benthic organisms close to dredging projects.

In summary, exposure over an extended period to multiple discrete sediment deposition events resulting in a near continuous covering of sediment on their surface did not alter the health of most adult sponges. Sponges possessed either active or passive self-cleaning strategies which allowed them to continue feeding, and were able to tolerate quite high levels of partial covering of their surfaces by sediment. These experiments were designed to examine a specific cause-effect pathway associated with sediment deposition alone. In reality, during dredging, sponges would be exposed to sediment deposition in combination with elevated SSCs and the associated light reduction from high turbidity. The results from this study will support the interpretation of experiments examining the combined effects of all three dredging-related pressures and aid the subsequent development of water quality thresholds for impact prediction purposes. Further research is also required to assess the effects of those stressors on reproduction and the early life-history stages, as higher vulnerability and reduced energy reserves available for those processes would have long-term consequences for sponge population dynamics.

Methods

Sample collection. This study used the phototrophic species *Cliona orientalis* Thiele, 1900, *Carteriospongia foliascens* (Pallas, 1766) and *Cymbastela coralliophila* Hooper & Berquist 1992 and the heterotrophic species *Coscinoderma matthewsi* (Lendenfeld, 1886) and *Stylissa flabelliformis* (Hentschel, 1912)^{22, 30, 58–60} to examine responses across different nutritional modes. The selected species are common throughout the Indo-Pacific, including the east and west coasts of tropical Australia, represent different morphologies and nutritional modes (Supplementary Table S3) and perform well in aquaria under experimental conditions²². All sponges were collected from 3–15 m depth from the Palm Islands, central Great Barrier Reef (GBR) (Supplementary Table S3). *C. orientalis* is an encrusting species that bioerodes coral, so cores of *C. orientalis* were air-drilled from dead colonies of *Porites* sp. ensuring > 2 cm of coral substrate below the sponge. For all species, sponges were cut into similar sized explants (~5 × 5 cm), and acclimated under natural light in flow-through seawater for 4 weeks until fully healed.

Experimental set up. The experiment was performed in the National Sea Simulator (SeaSim) at the Australian Institute of Marine Science (AIMS, Townsville, Queensland, Australia) using 150 L clear PVC acrylic tanks supplied with a continuous inflow of 5 µm filtered seawater at a rate of 600 mL min⁻¹ to ensure sponges received sufficient particulate and dissolved food. The seawater in experimental tanks was set to 27 °C, representing the temperature at the time of sponge collection. Experimental treatments comprised smothered v control tanks (in which no sediments were added) and 3 different exposure times (4, 16 and 30 d, see Fig. 1a). In the smothered treatments, sponges received repeated doses of sediment slurry every ~4 d, sufficient to cause continuous smothering (~30–45 mg cm⁻²). A VorTech™ MP10 propeller pump (EcoTech Marine, PA, US) was left on for 10 min after sediment was added to ensure homogenous turbidity throughout the tank. Pumps were then turned off for 24 h, to allow all sediments to settle out of suspension onto the sponges. After the sediments had settled, the pump was re-started to provide sufficient water flow to the sponges without lifting the sediments from the sponges' surfaces. The calcareous sediment used in this experiment was collected from the lagoon of Davies Reef, a mid-shelf reef centrally located in the GBR (S 18° 49.354' E 147° 38.253'). Sediments were first screened to 2 mm and then ground with a rod mill grinder until the mean particle size was 29 µm (with 80% of the sediment 3–64 µm, typical for dredge plumes⁶), measured using laser diffraction techniques (Mastersizer 2000, Malvern instruments Ltd, UK).

Tanks were illuminated by AI Hydra FiftyTwo™ HD LED lights (Aquaria Illumination, IA, US) on a 13:11 h L:D cycle, with a light regime designed to simulate daily conditions on the reef^{3, 61}. Each day there was a 6 h ramp up to a maximum instantaneous light level of 200 µmol photons m⁻² s⁻¹, followed by 1 h of constant illumination, and a 6 h ramp down to full darkness, resulting in a daily light integral (DLI) of 5 mols photons m⁻². Following the treatment period (4, 16 or 30 d), the surface of all sponges was gently brushed to remove any deposited sediments and all sponges were further exposed to clear seawater for a 14 d observation period (i.e. recovery, see Fig. 1a). Each treatment comprised 3 replicate tanks containing 4 sponge replicates per species (i.e. n = 12 replicates of each species per treatment).

Studied parameters. The effect of sediment smothering on the sponge holobiont was determined using a suite of response variables, with a particular focus on changes in sponge feeding activity and the associated symbiotic microbiome. To obtain baseline data on sponge health, 6 extra individuals were processed for each species immediately after collection (field controls) and after aquarium acclimation (t = 0 controls). Unless otherwise stated, statistical analyses and graphs were performed using the software SigmaPlot v.11.0 (Systat Software Inc.) and R⁶². Linear mixed models using tank as a random factor and treatment and time (B, E and O) as fixed factors were fitted by residual maximum likelihood (REML) for data pertaining to relative growth rates, respiration, lipid content, chlorophyll fluorescence and total pigments. For sediment clearance rates, the same method was used

but with time as the only fixed factor. For analyses with repeated measures of the same individual, i.e. clearance rates, growth, respiration rates, and chlorophyll fluorescence, individual was also included as a random factor. An analysis of variance (ANOVA) table was generated for each model and Tukey's post-hoc multiple comparisons were performed to compare treatment levels for each model⁶³.

Physical parameters. In order to measure sedimentation rates (SR), two SedPods⁶⁴ (surface area = 25.16 cm²) were placed in each tank before sediment addition and removed after the 24 h sedimentation period. SR were then measured by collecting and filtering sediments that accumulated on the SedPods using gravimetric techniques (filtration through 0.4 µm polycarbonate filters and calculating dry weight of the filters). Turbidity was monitored throughout the experiment using a manual WP 88 Turbidity Meter (TPS). Differences in sedimentation between replicate tanks and day of sediment pulse were assessed using two-way analysis of variance (ANOVA) with tank and time as fixed factors. A one-way ANOVA was used to study differences in the turbidity levels between replicate tanks (fixed factor) throughout the experiment.

Sediment smothering and clearance rates. Sponge surface area covered by sediments and sediment removal (i.e. clearance rates) were recorded throughout the experiment using a digital camera with underwater housing (Canon S120) and analysed using image analysis software (ImageJ⁶⁵).

Growth and necrosis. Initial and final thickness (in *C. foliascens*, *C. coralliophila* and *S. flabelliformis*), height (in *C. matthewsi*), or sponge tissue depth inside coral cores (in *C. orientalis*), of each sponge (± 0.1 mm) was measured as a proxy for growth. Callipers were used to take three measurements per sponge and averaged to calculate percentage change throughout the experiment and during the subsequent observational period. Partial mortality (necrosis) and loss of photosynthetic symbionts (bleaching) was recorded pre and post sediment exposure and at the end of the observational phase, using a digital camera (Canon S120) with underwater housing and analysed using ImageJ⁶⁵.

Respiration rates. Changes in sponge respiration rates were measured throughout the experiment and observational period. Samples were dark adapted for a minimum of 30 min before being transferred to 600 mL respiration chambers where they were incubated for 30 min at 27 °C. Constant mixing within the chambers was achieved using a magnetic stir bar and a submersible battery operated platform. An HDQ30D flexi meter (HACH LDO™, CA, US) was used to take 3 initial readings (i.e. initial O₂) and to measure the mg L⁻¹ of O₂ and the % O₂ in each chamber at the end of the incubation. The final oxygen concentration inside the chamber did not drop below 85% saturation in most cases. To control for microbial community respiration, a chamber containing only seawater (blank) was incubated under identical conditions. In order to normalize oxygen consumption among individuals, sponge volume was estimated by multiplying the surface area of each individual (derived from photos taken simultaneously and analysed using ImageJ) by its average thickness or height (as explained above). The same sponge volume was used to account for differences in water volume within the respiration chambers. In the case of *C. orientalis*, the height of the sponge layer within the coral cores was used to normalize oxygen consumption per sponge volume, whereas the height of the whole core (including the coral substrate) was used to calculate the specific volume of water within the chambers. Respiration data from *C. coralliophila* and *S. flabelliformis* were log and cube root transformed, respectively, in order to meet assumptions of homogeneity of variance.

Lipid analysis. The concentration of total lipids in sponge tissue was measured over time to assess whether sediment smothering interferes with sponge feeding. Samples were analysed from controls at the start of the experiment (T = 0), the 30 d treatment and its respective control, at the end of the exposure time and at the end of the observational period. Approximately 3 cm³ of sponge tissue was excised, wrapped in aluminium foil (to prevent plasticizer contamination) and immediately frozen in liquid nitrogen. Lipids were extracted from approximately 100 mg of sample as described in ref. 66 and following modifications in ref. 67, with total lipid content reported as percentage biomass based on a dry weight conversion factor.

Hyperspectral imaging. Hyperspectral imaging can be used to non-destructively estimate relative chlorophyll content *in situ* (e.g. refs 68, 69). A Pika II hyperspectral imaging camera (Resonon, MT, US), mounted on a moveable rig (Supplementary Fig. S4) captured back-reflected light in 480 spectral bands (~1 nm resolution) over the range of ~430–900 nm. Based on the methodologies described in refs 68, 70, the 3 phototrophic species, *C. orientalis*, *C. foliascens* and *C. coralliophila* were scanned after 8 d of being covered with sediment including i) before the sediment was removed, ii) after the sediment was removed and iii) after one day of recovery (n = 3). Scans were compared to control groups (n = 3) and the sponge's chlorophyll content was estimated by considering the logarithmic difference of the reflectance at chlorophyll absorption maximum (670 nm) and edge (745 nm). This calculation was performed at each pixel, and the values averaged over the imaged area of the specimen. Wavelength standards were selected based on optimal levels for control sponges, as each species had different chlorophyll content. One-way ANOVAs were performed to analyse changes in relative chlorophyll content for each species, separately. Significant differences were tested using pairwise, multiple Holm-Sidak comparisons. For *C. foliascens*, the ANOVA was performed on rank data to meet the assumption of homogenous variance, and a Tukey test was performed for *post hoc* comparison.

Based on the quick recovery of *C. orientalis* in the hyperspectral imaging trials, recovery was monitored using standard time-lapse photography. A partially bleached individual was monitored for 6 d after being covered with sediment for 30 d, with images taken every min.

Chlorophyll fluorescence. Changes in photosynthetic capacity (maximum quantum yield) of the sponge's phototrophic symbionts were measured with a Diving-PAM (pulse amplitude modulation) chlorophyll

fluorometer (Heinz Walz GmbH, Effeltrich, Germany) for *C. foliascens*, *C. coralliophila* and *C. orientalis*. Chlorophyll fluorescence measurements were taken 10 mm from the sponge tissue using a rubber space between the sponge and the end of the 6 mm fibre-optic probe. Sponges were dark-adapted for 30 min before measurement, and the initial fluorescence (F_0) determined using a pulse-modulated red measuring light (655 nm, $\sim 0.15 \mu\text{mol photons m}^{-2} \text{s}^{-1}$), and maximum fluorescence (F_m) then measured following a saturating pulse of light. Maximum quantum yield (F_v/F_m) was calculated from the ratio of variable fluorescence ($F_m - F_0$) to maximum fluorescence⁷¹. Three measurements were obtained before and after the sediment exposure time and at the end of the observational phase.

Pigment analysis. Pigment analyses were performed on tissue from all phototrophic sponges (*C. foliascens*, *C. coralliophila* and *C. orientalis*) at the end of the experimental time (4, 16 and 30 d) and after the 14 d observational phase. Pigments from samples incorporating pinacoderm and mesohyl regions were extracted and analysed as described in ref. 22 and standardized to sponge wet weight. The concentration of Chlorophyll a (hereafter Chl a) was used as a proxy for changes in photosymbiont health/bleaching³⁰. Pearson correlations were performed between all the studied pigments. All pigments retrieved by spectrophotometry (i.e. Chl a, b, c, d, total chlorophylls and carotenoids) were used to build resemblance matrices based on normalized data for each species, separately. Non-metric Multi-Dimensional Scaling (nMDS) plots were created using Euclidean distances. Two factors were determined (i.e. treatment and sampling time, nested to treatment) and examined by PERMANOVA (Permutational multivariate ANOVA based on distances). All multivariate analyses were performed using PRIMER 6 (Primer-E Ltd, UK).

Microbial community analysis. Microbial community composition was assessed using Illumina amplicon sequencing of the 16S rRNA taxonomic marker gene. Microbial analysis was performed on field controls, sponges collected at the start of the experiment, and at the end of the experimental and observational period for sponges smothered by sediments for 30 d and their corresponding controls. All samples were immediately frozen in liquid nitrogen and subsequently stored at -80°C . Water samples were simultaneously collected from each tank to facilitate a direct comparison with microbes present in the surrounding environment. DNA was extracted from ~ 0.2 g of sponge tissue using the PowerPlant[®] Pro DNA Isolation Kit (MoBio Laboratories, CA, US) according to the manufacturer's protocol. Microbial communities in seawater were filtered and their DNA extracted as previously described⁷². Sequencing of the 16S rRNA gene was performed at the Australian Centre for Ecogenomics using primers 515 f and 806r and the HiSeq2500 platform with the V2 chemistry (2×250 bp) (Illumina). Sequence data was deposited at the NCBI under the accession number SRP080232.

Amplicon sequence data was processed in Mothur v.1.35.1⁷³ according to the MiSeq standard operating procedure⁷⁴. Briefly, demultiplexed fastq paired-end reads were first quality-filtered and assembled into contigs (make.contigs and screen.seqs: maxambig = 0, maxhomop = 8, minlength = 100, maxlength = 292). Aligned reads were reduced to non-redundant sequences and chimeric sequences were detected using Uchime⁷⁵. Aligned sequences were phylogenetically classified based on the Silva reference file v.123, and all undersigned sequences removed (taxon = Chloroplast-Mitochondria-Unkown-Eukaryota). Samples with low read numbers were eliminated from the dataset. The remaining samples were sub sampled to 8,691 sequences. Pairwise distances were calculated and used for clustering and OTU assignment and OTUs were further classified based on the SILVA v.123 taxonomy.

OTU data was normalised to account for sampling depth and then square-root transformed to reduce the effect of abundant OTUs. Bray-Curtis distance matrices were constructed and visualised using non-metric multidimensional plots (nMDS) and principal coordinates analyses (PCO). Permutational analysis of variance (PERMANOVA, using 9,999 permutations) was used to determine significant differences in microbial communities based on source (sponge versus environmental control), time of sampling (field controls, time 0 controls, experimental and observational period samples), and treatment (control versus 30 d smothered). All multidimensional statistical analyses were performed in PRIMER 6/PERMANOVA. Similarity Percentage Analysis (SIMPER) was used to determine the OTUs that contribute to the differences between 30 d smothered and control samples for each species, separately. The 30 OTUs with the most discriminating power from the SIMPER analysis were used to create networks in Cytoscape 3.2.0 (www.cytoscape.org)⁷⁶.

References

- Hanley, J. Environmental monitoring programs on recent capital dredging projects in the Pilbara (2003–10): a Review. *Aust. Pet. Prod. Explor. Assoc.* **51**, 273–294 (2011).
- Masini, R., Jones, R. & Sim, C. Western Australian Marine Science Institution Dredging Node Science Plan (2011).
- Jones, R., Fisher, R., Stark, C. & Ridd, P. Temporal patterns in seawater quality from dredging in tropical environments. *PLoS One* **10**, e0137112 (2015).
- McCook, L. J. *et al.* Synthesis of current knowledge of the biophysical impacts of dredging and disposal on the Great Barrier Reef: Report of an Independent Panel of Experts (2015).
- Fisher, R., Stark, C., Ridd, P. & Jones, R. Spatial patterns in water quality changes during dredging in tropical environments. *PLoS One* **10**, e0143309 (2015).
- Jones, R., Bessell-Browne, P., Fisher, R., Klonowski, W. & Slivkoff, M. Assessing the impacts of sediments from dredging on corals. *Mar. Pollut. Bull.* **102**, 9–29 (2016).
- Pineda, M. C. *et al.* Effects of suspended sediments on the sponge holobiont with implications for dredging management. *Sci. Rep.* doi:10.1038/s41598-017-05241-z (2017).
- Pineda, M. C. *et al.* Effects of light attenuation on the sponge holobiont- implications for dredging management. *Sci. Rep.* **6**, 39038 (2016).
- Chartrand, K. M., Bryant, C. V., Carter, A. B., Ralph, P. J. & Rasheed, M. A. Light thresholds to prevent dredging impacts on the Great Barrier Reef seagrass, *Zostera muelleri* ssp. *capricorni*. *Front. Mar. Sci.* **3**, 1–17 (2016).
- Bak, R. P. M. & Elgershuizen, J. H. B. W. Patterns of Oil-Sediment rejection in corals. *Mar. Biol.* **37**, 105–113 (1976).
- Foster, T. *et al.* Dredging and port construction around coral reefs (2010).
- Bell, J. J. The functional roles of marine sponges. *Estuar. Coast. Shelf Sci.* **79**, 341–353 (2008).

13. de Goeij, J. M. *et al.* Surviving in a marine desert: the sponge loop retains resources within coral reefs. *Science* (80–) **342**, 108–10 (2013).
14. Wilkinson, C. R. & Cheshire, A. C. Patterns in the distribution of sponge populations across the central Great Barrier Reef. *Coral Reefs* **8**, 127–134 (1989).
15. Bell, J. J. & Barnes, D. K. A. A sponge diversity centre within a marine 'island'. in *Hydrobiologia* **440**, 55–64 (2000).
16. Murillo, F. J. *et al.* Deep-sea sponge grounds of the Flemish Cap, Flemish Pass and the Grand Banks of Newfoundland (Northwest Atlantic Ocean): Distribution and species composition. *Mar. Biol. Res.* **8**, 842–854 (2012).
17. Heyward, A. *et al.* The sponge gardens of Ningaloo Reef, Western Australia. *Open Mar. Biol. J.* **4**, 3–11 (2010).
18. Przeslawski, R., Alvarez, B., Battershill, C. & Smith, T. Sponge biodiversity and ecology of the Van Diemen Rise and eastern Joseph Bonaparte Gulf, northern Australia. *Hydrobiologia* **730**, 1–16 (2014).
19. Bell, J. J. *et al.* Sediment impacts on marine sponges. *Mar. Pollut. Bull.* **94**, 5–13 (2015).
20. Schönberg, C. H. L. Effects of dredging on filter feeder communities, with a focus on sponges. Report of Theme 6 - Project 6.1.1 prepared for the Dredging Science Node (2016).
21. Stubler, A. D., Duckworth, A. R. & Peterson, B. J. The effects of coastal development on sponge abundance, diversity, and community composition on Jamaican coral reefs. *Mar. Pollut. Bull.* **93**, 261–270 (2015).
22. Pineda, M. C., Duckworth, A. & Webster, N. Appearance matters: sedimentation effects on different sponge morphologies. *J. Mar. Biol. Assoc. United Kingdom* **96**, 481–492 (2016).
23. Webster, N. S. & Thomas, T. The Sponge Hologenome. *MBio* **7**, e00135–16 (2016).
24. Thomas, T. *et al.* Diversity, structure and convergent evolution of the global sponge microbiome. *Nat. Commun.* **7**, 11870 (2016).
25. Fan, L., Liu, M., Simister, R., Webster, N. S. & Thomas, T. Marine microbial symbiosis heats up: the phylogenetic and functional response of a sponge holobiont to thermal stress. *ISME J.* **7**, 991–1002 (2013).
26. López-Legentil, S., Erwin, P. M., Pawlik, J. R. & Song, B. Effects of sponge bleaching on ammonia-oxidizing Archaea: distribution and relative expression of ammonia monooxygenase genes associated with the barrel sponge *Xestospongia muta*. *Microb. Ecol.* **60**, 561–71 (2010).
27. Webster, N. S., Cobb, R. E. & Negri, A. P. Temperature thresholds for bacterial symbiosis with a sponge. *ISME J.* **2**, 830–42 (2008).
28. Arillo, A., Bavestrello, G., Burlando, B. & Sara, M. Metabolic integration between symbiotic cyanobacteria and sponges: a possible mechanism. *Mar. Biol.* **117**, 159–162 (1993).
29. Freeman, C. J. & Thacker, R. W. Complex interactions between marine sponges and their symbiotic microbial communities. *Limnol. Oceanogr.* **56**, 1577–1586 (2011).
30. Wilkinson, C. R. Net primary productivity in coral reef sponges. *Science* (80–) **219**, 410–412 (1983).
31. Hill, M., Allenby, A., Ramsby, B., Schönberg, C. & Hill, A. Symbiodinium diversity among host clonoid sponges from Caribbean and Pacific reefs: Evidence of heteroplasmy and putative host-specific symbiont lineages. *Mol. Phylogenet. Evol.* **59**, 81–8 (2011).
32. Thacker, R. W. & Freeman, C. J. In *Advances in Marine Biology* (eds Becerro, M. A., Uriz, M. J., Maldonado, M. & Turon, X.) **62**, 57–111 (Elsevier Ltd, 2012).
33. Wilkinson, C. & Trott, L. Light as a factor determining the distribution of sponges across the central Great Barrier Reef. *Proc. 5th int Coral Reef Symp., Tahiti* **5**, 125–130 (1985).
34. Erwin, P. & Thacker, R. Phototrophic nutrition and symbiont diversity of two Caribbean sponge–cyanobacteria symbioses. *Mar. Ecol. Prog. Ser.* **362**, 139–147 (2008).
35. Cheshire, A. C. & Wilkinson, C. R. Modelling the photosynthetic production by sponges on Davies Reef, Great Barrier Reef. *Mar. Biol.* **109**, 13–18 (1991).
36. Schönberg, C. H. L. Happy relationships between marine sponges and sediments – a review and some observations from Australia. *J. Mar. Biol. Assoc. United Kingdom* **96**, 493–514 (2016).
37. Ilan, M. & Abelson, A. The Life of a Sponge in a Sandy Lagoon. *Biol. Bull.* **189**, 363 (1995).
38. Tompkins-MacDonald, G. J. & Leys, S. P. Glass sponges arrest pumping in response to sediment: implications for the physiology of the hexactinellid conduction system. *Mar. Biol.* **154**, 973–984 (2008).
39. Hendler, G. The Association of Ophiothrix lineata and Callyspongia vaginalis: A Brittlestar-Sponge Cleaning Symbiosis? *Mar. Ecol.* **5**, 9–27 (1984).
40. Schönberg, C. H. L. Self-cleaning surfaces in sponges. *Mar. Biodivers.* **45**, 623–624 (2015).
41. Turon, X., Codina, M., Tarjuelo, I., Uriz, M. & Becerro, M. Mass recruitment of Ophiothrix fragilis (Ophiuroidea) on sponges: settlement patterns and post-settlement dynamics. *Mar. Ecol. Prog. Ser.* **200**, 201–212 (2000).
42. Weber, M., Lott, C. & Fabricius, K. E. Sedimentation stress in a scleractinian coral exposed to terrestrial and marine sediments with contrasting physical, organic and geochemical properties. *J. Exp. Mar. Bio. Ecol.* **336**, 18–32 (2006).
43. Gerodette, T. & Flechsig, A. Sediment-induced reduction in the pumping rate of the tropical sponge *Verongia lacunosa*. *Mar. Biol.* **55**, 103–110 (1979).
44. Carballo, J. L. Effect of natural sedimentation on the structure of tropical rocky sponge assemblages. *Ecoscience* **13**, 119–130 (2006).
45. Bythell, J. C. & Wild, C. Biology and ecology of coral mucus release. *J. Exp. Mar. Bio. Ecol.* **408**, 88–93 (2011).
46. Duerden, J. E. The role of mucus in corals. *Quart J Microsc Sci* **49**, 591–614 (1906).
47. Coffroth, M. A. The function and fate of mucus sheets produced by reef Coelenterates. In *Proceedings of the 6th International Coral Reef Symposium, Australia* 15–20 (1988).
48. Stafford-Smith, M. G. & Ormond, R. F. G. Sediment-rejection mechanisms of 42 species of Australian scleractinian corals. *Mar. Freshw. Res.* **43**, 683–705 (1992).
49. Kutti, T. *et al.* Metabolic responses of the deep-water sponge *Geodia barretti* to suspended bottom sediment, simulated mine tailings and drill cuttings. *J. Exp. Mar. Bio. Ecol.* **473**, 64–72 (2015).
50. Tjensvoll, I., Kutti, T., Fosså, J. H. & Bannister, R. J. Rapid respiratory responses of the deep-water sponge *Geodia barretti* exposed to suspended sediments. *Aquat. Biol.* **19**, 65–73 (2013).
51. Bannister, R. J., Battershill, C. N. & de Nys, R. Suspended sediment grain size and mineralogy across the continental shelf of the Great Barrier Reef: Impacts on the physiology of a coral reef sponge. *Cont. Shelf Res.* **32**, 86–95 (2012).
52. Biggerstaff, A., Smith, D. J., Jompa, J. & Bell, J. J. Photoacclimation supports environmental tolerance of a sponge to turbid low-light conditions. *Coral Reefs* **34**, 1049–1061 (2015).
53. Fang, J. K. H., Schönberg, C. H. L., Hoegh-Guldberg, O. & Dove, S. Day–night ecophysiology of the photosymbiotic bioeroding sponge *Cliona orientalis* Thiele, 1900. *Mar. Biol.* **163**, 100 (2016).
54. Thomas, S. & Ridd, P. V. Review of methods to measure short time scale sediment accumulation. *Mar. Geol.* **207**, 95–114 (2004).
55. Storlazzi, C. D., Field, M. E. & Bothner, M. H. The use (and misuse) of sediment traps in coral reef environments: Theory, observations, and suggested protocols. *Coral Reefs* **30**, 23–38 (2011).
56. Browne, N. K., Smithers, S. G., Perry, C. T. & Ridd, P. V. A Field-Based Technique for Measuring Sediment Flux on Coral Reefs: Application to Turbid Reefs on the Great Barrier Reef. *J. Coast. Res.* **284**, 1247–1262 (2012).
57. Whinney, J., Jones, R., Duckworth, A. & Ridd, P. Continuous *in situ* monitoring of sediment deposition in shallow benthic environments. *Coral Reefs*, [10.1007/s00338-016-1536-7](https://doi.org/10.1007/s00338-016-1536-7) (2017).
58. Ridley, C. P., Faulkner, D. & Haygood, M. G. Investigation of Oscillatoria spongeliae-dominated bacterial communities in four dictyoceratid sponges. *Appl. Environ. Microbiol.* **71**, 7366–75 (2005).

59. Schönberg, C. H. L. & Loh, W. K. W. Molecular identity of the unique symbiotic dinoflagellates found in the bioeroding demosponge *Cliona orientalis*. *Mar. Ecol. Prog. Ser.* **299**, 157–166 (2005).
60. Cheshire, A. *et al.* Preliminary study of the distribution and photophysiology of the temperate phototrophic sponge *Cymbastela* sp. from South Australia. *Mar. Freshw. Res.* **46**, 1211–1216 (1995).
61. Anthony, K. R. N., Ridd, P. V., Orpin, A. R., Larcombe, P. & Lough, J. Temporal variation of light availability in coastal benthic habitats: Effects of clouds, turbidity and tides. *Limnol. Oceanogr.* **49**, 2201–2211 (2004).
62. R Developmental Core Team. R: A Language and Environment for Statistical Computing. *R Foundation for statistical computing, Vienna, Austria*, doi:[10.1038/sj.hdy.6800737](https://doi.org/10.1038/sj.hdy.6800737) (2016).
63. Logan, M. Biostatistical design and analysis using R: a practical guide. (John Wiley & Sons, Ltd, 2010).
64. Field, M. E., Chezar, H. & Storlazzi, C. D. SedPods: a low-cost coral proxy for measuring net sedimentation. *Coral Reefs* **32**, 155–159 (2013).
65. Schneider, C. A., Rasband, W. S. & Eliceiri, K. W. NIH Image to ImageJ: 25 years of image analysis. *Nat. Methods* **9**, 671–675 (2012).
66. Folch, J., Lees, M. & Sloane-Stanley, G. A simple method for the isolation and purification of total lipids from animal tissues. *J. Biol. Chem.* **226**, 497–509 (1957).
67. Conlan, J., Jones, P., Turchini, G., Hall, M. & Francis, D. Changes in the nutritional composition of captive early-mid stage *Panulirus ornatus* phyllosoma over ecdysis and larval development. *Aquaculture* **434**, 159–170 (2014).
68. Chennu, A. *et al.* Hyperspectral imaging of the microscale distribution and dynamics of microphytobenthos in intertidal sediments. *Limnol. Oceanogr. Methods* **11**, 511–528 (2013).
69. Chennu, A., Grinham, A., Polerecky, L., de Beer, D. & Al-Najjar, M. A. A. Rapid Reactivation of Cyanobacterial Photosynthesis and Migration upon Rehydration of Desiccated Marine Microbial Mats. *Front. Microbiol.* **6**, 1–9 (2015).
70. Polerecky, L. *et al.* Modular Spectral Imaging System for Discrimination of Pigments in Cells and Microbial Communities. *Appl. Environ. Microbiol.* **75**, 758–771 (2009).
71. Genty, B., Briantais, J. & Baker, N. The relationship between the quantum yield of photosynthetic electron-transport and quenching of Chlorophyll fluorescence. *Biochim. Biophys. Acta* **990**, 87–92 (1989).
72. Webster, N. S. *et al.* Deep sequencing reveals exceptional diversity and modes of transmission for bacterial sponge symbionts. *Environ. Microbiol.* **12**, 2070–82 (2010).
73. Schloss, P. D. *et al.* Introducing mothur: Open-Source, Platform-Independent, Community-Supported Software for Describing and Comparing Microbial Communities. *Appl. Environ. Microbiol.* **75**, 7537–7541 (2009).
74. Kozich, J. J., Westcott, S. L., Baxter, N. T., Highlander, S. K. & Schloss, P. D. Development of a dual-index sequencing strategy and curation pipeline for analyzing amplicon sequence data on the miseq illumina sequencing platform. *Appl. Environ. Microbiol.* **79**, 5112–5120 (2013).
75. Edgar, R. C., Haas, B. J., Clemente, J. C., Quince, C. & Knight, R. UCHIME improves sensitivity and speed of chimera detection. *Bioinformatics* **27**, 2194–2200 (2011).
76. Shannon, P. *et al.* Cytoscape: A Software Environment for Integrated Models of Biomolecular Interaction Networks. *Genome Res.* **13**, 2498–2504 (2003).

Acknowledgements

This research was funded by the Western Australian Marine Science Institution (WAMSI) as part of the WAMSI Dredging Science Node, and made possible through investment from Chevron Australia, Woodside Energy Limited, BHP Billiton as environmental offsets and by co-investment from the WAMSI Joint Venture partners. The commercial entities had no role in data analysis, decision to publish, or preparation of the manuscript. The views expressed herein are those of the authors and not necessarily those of WAMSI. All collections were performed under Great Barrier Reef Marine Park Regulations 1983 (Commonwealth) and Marine Parks regulations 2006 (Queensland) Permit G12/35236.1 and Permit G13/35758.1. We are thankful to the crew of the San Miguel for helping with the sponge collection for this study. We also thank the staff at AIMS Marine Operations and AIMS National Sea Simulator for their technical assistance and expertise. Special thanks are due to E Arias for his valuable help in the field and while running the experiment. We thank Dr. A Chennu and the workshops of the Max Planck Institute for providing instruments and software for measurements. We also would like to acknowledge financial support from the BMBF grants 03F0666C (BIOACID) and 01DR14002. N.S.W was funded by an Australian Research Council Future Fellowship FT120100480.

Author Contributions

M.C.P., B.S., A.D., R.J. and N.S.W. designed the experiment. M.C.P. and B.S. undertook the experiment. M.C.P., B.S., M.S. and J.D.H. undertook laboratory analyses. M.C.P. and B.S. analysed the data. M.C.P., B.S., A.D., R.J. and N.S.W. wrote the manuscript. All authors reviewed the manuscript.

Additional Information

Supplementary information accompanies this paper at doi:[10.1038/s41598-017-05243-x](https://doi.org/10.1038/s41598-017-05243-x)

Competing Interests: The authors declare that they have no competing interests.

Publisher's note: Springer Nature remains neutral with regard to jurisdictional claims in published maps and institutional affiliations.



Open Access This article is licensed under a Creative Commons Attribution 4.0 International License, which permits use, sharing, adaptation, distribution and reproduction in any medium or format, as long as you give appropriate credit to the original author(s) and the source, provide a link to the Creative Commons license, and indicate if changes were made. The images or other third party material in this article are included in the article's Creative Commons license, unless indicated otherwise in a credit line to the material. If material is not included in the article's Creative Commons license and your intended use is not permitted by statutory regulation or exceeds the permitted use, you will need to obtain permission directly from the copyright holder. To view a copy of this license, visit <http://creativecommons.org/licenses/by/4.0/>.

© The Author(s) 2017

Supporting Online Material

Effects of sediment smothering on the sponge holobiont with implications for dredging management

Mari-Carmen Pineda^{1,2}, Brian Strehlow^{1,2,3}, Miriam Sternel⁴, Alan Duckworth^{1,2}, Joost den Haan⁵, Ross Jones^{1,2} and Nicole S. Webster^{1,2}

¹ *Australian Institute of Marine Science (AIMS), Townsville, QLD and Perth, WA, Australia*

² *Western Australian Marine Science Institution, Perth, WA, Australia*

³ *Centre for Microscopy Characterisation and Analysis, School of Plant Biology, and Oceans Institute, University of Western Australia, Crawley, WA, Australia*

⁴ *University of Bremen, Bremen, Germany*

⁵ *Max Plank Institute for Marine Microbiology, Bremen, Germany*

*Corresponding author:

Mari-Carmen Pineda

Australian Institute of Marine Science, PMB3, Townsville, QLD, 4810, Australia

E-mail: mcarmen.pineda@gmail.com.

Tel.: +61 7 4753 4522, fax: +61 7 4772 5852

Table S1. One-way ANOVA comparing relative chlorophyll content over time in smothered sponges immediately post cleaning, after 24h recovery and in control sponges. The ANOVA for *C. foliascens* was performed on ranks. Pairwise Multiple Comparison Procedures: Tukey Test for *C. foliascens*, and Holm-Sidak method for *C. orientalis* and *C. coralliophila*.

Source	df	<i>Cliona orientalis</i>		<i>Carteriospongia foliascens</i>		<i>Cymbastela coralliophila</i>	
		F	P	H	P	F	P
Treatment	3	38.693	<0.001	9.974	0.019	335.839	<0.001
Error	8						
Pairwise Multiple Comparisons:		Control > Sed. removal (P=0.016)		Control > Sed. removal (P<0.05)		Control > Sed. removal (P=0.002)	

Table S2. Similarity Percentage Analysis (SIMPER) for 30 most significant OTUs driving differences between controls and 30 d smothered samples combining experimental and observational periods.

OTU	Average relative abundance (%)		Contribution (%)	Taxonomic ID
	Control	30d-S		
<i>Cliona orientalis</i>				
Otu000001	6.05	3.86	2.59	Alphaproteobacteria
Otu000007	0.49	2.26	2	Alphaproteobacteria
Otu000020	0.96	1.76	1.6	Alphaproteobacteria
Otu000012	0.86	1.77	1.57	Deltaproteobacteria
Otu000017	1.27	1.8	1.44	Deltaproteobacteria
Otu000029	1.13	1.12	1.14	Alphaproteobacteria
Otu000013	1.67	1.69	1.04	Alphaproteobacteria
Otu000042	1.2	0.51	0.93	Alphaproteobacteria
Otu000061	1.04	0.65	0.91	Deltaproteobacteria
Otu000056	0.57	1.08	0.9	Alphaproteobacteria
Otu000053	0.64	1.25	0.88	Deltaproteobacteria
Otu000069	0.81	0.36	0.65	Deltaproteobacteria
Otu000081	0.78	0.49	0.62	Alphaproteobacteria
Otu000226	0.73	0.06	0.59	Deltaproteobacteria
Otu000131	0.32	0.56	0.59	Alphaproteobacteria
Otu000134	0.58	0.71	0.54	Alphaproteobacteria
Otu000165	0.09	0.69	0.53	Deltaproteobacteria
Otu000133	0.74	0.34	0.53	Alphaproteobacteria
Otu000174	0.33	0.5	0.52	Deltaproteobacteria
Otu000127	0.69	0.5	0.51	Deltaproteobacteria
Otu000192	0.53	0.34	0.51	Alphaproteobacteria
Otu000138	0.53	0.3	0.5	Deltaproteobacteria
Otu000152	0.41	0.37	0.5	Deltaproteobacteria
Otu000181	0.49	0.38	0.45	Alphaproteobacteria
Otu000274	0.17	0.5	0.45	Deltaproteobacteria
Otu000193	0.56	0.15	0.42	Alphaproteobacteria
Otu000217	0.58	0.21	0.42	Alphaproteobacteria
Otu000168	0.29	0.63	0.39	Alphaproteobacteria
Otu000304	0.19	0.32	0.38	Bacteroidetes
Otu000227	0.56	0.37	0.38	Alphaproteobacteria
<i>Carteriospongia foliascens</i>				
Otu000004	2.58	3.02	1.56	Cyanobacteria
Otu000019	1.39	0.86	1.14	Cyanobacteria
Otu000018	1.11	1.53	1.1	Cyanobacteria
Otu000021	1.28	0.77	0.86	Bacteroidetes
Otu000037	1.6	0.61	0.86	Gammaproteobacteria
Otu000008	2.51	2.3	0.84	Bacteroidetes
Otu000031	1.21	1.29	0.73	Cyanobacteria
Otu000030	1.08	1.16	0.71	Gammaproteobacteria
Otu000024	1.51	1.27	0.67	Alphaproteobacteria

Otu000052	0.58	0.86	0.62	Bacteroidetes
Otu000074	0.76	0.96	0.61	Gammaproteobacteria
Otu000044	1.06	1.25	0.58	Actinobacteria
Otu000086	0.5	1.17	0.57	Gammaproteobacteria
Otu000113	0.72	0.49	0.57	Alphaproteobacteria
Otu000054	0.8	0.55	0.55	Gammaproteobacteria
Otu000111	0.64	0.77	0.53	Alphaproteobacteria
Otu000036	1.57	1.3	0.52	Alphaproteobacteria
Otu000058	0.85	1.26	0.51	Gammaproteobacteria
Otu000100	0.94	0.56	0.51	Bacteroidetes
Otu000109	0.76	0.73	0.5	Gammaproteobacteria
Otu000097	0.71	0.73	0.5	Gammaproteobacteria
Otu000070	0.84	1.06	0.5	Bacteroidetes
Otu000093	0.86	0.73	0.47	Gammaproteobacteria
Otu000071	0.87	0.98	0.45	Bacteroidetes
Otu000175	0.4	0.64	0.45	Bacteroidetes
Otu000121	0.37	0.58	0.44	Bacteroidetes
Otu000116	0.73	0.39	0.4	Cyanobacteria
Otu000136	0.46	0.68	0.4	Gemmatimonadetes
Otu000214	0.52	0.35	0.39	Gammaproteobacteria
Otu000158	0.27	0.54	0.39	Alphaproteobacteria
<i>Cymbastela coralliophila</i>				
Otu000003	3.91	3.05	2.32	Cyanobacteria
Otu000009	0.95	1.15	1.3	Cyanobacteria
Otu000032	1.16	0.87	1.19	Cyanobacteria
Otu000035	0.68	1.41	1.09	Alphaproteobacteria
Otu000025	0.65	1.18	1.02	Cyanobacteria
Otu000041	0.82	0.78	0.98	Cyanobacteria
Otu000015	2.04	1.77	0.9	Gemmatimonadetes
Otu000026	1	1.6	0.84	Gammaproteobacteria
Otu000016	1.43	1.73	0.77	Acidobacteria
Otu000023	1.4	1.63	0.76	Alphaproteobacteria
Otu000039	0.81	1.26	0.76	Alphaproteobacteria
Otu000077	0.64	0.63	0.74	Cyanobacteria
Otu000115	0.74	0.23	0.68	Cyanobacteria
Otu000101	0.76	0.52	0.67	Cyanobacteria
Otu000064	0.68	0.44	0.66	Cyanobacteria
Otu000002	0.68	0.25	0.66	Gammaproteobacteria
Otu000045	0.87	1.33	0.63	Gammaproteobacteria
Otu000043	1.06	1.09	0.63	Alphaproteobacteria
Otu000084	0.76	0.67	0.61	Alphaproteobacteria
Otu000073	1.01	0.72	0.59	Acidobacteria
Otu000080	0.55	0.65	0.57	Alphaproteobacteria
Otu000072	0.88	0.89	0.57	Chloroflexi
Otu000118	0.58	0.39	0.53	Gemmatimonadetes
Otu000219	0.67	0.07	0.53	Cyanobacteria
Otu000132	0.48	0.6	0.53	Gammaproteobacteria
Otu000082	0.55	0.8	0.52	Acidobacteria
Otu000126	0.41	0.79	0.52	Acidobacteria
Otu000078	0.75	0.94	0.52	Acidobacteria
Otu000090	0.75	0.91	0.52	Gammaproteobacteria
Otu000057	0.81	0.67	0.48	Gammaproteobacteria
<i>Coscinoderma matthewsi</i>				
Otu000034	1.32	1.15	0.4	Chloroflexi
Otu000046	0.67	1.19	0.38	Chloroflexi
Otu000040	0.73	0.89	0.36	Acidobacteria
Otu000050	0.84	0.97	0.36	Acidobacteria
Otu000088	1.21	0.47	0.35	Gemmatimonadetes
Otu000033	0.97	1.61	0.34	Deltaproteobacteria
Otu000119	0.12	0.89	0.32	Gemmatimonadetes
Otu000089	0.39	0.82	0.3	Chloroflexi

Otu000075	0.85	0.62	0.29	Acidobacteria
Otu000067	0.85	0.58	0.28	Chloroflexi
Otu000128	0.57	0.51	0.28	Unclassified Bacteria
Otu000103	0.91	0.66	0.28	Unclassified Bacteria
Otu000094	0.66	0.79	0.28	Acidobacteria
Otu000144	0.9	0.35	0.27	Chloroflexi
Otu000051	0.99	0.94	0.26	Gemmatimonadetes
Otu000117	0.74	0.32	0.26	Acidobacteria
Otu000076	0.95	0.9	0.24	PAUC34f
Otu000140	0.34	0.52	0.24	Unclassified Bacteria
Otu000108	0.23	0.53	0.24	Chloroflexi
Otu000195	0.69	0.3	0.24	Acidobacteria
Otu000142	0.74	0.55	0.24	Alphaproteobacteria
Otu000156	0.72	0.29	0.23	Deltaproteobacteria
Otu000059	0.84	0.82	0.23	PAUC34f
Otu000153	0.71	0.55	0.23	Acidobacteria
Otu000096	0.7	0.83	0.23	Acidobacteria
Otu000203	0.64	0.37	0.22	Gemmatimonadetes
Otu000212	0.71	0.34	0.22	Actinobacteria
Otu000234	0.56	0.24	0.21	Acidobacteria
Otu000189	0.59	0.4	0.21	Acidobacteria
Otu000110	0.54	0.68	0.21	Unidentified Proteobacteria
<i>Stylissa flabelliformis</i>				
Otu000006	2.12	2.61	2.31	Archaea
Otu000014	1.03	1.23	1.78	Archaea
Otu000022	1.32	1.41	1.48	Unclassified Bacteria
Otu000028	1.52	1.05	1.44	Gammaproteobacteria
Otu000011	1.5	1.97	1.36	Gammaproteobacteria
Otu000002	5.2	4.69	1.3	Gammaproteobacteria
Otu000027	0.86	1.25	1.08	Unidentified Proteobacteria
Otu000049	0.74	0.92	1.08	Gammaproteobacteria
Otu000068	0.77	0.8	1.06	Unclassified Bacteria
Otu000055	0.6	0.95	1.04	Proteobacteria ARKDMS-49
Otu000083	0.51	0.66	1.03	Gammaproteobacteria
Otu000066	0.82	0.84	0.9	Archaea
Otu000095	0.43	0.66	0.88	Archaea
Otu000060	0.7	1.07	0.86	Nitrospirae
Otu000065	0.78	0.75	0.83	Unclassified Bacteria
Otu000085	0.48	0.29	0.76	Unclassified Bacteria
Otu000159	0.63	0.47	0.74	Proteobacteria ARKDMS-49
Otu000098	0.41	0.56	0.74	Archaea
Otu000038	1.05	1.19	0.7	Archaea
Otu000112	0.83	0.71	0.68	Gammaproteobacteria
Otu000176	0.38	0.4	0.66	Gammaproteobacteria
Otu000125	0.5	0.38	0.65	Proteobacteria ARKDMS-49
Otu000005	3.81	3.38	0.64	Proteobacteria ARKDMS-49
Otu000194	0.6	0.37	0.6	Nitrospirae
Otu000129	0.36	0.38	0.55	Gammaproteobacteria
Otu000163	0.45	0.36	0.54	Unclassified Bacteria
Otu000124	0.52	0.7	0.51	Gammaproteobacteria
Otu000010	2.39	2.3	0.5	Proteobacteria ARKDMS-49
Otu000177	0.5	0.26	0.49	Gammaproteobacteria
Otu000242	0.4	0.03	0.48	Gammaproteobacteria

Table S3. Sponge sampling details. List of species, morphologies, nutritional mode and sampling location.

Species Name (Author)	Functional Morphology	Primary Nutritional Mode	Sampling Location
<i>Cliona orientalis</i> Thiele, 1900	Encrusting (bioeroding)	Phototrophic ⁶³	Pelorus Is. (Palm Is.) S 18°32.903' E 146° 29.172'
<i>Carteriospongia foliascens</i> (Pallas, 1766)	Cup (wide cup)	Phototrophic ⁶²	Fantome Is. (Palm Is.) S 18°41.028' E 146° 30.706'
<i>Cymbastela coralliophila</i> Hooper & Bergquist, 1992	Encrusting (thick) Cup (table)	Phototrophic ⁶⁴	Pelorus Is. (Palm Is.) S 18°32.903' E 146° 29.172'
<i>Coscinoderma matthewsi</i> (Lendenfeld, 1886)	Massive	Heterotrophic (Wilkinson 1983)	Pelorus Is. (Palm Is.) S 18°32.903', E 146° 29.172'
<i>Stylissa flabelliformis</i> (Hentschel, 1912)	Erect (laminar)	Heterotrophic ²⁶	Pelorus Is. (Palm Is.) S 18°32.903' E 146° 29.172'

Figure S1. Photographs of the 5 sponge species before sediment addition, during sediment smothering and after sediment removal. Phototrophic species: a) *C. orientalis*, b) *C. foliascens*, c) *C. coralliophila*, and Heterotrophic species d) *C. matthewsi* and d) *S. flabelliformis*.

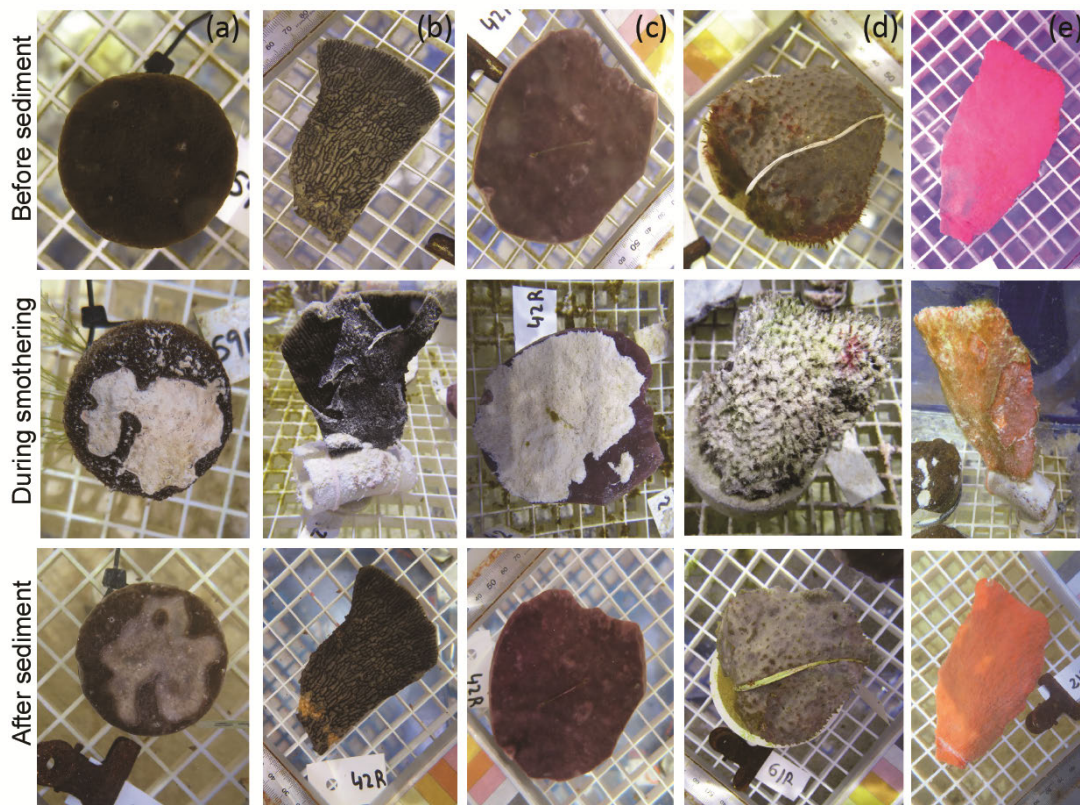


Figure S2. Non-metric Multi-Dimensional Scaling plots on microbial OTU data. nMDS of microbial communities for all 5 sponge species and the environmental control (seawater).

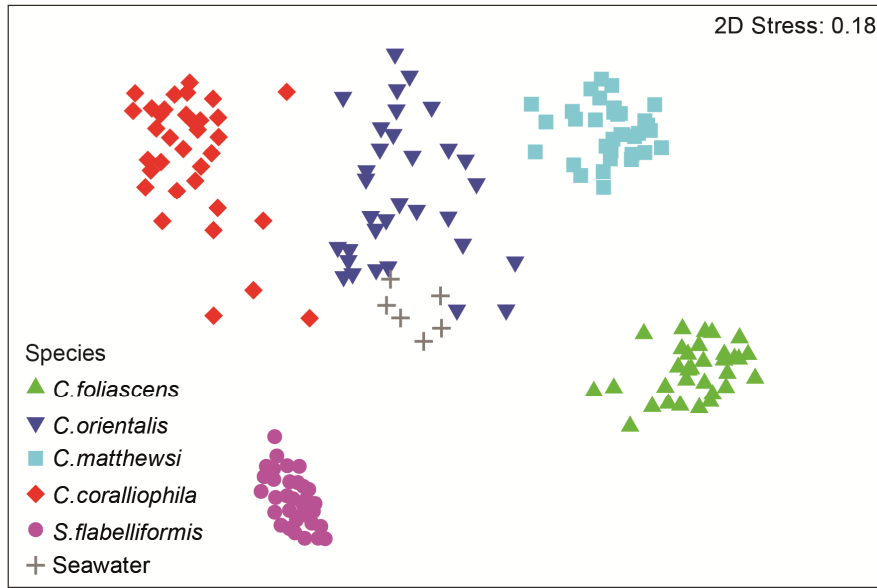


Figure S3. Phylum level bar chart for seawater (environmental control). Average relative abundance of each bacteria phylum (and class for Proteobacteria) for 3 replicate seawater samples within each targeted treatment (Control versus 30-days smothered). Only OTUs representing greater than 1% of the overall community were included.

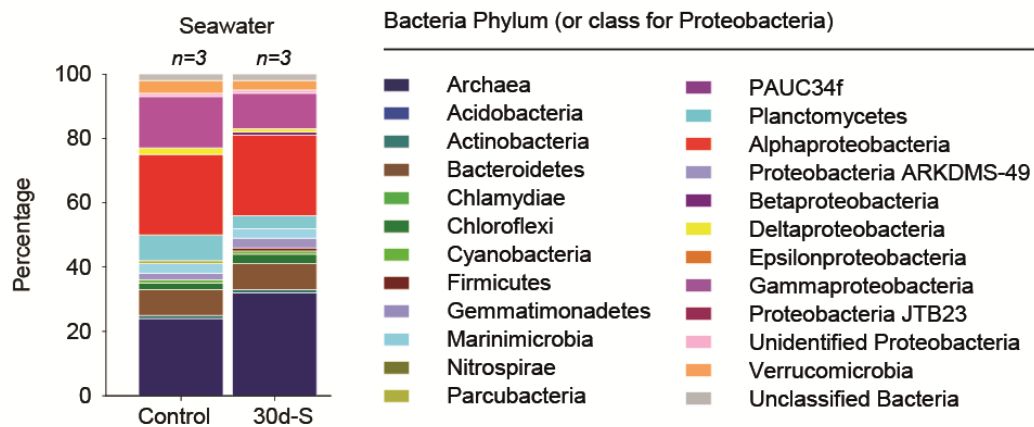
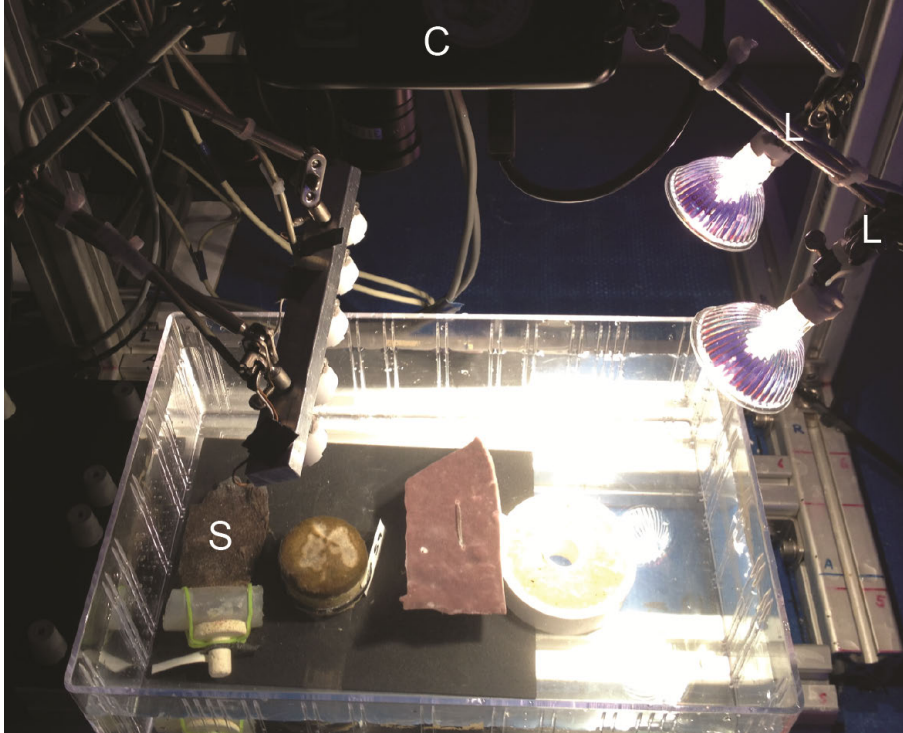


Figure S4. Hyperspectral imaging setup. The Hyperspectral camera (C) moves along a track (i.e. left to right), capturing the back-reflected light off the sponges to quantify chlorophyll concentrations *in situ* (based on the relative chlorophyll content). The external light (i.e. a clean white light spectrum) is provided by two halogen lights (L). Whilst incubated, the 3 sponge species (S) can be scanned simultaneously.



SCIENTIFIC REPORTS

OPEN

Effects of combined dredging-related stressors on sponges: a laboratory approach using realistic scenarios

Mari-Carmen Pineda^{1,2}, Brian Strehlow^{1,2,3}, Jasmine Kamp⁴, Alan Duckworth^{1,2}, Ross Jones^{1,2} & Nicole S. Webster^{1,2}

Dredging can cause increased suspended sediment concentrations (SSCs), light attenuation and sedimentation in marine communities. In order to determine the combined effects of dredging-related pressures on adult sponges, three species spanning different nutritional modes and morphologies were exposed to 5 treatment levels representing realistic dredging scenarios. Most sponges survived under low to moderate turbidity scenarios (SSCs of $\leq 33 \text{ mg L}^{-1}$, and a daily light integral of $\geq 0.5 \text{ photons m}^{-2} \text{ d}^{-1}$) for up to 28 d. However, under the highest turbidity scenario (76 mg L^{-1} , $0.1 \text{ photons m}^{-2} \text{ d}^{-1}$) there was 20% and 90% mortality of the phototrophic sponges *Cliona orientalis* and *Carteriospongia foliascens* respectively, and tissue regression in the heterotrophic *Ianthella basta*. All three sponge species exhibited mechanisms to effectively tolerate dredging-related pressures in the short term (e.g. oscula closure, mucus production and tissue regression), although reduced lipids and deterioration of sponge health suggest that longer term exposure to similar conditions is likely to result in higher mortality. These results suggest that the combination of high SSCs and low light availability can accelerate mortality, increasing the probability of biological effects, although there is considerable interspecies variability in how adult sponges respond to dredging pressures.

Sediments released into the water column by natural resuspension, river runoff and human activities such as dredging pose a potential risk to sensitive ecosystems such as coral reefs, seagrass meadows and sponge gardens^{1–4}. Sediments in suspension, or settling back out of suspension (i.e. sedimentation), can affect epi-benthic organisms in a number of ways, including clogging of the feeding and filtering mechanisms. Water turbidity (cloudiness) can also temporarily reduce or extinguish benthic light^{4–6}. These stressors can act alone but more often in combination, making impact prediction particularly difficult. Sponges are sessile filter-feeding organisms that play important roles in marine ecosystems, including substrate consolidation, habitat provision, seawater filtration and benthic-pelagic energy transfer^{7–9}. Despite their abundance and ecological importance, our understanding of how sponges respond to turbidity is still very basic^{10,11}. This knowledge gap poses significant challenges to their effective management, especially for anthropogenic turbidity-generating activities such as dredging, that can at least be subject to some regulation and control¹².

Most sponges obtain energy heterotrophically, by filtering seawater through an aquiferous system or internal canal network^{13,14}. However, many sponges can also obtain energy autotrophically from photosymbionts, of which *Cyanobacteria* are the most common^{15,16}. Some bioeroding sponge species also harbour dinoflagellates of the genus *Symbiodinium* as photosymbionts^{17,18}. The photosymbionts can provide >50% of the energy requirement of the host for some tropical sponge species^{15,19}. Overall, the diverse community of symbiotic microorganisms can comprise up to 35% of the sponge biomass and make other valuable contributions to many aspects of the sponge's physiology and ecology (e.g. production of secondary metabolites)²⁰. These microbial associations tend

¹Australian Institute of Marine Science (AIMS), Townsville, QLD and Perth, WA, Australia. ²Western Australian Marine Science Institution, Perth, WA, Australia. ³School of Biological Sciences, Centre for Microscopy Characterisation and Analysis, and Oceans Institute, University of Western Australia, Crawley, WA, Australia. ⁴James Cook University, Townsville, QLD, Australia. Mari-Carmen Pineda and Brian Strehlow contributed equally to this work. Correspondence and requests for materials should be addressed to M.-C.P. (email: mcarmen.pineda@gmail.com)

to be highly host specific, and are generally stable across broad geographic and environmental gradients²¹. This stable host-microbe consortium is often referred to as the ‘sponge holobiont’²⁰.

Sponges can be affected by dredging-related pressures in different ways depending on their nutritional mode, their morphology and their behavioural and physical adaptations to tolerate sediment. For instance, due to their high filter-feeding activity, heterotrophic sponges may be affected by elevated suspended sediment concentrations (SSCs), with long term exposure to high SSCs clogging their aquiferous systems and reducing the flow of oxygenated seawater to the mesohyl¹⁰. In addition, phototrophic sponges may be affected by the reduction in benthic light availability that occurs in sediment plumes^{5,6}. Sediment deposition could also cause smothering and suffocation of recruits and adult sponges, especially encrusting, massive, cups and plate-like morphologies^{10,11,22,23}. All these effects can have flow-on consequences for host energetics, health and reproductive output^{10,11}.

Nevertheless, some sponges can tolerate, and in some case thrive in, turbid environments, including endosymbiotic species which live partially buried within sediments^{10,11,24}. Knowing how they tolerate these conditions is important for understanding the consequences of turbidity generating activities. Some sponges can temporarily tolerate high SSCs through changes in their physiology, such as temporarily closing or reducing the size of their incurrent openings (ostia) or arresting pumping activity^{25–28}. Phototrophic species may be able to temporarily tolerate low light by photoacclimation and an increase in photosynthetic efficiency^{10,29,30}. To tolerate elevated sedimentation, some species have active cleaning mechanisms to remove sediments such as the production of mucus-like substances and tissue sloughing, selective rejection of inhaled particles and the use of water jets to unblock inhalant pores^{10,11,24}. These ‘active’ mechanisms (requiring energy expenditure) work in conjunction with more ‘passive’ mechanisms that reduce sediment accumulation such as the existence of self-cleaning surfaces, and micro and macro morphology and orientation that promotes sediment rejection under gravitational forces^{11,31}. The removal of sediment by epibionts is also a passive mechanism for self-cleaning that has been reported in some sponges¹¹.

Understanding physiological tolerance levels of sponges to turbidity and establishing dose-response relationships is essential for impact prediction purposes, i.e. to forecast the potential effect of turbidity-generating activities such as dredging at the environmental impact assessment stage. It is also essential for managing water quality during dredging, i.e. to alert dredging proponents to conditions which could harm local sponge populations. A key problem is that there are many different cause-effect pathways whereby sediment released into the water column can affect sponges and these cause-effect pathways may act alone or in combination, potentially confounding attempts to establish a dose and subsequent response in laboratory based or field studies^{4,32}. Elevated turbidity is clearly a hazard to sponge communities, as has been shown in many previous laboratory and field based studies^{10,11}, but whether it constitutes a risk depends on being able to place the results in the context of likely exposure scenarios. Recently, the spatial and temporal changes in water quality have been comprehensively described for several large scale dredging projects^{5,6,33}. These capital projects occurred in a range of marine settings from inshore turbid reef to offshore ‘clear water’ environments, providing a suitable spectrum of conditions to describe the range of likely exposure scenarios^{5,6}. The analyses included an examination of pre-dredging (baseline) data, and data collected at various distance from the dredging (excavation) activities, allowing characterization of spatial patterns and effects relative to background conditions (i.e. natural resuspension events).

Water quality information from these dredging programs has already been used in a sequence of laboratory-experiments to better understand the risks posed to sponges by individual stressors. Sponges were exposed to a range of different light intensity treatments (range: 0–8.1 mol photons m⁻² d⁻¹) under very low SSCs (<0.05 mg L⁻¹), so that light reduction was the primary variable examined³⁴. Subsequently, sponges were exposed to a range of different SSC treatments (range: 0–76 mg L⁻¹) and light was standardized across the treatments (to 5 mol photons m⁻² d⁻¹), such that SSC was the only variable being examined³⁵. Finally, to derive pressure response values to sedimentation, sponges were repeatedly exposed to multiple discrete sediment deposition events (of 30–45 mg cm⁻²)³⁶. These experiments were conducted with 5–6 sponge species, spanning heterotrophic and phototrophic nutritional modes, and a range of different morphologies. Endpoints included a range of physiological metrics encompassing respiration, survivorship, growth, lipid and chlorophyll content, production of mucus-like substances and changes in the microbial community (microbiome) composition. All experiments were conducted for an extended (chronic) time frame of 28 d, and included a 14 d post exposure monitoring or ‘observational’ period to see if there were any latent effects.

These studies showed that reducing the light levels clearly affected the phototrophic sponges³⁴, with little effect on the heterotrophic species. Among phototrophs, the boring sponge *Cliona orientalis* and the cup-shaped *Carteriospongia foliascens* rapidly bleached (discoloured) when held in the dark. *C. orientalis* survived the 28 d exposure period, rapidly regaining colour when returned to normal light levels; in contrast, *C. foliascens* died in the observational period. Less extreme light reduction treatments (0.8 mol photons m⁻² d⁻¹) resulted in some minor bleaching but no mortality in either species. Microbial community composition did not differ between light treatments for the heterotrophic species, but did for the two phototrophic species that bleached. In the sediment exposure experiments, high SSCs alone resulted in negative growth, decreased respiration rates and lipid depletion in most sponges³⁵. Significant necrosis and mortality occurred within most species, including *C. foliascens* and *C. orientalis* at 70 mg L⁻¹, while no mortality occurred at lower SSCs (<23 mg L⁻¹).

These studies are useful for identifying the physiological and behavioural responses specific to individual stressors, and for understanding the different susceptibility of species and nutritional modes. They also help in the interpretation of experiments when the stressors are combined — which is the subject of the current study. In this investigation, three different sponge species were exposed to five different treatments (referred to as ‘scenarios’) of elevated turbidity (i.e. combinations of elevated SSCs and associated reductions in light). As with the earlier experiments examining the individual stressors in isolation^{34–36}, the experiments were conducted over a 28 d exposure period and a subsequent 14 d observational period. The SSCs and light levels used are based on the

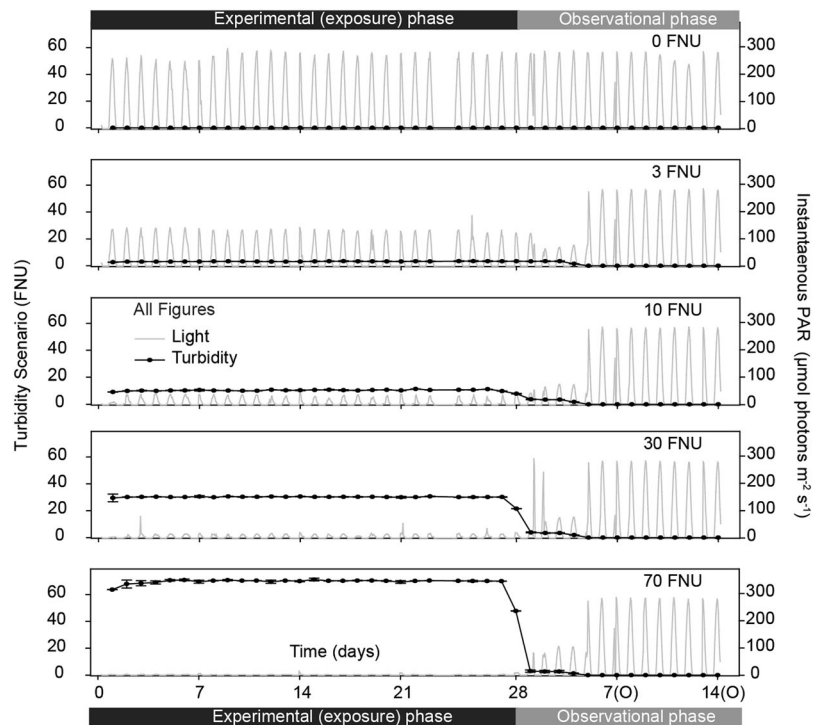


Figure 1. Physical parameters throughout the experiment. Turbidity (FNU) (mean \pm SE) and instantaneous light (PAR, $\mu\text{mol photon m}^{-2} \text{s}^{-1}$) (mean) ($n = 2$ replicate tanks per treatment) experienced in each scenario (0, 3, 10, 30 and 70 FNU, but see also Table 1) throughout the 28 d experimental (exposure) and 14 d observational periods.

Turbidity Scenario	nephelometrically-derived SSC	Measured SSCs (gravimetrically determined)	Light (mid-day max)	Daily Light Integral (DLI)	SedPod accumulation rate
FNU	mg L^{-1}	mg L^{-1}	$\mu\text{mol photons m}^{-2} \text{s}^{-1}$	$\text{mol photons m}^{-2} \text{d}^{-1}$	$\text{mg cm}^{-2} \text{d}^{-1}$
70	76	76.9 ± 2.6	12.3	0.15	5.2 ± 0.9
30	33	32.2 ± 2.2	18.7	0.46	3.3 ± 0.4
10	11	15.5 ± 1.8	35.4	0.87	2.5 ± 0.4
3	3	3.6 ± 0.4	119	3.07	1.1 ± 0.3
0	0	1.3 ± 0.3	267	6.34	0.2 ± 0.1
Observational	0	1.3 ± 0.3	271	6.53	0.2 ± 0.1

Table 1. Summary of exposure scenarios. Turbidity (FNU), mean nephelometrically-derived SSC (mg L^{-1}), measured SSCs determined gravimetrically at 7, 14, 21 and 28 d (mean \pm SE, $n = 3$ samples per tank and day), maximum daily (mid-day) light level (instantaneous), daily light integral (DLI) and SedPod accumulation rate determined gravimetrically at 7, 14, 21 and 28 d (mean \pm SE, $n = 2$ samples per tank and day), during the 28 d experimental period and subsequent 14 d observational period. Scenarios were based on *in situ* water quality data collected from three recent large scale capital dredging programs in Australia^{5,6} (see Discussion).

empirical data collected during several large scale capital dredging projects^{5,6}, allowing the results to be contextualized in a management framework.

Results

Physical parameters. Turbidity values as measured by the nephelometers (formazin nephelometric units, FNU) were constant (± 1 FNU) throughout the experiment (Fig. 1), and there were significant differences between all treatments during the exposure period (Table 1, Table 2). Gravimetrically determined SSCs were also significantly different between treatments throughout the experiment (Repeated measures (RM) ANOVA: $P < 0.001$). Daily Light Integrals (DLIs) were also significantly different between treatments (Fig. 1, Table 1, Table 2). Mean sediment deposition (\pm SE), measured using SedPods, increased as FNU increased from 0.2 – $5.2 \text{ mg cm}^{-2} \text{ d}^{-1}$, respectively, and was significantly different between treatments during the experimental period (Table 1, Table 2). During the observational phase, all tanks returned to control conditions and no significant differences were retrieved between treatments (Fig. 1, Table 1, Table 2). The term ‘scenario’ in combination with the nominal

	Source	df	Turbidity (FNU)		Light (DLI)		SedPod accumulation rate (mg cm ⁻² d ⁻¹)	
			F	P	F	P	F	P
Experimental phase	Scenario	4	686.1	<0.001	212.1	<0.001	19.772	<0.001
	Error	65						
	Tukey		0 < 3 < 10 < 30 < 70		0 < 3 < 10 < 30 < 70		0, 3 < 10, 30 < 70	
Observational phase	Scenario	4	1.000	1.000	0.081	0.988	1.000	1.000
	Error	65						

Table 2. Analyses of variance on the effect of turbidity scenario on the physical parameters. One-way ANOVA on turbidity (FNU), light (DLI) and sedimentation data, at the end of the experimental and observational phase. Tukey tests have been performed for significant pairwise multiple comparisons between scenarios (scenarios: 0, 3, 10, 30 and 70 FNU).

turbidity value is used hereafter to refer to the treatments, and thus, for instance, the 70 FNU scenario refers to the SSC combination and DLI specified in Table 1 (76 mg L⁻¹ and 0.15 mol photons m⁻² d⁻¹, respectively).

Sponge health, growth and stress responses to sediments. Overall sponge health was negatively affected by the scenarios ≥ 10 FNU although the extent of the impact and the ability to recover during the observational phase were species-specific. Changes in biomass per unit area (mg cm⁻²) in *Cliona orientalis*, which are related to its bioerosion rate, varied greatly among scenarios. During the experimental period, the decrease in biomass in this species was higher under 3, 10 and 70 FNU scenarios, suggesting a continuous bioeroding activity (Fig. 2). The increase in biomass in the 30 FNU scenario was unexpected, and possibly due to an accumulation of sediments within the cores of some replicates, particularly in the necrotic regions which exposed the rugose and porous coral substrate and could accumulate sediments (see Fig. 3a). Overall, the variability among replicates was very high, and significant differences were only detected between the 10 and 30 FNU scenarios (Table 3a). For *Carteriospongia foliascens* and *Ianthella basta*, growth based on surface area throughout the experiment (i.e. experimental plus observational periods) had a negative relationship with increasing FNU, with greatest regression from both species at the 70 FNU scenario (Fig. 2a, Table 3a). Positive growth was only detected in *C. foliascens* in the ≤ 3 FNU scenarios, while negative growth occurred in the ≥ 30 FNU scenarios, during both the experimental and observational periods. *I. basta* showed negative growth under all dredging scenarios except for the control (Fig. 2a, Table 3a).

For *C. orientalis*, 20% of individuals (n = 4 replicates) died after 14–28 d in the 70 FNU scenario (Supplementary Fig. S1). While all remaining individuals in the ≥ 10 FNU scenarios had minor to moderate bleaching (discolouration) during the experimental period. These partially bleached sponges recovered their initial pigmentation during the observational phase (Fig. 2b). In contrast, *C. foliascens* was particularly sensitive, showing significantly higher rates of necrosis and mortality under the ≥ 30 FNU scenarios. Mortality affected 10, 55 and 85% of *C. foliascens* individuals in the 10, 30 and 70 FNU scenarios, respectively, with necrosis and mortality observed after 28, 21 and 7 d, respectively (Fig. 2b, Supplementary Fig. S1). No mortality was evident in the heterotrophic *I. basta* throughout the experiment; however some individuals had partial mortality with most tissue lost in sponges exposed to ≥ 30 FNU (Fig. 2b, Table 3b).

Mortality data for *C. foliascens* was fitted to nonlinear regression curves to calculate the lethal concentration (LC) at which 50% (LC₅₀) and 10% (LC₁₀) of the population died. Nonlinear regression of the dose–response curve ($R^2 = 0.9567$, AICc = 48.11) met assumptions of normality and homoscedasticity and the replicates test showed no evidence for lack of fit ($P = 0.694$). After the 28 d exposure period, the LC₅₀ (and 95% confidence intervals range) for mortality in *C. foliascens* was 47 mg L⁻¹ (range: 40–56 mg L⁻¹) and the LC₁₀ was 22 mg L⁻¹ (range: 14–31 mg L⁻¹). These SSCs corresponded to an LC₅₀ value for DLI of 0.3 mol photons m⁻² d⁻¹ (range: 0.21–0.33), and an LC₁₀ DLI of 0.9 mol photons m⁻² d⁻¹ (range: 0.61–1.26 mol photons m⁻² d⁻¹). Mortality data from *C. orientalis* did not meet model assumptions and LC values could not be calculated.

In addition to partial or total mortality, sponges showed different sublethal responses to dredging-related pressures. Visual assessments of *C. orientalis* throughout the experiment revealed a significantly higher percentage of open oscula in the lower turbidity scenarios (<10 FNU) from day 7 until the end of the experimental phase (ANOVA: $P < 0.05$, Fig. 2c), indicating reduced pumping activity in this species within the higher turbidity scenarios (≥ 10 FNU). However, all oscula appeared open again once sponges were returned to control conditions during the observational phase (Fig. 2c, Fig. 3a, Table 3c). In contrast, *C. foliascens* produced layers of mucus when exposed to any sediment (Fig. 2c, Fig. 3b). The percentage of mucus cover was significantly higher in the 10 and 30 FNU scenarios at the end of the experimental phase, although no mucus was produced during the observational period (Fig. 2c, Table 3c). *I. basta* produced a moderate amount of mucus when exposed to sediments (Fig. 3c); with a significantly higher percentage of mucus cover in samples from the 30 and 70 FNU scenarios at the end of the 28 d exposure period and no mucus production observed during the recovery period (Fig. 2c, Table 3c). In both species the mucus layers were observed to eventually slough off the sponge surface leaving clean tissue relatively free of sediments (Fig. 3b–c). The observed sublethal responses to sediments were directly related to the percentage of sediment cover observed on top of sponges during the experiment (Fig. 2d).

Lipid analysis. No depletion of total lipid content per sponge biomass was detected in the control samples throughout the experiment (i.e. from Time 0 until the end of the observational phase, T-tests: $P > 0.05$ for all

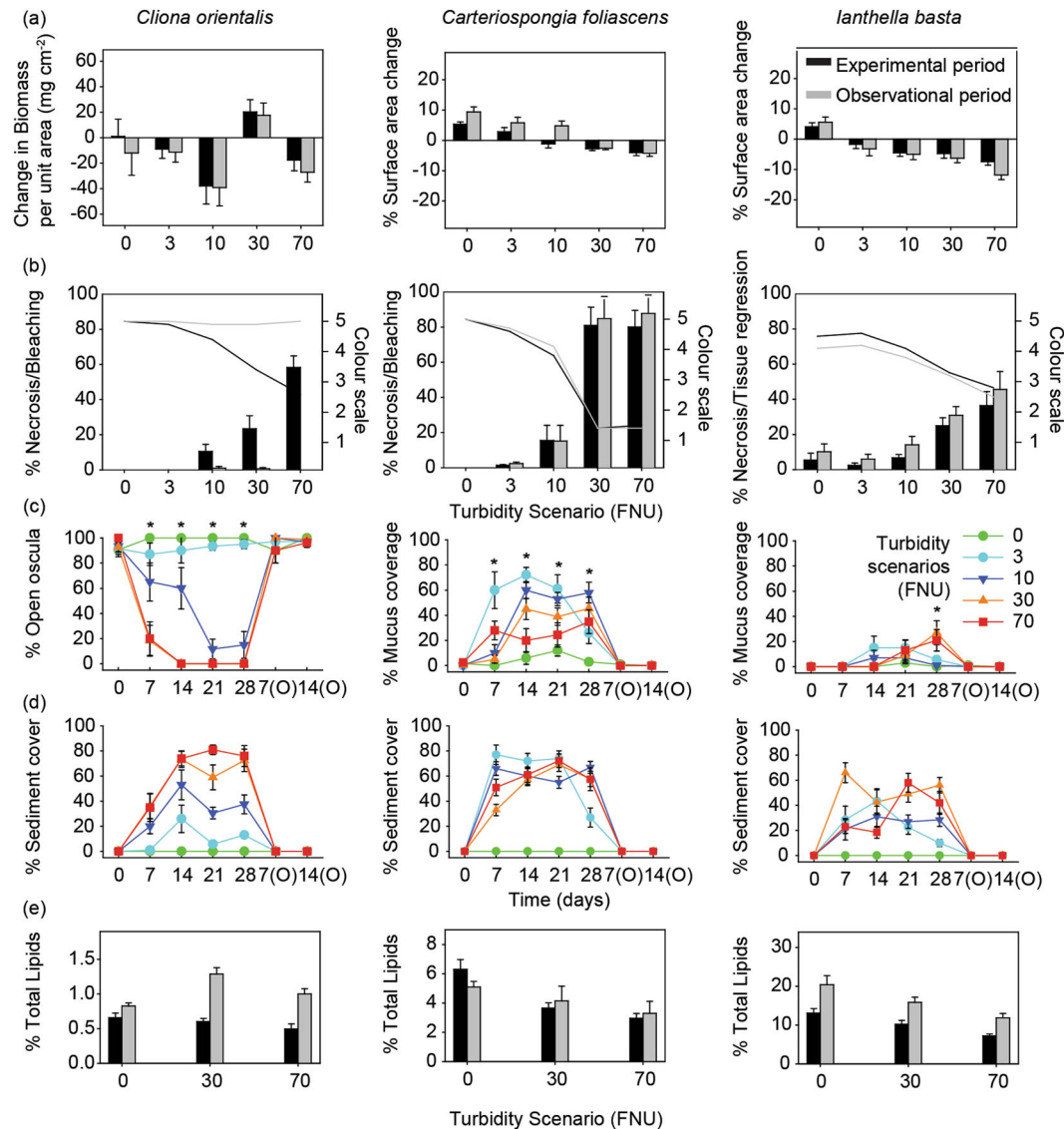


Figure 2. Sponge health, growth and behavioural responses. **(a)** Growth based on changes in biomass per unit area in *C. orientalis* (mg cm^{-2}) and percentage change in surface area in *C. foliascens* and *I. basta*, **(b)** percentage of necrotic, bleached, or regressed tissue (bars) and colour scale (lines), **(c)** percentage of open oscula in *C. orientalis* and mucus production in *C. foliascens* and *I. basta* as stress responses to sediments, **(d)** percentage of sediment cover on sponges, and **(e)** percentage of sponge biomass comprised of lipids, for all species and targeted scenarios (0, 3, 10, 30 and 70 FNU) after the 28 d experimental period and 14 d observational period in **a**, **b** and **e** and throughout the experiment in **c** and **d** (mean \pm SE). Asterisks in **c** show statistically significant differences between scenarios (ANOVA: $P < 0.05$).

species). However, total lipid content was lower in all species exposed to the ≥ 30 FNU scenarios by the end of the exposure period, although this was not statistically significant in *C. orientalis* (Fig. 2e, Table 3d). The percentage of total lipids in *C. foliascens* decreased from $6.3\% \pm 0.66$ (mean \pm SE) in the control to $2.9\% \pm 0.32$ in the 70 FNU scenario, and no significant recovery of lipid content occurred during the observational phase. Similarly, the percentage of total lipids in *I. basta* decreased from $13.1\% \pm 1.13$ (mean \pm SE) in the control to $7.2\% \pm 0.47$ in the 70 FNU scenario. Some recovery of lipid content was evident in *I. basta* towards the end of the observational phase (Fig. 2e, Table 3d). Finally, *C. orientalis* exposed to the 30 and 70 FNU scenarios exhibited a dramatic recovery in percent total lipids during the observational period (Fig. 2e, Table 2d).

Chlorophyll fluorescence. Maximum quantum yields were highly stable among scenarios in the phototrophic sponge *C. orientalis* throughout the experimental and observational phases (Fig. 4a, Table 4a). In *C. foliascens*, maximum quantum yields were significantly lower in bleached (discoloured) individuals from day 21 and 28 under the 70 and 30 FNU scenarios, respectively (Fig. 4a, Table 4a). High rates of bleaching, necrosis and subsequent mortality precluded recovery in this species.

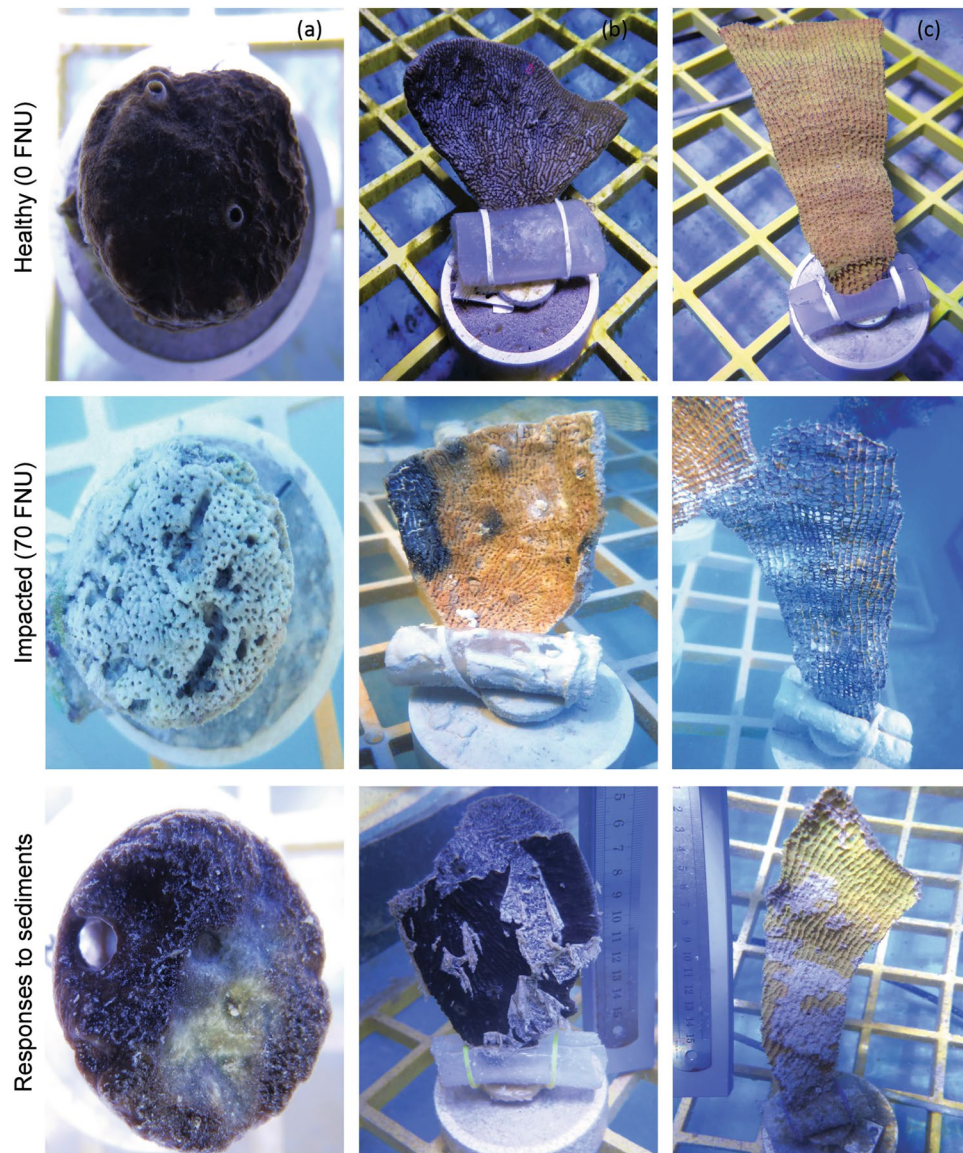


Figure 3. Sponge behavioural responses to sediments. (a) *C. orientalis*, (b) *C. foliascens*, and (c) *I. basta*. Healthy and impacted sponges under the control (0 FNU) and highest turbidity scenario (70 FNU), respectively, and their visual responses to sediment stress (i.e. oscula closure, mucus production and tissue regression).

Pigment analysis. Chl *a* concentration was highly correlated to total chlorophyll in both *C. orientalis* and *C. foliascens* ($R^2 = 0.997$ and 0.998 and $P < 0.001$, respectively). In addition, Chl *a* was highly correlated to Chl *c* in *C. orientalis* and negatively correlated to Chl *d* in *C. foliascens* ($R^2 = 0.993$, -0.392 and $P < 0.001$, respectively). Overall, concentrations of Chl *a* were stable throughout the experiment in the controls and lower turbidity scenarios (≤ 3 FNU) (Fig. 4b). However, significantly lower concentrations of Chl *a* were observed under higher turbidity scenarios (≥ 30 FNU) at the end of the experimental period for both species (Fig. 4b, Table 4b). Accordingly, Chl *c* in *C. orientalis* also decreased significantly in the 70 FNU scenario (ANOVA: $P < 0.001$) at the end of the experimental period (Supplementary Fig. S2). At the end of the 14 d observational period, *C. orientalis* did not show any significant differences between scenarios, consistent with a recovery of its original health status, colour and quantum yields after temporary bleaching (Fig. 4b, Table 4b, Fig. S2). *C. foliascens* did not recover during the observational period, and significantly lower values of Chl *a* were retrieved from scenarios ≥ 10 FNU (Fig. 4b, Table 4b). However, the negative correlation between Chl *a* and Chl *d* in *C. foliascens*, and a significant increase in Chl *d* in samples exposed to ≥ 30 FNU scenarios (ANOVA: $P < 0.001$), suggests an increase in some Chl *d*-containing Cyanobacteria under the higher turbidity scenarios (Fig. S2).

Non-metric Multi-Dimensional Scaling (nMDS) analysis of normalized data for all pigments retrieved by spectrophotometry (Chl *a*, Chl *b*, Chl *c*, Chl *d*, Total Chlorophyll and Carotenoids) showed some grouping of the samples according to scenarios for both species (Fig. 4c). This was most evident for *C. foliascens* exposed to ≥ 10 FNU (Fig. 4c), which is consistent with patterns observed for Chl *a*. PERMANOVA analysis confirmed

Parameter	Phase	Source	df	<i>Cliona orientalis</i>		<i>Carteriospongia foliascens</i>		<i>Ianthella basta</i>	
				F	P	F	P	F	P
(a) growth	Expt.	Scenario	4	3.864	0.009	14.348	<0.001	10.674	<0.001
		Error	45						
		Tukey		10 < 30		0, 3 > 10, 30, 70		0 > 3, 10, 30, 70	
	Obs.	Scenario	4	3.116	0.024	17.623	<0.001	12.283	<0.001
		Error	45						
		Tukey		10 < 30		0, 3, 10 > 30, 70		0 > 3, 10, 30, 70	
(b) % necrosis, bleaching & tissue regression	Expt.	Scenario	4	39.639	<0.001	31.694	<0.001	31.435	<0.001
		Error	45						
		Tukey		0, 3 < 30, 70		0, 3, 10 < 30, 70		0, 3 < 30, 70	
	Obs.	Scenario	4	3.063	0.547	36.878	<0.001	22.751	<0.001
		Error	45						
		Tukey				0, 3, 10 < 30, 70		0, 3 < 30, 70	
(c) stress responses	Expt.	Scenario	4	103.028	<0.001	7.439	<0.001	19.567	<0.001
		Error	45						
		SNK		0, 3 > 10, 30, 70		0, 3 < 10, 30		0, 3, 10 < 30, 70	
	Obs.	Scenario	4	0.367	0.831	1.000	1.000	1.000	1.000
		Error	45						
		SNK							
(d) % lipids	Expt.	Scenario	2	1.709	0.200	13.913	<0.001	10.400	<0.001
		Error	27						
		SNK				0 > 30, 70		0 > 30 > 70	
	Obs.	Scenario	2	9.874	<0.001	1.292	0.291	6.293	0.006
		Error	27						
		SNK		0 < 30 > 70				0 > 70	

Table 3. Analyses of variance on the effects of dredging on the physiological responses of sponges. (a) One-way ANOVA on sponge growth (changes in biomass per unit area in *C. orientalis*, and relative growth rate based on surface area in *C. foliascens* and *I. basta*), (b) One-way ANOVA on ranks of the percentage of necrotic, bleached and regressed tissue, (c) One-way ANOVA on percentage of open oscula in *C. orientalis* and on percentage of mucus coverage in *C. foliascens* and *I. basta*, (d) One-way ANOVA on the percentage of sponge biomass comprised of lipids, for each species separately, at the end of the experimental and observational phase. Tukey and Student Newman-Keuls (SNK) tests have been performed for significant pairwise multiple comparisons in a-b and c-d, respectively (scenarios: 0, 3, 10, 30 and 70 FNU).

significant differences between scenarios in both species, with subsequent pair-wise testing showing main differences between low and high turbidity scenarios (Table 4c).

Discussion

Turbidity associated with the release of sediments into the water column by dredging or natural resuspension can affect the sponge holobiont in many ways, primarily involving suspended sediment, light attenuation and sediment deposition. These stressors can act either alone or, more frequently, in combination and can change rapidly according to sea-state, cloud cover, and diel and tidal cycles^{4,32}. The 'protean' characteristic of turbidity makes it very difficult to predict impacts for management purposes. The results from this study show a range of responses from three sponge species to the combined effects of elevated SSC, light attenuation and sedimentation, with sponge health being negatively affected by moderate to high turbidity scenarios ($\geq 10 \text{ mg L}^{-1}$, $\leq 0.8 \text{ mol photons m}^{-2} \text{ d}^{-1}$). Responses included the production of mucus-like substances, bleaching, oscula (excurrent openings) closure, lipid depletion and tissue regression. Reduced chlorophyll content and low maximum quantum yield under the highest turbidity scenarios ($\geq 33 \text{ mg L}^{-1}$, $\leq 0.5 \text{ mol photons m}^{-2} \text{ d}^{-1}$) also indicated negative effects on the photosymbionts within the phototrophic sponges. In fact, for the phototrophic species, when light reduction and elevated suspended sediments were combined, it resulted in greater sub-lethal and lethal effects than seen previously when the stressors were applied in isolation^{23,34-36}. In addition, mortality occurred in *C. foliascens* and *C. orientalis* under the highest turbidity scenario (90% and 20%, respectively), although most *C. orientalis* and all individuals of *I. basta* survived and recovered once returned to clear water conditions.

The response of the sponges to the combined stressors and even to isolated stressors in the studies described in³⁴⁻³⁶ was varied and particular to the sponge species and nutritional mode being examined. Elevated turbidity caused some sponges, especially *C. foliascens*, to produce mucus-like sheets which trapped sediments. The sheets eventually sloughed off the surface into the water column removing sediments from the sponge. The term mucus has been used here in a broad sense³⁷, as the composition of the sponge mucus layer has not been characterised. Production of mucus-like substances in sponges has been anecdotally noted before in *Hemectyon felix*²⁵, *Crambe crambe*³⁸, *Mycale acerata*³⁹, *Rhopaloeides odorabile*⁴⁰, *Carteriospongia foliascens*, *Coscinoderma matthewsi*, *Cymbastela coralliophila* and *Stylissa flabelliformis*³⁶. The formation of mucus sheets has been previously reported in hard corals, particularly from the genus *Porites*^{41,42}. A number of studies have inferred this plays a role in

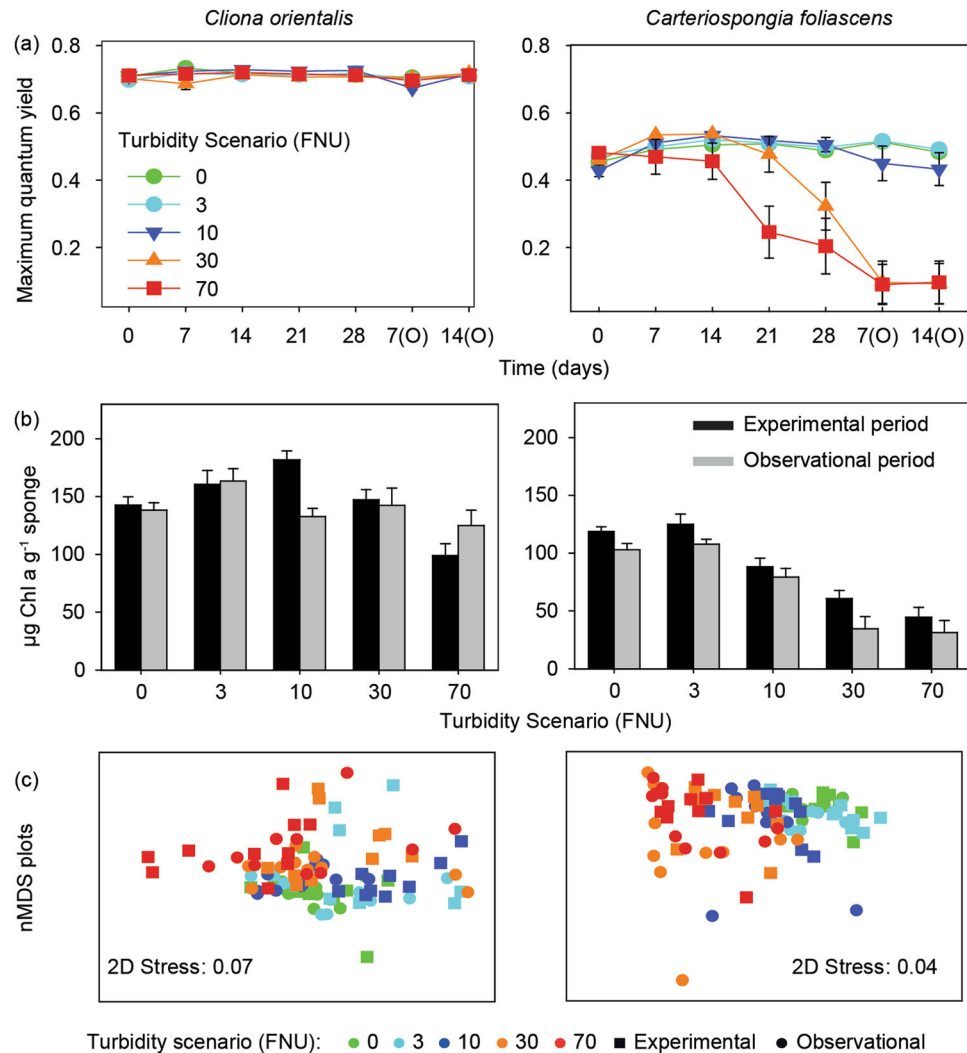


Figure 4. Photosymbiont response to the 5 different scenarios. (a) Mean values (\pm SE) of maximum quantum yield, (b) Mean values (\pm SE) of Chl *a*, and (c) Non-metric Multi-Dimensional Scaling (nMDS) of all photopigments retrieved by spectrophotometry, for the two phototrophic species and for all scenarios in the experimental and observational phases.

self-cleaning in *Porites* spp. to combat sedimentation, although others have suggested this is a secondary phenomenon^{42,43}. Certainly for species such as *C. foliascens* and *I. basta* the episodic shedding of sediment-impregnated mucus-sheet was an effective mechanism to remove surface accumulated sediments (Fig. 3b). As also noted for corals, the production of the layer is expected to come at an energetic cost⁴⁴, which would make it a difficult process to sustain during chronically elevated suspended sediments loads^{11,35} and/or repeated smothering³⁶.

To our knowledge, this is the first study to quantify the production of the mucus-like substance over time in sponges, and specifically, in response to sediment exposure. *C. foliascens* and *I. basta* both produced mucus layers under all sediment treatments (≥ 3 mg L⁻¹), although *C. foliascens* showed the highest percentage of mucus cover (i.e. up to 80%) from the start of the experiment. *C. foliascens* also experienced a depletion in energy reserves and high mortality towards the end of the exposure, which may be due to an inability to maintain phototrophic feeding under low light conditions (as suggested by decreased Chl *a* and reduced maximum quantum yields under the high turbidity scenarios). These results are consistent with previous research reporting that *C. foliascens* is unable to shift between nutritional modes (i.e. increasing heterotrophic feeding), and its intimate and potentially obligate symbioses with *Cyanobacteria* is adversely impacted by high SSCs and light attenuation^{34,35}. Therefore, formation and sloughing of mucus sheets in *C. foliascens* may only be effective under low SSCs with limited light attenuation or as a short-term response (<7 d) under higher turbidity scenarios before irreversible effects occur.

C. orientalis showed a significant reduction in the number of open oscula under high SSCs, with total oscula closure in the highest turbidity scenario. Oscula closure in this species is strongly correlated with reduced pumping²⁸, which is a common response of sponges to elevated SSCs^{25,26,28,35,39,45,46}. This response can be effective in the short term as it prevents clogging of the aquiferous system. However, it can also adversely affect filter-feeding, reducing food-retention efficiency and potentially leading to starvation in obligate heterotrophs^{35,39,40}. Increased

Parameter	Phase	Source	df	<i>Cliona orientalis</i>		<i>Carteriospongia foliascens</i>	
				F	P	F	P
(a) maximum quantum yield	Expt.	Scenario	4	2.920	0.031	7.338	<0.001
		Error	45				
		SNK		10 > 30		0, 3, 10 > 70	
	Obs.	Scenario	4	0.914	0.464	20.824	<0.001
		Error	45				
		SNK				0, 3, 10 > 30, 70	
(b) Chl <i>a</i>	Expt.	Scenario	4	10.520	<0.001	23.286	<0.001
		Error	45				
		SNK		3, 10 > 30 > 70		0, 3 > 10 > 30, 70	
	Obs.	Scenario	4	1.726	0.161	20.077	<0.001
		Error	45				
		SNK				0, 3 > 10 > 30, 70	
(c) PERMANOVA of all pigment data	Expt. + Obs.	Scenario	4	5.4241	0.0001	24.9	0.0001
		Time (Scenario)	5	3.6263	0.0009	2.3848	0.0071
		Error	90				
		Pair-wise Tests		0 ≠ 3, 10, 30 ≠ 70		0, 3 = 10 = 30, 70	

Table 4. Analyses of variance on the effects of turbidity scenarios on photosymbionts. One-way ANOVA examining the effects of turbidity scenarios on (a) maximum quantum yield and (b) Chl *a* concentrations, at the end of the experimental and observational periods, with Student Newman-Keuls (SNK) tests performed for significant pairwise multiple comparisons, and (c) Two-way PERMANOVA of all pigment data (Chl *a*, *b*, *c*, *d*, total Chlorophyll and Carotenoids) with scenario and time as factors, for the two phototrophic species (scenarios: 0, 3, 10, 30 and 70 FNU).

ocular closure together with potential canal blockage may explain the mortality of 20% of *C. orientalis* individuals in this study and is likely to be a response to the suspended sediment concentration.

A common feature in the higher turbidity scenarios in the phototrophic species was sponge bleaching or tissue discolouration concomitant with reductions in chlorophyll concentration. This was often a sublethal response, and in many cases sponges regained their pigmentation in the post exposure observation period. However, in the high turbidity scenarios, bleaching and partial and whole sponge mortality were intimately linked. Bleaching in these species has been reported previously solely in response to light deprivation³⁴, and the response is most likely a function of the low light levels associated with the turbidity scenario, as opposed to the high SSCs.

In addition to the production of mucus layers, *I. basta* also underwent tissue regression in response to high SSCs, which reduces the number of choanocyte chambers and results in more densely packed cells^{47, 48}. This mechanism for coping with sediment stress reduces the risk of the aquiferous system becoming clogged, but also causes the sponge to enter a stress-induced 'dormant' state⁴⁷. This dormant state may not be energetically sustainable in the long term as suggested by the reduction in total lipids in *I. basta* under high turbidity scenarios. Hence, although all 3 species possess mechanisms to cope with different sediment-related stressors, and despite the ability of both *C. orientalis* and *I. basta* to survive and recover from sediment stress in this 28 d experiment, we hypothesize that all 3 species would undergo higher mortalities if the stressors persist in time.

The development and use of sub-lethal stress indicators would alert dredging proponents of water quality conditions before they could detrimentally impact sponge populations. Discolouration and necrosis of sponge tissue have been previously described as effective bioindicators for dredging related stress³⁵. However, discolouration could also be related to natural causes or diel patterns in some species, such as the day-night migration of *Symbiodinium* sp. in *C. orientalis*⁴⁹ which would require the use of this bioindicator with caution and at defined times. On the other hand, lesion formation (i.e. partial mortality) may be irreversible in some sponge species and lead to rapid mortality as observed here and in previous studies for *C. foliascens*^{34, 35}. Although it is challenging to identify universal bioindicators that could be applied to all sponges, our results suggest that mucus sheet production, oscula closure and tissue regression could be effective bioindicators of turbidity-related stress in some sponge species and could be incorporated into future sponge monitoring programs. Mucus excretion has previously been proposed as a useful indicator for sediment stress in sponges^{10, 11} and corals^{50, 51} and tissue regression has previously been described as a symptom of stress⁴⁷.

The response of some of the species to the combined effects of elevated suspended sediment and reduced light availability was more immediate and severe than when applied alone in previous studies conducted under the same or similar conditions and species^{34, 35}. Specifically, decreased light levels coupled with high SSCs affected both phototrophic and heterotrophic feeding strategies simultaneously and likely contributed to the earlier and higher mortalities observed in *C. foliascens* and *C. orientalis* in comparison to previous studies assessing these factors independently^{34, 35}. For example, in this study, exposure of *C. foliascens* to high SSCs (33 mg L⁻¹) in combination with low light (0.5 mol photons m⁻² d⁻¹) resulted in tissue bleaching and 55% mortality within 28 d. In contrast, exposure to 0.8 mol photons m⁻² d⁻¹ (with a SSC of 0 mg L⁻¹) did not cause any mortality³⁴, and exposure to 23 mg L⁻¹ (with a DLI of 5 mol photons m⁻² d⁻¹) resulted in lower mortality³⁵ (Supplementary Table S1). Similarly, exposure to 76 mg L⁻¹ in combination with a DLI of 0.15 mol photons m⁻² d⁻¹ resulted in tissue

Species Name (Author)	Functional Morphology	Primary Nutritional Mode	Sampling location
<i>Cliona orientalis</i> (Thi le, 1900)	Encrusting (bioeroding)	phototrophic ⁵⁵	Pelorus Is. (Palm Is.) S 18°32.903' E 146° 29.172'
<i>Carteriospongia foliascens</i> (Pallas, 1766)	Cup (wide cup)	phototrophic ⁵⁶	Fantome Is. (Palm Is.) S 18°41.028' E 146° 30.706'
<i>Ianthella basta</i> (Pallas, 1766)	Erect (laminar)	heterotrophic ⁵⁷	Fantome Is. (Palm Is.) S 18° 42.291' 146° 30.591'

Table 5. List of sponge species, morphologies, nutrition mode and sampling locations.

bleaching and 85% mortality within 7 d, whilst exposure to 73 mg L^{-1} alone resulted in mortality only after 14 d, and $0 \text{ mol photons m}^{-2} \text{ d}^{-1}$ alone resulted in mortality only during the recovery period ($>28 \text{ d}$) (Supplementary Table S1). There was some sediment deposition on the sponges in this study which is another potential known stressor; however, the accumulation rate of sediment was low, reaching up to $5.2 \text{ mg cm}^{-2} \text{ d}^{-1}$. In previous studies, exposure to repeated sediment deposition events of up to 44 mg cm^{-2} for over a similar period (28 d) did not result in any bleaching or mortality in a range of species, including *C. foliascens*³⁶. For *C. orientalis*, it occasionally resulted in small accumulations of sediment in local surface depressions which led to small bleached patches and eventually to lesions. Although deposition rates in the present study were lower, similar bleached patches were observed where sediments accumulated.

It is possible to place the results of this study and previous studies^{34, 35} into context, using recent analyses of water quality monitoring data from several large scale dredging projects in tropical waters^{5, 6, 33}. The impacts of dredging on light attenuation and SSCs followed a power-law decay relationship, with sites near the excavation activities experiencing greater changes to water quality than more distant ones⁵. One of the dredging campaigns was conducted in a clear-water environment (Barrow Island, Western Australia⁴), with similar water quality to the collection location of sponges in this study. The average nephelometrically-derived SSCs and DLIs were calculated for five sites located $<1 \text{ km}$ from the dredging⁵. Over 30 d running mean periods determined for the duration of the 1.5 year program, the P_5 of mean DLIs was $0.4 \text{ mol photons m}^{-2} \text{ d}^{-1}$, as opposed to $1.9 \text{ mol photons m}^{-2} \text{ d}^{-1}$ during the baseline phase. Based on the laboratory studies examining the effects of light reduction alone over a similar period, a DLI of $0.8 \text{ mol photons m}^{-2} \text{ d}^{-1}$ resulted in bleaching in *C. orientalis* and *C. foliascens*³⁴. During the dredging, the P_{95} of SSCs over a 30 d running mean period was 23 mg L^{-1} , as opposed to 3.2 mg L^{-1} during the baseline phase. The laboratory based studies, examining the effects of elevated SSCs alone over a 30 d period, showed a range of effects at $\geq 23 \text{ mg L}^{-1}$ and few negative effects at SSC of $\leq 10 \text{ mg L}^{-1}$ ³⁵. Both of these laboratory-based studies suggest that even when applied in isolation, exposure to environmentally realistic conditions (of light reduction and elevated SSCs during dredging) could have negative effects on sponge communities. The results from this study, suggests that combinations of high SSCs and low light availability can accelerate and increase mortality increasing the probability of biological effects.

Finally, although sponges have mechanisms or adaptations to cope with dredging-related pressures in the short term, these tolerance mechanisms come at a cost, as evidenced by reduced lipids and deterioration of sponge health in all species towards the end of the experiment, suggesting that longer term exposure to similar conditions is likely to result in higher mortality. The LC_{50} and LC_{10} values derived for *C. foliascens* in this study and a previous study³⁵ could be used by managers and dredging proponents when implementing zones of impact based on dredge plume models. Priorities for future research include (i) assessing longer term impacts, (ii) assessing the effect of different frequency events and (iii) assessing the effects on potentially sensitive early life history stages.

Methods

Sample collection. The three sponge species, representing three general morphologies (encrusting, cup and fan) and nutritional modes (i.e. phototrophic and heterotrophic), were collected from 3–15 m depth from the Palm Islands, central Great Barrier Reef (GBR) in March 2016 (Table 5). *Cliona orientalis* (Thi le, 1900), *Carteriospongia foliascens* (Pallas, 1766) and *Ianthella basta* (Pallas, 1766) are common throughout the Indo-Pacific, including the east and west coasts of tropical Australia⁵². At least one quarter of each sponge individual was left in the field in order to facilitate recovery³³. *C. foliascens* and *I. basta* were cut into large explants ($\sim 5 \times 5 \text{ cm}$) and cores (radius: 2.45 cm, height: 2 cm) of the encrusting sponge *C. orientalis* were drilled from dead colonies of *Porites* spp. Sponges were transported to the Australian Institute of Marine Science (AIMS, Townsville) and acclimated for two weeks under natural light conditions in a 5000 L tank with flow-through seawater at 28°C and 36‰ salinity. Experiments were conducted with calcareous sediment collected from the lagoon of Davies Reef, a mid-shelf reef centrally located in the GBR (S $18^\circ 49.354'$ E $147^\circ 38.253'$) and processed to a predominately silt-size typical for dredge plumes⁵⁴ (mean particle size of $29 \mu\text{m}$, range: $3\text{--}64 \mu\text{m}$) as described in³⁵.

Experimental set up. Experiments were conducted in $10 \times 1200 \text{ L}$ fibreglass tanks with $5 \mu\text{m}$ filtered seawater in an environmentally controlled room within the National Sea Simulator (SeaSim) at AIMS (see Supplementary Fig. S3). Sponges were placed on a false bottom floor or made from fibre reinforced plastic grating (80% open) at a depth of 50 cm below the surface. Each tank had a Perspex window for observations during the experiments.

Sponges were exposed to 5 different situations representing different intensities of increased suspended sediment concentrations (SSCs), and associated light attenuation and sedimentation rate (see Table 1). Hereafter, the different treatments are referred to as 'scenarios' and based on the nominal turbidity (0, 3, 10, 30 and 70 NTU)

(Table 1). Two tank replicates were used for each scenario, with 10 replicate sponges per species in each tank. As replicate tanks within each treatment behaved similarly throughout the experiment for all physical parameters (i.e. turbidity, light and sediment deposition, T-tests: $P > 0.05$), and sponges were unlikely to influence each other within the large 1200 L tanks (i.e. sponges were >20 cm apart), sponges rather than tanks were used as replicates for statistical analyses. Sponges were acclimated to experimental control conditions in the tanks for one week prior to commencing the experiment. The experiment ran for a 28 d 'experimental period' followed by a 14 d 'observational' period where all sponges were returned to sediment-free seawater (Table 1).

The SSCs and associated light combinations were based on recently reported data from several large scale capital dredging programs^{5,6} (Table 1). Because the experiments were conducted in shallow containers (with only 50 cm water depth), the light attenuation associated with a given SSC would be much less than would occur *in situ* on a typical reef and it was therefore necessary to adjust the light accordingly. We nominally chose a water depth similar to the sponge collection depth (7 m) and used the relationships between water depth, SSC and PAR described in⁶ (which was based on empirical data collected by multiple light profiles through a dredging plume) to simulate the maximum down welling irradiance for a clear (cloud-free) sky at solar noon (with an initial underwater, 0 m depth PAR value of $\sim 1530 \mu\text{mol photons m}^{-2} \text{s}^{-1}$)⁶. During cloudy days, at lower azimuth angles and at different sea states, underwater light quality and quantity would differ substantially.

Lighting was provided by 2 custom-made sets of Light Emitting Diodes (LED) positioned above each tank. Light within each tank was measured using a photosynthetically active radiation (PAR) Quantum Sensor (Skye, UK) positioned on the fiber reinforced plastic grating next to the sponges. Both the lights and the light sensor were connected to a programmable logic controller (PLC) system which controlled the light based on the SSC (see above). In addition, light intensity in each tank simulated daylight variation, with a 6 h ramping up from 05:30 h (sunrise) to full light from 11:30–12:30, followed by a 6 h ramping down to sunset at 18:30 h. Light levels were expressed as the daily light integral (DLI) in units of $\text{mol photons m}^{-2} \text{d}^{-1}$, which is the sum of the per second quantum flux measurements over the course of 24 h.

Water fl w into the tanks was standardized to 1000 mL min^{-1} to ensure ~ 1.5 complete turnover per day. Water temperature was 28 ± 1 °C in all tanks over the duration of the experiment. SSCs were mixed within the experimental tanks using a recirculating Iwaki MX pump (Iwaki Co., Ltd., Japan) at 45 Hz and an underwater Hydrowizard pump (Panta Rhei, Germany) which was set to oscillate from 24–25% power in 'wave' mode (0.6 s pulse: 0.6 s no pulse). The combined pumps created a turbulent, fl w typical on shallow coral reefs⁵⁸, generating in-tank fl w rates of $\sim 4 \text{ cm s}^{-1}$, as measured using a mini acoustic doppler velocimeter (ADCP, SonTek 16-MHz MicroADV Sontek, US). To bring the SSC to the desired levels and to replace sediment lost from the tanks (by the water exchange) short pulses of a high SSC ($\sim 6 \text{ g L}^{-1}$) sediment slurry from a 500 L stock tank was episodically injected into the tanks through a solenoid valve. SSCs were continually measured in each tank using turbidity as a proxy, using Turbimax CUS31 nephelometers (Endress and Hauser, Germany) connected to the PLC system. Nephelometers were calibrated to formazin nephelometric units (FNU), and a near 1:1 correlation was established between FNU and mg L^{-1} of sediment (see equation below). SSCs in the tanks were kept constant by a continuous feedback mechanism from the nephelometer probes through the PLC which also controlled the opening and closing of the solenoids as required. Associated with the SSC, and corresponding light level, there was also some sedimentation that occurred on the sponges in the tanks (Table 1).

Physical parameters. Water samples ($3 \times 200 \text{ mL}$) were collected from each tank each week and the SSCs were determined gravimetrically by filtering the samples through pre-weighed $0.4 \mu\text{m}$ polycarbonate filters, drying the samples (60 °C for 24 h) and re-weighing the filters.

Throughout the experiment, FNU values related to SSCs according to the following equation:

$$\text{SSC}(\text{mg L}^{-1}) = 1.089 \times \text{FNU}(F_{1,9} = 578.5, P < 0.01, R^2 = 0.985)$$

Sediment deposition was measured in real-time using a deposition sensor⁵⁹ located in the middle of the grate fl or and two SedPods⁶⁰ (Surface Area = 25.2 cm^2) randomly placed in each tank. SedPod sediment accumulation rates were measured weekly by collecting and filtering sediments that settled on the surface for 24 h.

Differences in turbidity and DLIs were analysed between replicate tanks with T-tests and with a one-way repeated measures analysis of variance (ANOVA) at the end of the experimental and observational phase with treatment as fi ed factor. Differences in SSCs and SR between treatments were furthered assessed throughout the experiment with a two-way repeated measures ANOVA using treatment (i.e. scenario) and day as fi ed factors.

Unless otherwise stated, statistical analyses and graphs were performed using the software R v. 3.1.0⁶¹ and SigmaPlot v.11.0 (Systat Software Inc.).

Studied parameters. After the 28 d experimental period, 10 individuals from each species were sampled from each scenario (and removed from the experiment), and a further 10 individuals were sampled after the 14 d observational period, for all 'destructive' analyses (i.e. lipids and pigments). To obtain baseline data on sponge health, 5 extra individuals were processed for each species after aquarium acclimation ($t = 0$ controls).

In order to enable weekly 'non-destructive' measurements (i.e. pictures, visual assessments and fluorescence measurements), sediment dosing was interrupted and the power in the Iwaki and Hydrowizard pumps decreased to 20 Hz and 1% respectively, causing a subsequent drop in turbidity levels in the tanks for a period of < 20 h from 16.00 h on Tuesday until 12.00 h on Wednesday, each week. Light values, however, were maintained at the corresponding levels irrespectively of SSCs to minimize effects on the experimental scenarios.

Sponge health, growth and stress responses to sediments. A 2-dimensional approach for growth (i.e. surface area), partial mortality (necrosis), tissue regression and loss of photosynthetic symbionts

(discolouration or bleaching) were recorded weekly using a digital camera and analysed using image analysis software (ImageJ⁶²). Growth and bioerosion in *C. orientalis* cores was determined using buoyant weights (± 0.001 g) before and after the experimental and observational periods, and normalized to surface area to obtain changes in biomass per unit area, which are correlated to bioerosion rates in this species⁶³. Relative growth rates in *C. foliascens* and *I. basta* were calculated as the \log_{10} of their final surface area (SA) measure divided by their initial SA.

In addition, sponges were visually assessed at midday once a week to check for stress responses, including percent mucus cover, sediment cover, bleaching and necrosis. Sponges presenting >50% necrosed tissue were considered effectively dead and were sampled for 'destructive' analyses. The percentage of tissue regression was also assessed in *I. basta*, which presents a dynamic pattern of regression/recovery⁴⁷. The contractile behaviour of the oscula in *C. orientalis* was used as an additional stress response. This involved comparing the numbering of open oscula to the total number of oscula per individual throughout the experiment.

All treatment effects were tested with one-way ANOVAs; statistical analyses found that there was no significant difference between tanks within scenarios, thus tank effect was not considered further. In any instances where homogeneity of variances and normality were not met, a Kruskal-Wallis one-way ANOVA on ranks was performed. Mortality data was fitted to nonlinear regression curves using the program Prism v7.01 (GraphPad Software Inc, US). Regression curves were used to calculate the lethal concentrations (LC) of SSC and DLI at which 50% (LC₅₀) and 10% (LC₁₀) of the population died. The models were constrained between 0 and 100 with F values set at 50 and 10, for LC₅₀ and LC₁₀, respectively. The curve was tested for normality of the residuals and a replicate test was applied to assess goodness of fit. Asymmetrical confidence intervals were calculated for the LC values.

Lipid analysis. The concentration of total lipids in sponge tissue was measured over time as a proxy for health (i.e. energetic stress). Samples were analysed at the start of the experiment and at the end of the experimental and observational periods in the 0, 30 and 70 NTU scenarios. Lipids were extracted from ~100 mg of freeze-dried ground sample as described elsewhere^{35, 64, 65}. Total lipid content was reported as percentage biomass based on a dry weight conversion factor. T-tests were used to assess changes in lipid content throughout the experiment in control samples, whereas differences between scenarios at the end of each sampling point were assessed for each species separately using a one-way ANOVA.

Chlorophyll fluorescence. Photosynthetic capacity (maximum quantum yield) of the phototrophic symbionts in *C. orientalis* and *C. foliascens* was measured with a Diving-PAM (pulse amplitude modulation) chlorophyll fluorometer (Heinz Walz GmbH, Effeltrich, Germany) as described in³⁴. Briefly, maximum quantum yield (F_v/F_m)⁶⁶ measurements were obtained from dark-adapted sponges (measured before sunrise) at weekly intervals throughout the experimental and observational periods. Bleached individuals of *C. foliascens* that died during the experiment were assumed to have the lowest detected quantum yield value (zero) in subsequent weeks after mortality throughout the time series. Changes in maximum quantum yield at the end of the experimental and observational periods were assessed for each species separately using a one-way ANOVA with scenario as the fixed factor.

Pigment analysis. Pigment analyses were performed on tissue from the phototrophic sponges *C. orientalis* and *C. foliascens* at the end of the experimental and observational periods. Pigments from samples incorporating pinacoderm and mesohyl regions were extracted and analysed as described in²³ and standardized to sponge wet weight. The concentration of Chlorophyll *a* (hereafter Chl *a*) was used as a proxy for changes in photosymbiont health/activity (i.e. bleaching)¹⁵. Changes in Chl *a* concentration at the end of the experimental and observational periods were assessed for each species separately using a one-way ANOVA with scenario as the fixed factor. Pearson correlations were performed between all studied pigments. All pigments measured by spectrophotometry (i.e. chlorophylls *a*, *b*, *c*, *d*, Total chlorophylls and carotenoids) were used to build resemblance matrices based on normalized data for each species separately. Non-metric Multi-Dimensional Scaling (nMDS) plots were created using Euclidean distances. Two factors were determined (i.e. scenario and sampling time, nested to scenario) and examined by PERMANOVA (Permutational multivariate ANOVA based on distances). All multivariate analyses were performed using Primer 6 (Primer-E Ltd, UK).

References

- Schönberg, C. H. L. & Fromont, J. Sponge gardens of Ningaloo Reef (Carnarvon Shelf, Western Australia) are biodiversity hotspots. *Hydrobiologia* **687**, 143–161 (2011).
- Jones, R., Ricardo, G. F. & Negri, A. P. Effects of sediments on the reproductive cycle of corals. *Mar. Pollut. Bull.* **100**, 13–33 (2015).
- Erfemeijer, P. L. A. & Lewis, R. R. Environmental impacts of dredging on seagrasses: a review. *Mar. Pollut. Bull.* **52**, 1553–72 (2006).
- Jones, R., Bessell-Browne, P., Fisher, R., Klonowski, W. & Slivkoff, M. Assessing the impacts of sediments from dredging on corals. *Mar. Pollut. Bull.* **102**, 9–29 (2016).
- Fisher, R., Stark, C., Ridd, P. & Jones, R. Spatial patterns in water quality changes during dredging in tropical environments. *PLoS One* **10**, e0143309 (2015).
- Jones, R., Fisher, R., Stark, C. & Ridd, P. Temporal patterns in seawater quality from dredging in tropical environments. *PLoS One* **10**, e0137112 (2015).
- Bell, J. J. The functional roles of marine sponges. *Estuar. Coast. Shelf Sci.* **79**, 341–353 (2008).
- Goeij, J. M. De *et al.* Surviving in a marine desert: the sponge loop retains resources within coral reefs. *Science (80-)* **342**, 108–110 (2013).
- Maldonado, M. Sponge waste that fuels marine oligotrophic food webs: a re-assessment of its origin and nature. *Mar. Ecol.* **37**, 477–491 (2016).
- Bell, J. J. *et al.* Sediment impacts on marine sponges. *Mar. Pollut. Bull.* **94**, 5–13 (2015).
- Schönberg, C. H. L. Effects of dredging on filter feeder communities, with a focus on sponges. Report of Theme 6 - Project 6.1.1 prepared for the Dredging Science Node (2016).

12. Environmental Protection Authority WA. Environmental Assessment Guidelines (2013).
13. Reiswig, H. Particle feeding in natural populations of three marine demosponges. *Biol. Bull.* **141**, 568–591 (1971).
14. Wilkinson, C. R., Garrone, R. & Vacelet, J. Marine Sponges Discriminate between Food Bacteria and Bacterial Symbionts: Electron Microscope Radioautography and *in situ* Evidence. *Proc. R. Soc. London. Ser. B. Biol. Sci.* **220**, 519 LP–528 (1984).
15. Wilkinson, C. R. Net primary productivity in coral reef sponges. *Science (80-)* **219**, 410–412 (1983).
16. Thacker, R. W. & Freeman, C. J. In *Advances in Marine Biology* (eds Becerro, M. A., Uriz, M. J., Maldonado, M. & Turon, X.) **62**, 57–111 (Elsevier Ltd, 2012).
17. Hill, M., Allenby, A., Ramsby, B., Schönberg, C. & Hill, A. Symbiodinium diversity among host clonoid sponges from Caribbean and Pacific reefs: Evidence of heteroplasmy and putative host-specific symbiont lineages. *Mol. Phylogenet. Evol.* **59**, 81–8 (2011).
18. Schönberg, C. H. L. & Loh, W. K. W. Molecular identity of the unique symbiotic dinoflagellates found in the bioeroding demosponge *Cliona orientalis*. **299**, 157–166 (2005).
19. Erwin, P. & Thacker, R. Phototrophic nutrition and symbiont diversity of two Caribbean sponge–cyanobacteria symbioses. *Mar. Ecol. Prog. Ser.* **362**, 139–147 (2008).
20. Webster, N. S. & Thomas, T. The Sponge Hologenome. *MBio* **7**, e00135–16 (2016).
21. Thomas, T. *et al.* Diversity, structure and convergent evolution of the global sponge microbiome. *Nat. Commun.* **7**, 11870 (2016).
22. Maldonado, M., Giraud, K. & Carmona, C. Effects of sediment on the survival of asexually produced sponge recruits. *Mar. Biol.* **154**, 631–641 (2008).
23. Pineda, M. C., Duckworth, A. & Webster, N. Appearance matters: sedimentation effects on different sponge morphologies. *J. Mar. Biol. Assoc. United Kingdom* **96**, 481–492 (2016).
24. Schönberg, C. H. L. Happy relationships between marine sponges and sediments – a review and some observations from Australia. *J. Mar. Biol. Assoc. United Kingdom* **96**, 493–514 (2016).
25. Gerrodette, T. & Flechsig, A. Sediment-induced reduction in the pumping rate of the tropical sponge *Verongia lacunosa*. *Mar. Biol.* **55**, 103–110 (1979).
26. Tompkins-MacDonald, G. J. & Leys, S. P. Glass sponges arrest pumping in response to sediment: implications for the physiology of the hexactinellid conduction system. *Mar. Biol.* **154**, 973–984 (2008).
27. Ilan, M. & Abelson, A. The Life of a Sponge in a Sandy Lagoon. *Biol. Bull.* **189**, 363 (1995).
28. Strehlow, B. W., Jorgensen, D., Webster, N. S., Pineda, M. C. & Duckworth, A. Using a thermistor flowmeter with attached video camera for monitoring sponge excurrent speed and oscular behaviour. *PeerJ* **4**, e2761 (2016).
29. Roberts, D. E., Davis, A. R. & Cummins, S. P. Experimental manipulation of shade, silt, nutrients and salinity on the temperate reef sponge *Cymbastela concentrica*. **307**, 143–154 (2006).
30. Biggerstaff, A., Smith, D. J., Jompa, J. & Bell, J. J. Photoacclimation supports environmental tolerance of a sponge to turbid low-light conditions. *Coral Reefs* **34**, 1049–1061 (2015).
31. Schönberg, C. H. L. Self-cleaning surfaces in sponges. *Mar. Biodivers.* **45**, 623–624 (2015).
32. Chartrand, K. M., Bryant, C. V., Carter, A. B., Ralph, P. J. & Rasheed, M. A. Light thresholds to prevent dredging impacts on the Great Barrier Reef seagrass, *Zostera muelleri* ssp. *capricorni*. *Front. Mar. Sci.* **3**, 1–17 (2016).
33. Abdul Wahab, M. A., Fromont, J., Gomez, O., Fisher, R. & Jones, R. Comparisons of benthic filter feeder communities before and after a large-scale capital dredging program. *Mar. Poll. Bull. (In Press)*.
34. Pineda, M. C. *et al.* Effects of light attenuation on the sponge holobiont- implications for dredging management. *Sci. Rep.* **6**, 39038 (2016).
35. Pineda, M. C. *et al.* Effects of suspended sediments on the sponge holobiont with implications for dredging management. *Sci. Rep.* doi:10.1038/s41598-017-05241-z (2017).
36. Pineda, M. C. *et al.* Effect of sediment smothering on the sponge holobiont with implications for dredging management. *Sci. Rep.* doi:10.1038/s41598-017-05243-x (2017).
37. Bythell, J. C. & Wild, C. Biology and ecology of coral mucus release. *J. Exp. Mar. Bio. Ecol.* **408**, 88–93 (2011).
38. Turon, X., Uriz, M. J. & Willenz, P. Cuticular linings and remodelisation processes in *Crambe crambe* (Demospongiae: Poecilosclerida). *Mem. Queensl. Museum* 617–625 (1999).
39. Kowalke, J. Ecology and energetics of two Antarctic sponges. **247**, 85–97 (2000).
40. Bannister, R. J., Battershill, C. N. & de Nys, R. Suspended sediment grain size and mineralogy across the continental shelf of the Great Barrier Reef: Impacts on the physiology of a coral reef sponge. *Cont. Shelf Res.* **32**, 86–95 (2012).
41. Duerden, J. E. The role of mucus in corals. *Quart J Microsc Sci* **49**, 591–614 (1906).
42. Lewis, J. B. The formation of mucus envelopes by hermatypic corals of the genus *Porites*. *Caribb J Sci* **13**, 3–4 (1973).
43. Coffroth, M. Mucous sheet formation on Poritid corals: effects of altered salinity and sedimentation. In *Proceedings of the 5th International Coral Reef Congress, Tahiti, French Polynesia* (1985).
44. Brown, B. & Bythell, J. Perspectives on mucus secretion in reef corals. *Mar. Ecol. Prog. Ser.* **296**, 291–309 (2005).
45. Kutti, T. *et al.* Metabolic responses of the deep-water sponge *Geodia barretti* to suspended bottom sediment, simulated mine tailings and drill cuttings. *J. Exp. Mar. Bio. Ecol.* **473**, 64–72 (2015).
46. Tjensvoll, I., Kutti, T., Fosså, J. H. & Bannister, R. J. Rapid respiratory responses of the deep-water sponge *Geodia barretti* exposed to suspended sediments. *Aquat. Biol.* **19**, 65–73 (2013).
47. Luter, H. M., Whalan, S. & Webster, N. S. The marine sponge *Ianthella basta* can recover from stress-induced tissue regression. *Hydrobiologia* **687**, 227–235 (2012).
48. Leys, S. P. & Meech, R. W. Physiology of coordination in sponges. *Can. J. Zool.* **84**, 288–306 (2006).
49. Fang, J. K. H., Schönberg, C. H. L., Hoegh-Guldberg, O. & Dove, S. Day–night ecophysiology of the photosymbiotic bioeroding sponge *Cliona orientalis* Thiele, 1900. *Mar. Biol.* **163**, 100 (2016).
50. Bessell-Browne, P., Fisher, R., Duckworth, A. & Jones, R. Mucous sheet production in *Porites*: an effective bioindicator of sediment related pressures. *Mar. Poll. Bull.*, doi:10.1016/j.ecolind.2017.02.023 (2017).
51. Erfemeijer, P. L. A., Riegl, B., Hoeksema, B. W. & Todd, P. A. Environmental impacts of dredging and other sediment disturbances on corals: A review. *Mar. Pollut. Bull.* **64**, 1737–1765 (2012).
52. Fromont, J. Porifera (sponges) of the Dampier Archipelago, Western Australia: habitats and distribution. *Rec. West. Aust. Museum* **66**, 69–100 (2004).
53. Duckworth, A. R. Effect of wound size on the growth and regeneration of two temperate subtidal sponges. *J. Exp. Mar. Bio. Ecol.* **287**, 139–153 (2003).
54. McCook, L. J. *et al.* Synthesis of current knowledge of the biophysical impacts of dredging and disposal on the Great Barrier Reef: Report of an Independent Panel of Experts (2015).
55. Schönberg, C. H. L. & Loh, W. K. W. Molecular identity of the unique symbiotic dinoflagellates found in the bioeroding demosponge *Cliona orientalis*. *Mar. Ecol. Prog. Ser.* **299**, 157–166 (2005).
56. Ridley, C. P., Faulkner, D. & Haygood, M. G. Investigation of Oscillatoria spongeliae-dominated bacterial communities in four didymoceratid sponges. *Appl. Environ. Microbiol.* **71**, 7366–75 (2005).
57. Cheshire, A. C. A., Wilkinson, C. R. C., Seddon, S. & Westphalen, G. Bathymetric and seasonal changes in photosynthesis and respiration of the phototrophic sponge *Phyllospongia lamellosa* in comparison with respiration by the heterotrophic sponge *Ianthella basta* on Davies Reef, Great Barrier Reef. *Mar. Freshw. Res.* **48**, 589–599 (1997).

58. Koehl, M. A. R. & Hadfi ld, M. G. Hydrodynamics of larval settlement from a larva's point of view. *Integr. Comp. Biol.* **50**, 539–551 (2010).
59. Whinney, J., Jones, R., Duckworth, A. & Ridd, P. Continuous *in situ* monitoring of sediment deposition in shallow benthic environments. *Coral Reefs* doi:10.1007/s00338-016-1536-7 (2017).
60. Field, M. E., Chezar, H. & Storlazzi, C. D. SedPods: a low-cost coral proxy for measuring net sedimentation. *Coral Reefs* **32**, 155–159 (2013).
61. R Core Team. R: A Language and Environment for Statistical Computing. *R Foundation for statistical computing, Vienna, Austria* Available at: <http://www.r-project.org/> (2015).
62. Schneider, C. A., Rasband, W. S. & Eliceiri, K. W. NIH Image to ImageJ: 25 years of image analysis. *Nat. Methods* **9**, 671–675 (2012).
63. Fang, J. K. H., Schönberg, C. H. L., Kline, D. I., Hoegh-Guldberg, O. & Dove, S. Methods to quantify components of the excavating sponge *Cliona orientalis* Thiele, 1900. *Mar. Ecol.* **34**, 193–206 (2013).
64. Folch, J., Lees, M. & Sloane-Stanley, G. A simple method for the isolation and purification of total lipids from animal tissues. *J. Biol. Chem.* **226**, 497–509 (1957).
65. Conlan, J. A., Jones, P. L., Turchini, G. M., Hall, M. R. & Francis, D. S. Changes in the nutritional composition of captive early-mid stage *Panulirus ornatus* phyllosoma over ecdysis and larval development. *Aquaculture* **434**, 159–170 (2014).
66. Genty, B., Briantais, J. & Baker, N. The relationship between the quantum yield of photosynthetic electron-transport and quenching of Chlorophyll fluorescence. *Biochim. Biophys. Acta* **990**, 87–92 (1989).

Acknowledgements

This research was funded by the Western Australian Marine Science Institution (WAMSI) as part of the WAMSI Dredging Science Node, and made possible through investment from Chevron Australia, Woodside Energy Limited, BHP Billiton as environmental offsets and by co-investment from the WAMSI Joint Venture partners. The commercial entities had no role in data analysis, decision to publish, or preparation of the manuscript. The views expressed herein are those of the authors and not necessarily those of WAMSI. All collections were performed under Great Barrier Reef Marine Park Regulations 1983 (Commonwealth) and Marine Parks regulations 2006 (Queensland) Permit G12/35236.1 and Permit G13/35758.1. We are thankful to the crew of the San Miguel for helping with the sponge collection for this study. We also thank the staff at AIMS Marine Operations and AIMS National Sea Simulator for their technical assistance and expertise, to P Bessell-Browne and N Giofre for their time and efforts on the WAMSI tank prototyping and to M Sternel and E Arias for their valuable help in the field and while running the experiment. N.S.W. was funded by an Australian Research Council Future Fellowship FT120100480.

Author Contributions

M.C.P., B.S., A.D., R.J. and N.S.W. designed the experiment. M.C.P. and B.S. undertook the experiment. M.C.P., B.S. and J.K. undertook laboratory analyses. M.C.P. and B.S. analysed the data. M.C.P., B.S., A.D., R.J. and N.S.W. wrote the manuscript. All authors reviewed the manuscript.

Additional Information

Supplementary information accompanies this paper at doi:10.1038/s41598-017-05251-x

Competing Interests: The authors declare that they have no competing interests.

Publisher's note: Springer Nature remains neutral with regard to jurisdictional claims in published maps and institutional affiliations.



Open Access This article is licensed under a Creative Commons Attribution 4.0 International License, which permits use, sharing, adaptation, distribution and reproduction in any medium or format, as long as you give appropriate credit to the original author(s) and the source, provide a link to the Creative Commons license, and indicate if changes were made. The images or other third party material in this article are included in the article's Creative Commons license, unless indicated otherwise in a credit line to the material. If material is not included in the article's Creative Commons license and your intended use is not permitted by statutory regulation or exceeds the permitted use, you will need to obtain permission directly from the copyright holder. To view a copy of this license, visit <http://creativecommons.org/licenses/by/4.0/>.

© The Author(s) 2017

Supporting Online Material

Effects of combined dredging-related stressors on sponges: a laboratory approach using realistic scenarios

Mari-Carmen Pineda^{1,2^*}, Brian Strehlow^{3^}, Jasmine Kamp⁴, Alan Duckworth^{1,2}, Ross Jones^{1,2} and Nicole S. Webster^{1,2}

¹ *Australian Institute of Marine Science (AIMS), Townsville, QLD and Perth, WA, Australia*

² *Western Australian Marine Science Institution, Perth, WA, Australia*

³ *Centre for Microscopy Characterisation and Analysis, School of Plant Biology and Oceans Institute, University of Western Australia, Crawley, WA, Australia*

⁴ *James Cook University, Townsville, QLD, Australia*

[^]represents joint 1st authors

*Corresponding author:

Mari-Carmen Pineda

Australian Institute of Marine Science, PMB3, Townsville, QLD, 4810, Australia

E-mail: mcarmen.pineda@gmail.com.

Tel.: +61 7 4753 4522, fax: +61 7 4772 5852

Figure S1. Percentage of mortality for each scenario across the experiment in *C. orientalis* and *C. foliascens*.

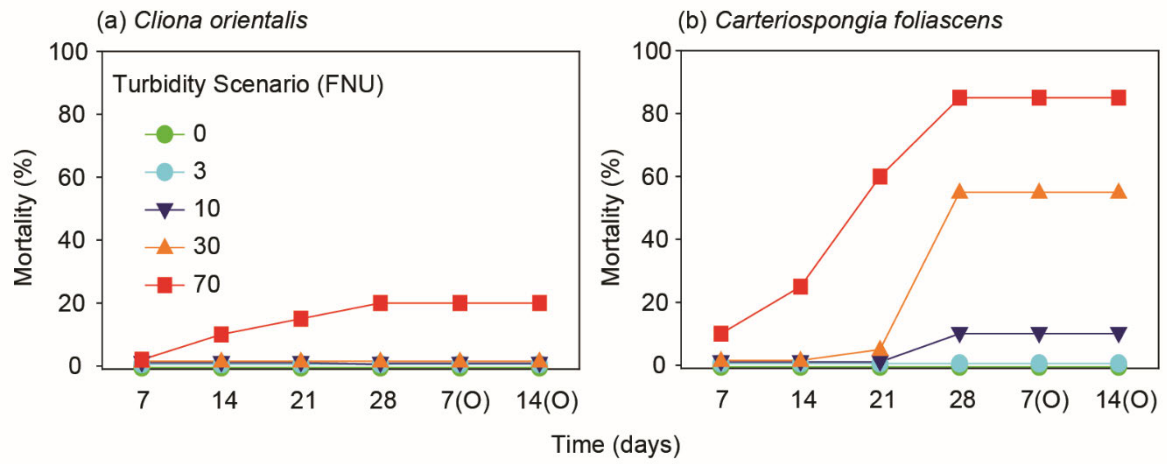


Figure S2. Mean values (\pm SE) of (a) Chl c and (b) Chl d in *C. orientalis* and *C. foliascens*, respectively, at 5 turbidity scenarios after the experimental and observational periods.

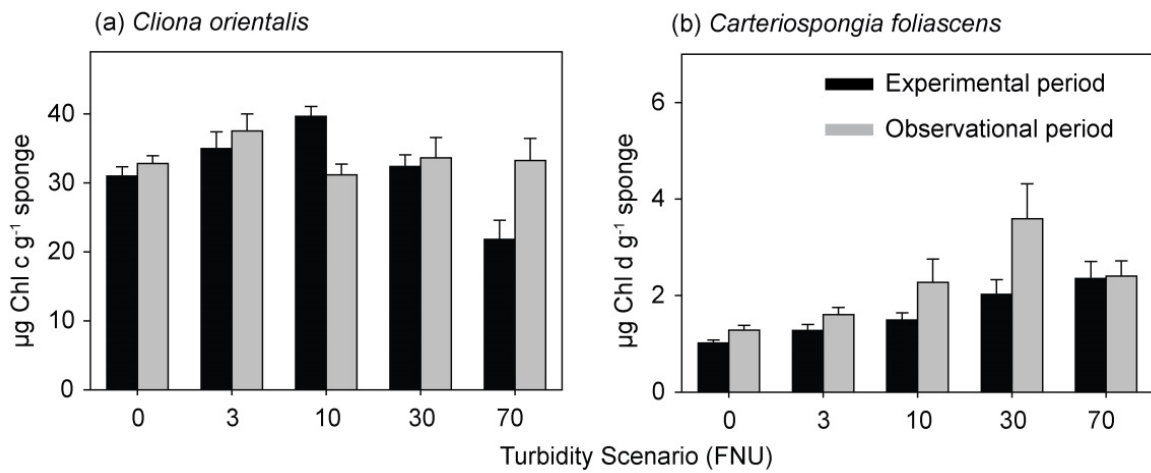


Figure S3. Experimental set up. Experimental set up in an environmentally controlled room within the National Sea Simulator (SeaSim) at the Australian Institute of Marine Science (AIMS, Townsville, Australia).



Table S1. Response of phototrophic sponges to stressors in isolation and combined. Response of the boring sponge *C. orientalis* and the foliose sponge *C. foliascens* to light reduction (as daily light integral [DLI], mol photons $\text{m}^{-2} \text{d}^{-1}$) and elevated SSCs (nephelometrically-derived SSC, mg L^{-1}) alone or in combination over a 28 d experimental exposure period (exp.) and subsequent 14 d observational period (obs.).

Experiment (Source)	SSC (mg L^{-1})	Light (DLI) (mol photons $\text{m}^{-2} \text{d}^{-1}$)	<i>Cliona orientalis</i>	<i>Carteriospongia foliascens</i>
SSC constant light variable (³⁴)	0	0	Bleaching (>3 d) but no mortality	Bleaching (>7 d). No mortality in exp. 100% mortality during obs.
	0	0.8	Minor bleaching at end of the 28 d exp. but no mortality	Minor bleaching towards the end of exp. but no mortality
Light constant SSC variable (³⁵)	10	5	~5% bleaching (28 d) but no mortality	5–20% bleaching (>21 d) and 20% mortality (from 28 d)
	23	5	5–10% bleaching in exp. but no mortality	5–20% bleaching (>21 d) and 20% mortality (>28 d)
	73	5	40% bleaching (>7 d) but no mortality	40–80% bleaching (>14 d) and 90% mortality (>14 d)
Light variable SSC variable (this study)	11	0.87	~10% bleaching (>21 d) but no mortality	20% bleaching (>14 d) and 10% mortality (>21 d)
	33	0.5	20% bleaching (>14 d) but no mortality	90% bleaching (>14 d) and 55 % mortality (>14 d)
	76	0.15	60% bleaching (>14 d), 20% mortality (> 14 d)	90% bleaching (>7 d) and 85% mortality (>7 d)



Using a thermistor flowmeter with attached video camera for monitoring sponge excurrent speed and oscular behaviour

Brian W. Strehlow^{1,2,3}, Damien Jorgensen³, Nicole S. Webster^{2,3}, Mari-Carmen Pineda^{2,3} and Alan Duckworth^{2,3}

¹ Centre for Microscopy, Characterisation and Analysis, School of Plant Biology, and Oceans Institute, University of Western Australia, Crawley, WA, Australia

² Western Australian Marine Science Institution, Crawley, WA, Australia

³ Australian Institute of Marine Science, Townsville, QLD, Australia

ABSTRACT

A digital, four-channel thermistor flowmeter integrated with time-lapse cameras was developed as an experimental tool for measuring pumping rates in marine sponges, particularly those with small excurrent openings (oscula). Combining flowmeters with time-lapse imagery yielded valuable insights into the contractile behaviour of oscula in *Cliona orientalis*. Osculum cross-sectional area (OSA) was positively correlated to measured excurrent speeds (ES), indicating that sponge pumping and osculum contraction are coordinated behaviours. Both OSA and ES were positively correlated to pumping rate (Q). Diel trends in pumping activity and osculum contraction were also observed, with sponges increasing their pumping activity to peak at midday and decreasing pumping and contracting oscula at night. Short-term elevation of the suspended sediment concentration (SSC) within the seawater initially decreased pumping rates by up to 90%, ultimately resulting in closure of the oscula and cessation of pumping.

Submitted 15 June 2016

Accepted 5 November 2016

Published 13 December 2016

Corresponding author

Brian W. Strehlow,

brian.strehlow@research.uwa.edu.au

Academic editor

Joseph Pawlik

Additional Information and
Declarations can be found on
page 16

DOI 10.7717/peerj.2761

© Copyright
2016 Strehlow et al.

Distributed under
Creative Commons CC-BY 4.0

OPEN ACCESS

Subjects Animal Behavior, Marine Biology

Keywords Flowmeter, Sponge, Thermistor, Pumping, Behaviour, Contraction

INTRODUCTION

Marine sponges (Porifera), and their associated microbial symbionts, perform many ecologically important functions including: creating and bioeroding substrate, coupling benthic-pelagic biogeochemical fluxes (e.g., carbon, nitrogen, silicon, and phosphorus cycling), forming intricate associations with other organisms (*Bell, 2008; Maldonado, Ribes & Van Duyl, 2012*), and converting dissolved organic matter to particulate organic matter for use in oligotrophic food webs (*De Goeij et al., 2013; Maldonado, 2016*). Furthermore, marine sponges are present in a wide variety of habitats from the polar regions to the tropics and from the shallows to the deep sea (*Van Soest et al., 2016*), and they are often the most abundant, macrobenthic taxa present (*Flach et al., 1998; Diaz & Rützler, 2001; Heyward et al., 2010*).

Sponges are generally considered 'simple' animals, yet they have surprisingly complex physiologies. Sponges actively pump water through their tissues using specialised chambers of flagellated cells called choanocytes. Water is pumped through small incurrent pores (ostia) to a system of channels leading to chambers full of choanocytes before flowing out via larger excurrent openings (oscula) (Bergquist, 1978). They depend on this water circulation for most of their essential physiological processes, i.e., food capture, waste elimination, gas exchange and reproduction (Bergquist, 1978). Sponges filter large volumes of water, with retention efficiencies between 75 and 99% for particles and biota of various sizes (Reiswig, 1971; Reiswig, 1975; Pile et al., 1997). Sponge populations can filter the equivalent volume of the overlaying water column in <1 to 56 days, depending on density, water depth and community composition (Reiswig, 1974; Pile et al., 1997; Savarese et al., 1997).

Despite the global abundance and ecological importance of sponges, sponge physiology is understudied, comprising <1% of published literature on sponges (Becerro, 2008). Currently, pumping rates (Q) have been measured for <0.01% (Weisz, Lindquist & Martens, 2008; Massaro et al., 2012; McMurray, Pawlik & Finelli, 2014) of the approximately 8,700 described species (Hooper & Van Soest, 2002; Van Soest et al., 2016). Sponge pumping is highly variable depending on the species, being continuous with occasional, temporary cessation for species with thick tissue layers (Reiswig, 1971; Reiswig, 1974; McMurray, Pawlik & Finelli, 2014) or periodic in species that are more behaviourally active (Reiswig, 1971; Reiswig, 1974). Generally, sponges with high microbial abundances (HMA) have lower pumping rates than low microbial abundance (LMA) species (Weisz, Lindquist & Martens, 2008). Sponge behaviour is also highly variable depending on the species. Some species can actively open and close their ostia and oscula (Reiswig, 1974; Harrison, 1972; Weissenfels, 1976; Ilan & Abelson, 1995; Leys & Meech, 2006; Elliott & Leys, 2007); expand and contract aquiferous systems and pinacoderm (outer layer) (Nickel, 2004; Ellwanger & Nickel, 2006; Nickel et al., 2011); and even execute coordinated behaviour patterns (Leys & Meech, 2006; Ludeman et al., 2014).

Contractile behaviours have only been directly linked to sponge pumping rates in two species: *Tectitethya crypta* and *Verongia reiswigi* (*Tethya crypta* and *V. gigantea* in Reiswig, 1971; Reiswig, 1974). *T. crypta* opens its oscula, increasing its osculum cross-sectional area (OSA) during the day and decreasing it at night. The increased OSA corresponds to increased pumping rates during the day, which drop off after sunset as the oscula close. *V. reiswigi*, on the other hand, exhibits steady pumping with periodic cessations. During these cessations, the excurrent pores that channel water into the atrium of the osculum close (Reiswig, 1971).

An enhanced understanding of how sponge physiology and ecophysiology respond to anthropogenic stressors will be particularly valuable in the current period of rapid environmental change. Previous studies have shown that pumping rates in sponges significantly decrease or arrest when exposed to elevated SSCs (Reiswig, 1971; Gerrodette & Flechsig, 1979; Leys, Mackie & Meech, 1999; Tompkins-MacDonald & Leys, 2008). However, it remains to be seen if this response is ubiquitous across the Porifera, as it has only been reported in a few species. During dredging operations, where sediments are removed from the seabed to either maintain or create ports, SSCs can range from 100–300 mg L⁻¹

for periods of several hours and from 10–30 mg L⁻¹ over several days in areas within 500 m of dredging activities (Jones *et al.*, 2015). The physiological and ecological impacts of sediments at these levels on sponges, even for those species well adapted to turbid environments, remain largely unknown (Bell *et al.*, 2015; Schönberg, 2015; Schönberg, 2016).

In order to elucidate the relationship between sponge oscula opening/closing behaviour and pumping rate, we examined the common, Indo-pacific bioeroding sponge *Cliona orientalis* (Thiele, 1900). This species contains phototrophic, intracellular symbionts (*Symbiodinium* sp.) (Schönberg & Loh, 2005), and it can open and close its oscula (Schönberg, 2000), consistent with other Clionoids (e.g., Grant, 1826; Friday, Poppell & Hill, 2013; B Strehlow, pers. obs., 2012 *Cliona viarians*). *C. orientalis* exhibits increased bioerosion during the day as well as a diurnal change in symbiont distribution (Fang *et al.*, 2016b), which indicate that, like *T. crypta*, it could have a diurnal, physiological rhythm. However, the pumping and behavioural patterns of *C. orientalis* have not yet been described over time.

The central aim of this study was to characterise the pumping and behaviour of *C. orientalis*, which was achieved by developing a multi-channel digital thermistor flowmeter that incorporates time-lapse cameras to observe oscula behaviour and excurrent speeds (ES) concurrently. These values were used to calculate pumping rates under ambient environmental conditions. The pumping rate was hypothesised to be periodic and not continuous, hence the relationship between ES and OSA during contractions was also examined. It was further hypothesized that a positive correlation existed between ES and OSA and that *C. orientalis* pumping would follow a diel pattern, increasing during the day and decreasing at night. In addition, the flowmeter and camera apparatus was used to determine the pumping and contractile responses of *C. orientalis* to elevated SSCs from both single and multi-pulse events. It was predicted that *C. orientalis* pumping rates would decrease in response to elevated SSCs comparable to those of a dredging plume.

MATERIALS AND METHODS

Thermistor flowmeter construction and calibration

A four-channel thermistor flowmeter with integrated video camera was designed, constructed and validated in order to simultaneously measure sponge excurrent speed and observe sponge behaviour. The thermistor flowmeter was designed and built at the Australian Institute of Marine Science (AIMS) in Townsville with all testing done at the AIMS National Sea Simulator (SeaSim). The flowmeter incorporated four independent thermistor probes and a thermometer to determine ambient temperature. Each glass thermistor probe (120 series, 1,000 Ω at 25 °C, Honeywell, USA) was set to hold at 10 °C above ambient temperature. In high flow conditions, the probes drew more power to maintain this temperature difference hence power could be directly correlated to flow rate. This design is similar to thermistor flow meters used by Reiswig (1971) and Labarbera & Vogel (1976); however, in the current model, measurements were recorded digitally and four probes could measure flow simultaneously.

For calibration, each probe was attached to a carriage running along a rail on top of the tank and driven by a stepper motor through a belt and pulley system. The probes were

run across the track at 8 different speeds from 5 to 200 mm s⁻¹. Three calibration runs were performed for each speed, and the power used to maintain thermistor temperature was averaged across the three trials. To confirm precision at different temperatures, the same calibration runs were performed between 24–29 °C (at 1 °C intervals). Curves were fitted to a polynomial regression model for power compensation developed by Moore (2003) using R64 (R Core Team, 2013). R-squared values for polynomial regression models for all four probes calibrated at four temperatures were greater than 0.99. A successive approximation method based on the calibration curve was used to back-calculate flow rate from power output. Custom designed software facilitated modification of the calibration equations according to temperature. The reliable range of the instrument was defined as 5–200 mm s⁻¹ with an accuracy of ±5 mm s⁻¹.

As a consequence of having the probes heated to 10 °C above the ambient temperature, no clear trend could be determined between ambient temperature and power, with curves from different temperatures intersecting at two points. Under identical flow conditions, differences in measured flow of 5 mm s⁻¹ could be recorded if temperatures changed by >1 °C. Experiments were therefore conducted at a controlled temperature for which a specific calibration curve was generated. As the logging software records changes in temperature to ±0.01 °C, experiments can be monitored effectively, quality controlled and were aborted if temperatures changed by ≥0.5 °C.

Sample collection and experimental setup

Small sponge explants (50 mm in diameter and containing several oscula) air drilled from large colonies of *C. orientalis* inhabiting (bioeroding) the skeleton of dead *Porites* sp. coral. Explants were collected at a depth of 3 m from reefs around Pelorus Island on the inshore Great Barrier Reef (GBR) (S18°32.903' E146°29.172', GBR Marine Park Authority Permit:G13/35758.1) and were acclimated to aquarium conditions for two weeks before experimentation. Aquaria consisted of 100 L tanks (Fig. 1) held at 27 °C. Seawater (5 µm filtered) flowed into tanks at 600 mL min⁻¹ (~9 turnovers per day) ensuring abundant food and nutrients for the animals. Water in each tank was recirculated using an Iwaki MD magnetic drive centrifugal pump (Iwaki Pumps, Sydney, Australia) that collected water from the surface and forced it up through the centre point of the inverted pyramid at the tank's base (Fig. 1A, IP) in conjunction with a VorTech MP10 pump (EcoTech Marine, Allentown, PA, USA) mounted inside the tank (Fig. 1, V). Hydra 52 LED lights (AquaIllumination, Ames, IA, USA) ramped up to 200 µmol photons m⁻² s⁻¹ from 5:30 to 11:30, held at the maximum for one hour and then decreased to 0 from 12:30 to 17:30. This natural daily pattern of light provided sufficient intensity for the phototrophic *C. orientalis*.

Observations of oscula behaviour, ES, OSA and Q

Waterproof USB endoscopes (7 mm USB waterproof endoscope; Shenzhen Dowdon Tech Co, Shenzhen, China) aided in accurate positioning of the probes over the oscula (item C in Fig. 1). 3D flow patterns were measured for a single osculum. The probe was positioned in three dimensions around the osculum, with flow rates measured for 1 min per location. ESs across the osculum plane were integrated gravimetrically based on the area measured

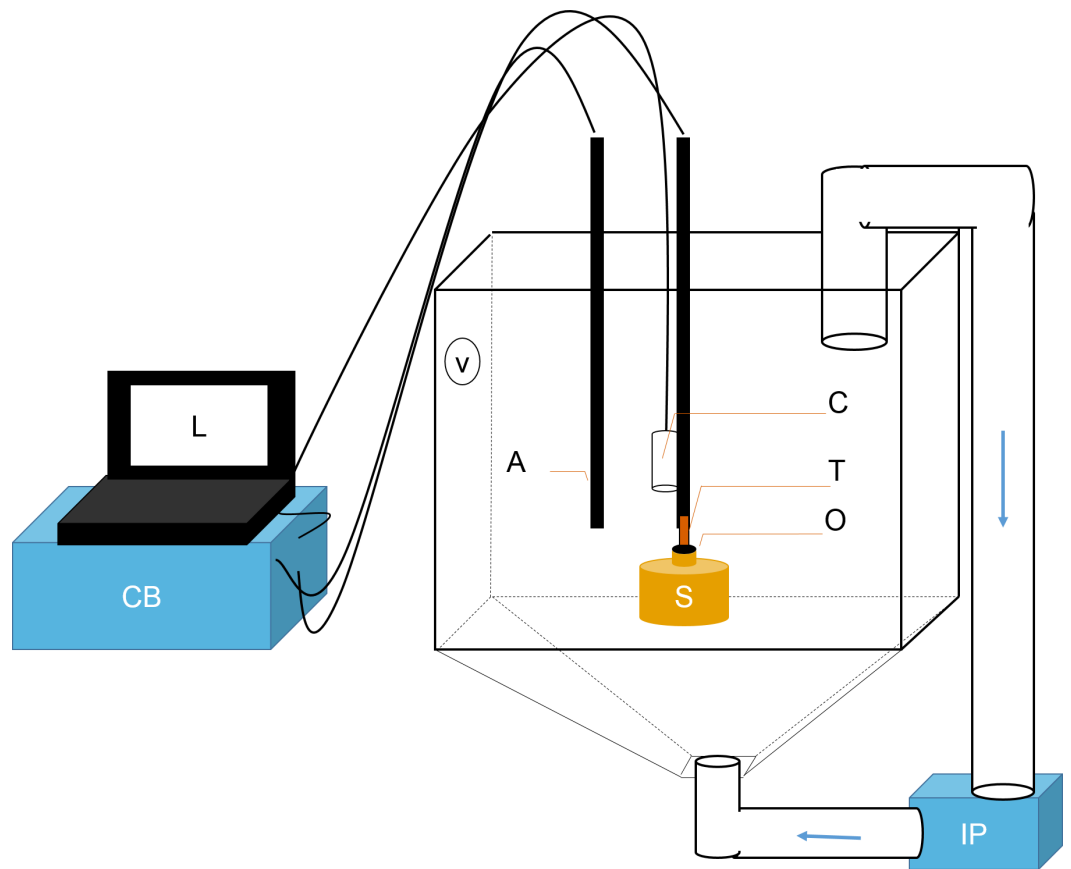


Figure 1 Schematic representation of flowmeter and experimental tank. A laptop computer (L) controlled the time-lapse USB camera (C). The ambient temperature probe (A) and the thermistor flowmeter (T) were controlled by the control box (CB). Data was sent from CB to L for processing. T was positioned directly over sponge (S) osculum (O). Sediments were kept in suspension using two pumps: a Vortech MP10 (V) and an Iwaki MD (IP). The latter recirculated water and sediments from below (flow direction is shown with blue arrows).

to determine the mean ES over the entire OSA (Reiswig, 1974). The ratio of the mean ES to the centreline ES (ES_{centre}), i.e., the ES recorded at the centre of the OSA, was 0.90, and this value was used as the profile correction factor (see Eq. (2)), which accounted for any decrease in speed at the edge of the osculum (Reiswig, 1974; McMurray, Pawlik & Finelli, 2014). Based on 3D measures of ES, the excurrent stream was considered to be laminar with a plug-like flow profile.

The OSA and centreline ES (ES_{centre}) were measured for all oscula ($n = 10$) on two different sponge explants (E1 and E2) for approximately 40 min per oscula. Reported measurements of ES should be considered as ES_{centre} unless otherwise specified. The OSA was based on the diameter of the osculum as measured by ImageJ (Schneider, Rasband & Eliceiri, 2012), with area calculated assuming a circle. Reduced major axis (RMA) regressions were performed using the lmodel2 package in R64 (R Core Team, 2013) to correlate OSA to ES_{centre} (sensu McMurray, Pawlik & Finelli, 2014). Additionally one-way

Analyses of Variance (ANOVAs) were run to determine if the ratio of ES: OSA was different between oscula on the same explant.

At each time point, the instantaneous pumping rate (Q), i.e., “point rate” (Reiswig, 1974), was calculated as follows:

$$Q = \text{OSA} \times \text{ES}_{\text{centre}} \times \text{profile correction factor} \quad (\text{Adapted from Reiswig, 1974}). \quad (1)$$

RMA regressions were also performed to relate OSA to Q and ES to Q . This equation was used to approximate Q based on ES in future experiments:

$$Q = 5.42 \times 10^{-3} (\text{ES})^{1.60} \quad (2)$$

Mean Q values for each osculum were summed to calculate specific pumping rate based on explant volume. Explant volume was approximated by measuring the surface area on the top of the core and the depth that the sponge eroded into the substrate and calculating the volume of the cylinder.

Effects of elevated SSC

If probes were exposed to elevated SSCs, a layer of sediment deposited on them over time. This layer significantly decreased the probe readings. To counteract this effect, probes were cleaned twice a day using small burst of water from a submerged transfer pipette. Two experiments were run exposing *C. orientalis* to elevated SSCs: (i) a single, short term exposure and (ii) a long term exposure with three pulses of sediment. Sediments were prepared from biogenic calcium carbonate sediment collected from Davies Reef (a clear-water, mid-shelf reef in the central GBR). Sediment was dried and ground using a rod mill grinder until the mean grain size was $\sim 29 \mu\text{m}$ with 80% of the sediment ranging in size between 3 and $64 \mu\text{m}$, as measured using laser diffraction techniques (Mastersizer 2000; Malvern Instruments Ltd, Malvern, UK). Suspended sediments were added to the experiments gradually (over approximately five min) to reach a level of 100 mg L^{-1} . This level was chosen to reflect SSC within 500 m of dredging activities, where SSCs exceeded 100 mg L^{-1} for periods of several hours (Jones et al., 2015).

In the short term SSC exposure, four explants (E3–6) were tested individually on separate days. Each of the four trials was independent, and the tanks were cleaned between trials. For consistency, each trial was conducted at the same time of day. To obtain ‘normal’ pumping rates (i.e., unaffected by sediment), excurrent speeds from each sponge were measured for 30 min. Each sponge explant was subsequently exposed to a single pulse of 100 mg L^{-1} sediment and monitored for 3.5 h. Sediments settled quickly, with SSC decreasing to $\sim 50 \text{ mg L}^{-1}$ in the tanks after 1.5 h and to $\sim 40 \text{ mg L}^{-1}$ after 3 h. Temperature was held constant at 28°C for explants 3 and 4, and 27°C for explants 5 and 6. Q was calculated using Eq. (2).

In the long term SSC exposure experiment, ES and OSA were recorded for an additional four explants (E7–10) for 2.5 d before and after three separate sediment pulses of 100 mg L^{-1} , each applied over a 4 h period. Again, Q was approximated using Eq. (2). The diurnal pattern of *C. orientalis* pumping was also assessed. During the first 24 h of observation,

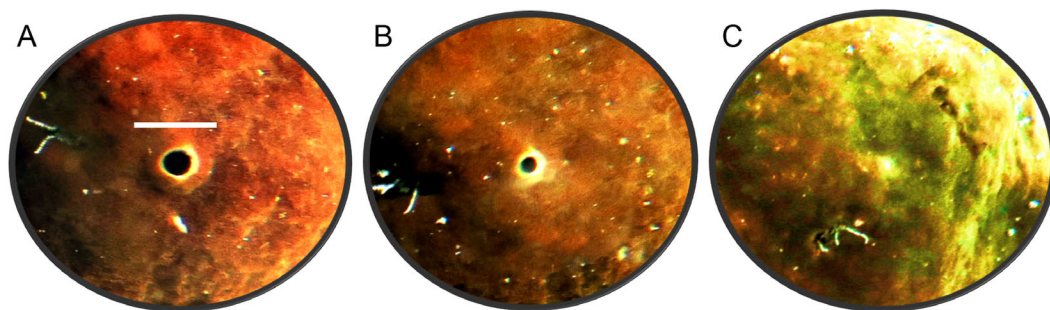


Figure 2 Time-lapse images of *Cliona orientalis* oscular states. (A) Osculum fully open (scale bar: 10 mm). (B) Osculum partially contracted (+10 min) (C) Osculum fully contracted, i.e., closed, following mechanical disturbance.

diurnal pumping patterns were assessed based on 20 min moving averages of calculated pumping rates.

Since pumping rates oscillated regularly throughout the day, percentage change was recorded based on the local maxima (Reiswig, 1974; Reiswig, 1975). SSCs were monitored using a nephelometer (TPS, Australia), and nephelometric turbidity units (NTUs) converted to SSCs (as mg L^{-1}) by applying a sediment-specific conversion factor. Sedimentation rates were measured using SedPods (Field, Chezar & Storlazzi, 2013), which were capped after 24 h in the tank with deposited sediment filtered through pre-weighed $0.4 \mu\text{m}$ 47 mm diameter polycarbonate filters, incubated at 60°C for 24 h, and weighed to 0.0001 g to determine sediment mass. Sedimentation rates during this experiment were $\sim 6 \text{ mg cm}^{-2} \text{ day}^{-1}$. Tank temperature was maintained at $27 \pm 0.2^\circ\text{C}$ during the experiment.

RESULTS

Observations of oscular behaviour, OSA, ES and Q

The oscula of *C. orientalis* contracted and partially closed (Figs. 2A and 2B) on a regular basis. When an osculum closed completely the adjacent area also contracted (Fig. 2C), leaving a small indentation in the tissue. Interestingly oscula on the same explant were observed to undergo partial contractions asynchronously. If a single osculum was disturbed mechanically, it closed and ceased pumping within 2 min. If the whole explant was disturbed or moved within the tank, all oscula on the explant closed within two minutes.

When the oscula opened, the OSA, ES and Q increased. Once open, the osculum partially contracted regularly again (decreasing OSA), but it did not fully close (Fig. 3A). These partial contractions coincided with decreased ES. As Q is the product of OSA and ES, it follows the same periodic increase and decrease. The same partial contractions occurred when a different osculum was pumping actively (Fig. 3B). Again, Q followed a regular period. When a third osculum closed (Fig. 3C), the ES decreased proportionally with a lag of approximately one min.

Summaries of centreline ES, OSA, Q and partial contraction period for ten oscula of two separate explants are presented in Table 1. Factoring in all oscular flow rates, explants

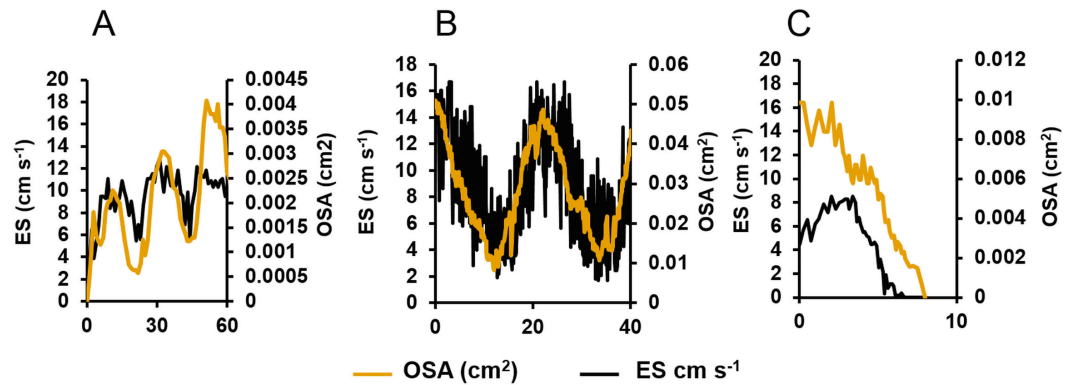


Figure 3 Centrelines excurrent speeds (ES) and osculum cross-sectional area (OSA) for three different oscula exhibiting different contractile behaviours. (A) The osculum was actively opening (from a state of complete closure) and initiating pumping. (B) The osculum was open and actively pumping. (C) The osculum was closing and decreasing pumping.

Table 1 Summary of centrelines excurrent speeds (ES), osculum cross sectional area (OSA), pumping rates (\pm SD) and contraction periods from ten oscula on two explants of *Cliona orientalis* during different states of contraction: opening, open (with periodic partial contraction), and closing (full contraction).

Explant	Osculum	State	Mean ES (cm s ⁻¹)	Max ES (cm s ⁻¹)	Mean OSA (cm ²)	Max OSA (cm ²)	Mean pumping rate (mL s ⁻¹)	Max pumping rate (mL s ⁻¹)	Osculum partial contraction period (min)
1	1	Open	8.27 \pm 3.91	16.66	0.027 \pm 0.012	0.052	0.234 \pm 0.185	0.720	22.25
	2	Closing	4.83 \pm 2.79	8.51	0.006 \pm 0.002	0.010	0.031 \pm 0.0212	0.076	17.67
	3	Open	7.64 \pm 1.49	10.59	0.033 \pm 0.006	0.045	0.237 \pm 0.081	0.408	19.83
	4	Open	5.74 \pm 0.83	7.76	0.140 \pm 0.030	0.188	0.723 \pm 0.189	1.212	20.86
	5	Open	7.62 \pm 2.87	14.45	0.017 \pm 0.003	0.021	0.112 \pm 0.040	0.188	23.50
2	1	Open	8.33 \pm 2.98	12.28	0.016 \pm 0.003	0.022	0.129 \pm 0.062	0.225	25.91
	2	Opening	9.32 \pm 2.36	12.84	0.002 \pm 0.001	0.004	0.018 \pm 0.011	0.043	21.75
	3	Open	4.69 \pm 0.96	6.50	0.010 \pm 0.002	0.013	0.041 \pm 0.013	0.076	18.67
	4	Open	7.47 \pm 1.27	9.38	0.033 \pm 0.003	0.037	0.224 \pm 0.047	0.291	17.08
	5	Open	4.81 \pm 1.61	7.03	0.011 \pm 0.001	0.013	0.051 \pm 0.020	0.077	N/A

1 and 2 had a mean specific volume flow (per litre of sponge tissue) of 0.020 ± 0.008 and 0.007 ± 0.002 L water s⁻¹ L sponge⁻¹ (mean \pm SD). The estimated mean cycle times, i.e., the time required for all oscula to pump a sponge's volume, were 41 and 151 s, respectively. During active pumping, the osculum partially contracted and then reopened following a regular period of 20.84 ± 2.86 min.

During partial contraction, full contraction, and reopening, ES was positively related to OSA (Eq. (3); $R^2 = 0.431$, $P < 0.001$, $n = 1,335$, Fig. 4A). On closer examination of the ratio of ES to OSA for each oscula, significant differences were demonstrated between values from O2 and all other oscula, O3 and O4, O4 and O1 in E1 ($P < 0.05$). The difference in O2 was due its active closure, whereas all other oscula were undergoing regular partial contraction (Table 1). There are also significant differences between O1 and O3 as well

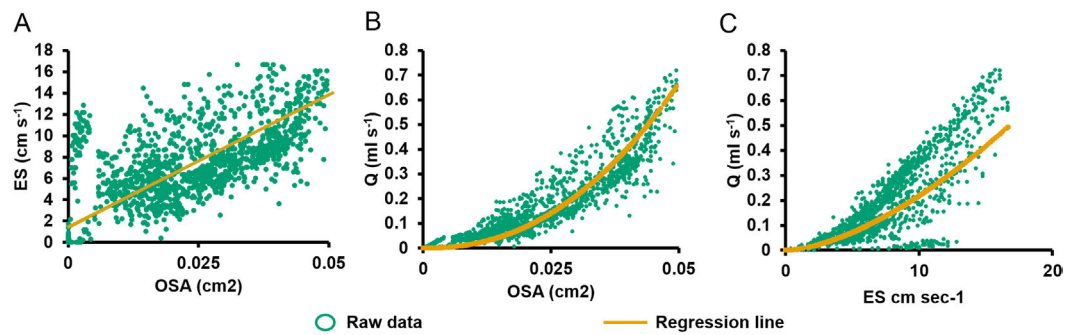


Figure 4 Relationships between pumping variables. (A) Excurent speed (ES) vs. osculum cross-sectional area (OSA). Regression lines were computed using reduced major axis (RMA) regression. (B) Volume flow (Q) vs. OSA. (C) Q vs. ES.

as O3 and O6 in E2. These differences probably account for the $\sim 50\%$ of variation not explained by the RMA model. Q was positively related to OSA (Eq. (4); $R^2 = 0.880$, $P < 0.001$, $n = 1,335$; Fig. 4B) and ES (Eq. (2), $R^2 = 0.946$, $P < 0.001$, $n = 1,335$, Fig. 4C). Despite the variation caused by different oscula, both ES and OSA were strongly correlated to Q. The regression equations were as follows:

$$ES = 250.48(OSA) + 1.35 \quad (3)$$

$$Q = 539(OSA)^{2.24} \quad (4)$$

Effects of elevated SSC

In the short term SSC exposure experiment, small temperature fluctuations did not have an effect on recorded ESs (Fig. 5). Immediately after exposure to the high SSC, three of the four explants decreased Q by 42–90%, and minimum pumping rates were reached after 15 min (Fig. 5). E3 started closing immediately after sediment exposure but partially reopened its osculum and restarted pumping at $\sim 50\%$ of pre-treatment levels after ~ 25 min. E4 exhibited a short burst of increased pumping, and then partially closed its osculum in response to SSC before reducing pumping rates to $\sim 50\%$ of the pre-treatment level. After 80 mins of reduced pumping, both E3 and E4 closed their oscula and ceased pumping. E5 continued pumping in a “normal,” periodic manner for ~ 20 min after exposure, then maximal pumping decreased by $\sim 50\%$ and osculum closure and pumping cessation occurred after 180 min. E6 closed its osculum and pumping ceased after 30 min. All explants exhibited osculum closure and pumping cessation after treatment. On average, explants kept their oscula open for 99 ± 4 min (mean \pm SD) after exposure to sediment. When explants reduced their pumping rates, partial contraction periods of ~ 20 min were similar to those explants not exposed to SSC (see Fig. 3).

In the long term sediment dosing experiment, explants 7 to 9 increased pumping rates towards midday, reaching a maximum around the time of highest light intensity (Fig. 6), and then decreased into the night. Although the ~ 28 min period of partial contraction of each oscula was consistent throughout the day, excurent speeds and pumping rates varied during the day. Generally, ES and Q increased during the morning to peak approximately

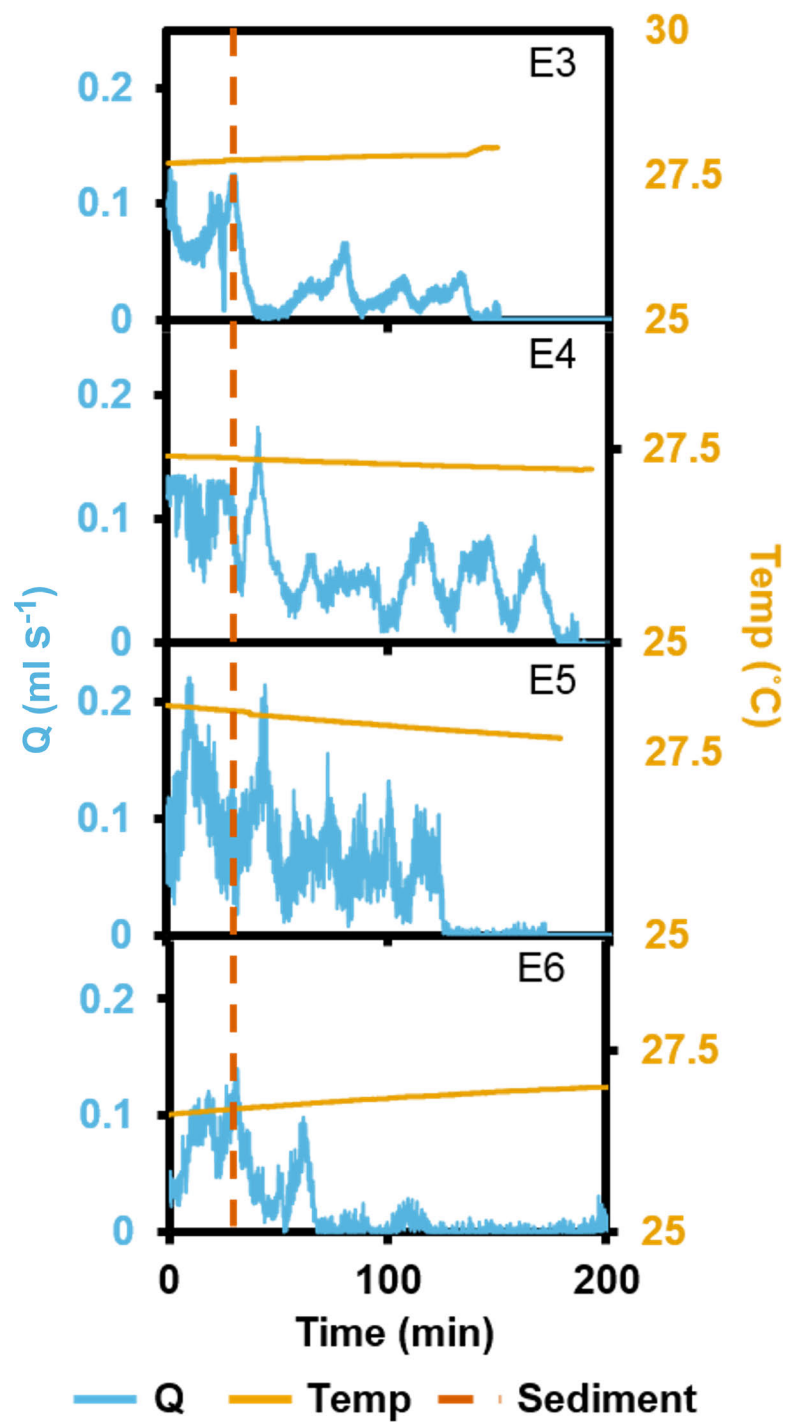


Figure 5 Pumping rates (Q) from four oscula of four separate explants (E3–6) exposed to a single dose of high SSC with ambient temperature (temp) recorded. The vertical, dashed line indicates when sediment was introduced.

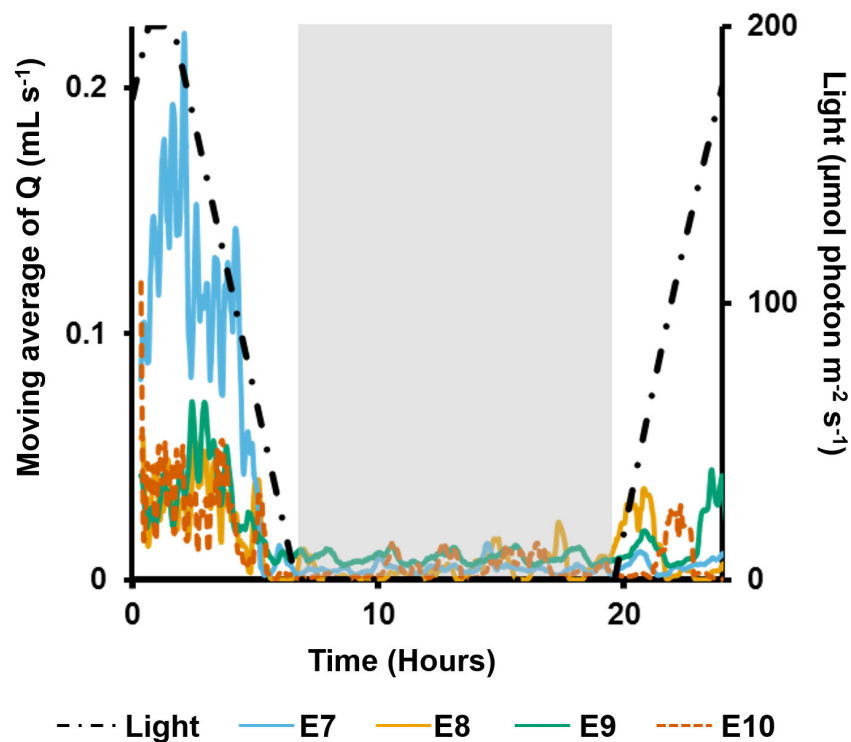


Figure 6 Moving average (period: 20 min) of pumping rates (Q) for four explants (E3–6) over 24 h. Light intensity is shown on the secondary y -axis, and the grey rectangle represents night.

1 h after midday (maximum light intensity), and decreased during the afternoon and were very low during night-time. During the night, pumping activity was markedly depressed and all oscula were either fully or partially contracted. Some pumping occurred at night, but maximal rates were <50% of those during the day.

On the second day, pumping rates were generally lower and the diel cycle was less obvious, although night-time speeds decreased for all individuals (Fig. 7). The first sediment pulse reduced excurrent speeds for all measured oscula (Fig. 7). Maximal excurrent speed decreased by 41%, 11% and 36% for explants 7–9, respectively (mean: $29 \pm 9\%$). Calculated maximal pumping rates decreased by 57%, 27% and 51%, respectively, with a mean decrease of $41\% \pm 12\% \text{ mL s}^{-1}$ (Fig. 7B). In contrast, the maximal excurrent speed of E10 increased by 7%, and pumping rates increased by 12%. All four explants closed their oscula following the first sediment dose after an average of 56 ± 67 min. E9 exhibited a very rapid closure, arresting pumping and closing after 6 min. After the first sediment pulse, all explants except E8, reopened their oscula and restarted pumping 68 ± 26 mins after closure, albeit at lower flow rates than before.

Maximal excurrent speeds after the second sediment dosing decreased by $59 \pm 19\%$ from pre-treatment maxima and pumping rates decreased by $71 \pm 19\%$. However, variability was again detected between explants. E7 ceased pumping and closed its osculum after 70 mins. E8 kept its osculum closed. E10 closed its osculum after <1 min, and E9 kept its

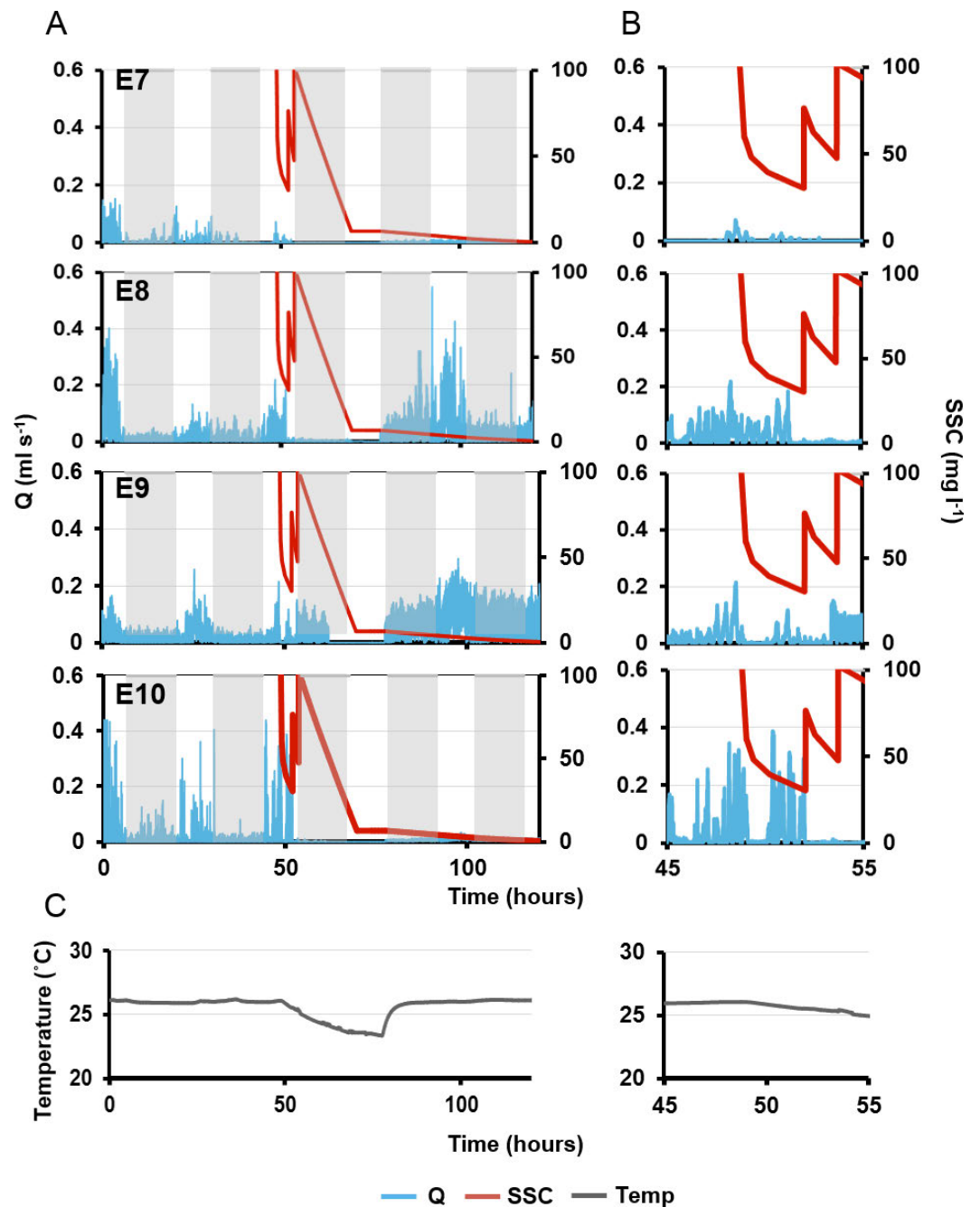


Figure 7 Pumping rates (Q, blue line) in four explants over five days. (A) The grey rectangles represent night. The red line on the third day represents suspended sediment concentrations (SSC) (right-side y-axis). Panels E7–10 represent a single osculum of different individual explants measured simultaneously. (B) Close-up of ‘A’ graphs on the third day, when sediment was added. (C) Ambient temperature over time corresponding to times shown in (A) and (B).

osculum open even after the second dose (although maximal excurrent speed and pumping rate decreased by 23% and 34%, respectively).

After the third sediment dose, all individuals except E9 closed their oscula and ceased pumping until nightfall. Pumping ceased through the night, in concordance with the diel pumping pattern observed before treatment. E9 kept its oscula open although excurrent speed and pumping rates were reduced by 39% and 55% respectively. Approximately 48 h after the first sediment treatment, E8 and E9 exhibited excurrent speeds and pumping rates similar to pre-treatment levels, and the diel pattern was re-established with maximal excurrent speeds at peak light intensity. A similar pattern was observed in E8, although excurrent speeds did not return to pre-sediment levels. Explant 10 did not restart pumping or reopen its osculum for at least 72 h post-exposure to sediment.

DISCUSSION

Although sponge pumping behaviour is paramount to sponge biology, physiology and ecology, it has been examined in relatively few sponge species. This study, combining flowmeters with time-lapse imagery yielded useful insights into the contractile behaviours and pumping rates of *Cliona orientalis*. Both OSA and ES strongly correlated to pumping rates and either could be used to accurately calculate Q based on Eqs. (1) or (4). Affordable, user-friendly time-lapse cameras could therefore be used in future studies to determine pumping rates in *C. orientalis*. This method, using only cameras, could be easily paired with incubation methods in order to relate respiration, oxygen production, feeding, and/or POM production to pumping rates (e.g., Fang *et al.*, 2013b), provided incubation chambers are transparent. However, the equations provided should only be used for studies of *C. orientalis* pumping rates. Standards would need to be calculated to determine Q from OSA in other species with contractile oscula. As *C. orientalis* has multiple oscula per sponge, pumping in all oscula could be observed simultaneously so that specific volume flow rates could be calculated. This calculation was hitherto limited only to sponge species or individuals with one osculum due to logistical limitations.

C. orientalis is widely distributed in the Indo-Pacific (Van Soest *et al.*, 2016) and an emerging model organism in the study of the effect of climate change and ocean acidification. As a bioeroder with photosymbionts, *C. orientalis* competes with hard corals for space (Fang *et al.*, 2016a), and it increases its growth and bioerosion rates in response to ocean warming and ocean acidification (Fang *et al.*, 2013a). Given potential decreases in carbonate accretion by corals (Hoegh-Guldberg *et al.*, 2007), *C. orientalis* abundance may increase in the future. Furthermore, sponges in general (Bell *et al.*, 2013) and photosynthetic sponges in particular (Bennett *et al.*, 2016) will likely increase in abundance under projected climate change scenarios. This increase would be concurrent with an increased effect of sponge pumping on ecosystem processes (e.g., element cycling), and could even lead to a positive feedback loop that enhances sponge and algal growth while decreasing coral recovery potential (Pawlik, Burkepile & Thurber, 2016).

It is therefore important to understand the baseline physiology of *C. orientalis*. In this study we report the first specific volume pumping rates for *C. orientalis*. Pumping rates of

0.020 ± 0.008 and 0.007 ± 0.002 L water s^{-1} L sponge $^{-1}$ calculated here were comparable to those of other sponge species (see [Weisz, Lindquist & Martens, 2008](#)). *C. orientalis* is classified as a low microbial abundance (LMA) species like *Cliona varians* ([Poppell et al., 2013](#)); however, the specific pumping rate of *C. orientalis* was considerably lower than the mean specific pumping rate of other LMA sponges (~ 0.27 L water s^{-1} L sponge $^{-1}$) ([Weisz, Lindquist & Martens, 2008](#)) and more comparable to the mean specific pumping rate of high microbial abundance (HMA) sponges (~ 0.09 L water s^{-1} L sponge $^{-1}$) ([Weisz, Lindquist & Martens, 2008](#); [McMurray, Pawlik & Finelli, 2014](#)). *C. orientalis* likely has a lower pumping rate due to its high abundance of eukaryotic photosymbionts ([Schönberg & Loh, 2005](#)), compared to other LMA sponges, and consequent reliance on phototrophy over heterotrophic filter feeding ([Fang et al., 2013b](#)).

C. orientalis pumping rates and oscular behaviour exhibited diel patterns. Pumping rates increased during the morning to peak after noon, decreased during the afternoon and were minimal at night. This coincided with an observed decrease in osculum area at night. The Caribbean sponge *Cliona varians* also contracts its oscula at night (B Strehlow, pers. obs., 2012), as does *T. crypta*, which concurrently decreases its excurrent speed overnight ([Reiswig, 1971](#)). This increased activity during the day could explain why *C. orientalis* increases its chemical bioerosion rate during the day compared to night ([Fang et al., 2016b](#)). Interestingly, the distribution of endosymbiotic *Symbiodinium* within *C. orientalis* follows a diel rhythm, with algal cells appearing closer to the pinacoderm during the day ([Schönberg & Suwa, 2007](#); [Fang et al., 2016b](#)). Changes in pumping activity may be a central part of the diel rhythms of the *C. orientalis* holobiont, as pumping is critical to physiological maintenance of the holobiont. Hence, establishing a direct, causal link between increased pumping rates, increased bioerosion and altered symbiont distribution should be an area of further research.

Osculum area was previously found to be directly correlated with excurrent speed in *Tectitethya crypta* ([Reiswig, 1971](#)). Mechanistically, this correlation indicates that either the osculum acts as a passive, elastic valve that closes when no pressure is applied by the pumping choanocytes or that there is communication between choanocytes and contractile pinacocytes in the osculum. According to [Ludeman et al. \(2014\)](#), the osculum itself may now be considered a sensory organ that coordinates behavioural responses, sensing and reacting to decreased pumping by choanocytes. Flow sensing ciliated pinacocytes have been identified in oscula from numerous sponge species and classes ([Hammel & Nickel, 2014](#); [Ludeman et al., 2014](#)). Although flow sensing cilia structures have not yet been observed in *C. orientalis*, it is likely that they are present given our results. If so, then the oscula of *C. orientalis* sense low flow from the choanocytes and close in response. This is supported by the lag of approximately one min between pumping cessation and full osculum closure (see [Fig. 4C](#)). This is also consistent with the observation that *Xestospongia muta*, which has rigid oscula and excurrent pores, can exhibit full pumping cessation via a coordinated, intrinsically generated decrease in choanocyte activity ([McMurray, Pawlik & Finelli, 2014](#)).

Elevated SSCs decreased pumping and eventually caused osculum closure and arrested pumping in *C. orientalis*. The decrease in maximal pumping rates was likely caused by suspended sediments clogging the aquiferous system. However the deposition of sediment

may have been a mechanical stimulus that caused the prolonged osculum closure. Partial contraction periods were unchanged, even when pumping rates were reduced. This indicated that periodic, partial contraction is an intrinsic aspect of *C. orientalis* pumping behaviour.

Decreased pumping rates in response to elevated SSCs have been reported in numerous sponge species. In *Aplysina lacunosa*, pumping rates decrease by 41% after exposure to sediment concentrations of $\sim 100 \text{ mg L}^{-1}$ (Gerrodette & Flechsig, 1979) and oscula of *Tectitethya crypta* close rapidly in response to wave action and sand score, with storms causing pumping activity to drop by 27% (Reiswig, 1971). Similarly, *Rhabdocalyptus dawsoni* reduces pumping by 32% within five min after exposure to sediments and can also arrest pumping in response to mild tactile stimulation (Leys, Mackie & Meech, 1999; Tompkins-MacDonald & Leys, 2008). However, not all sponges are equally sensitive to tactile disturbance. The glass sponge *Aphrocallistes vastus* only arrested pumping after a very intense tactile response, i.e., when stabbed with a pipette (Tompkins-MacDonald & Leys, 2008). *A. vastus* also reacted rapidly (within 2 s) to deposited sediment with cessation of pumping lasting for intervals of 30–40 s (Tompkins-MacDonald & Leys, 2008). These intervals are comparatively shorter than what was observed in *C. orientalis*, and this may be due to the ability of glass sponges to rapidly propagate action potentials across syncytial tissue (Leys, Mackie & Meech, 1999).

C. orientalis has multiple oscula per individual that contract asynchronously under normal conditions. The level of connection and coordination among oscula on a single sponge and, more importantly, the aquiferous system related to each osculum, remains to be determined for this species. However, sponges with encrusting morphologies and contractile oscula likely have connected (confluent) aquiferous systems (Reiswig, 1975). If disturbed locally, an osculum could contract and flow from associated choanocyte chambers would be channelled to adjacent oscula. However, elevated SSC and sedimentation caused all oscula on *C. orientalis* to contract and close. Although possibly a good short term acclimation strategy to localised disturbance, these reductions in pumping rates and prolonged osculum closures are implicitly detrimental to sponges in the long term. If sediment stressors were applied chronically, decreased pumping could lead to hypoxia, starvation and the inability to effectively eliminate waste. However, the long term effects of dredging-related stressors still need to be determined in future work.

CONCLUSION

Understanding the baseline physiology of sponges is increasingly important due to the demonstrated ecological importance of sponges in oligotrophic food webs and the changes in coral reef community composition forecasted with increasing anthropogenic stress, e.g., dredging. Here we have elucidated diurnal previously unknown patterns in pumping and contractile behaviour in *Cliona orientalis*. The correlation of OSA to Q will provide a valuable metric for future studies of *C. orientalis* physiology. Finally, acute exposures to elevated SSCs caused pumping rates in *C. orientalis* to decrease by up to 90%. This decrease was generally followed by a coordinated closure of the oscula and the cessation of pumping.

However, longer term studies are still needed to confirm the effects of chronic sediment stress.

ACKNOWLEDGEMENTS

We are thankful to SeaSim staff for their help during experiment set up. Many thanks to Dr. CHL Schönberg for initial discussions and design input in the development of the thermistor flowmeter. Thanks also to Dr. M. Abdul Wahab and Dr. RJ Jones for comments on a previous version of the manuscript.

ADDITIONAL INFORMATION AND DECLARATIONS

Funding

This research was funded by the Western Australian Marine Science Institution (WAMSI) as part of the WAMSI Dredging Science Node, and made possible through investment from Chevron Australia, Woodside Energy Limited, BHP Billiton as environmental offsets and by co-investment from the WAMSI Joint Venture partners. The views expressed herein are those of the authors and not necessarily those of WAMSI. NSW was funded by an Australian Research Council Future Fellowship FT120100480. The funders had no role in study design, data collection and analysis, decision to publish, or preparation of the manuscript.

Grant Disclosures

The following grant information was disclosed by the authors:
Western Australian Marine Science Institution (WAMSI) Dredging Science Node.
Australian Research Council Future Fellowship: FT120100480.

Competing Interests

The authors declare there are no competing interests.

Author Contributions

- Brian W. Strehlow conceived and designed the experiments, performed the experiments, analyzed the data, contributed reagents/materials/analysis tools, wrote the paper, prepared figures and/or tables, reviewed drafts of the paper.
- Damien Jorgensen conceived and designed the experiments, performed the experiments, analyzed the data, contributed reagents/materials/analysis tools, wrote the paper, reviewed drafts of the paper.
- Nicole S. Webster conceived and designed the experiments, wrote the paper, reviewed drafts of the paper.
- Mari-Carmen Pineda conceived and designed the experiments, performed the experiments, contributed reagents/materials/analysis tools, wrote the paper, reviewed drafts of the paper.
- Alan Duckworth conceived and designed the experiments, contributed reagents/materials/analysis tools, wrote the paper, reviewed drafts of the paper.

Field Study Permissions

The following information was supplied relating to field study approvals (i.e., approving body and any reference numbers):

All collections were performed under GBR Marine Park Authority Permit:G13/35758.1.

Data Availability

The following information was supplied regarding data availability:

The raw data has been supplied as a [Supplemental File](#).

Supplemental Information

Supplemental information for this article can be found online at <http://dx.doi.org/10.7717/peerj.2761#supplemental-information>.

REFERENCES

- Becerro MA. 2008.** Quantitative trends in sponge ecology research. *Marine Ecology* 29:167–177 DOI 10.1111/j.1439-0485.2008.00234.x.
- Bell JJ. 2008.** The functional roles of marine sponges. *Estuarine, Coastal and Shelf Science* 79:341–353 DOI 10.1016/j.ecss.2008.05.002.
- Bell JJ, Davy SK, Jones T, Taylor MW, Webster NS. 2013.** Could some coral reefs become sponge reefs as our climate changes? *Global Change Biology* 19:2613–2624 DOI 10.1111/gcb.12212.
- Bell JJ, McGrath E, Biggerstaff A, Bates T, Bennett H, Marlow J, Shaffer M. 2015.** Sediment impacts on marine sponges. *Marine Pollution Bulletin* 94:5–13 DOI 10.1016/j.marpolbul.2015.03.030.
- Bennett HM, Altenrath C, Woods L, Davy SK, Webster NS, Bell JJ. 2016.** Interactive effects of temperature and pCO₂ on sponges: from the cradle to the grave. *Global Change Biology* Epub ahead of print Aug 23 2016.
- Bergquist PR. 1978.** *Sponges*. London: Hutchinson, 268 pp.
- De Goeij JM, Van Oevelen D, Vermeij MJA, Osinga R, Middelburg JJ, De Goeij AFPM, Admiraal W. 2013.** Surviving in a marine desert: the sponge loop retains resources within coral reefs. *Science* 342:108–110 DOI 10.1126/science.1241981.
- Diaz MC, Rützler K. 2001.** Sponges: an essential component of Caribbean coral reefs. *Bulletin of Marine Science* 69:535–546.
- Elliott GRD, Leys SP. 2007.** Coordinated contractions effectively expel water from the aquiferous system of a freshwater sponge. *The Journal of Experimental Biology* 210:3736–3748 DOI 10.1242/jeb.003392.
- Ellwanger K, Nickel M. 2006.** Neuroactive substances specifically modulate rhythmic body contractions in the nerveless metazoon *Tethya wilhelma* (Demospongiae, Porifera). *Frontiers in Zoology* 3:1–14 DOI 10.1186/1742-9994-3-7.
- Fang JKH, Mason RAB, Schönberg CHL, Hoegh-Guldberg O, Dove S. 2016a.** Studying interactions between excavating sponges and massive corals by the use of hybrid cores. *Marine Ecology* Epub ahead of print Oct 15 2016 DOI 10.1111/maec.12393.

- Fang JKH, Mello-Athayde MA, Schönberg CHL, Kline DI, Hoegh-Guldberg O, Dove S. 2013a. Sponge biomass and bioerosion rates increase under ocean warming and acidification. *Global Change Biology* 19:3581–3591 DOI 10.1111/gcb.12334.
- Fang JKH, Schönberg CHL, Hoegh-Guldberg O, Dove S. 2016b. Day–night ecophysiology of the photosymbiotic bioeroding sponge *Cliona orientalis* Thiele, 1900. *Marine Biology* 163:100–112 DOI 10.1007/s00227-016-2848-4.
- Fang JKH, Schönberg CHL, Mello-Athayde MA, Hoegh-Guldberg O, Dove S. 2013b. Effects of ocean warming and acidification on the energy budget of an excavating sponge. *Global Change Biology* 20:1043–1054 DOI 10.1111/gcb.12369.
- Field ME, Chezar H, Storlazzi CD. 2013. SedPods: a low-cost coral proxy for measuring net sedimentation. *Coral Reefs* 32:155–159 DOI 10.1007/s00338-012-0953-5.
- Flach E, Lavaleye M, De Stigter H, Thomsen L. 1998. Feeding types of the benthic community and particle transport across the slope of the N.W. European Continental Margin (Goban Spur). *Progress in Oceanography* 42:209–231 DOI 10.1016/S0079-6611(98)00035-4.
- Friday S, Poppell E, Hill M. 2013. *Cliona tumula* sp. nov., a conspicuous, massive symbiodinium-bearing clionaid from the lower florida keys (usa) (Demospongiae: Hadromerida: Clionaidae). *Zootaxa* 3750:375–382 DOI 10.11646/zootaxa.3750.4.6.
- Gerrodette T, Flechsig AO. 1979. Sediment-induced reduction in the pumping rate of the tropical sponge *Verongia lacunosa*. *Marine Biology* 55:103–110 DOI 10.1007/BF00397305.
- Grant R. 1826. Notice of a New Zoophyte (*Cliona celata* Gr.) from the Firth of Forth. *Edinburgh New Philosophical Journal* 1:78–81.
- Hammel JU, Nickel M. 2014. A new flow-regulating cell type in the Demosponge *Tethya wilhelma*—functional cellular anatomy of a leuconoid canal system. *PLoS ONE* 9:e113153 DOI 10.1371/journal.pone.0113153.
- Harrison FW. 1972. Phase contrast photomicrography of cellular behaviour in spongillid porocytes (Porifera: Spongillidae). *Hydrobiologia* 40:513–517 DOI 10.1007/BF00019986.
- Heyward A, Fromont J, Schönberg C, Colquhoun J, Radford B, Gomez O. 2010. The sponge gardens of Ningaloo reef, Western Australia. *The Open Marine Biology Journal* 4:3–11 DOI 10.2174/1874450801004010003.
- Hoegh-Guldberg O, Mumby PJ, Hooten AJ, Steneck RS, Greenfield P, Gomez E, Harvell CD, Sale PF, Edwards AJ, Caldeira K, Knowlton N, Eakin CM, Iglesias-Prieto R, Muthiga N, Bradbury RH, Dubi A, Hatziolos ME. 2007. Coral reefs under rapid climate change and ocean acidification. *Science* 318:1737–1742 DOI 10.1126/science.1152509.
- Hooper JNA, Van Soest RWM. 2002. *Systema Porifera: a guide to the classification of Sponges*. New York: Kluwer Academic/Plenum Publishers.
- Ilan M, Abelson A. 1995. The life of a sponge in a sandy lagoon. *Biological Bulletin* 189:363–369 DOI 10.2307/1542154.

- Jones R, Fisher R, Stark C, Ridd P. 2015.** Temporal patterns in seawater quality from dredging in tropical environments. *PLoS ONE* **10**:e0137112
[DOI 10.1371/journal.pone.0137112](https://doi.org/10.1371/journal.pone.0137112).
- Labarbera M, Vogel S. 1976.** An inexpensive thermistor flowmeter for aquatic biology. *Limnology and Oceanography* **21**:750–756 [DOI 10.4319/lo.1976.21.5.0750](https://doi.org/10.4319/lo.1976.21.5.0750).
- Leys SP, Mackie GO, Meech RW. 1999.** Impulse conduction in a sponge. *The Journal of Experimental Biology* **202**:1139–1150.
- Leys SP, Meech RW. 2006.** Physiology of coordination in sponges. *Canadian Journal of Zoology* **84**:288–306 [DOI 10.1139/z05-171](https://doi.org/10.1139/z05-171).
- Ludeman DA, Farrar N, Riesgo A, Paps J, Leys SP. 2014.** Evolutionary origins of sensation in metazoans: functional evidence for a new sensory organ in sponges. *BMC Evolutionary Biology* **14**:1–11 [DOI 10.1186/1471-2148-14-3](https://doi.org/10.1186/1471-2148-14-3).
- Maldonado M. 2016.** Sponge waste that fuels marine oligotrophic food webs: a re-assessment of its origin and nature. *Marine Ecology* **37**:477–491
[DOI 10.1111/maec.12256](https://doi.org/10.1111/maec.12256).
- Maldonado M, Ribes M, Van Duyl FC. 2012.** Nutrient fluxes through sponges: biology, budgets, and ecological implications. *Advances in Marine Biology* **62**:113–182
[DOI 10.1016/B978-0-12-394283-8.00003-5](https://doi.org/10.1016/B978-0-12-394283-8.00003-5).
- Massaro AJ, Weisz JB, Hill MS, Webster NS. 2012.** Behavioral and morphological changes caused by thermal stress in the Great Barrier Reef sponge *Rhopaloeides odorabile*. *Journal of Experimental Marine Biology and Ecology* **416–417**:55–60
[DOI 10.1016/j.jembe.2012.02.008](https://doi.org/10.1016/j.jembe.2012.02.008).
- McMurray SE, Pawlik JR, Finelli CM. 2014.** Trait-mediated ecosystem impacts: how morphology and size affect pumping rates of the Caribbean giant barrel sponge. *Aquatic Biology* **23**:1–13 [DOI 10.3354/ab00612](https://doi.org/10.3354/ab00612).
- Moore JP. 2003.** A thermistor based sensor for flow measurement in water. MSc Thesis, School of Physical Sciences Dublin City University, Ireland.
- Nickel M. 2004.** Kinetics and rhythm of body contractions in the sponge *Tethya wilhelma* (Porifera: Demospongiae). *The Journal of Experimental Biology* **207**:4515–4524
[DOI 10.1242/jeb.01289](https://doi.org/10.1242/jeb.01289).
- Nickel M, Scheer C, Hammel JU, Herzen J, Beckmann F. 2011.** The contractile sponge epithelium sensu lato—body contraction of the demosponge *Tethya wilhelma* is mediated by the pinacoderm. *The Journal of Experimental Biology* **214**:1692–1698
[DOI 10.1242/jeb.049148](https://doi.org/10.1242/jeb.049148).
- Pawlik JR, Burkepille DE, Thurber RV. 2016.** A vicious circle? Altered carbon and nutrient cycling may explain the low resilience of caribbean coral reefs. *BioScience* **XX**:1–7 [DOI 10.1093/biosci/biw047](https://doi.org/10.1093/biosci/biw047).
- Pile AJ, Savarese M, Chernykh VI, Fialkov VA. 1997.** Trophic effects of sponge feeding within Lake Baikal's littoral zone. 2. Sponge abundance, diet, feeding efficiency, and carbon flux. *Limnology and Oceanography* **42**:184–192
[DOI 10.4319/lo.1997.42.1.0178](https://doi.org/10.4319/lo.1997.42.1.0178).

- Poppell E, Weisz J, Spicer L, Massaro A, Hill A, Hill M. 2013.** Sponge heterotrophic capacity and bacterial community structure in high- and low-microbial abundance sponges. *Marine Ecology* **35**:414–424 DOI [10.1111/maec.12098](https://doi.org/10.1111/maec.12098).
- R Core Team. 2013.** R: a language and environment for statistical computing. Vienna: R Foundation for Statistical Computing. Available at <http://www.R-project.org/>.
- Reiswig HM. 1971.** *In situ* pumping activities of tropical Demospongiae. *Marine Biology* **9**:38–50 DOI [10.1007/BF00348816](https://doi.org/10.1007/BF00348816).
- Reiswig HM. 1974.** Water transport, respiration and energetics of three tropical marine sponges. *Journal of Experimental Marine Biology and Ecology* **14**:231–249 DOI [10.1016/0022-0981\(74\)90005-7](https://doi.org/10.1016/0022-0981(74)90005-7).
- Reiswig HM. 1975.** The aquiferous systems of three marine Demospongiae. *Journal of Morphology* **145**:493–502 DOI [10.1002/jmor.1051450407](https://doi.org/10.1002/jmor.1051450407).
- Savarese M, Patterson MR, Chernykh VI, Fialkov VA. 1997.** Trophic effects of sponge feeding within Lake Baikal's littoral zone .1. *In situ* pumping rates. *Limnology and Oceanography* **42**:171–178.
- Schneider CA, Rasband WS, Eliceiri KW. 2012.** NIH Image to ImageJ: 25 years of image analysis. *Nature Methods* **9**:671–675.
- Schönberg CHL. 2000.** Bioeroding sponges common to the central Australian great barrier reef: descriptions of three new species, two new records, and additions to two previously described species. *Senckenbergiana Maritima* **30**:161–221 DOI [10.1007/BF03042965](https://doi.org/10.1007/BF03042965).
- Schönberg CHL. 2015.** Happy relationships of marine sponges with sediments — a review and some observations from Australia. *Journal of the Marine Biological Association of the United Kingdom* **96**:493–514 DOI [10.1017/S0025315415001411](https://doi.org/10.1017/S0025315415001411).
- Schönberg C.HL. 2016.** Effects of dredging on benthic filter feeder communities, with a focus on sponges. Report of theme 6—project 6.1.1 prepared for the Dredging Science Node, Western Australian Marine Science Institution, Perth, Western Australia, 139.
- Schönberg C.HL, Loh WKW. 2005.** Molecular identity of the unique symbiotic dinoflagellates found in the bioeroding demosponge *Cliona orientalis*. *Marine Ecology-Progress Series* **299**:157–166 DOI [10.3354/meps299157](https://doi.org/10.3354/meps299157).
- Schönberg C.HL, Suwa R. 2007.** Why bioeroding sponges may be better hosts for symbiotic dinoflagellates than many corals. *Porifera Research: Biodiversity, Innovation and Sustainability* **28**:569–580.
- Tompkins-MacDonald GJ, Leys SP. 2008.** Glass sponges arrest pumping in response to sediment: implications for the physiology of the hexactinellid conduction system. *Marine Biology* **154**:973–984 DOI [10.1007/s00227-008-0987-y](https://doi.org/10.1007/s00227-008-0987-y).
- Van Soest RWM, Boury-Esnault N, Hooper JNA, Rützler K, De Voogd NJ, Alvarez de Glasby B, Hajdu E, Pisera AB, Manconi R, Schönberg C, Klautau M, Picton B, Kelly M, Vacelet J, Dohrmann M, Díaz MC, Cárdenas P, Carballo JL. 2016.** World Porifera database. Available at <http://www.marinespecies.org/porifera> (accessed on 26 October 2016).

Weissenfels N. 1976. Bau und Function des SuBwasserschwamms *Ephydatia fluviatilis* L. (Porifera), Nahrungsaufnahme, I I I, Verdauung und Defaekation. *Zoomorphologie* **85**:73–88.

Weisz JB, Lindquist N, Martens CS. 2008. Do associated microbial abundances impact marine demosponge pumping rates and tissue densities? *Oecologia* **155**:367–376
[DOI 10.1007/s00442-007-0910-0](https://doi.org/10.1007/s00442-007-0910-0).



Sediment tolerance mechanisms identified in sponges using advanced imaging techniques

Brian W. Strehlow^{1,2,3,4,5}, Mari-Carmen Pineda^{4,5}, Alan Duckworth^{4,5}, Gary A. Kendrick^{1,3,5}, Michael Renton^{1,6}, Muhammad Azmi Abdul Wahab^{4,5}, Nicole S. Webster^{4,5,7} and Peta L. Clode^{1,2,3}

¹ School of Biological Sciences, University of Western Australia, Crawley, WA, Australia

² Centre for Microscopy, Characterisation and Analysis, University of Western Australia, Crawley, WA, Australia

³ Oceans Institute, University of Western Australia, Crawley, WA, Australia

⁴ Australian Institute of Marine Science, Cape Ferguson, QLD, Australia

⁵ Western Australian Marine Science Institution, Crawley, WA, Australia

⁶ School of Agriculture and Environment, University of Western Australia, Crawley, WA, Australia

⁷ Australian Centre for Ecogenomics, University of Queensland, Brisbane, QLD, Australia

ABSTRACT

Terrestrial runoff, resuspension events and dredging can affect filter-feeding sponges by elevating the concentration of suspended sediments, reducing light intensity, and smothering sponges with sediments. To investigate how sponges respond to pressures associated with increased sediment loads, the abundant and widely distributed Indo-Pacific species *Ianthella basta* was exposed to elevated suspended sediment concentrations, sediment deposition, and light attenuation for 48 h (acute exposure) and 4 weeks (chronic exposure). In order to visualise the response mechanisms, sponge tissue was examined by 3D X-ray microscopy and scanning electron microscopy (SEM). Acute exposures resulted in sediment rapidly accumulating in the aquiferous system of *I. basta*, although this sediment was fully removed within three days. Sediment removal took longer (>2 weeks) following chronic exposures, and *I. basta* also exhibited tissue regression and a smaller aquiferous system. The application of advanced imaging approaches revealed that *I. basta* employs a multilevel system for sediment rejection and elimination, containing both active and passive components. Sponges responded to sediment stress through (i) mucus production, (ii) exclusion of particles by incurrent pores, (iii) closure of oscula and pumping cessation, (iv) expulsion of particles from the aquiferous system, and (v) tissue regression to reduce the volume of the aquiferous system, thereby entering a dormant state. These mechanisms would result in tolerance and resilience to exposure to variable and high sediment loads associated with both anthropogenic impacts like dredging programs and natural pressures like flood events.

Submitted 8 June 2017
Accepted 18 September 2017
Published 16 November 2017

Corresponding author
Brian W. Strehlow,
brian.strehlow@research.uwa.edu.au

Academic editor
Joseph Pawlik

Additional Information and
Declarations can be found on
page 20

DOI 10.7717/peerj.3904

© Copyright
2017 Strehlow et al.

Distributed under
Creative Commons CC-BY 4.0

OPEN ACCESS

Subjects Ecology, Marine Biology, Biosphere Interactions

Keywords Sponge, Sediments, 3D X-ray microscopy, Scanning electron microscopy

INTRODUCTION

Sediments are an important component of all aquatic ecosystems, and they are particularly evident in coastal zones, where sediment loads and suspended sediment concentrations

(SSCs) can be high and variable. High sediment concentrations in the water column can be caused by flooding or resuspension events driven by severe storms. Wave action and currents can also resuspend sediments introduced via river discharge and flooding, resulting in sediments being transported throughout nearshore marine ecosystems. Due to increased land development in coastal areas, sediment loads from riverine discharge are increasing in many coastal zones (e.g., [Kroon et al., 2013](#)). Coastal development can also have a direct impact on sediment loads through dredging activities, which involves the removal of sediment from the seafloor and generation of a sediment plume. Dredging is typically undertaken to improve access and navigation by ships, and both the number and size of dredging programs are increasing with increased port developments in Australia and globally ([Ports Australia, 2014](#); [Ports Australia, 2015](#)). However, the potential impact of increased sediment loads from dredging and coastal runoff on marine organisms and ecosystems is understudied (reviewed in [Jones et al., 2016](#); [Jones, Ricardo & Negri, 2015](#); [Schönberg, 2016](#); [Fraser et al., 2017](#)).

Sediment causes three main abiotic stressors to marine organisms: (i) elevated SSCs, (ii) increased light attenuation, and (iii) increased sediment deposition on the benthos ([Jones et al., 2016](#)). Elevated SSCs can clog gills and filter feeding apparatuses ([Bell et al., 2015](#); [Jones et al., 2016](#); [Schönberg, 2016](#)) and can reduce the total amount of photons and change the spectral attenuation of photosynthetically active radiation (PAR) reaching the benthos, thereby inhibiting photosynthesis ([Bell et al., 2015](#); [Jones et al., 2016](#); [Schönberg, 2016](#)). High sediment deposition can smother benthic organisms and impair recruitment ([Jones, Ricardo & Negri, 2015](#)).

Sponges are ecologically important benthic filter feeders ([Bell, 2008](#); [De Goeij et al., 2013](#); [Maldonado, 2016](#)) that are abundant ([Flach et al., 1998](#); [Diaz & Rützler, 2001](#); [Heyward et al., 2010](#); [Schönberg, 2016](#)) and widely distributed ([Van Soest et al., 2017](#)) in coastal habitats where natural sediment loads can be high and dredging typically occurs ([Abdul Wahab et al., 2017](#)). Sponges feed, exchange gases, eliminate waste, and reproduce by pumping and filtering water through a complex system of internal channels and chambers known collectively as the aquiferous system ([Bergquist, 1978](#)). In the Caribbean, for example, dense populations of *Xestospongia muta* can pump the equivalent volume of the overlying water column (at 30 m) in less than three days ([McMurray, Pawlik & Finelli, 2014](#)). Sponges can filter out between 75% and 99% of biotic and abiotic particles in the water, depending on particle size and the sponge species ([Reiswig, 1971](#); [Reiswig, 1974](#); [Reiswig, 1975](#); [Pile et al., 1997](#); [Savarese et al., 1997](#)). Considering these pumping rates and filtration efficiencies, elevated SSCs are predicted to cause sediments to enter and clog the sponge aquiferous system ([Bell et al., 2015](#); [Schönberg, 2015](#); [Schönberg, 2016](#)).

Some species appear well adapted to living in environments with high sediment loads, and there are at least 11 sponge genera explicitly named for their psammobiosis, i.e., living partially embedded in sediments, e.g., *Psammoclema*, *Psammocinia* ([Schönberg, 2015](#)). Others sponge species may be limited in distribution to areas with lower sediment loads, e.g., *Scopalina lophyropoda* ([Maldonado, Giraud & Carmona, 2008](#)). Possible mechanisms for, and rates of, sediment clogging of the aquiferous system are largely unknown and have only been experimentally demonstrated in two sponge species from one location

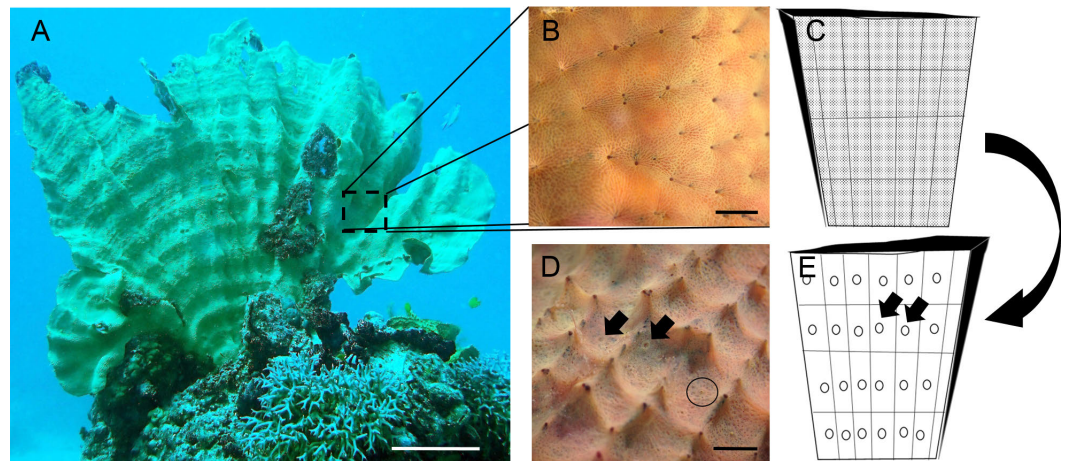


Figure 1 *Ianthella basta* body plan. (A) *In situ* photo of *I. basta* at Davies Reef (S 18°49.354', E 147°38.253'). *I. basta* is generally thin (2–5 mm) and fan-shaped (scale = 5 cm). One side, the incurrent side (B), is studded with ostia (incurrent pores), and the opposite excurrent side (D), contains larger oscula (excurrent pores). (B) Close up image of incurrent surface with clusters of ostia (scale = 1 cm). (C) Schematic of incurrent surface showing many dots (ostia) and the regular structure of skeletal elements (black lines/grid). (D) Close up image of excurrent surface on the opposite side of the incurrent surface, as indicated by the large, curved arrow. Open oscula are indicated with black arrows. A contracted osculum is circled (Scale = 1 cm). (E) Schematic of excurrent surface showing many circles (oscula) and the regular structure of skeletal elements (black lines/grid). Each grid formed by the skeleton generally contains one or more contractile oscula (arrows). Photo credits: (A) Mari-Carmen Pineda; (B) and (D) Brian W. Strehlow.

Full-size DOI: [10.7717/peerj.3904/fig-1](https://doi.org/10.7717/peerj.3904/fig-1)

(Tompkins-MacDonald & Leys, 2008). Sponges likely employ a mixture of passive and active mechanisms to reduce and prevent sediment accumulation within their aquiferous system. Passive mechanisms, such as self-cleaning surfaces, morphology, and orientation, could limit sediment accumulation inside and on top of sponges (Bell et al., 2015; Schönberg, 2015; Schönberg, 2016). Active mechanisms, including the production of mucus, expulsion of particles from the aquiferous system, pumping cessation and tissue sloughing, involve additional energy expenditure and may not be sustainable in the long term (Bell et al., 2015; Schönberg, 2015; Schönberg, 2016; Strehlow et al., 2016a). Note that the term ‘mucus’ is used in its broadest sense as sponge mucus has not been chemically characterised (Bythell & Wild, 2011). The details of these sediment exclusion mechanisms are not known for most sponge species and some have only been reported anecdotally.

To further explore the mechanistic responses of sponges to sediment we used the model species *Ianthella basta* (Pallas 1766). The widely distributed, Indo-Pacific sponge *I. basta* (Van Soest et al., 2017) is found in naturally turbid environments (Abdul Wahab et al., 2017). It is tolerant to sediment-related stress, is unaffected by light attenuation (Luter, Whalan & Webster, 2012a; Pineda et al., 2016; Pineda et al., 2017a), has a high thermal threshold (Luter, Whalan & Webster, 2012a), and is known to recover from stress-induced tissue regression (Luter, Whalan & Webster, 2012b). It is generally thin (2–5 mm), erect and laminar (Gray, 1869; Andreakis, Luter & Webster, 2012) (Fig. 1A). Due to this thin tissue, relatively small samples (8–125 mm³) can be representative of the entire aquiferous

system because the incurrent (ostia) and excurrent pores (oscula) are generally on opposite sides of the sponge (Figs. 1B and 1C). These features make *I. basta* an ideal candidate to investigate how sponges internally process sediments. In this study, we identified and characterised the mechanisms for internal sediment processing and tolerance in *I. basta* using high resolution three-dimensional (3D) X-ray microscopy and scanning electron microscopy (SEM).

MATERIALS AND METHODS

Sponge and sediment collection

I. basta ($n = 5$, representing a single evolutionary significant unit, see [Andreakis, Luter & Webster, 2012](#), verified via examination of skeletal structure and morphology) was collected at 10 m depth near Fantome Island (S 18°41.028', E 146°30.706') in the inshore, central region of the Great Barrier Reef (GBR) in Australia, leaving at least one quarter of the remaining sponge to recover ([Duckworth, 2003](#)). The number of sponges collected was limited by to five due to logistical constraints in the field. All collections from the Great Barrier Reef were performed under Great Barrier Reef Marine Park Regulations 1983 (Commonwealth) and Marine Parks regulations 2006 (Queensland) Permit G12/35236.1 and Permit G13/35758.1. Collected *I. basta* were transported in flowing seawater to the National Sea Simulator (SeaSim) at the Australian Institute of Marine Science (AIMS, Townsville), and then cut into small explants, i.e., clones, ($\sim 1 \times 3$ cm) and allowed to heal for >2 weeks in large holding tanks (5,000 L) with flow-through seawater (600 mL min⁻¹, 5 µm filtered) at conditions similar to the collection location (28 °C and 36‰ salinity).

Sediments were collected from two geographically diverse locations where *I. basta* is common: (i) Davies Reef, a mid-shelf reef on the central GBR (S 18°49.354', E 147°38.253') and (ii) a coastal habitat approximately 10 km offshore, near the township of Onslow in the Pilbara region, Western Australia (S 21°38.642', E 114°55.924'). Sediment composition differed between collection sites, with Davies Reef sediment predominantly calcium carbonate (~80% aragonite) and Pilbara sediment primarily siliciclastic (~50% quartz) in nature ([Ricardo et al., 2015](#)). As such, the sediments are referred to as 'carbonate' or 'siliciclastic', respectively. Carbonate sediment were representative of sediments in offshore environments as well as sediment from specific dredging operations, including the Barrow Island in north-western Australia (see [Bessell-Browne et al., 2017b](#)). Siliciclastic sediment was representative of inshore environments as its composition was highly influenced by terrigenous discharge from a neighbouring river. The collected sediments were ground with a rod mill grinder to a mean grain size of 29 µm (range: 3–64 µm) and 18 µm (range: 2–42 µm) for carbonate and siliciclastic, respectively. Sediments were ground because fine and medium silts (<60 µm) stay in suspension longer and travel farther than other particles ([Bainbridge et al., 2012](#)), so these particles are predicted to have the largest impact in coastal areas across space and time during natural sediment resuspension events and during dredging ([Jones et al., 2016](#)). Furthermore, dredging and natural resuspension occur in both inshore and offshore environments, so it is important to understand the effects of different sediment types.

Acute exposure to sediments

To determine if passive accumulation of internal sediments could occur without active pumping by the sponge, initial experiments were undertaken to compare sediment accumulation in living, anaesthetised, and dead sponge explants. Sponges were anaesthetised in a solution of 7.5% MgCl_2 in filtered seawater (FSW) (Messenger, Nixon & Ryan, 1985) for 10 min prior to sediment exposure, resulting in closure of sponge oscula and cessation of pumping (see Strehlow et al., 2016a). To obtain dead individuals, sponges were euthanized by immersion in 100% ethanol for 10 min (Bell, 2004). Living, anaesthetised, and dead explants ($n = 3$ per treatment) were exposed to elevated SSC (siliciclastic sediment, approximately 100 mg L^{-1}) for 48 h. Sediments were kept in suspension using specialised 115 L tanks, as previously described (see Bessell-Browne et al., 2017a; Bessell-Browne et al., 2017b; Pineda et al., 2017b). 3D X-ray microscopy scans were assessed qualitatively for the presence of sediment (see “X-ray microscopy settings and data quantification”). These comparisons showed that sediment accumulated within living explants only. For dead and anaesthetised explants, sediment was only present on their surfaces, validating the experimental and analytical X-ray microscopy approach and confirming that water had to be actively pumped by the sponge in order for sediment to enter the aquiferous system.

After sediment uptake by live sponges was verified, a second, acute sediment exposure experiment was performed. The experiment used the same tanks and siliciclastic sediment, and tested three SSCs: high ($135 \pm 30 \text{ mg L}^{-1}$, mean \pm standard error), medium ($42 \pm 8 \text{ mg L}^{-1}$), and control (0 mg L^{-1}), with three tank replicates per treatment, resulting in a total of nine tanks, each with five sponge explants. Sponges cloned from different ‘parent’ individuals were randomly distributed across the tanks and treatments to minimise the potential impact of genetic identity. Sediment was added every 6 h over 48 h, after which sediment addition was stopped and explants were observed for a subsequent three-week recovery period. During this recovery period, both high and medium sediment treatments returned to control levels. These SSCs correspond to levels that can be observed during dredging (Jones et al., 2015; Fisher et al., 2015) and following flooding and natural resuspension events (Bainbridge et al., 2012). Sedimentation rates, i.e., the rate at which sediments deposited on the bottom of the tank, was measured for each SSC treatment using SedPods (Field, Chezar & Storlazzi, 2013). Sedimentation rates were 1.29 ± 0.07 , 1.03 ± 0.05 , and $0.14 \pm 0.01 \text{ mg cm}^{-2} \text{ d}^{-1}$ in the high medium and control, respectively. The deposition detected in the control treatment was comparatively low, and was likely caused by algal growth or the particulate waste produced by the sponges, i.e., not sediments. The natural orientation, i.e., erect and perpendicular to the substratum, of *I. basta* was preserved during all experiments. Therefore sediment deposition on the sponge surface was not equal to the sedimentation rates on the SedPods, and the effect of sedimentation on the sponges was presumed to be minimal. Daily light integrals were approximately 1.2, 3.0, and $6.5 \text{ mol photons m}^{-2} \text{ d}^{-1}$, respectively. However, as *I. basta* is a heterotroph, decreased light levels have no effect its physiology (Pineda et al., 2016). Therefore, due to its orientation and heterotrophy, the potentially confounding effects of light attenuation and sediment smothering were eliminated in *I. basta*.

Sponges were sampled 24 h after sediment dosing commenced and after 1 h, 24 h, 78 h, and 3 weeks (w) of recovery under control conditions and fixed for X-ray microscopy and SEM analysis. Three separate sponges were processed per time point, one from each tank. Oscula on each sponge at each sampling time, as well as after 3 h of recovery, were recorded as either open or closed where visible. Sponge explants contained between 3–10 oscula.

Chronic exposure to sediments

In the longer-term (chronic) exposure experiment, large ($\sim 5 \times 5$ cm) *I. basta* explants were exposed to elevated SSCs (76 mg L^{-1}), reduced light (daily light integral: $0.15 \text{ mol photons m}^{-2} \text{ d}^{-1}$), and high sedimentation rates ($5.2 \text{ mg cm}^{-2} \text{ d}^{-1}$) for four weeks using the carbonate sediment. In the control treatment, sponges were exposed to no suspended sediments, no sedimentation, and a higher daily light integral of $6.53 \text{ mol photons m}^{-2} \text{ d}^{-1}$, typical levels for clear water reef environment (Jones et al., 2015; Fisher et al., 2015). Experiments were performed in $4 \times 1,200$ L fibreglass tanks with $5 \mu\text{m}$ filtered seawater in an environmentally controlled room at the SeaSim. The chronic exposure formed part of a larger collection of studies (Pineda, Duckworth & Webster, 2016; Pineda et al., 2017a; Pineda et al., 2017b; Pineda et al., 2017c) using carbonate sediment. Sediment was kept in suspension using two recirculating pumps (see Pineda et al., 2017a). When sediment concentrations dropped, doses of concentrated sediment ($\sim 6 \text{ g L}^{-1}$) were added automatically. The doses were monitored and controlled throughout the experiment by integrated nephelometers, which measured sediment levels, connected to a programmable logic controller (PLC) (see Pineda et al., 2017a). Two tank replicates were used for each treatment, making four tanks in total. At each time point, one sponge was taken from one tank and two sponges were taken from the corresponding tank replicate, making three replicates per time point per treatment and a total of 12 sponges. A piece ($\sim 1 \times 3$ cm) was fixed for X-ray microscopy, as outlined below, after four weeks of exposure to both control and high sediment conditions from each replicate ($n = 6$). After four weeks, tanks with high sediment loads were returned to control conditions to allow sponges to recover. After 2 w of recovery, a piece ($\sim 1 \times 3$ cm) was taken from each replicate ($n = 6$) as described above and fixed for examination using X-ray microscopy. For a full account of the methods and specifications of this experiment see: Pineda et al. (2017b).

X-ray microscopy settings and data quantification

Sponges were fixed in 2.5% glutaraldehyde and 1% paraformaldehyde in FSW for 1 h at 23°C and stored at 4°C . Sponges were stained in diluted Lugol's Iodine (I_2 : 1%, KI: 2%) for 24 h, to increase the contrast of tissue elements in X-ray scans. Three-dimensional X-ray scans were performed using an Xradia Versa XRM520 X-ray microscope, using the following specifications: $\sim 5 \mu\text{m}$ pixel size; voltage: 80 kV; power: 7 W; exposure time: 12 s; and binning: 2. Scanning time was approximately 6 h per sample. Projections were reconstructed using XMReconstructor software (Xradia Inc., Pleasanton, CA, USA).

Avizo Fire software (FEI, Hillsboro, OR, USA) was used to extract quantitative data from the 3D reconstructions. The Edit New Label Field tool was used to segment scans. Due to the porous nature of sponges, the sponge tissue could not be segmented out from the

background using thresholding. Instead, the lasso selection tool was used to manually select the internal edge of the pinacoderm (outer layer) on 2D X – Y cross sections. Selections were performed every 50 cross-sections (~ 250 μm), and then the interpolate function was used to create a 3D selection between the two selections. This process was repeated across 800 cross-sections (~ 4 mm) to select the internal volume of the sponge. This procedure also served to exclude sediments on the surface of the sponge since the concentration of these sediments was highly variable due to handling effects and mucus production (Pineda *et al.*, 2017a). Internal organisms, such as polychaetes and barnacles, were manually excluded from analysis using the lasso selection tool. The internal sediment, within the selected volume, was then segmented via the Interactive Thresholding tool, and the number of sediment particles and sediment particle volumes was quantified using the Label Analysis tool. Sediment particle diameter, was estimated assuming that the particles were spherical. Sponge tissue and skeletal elements were also segmented, labelled, and quantified within the selected volume. The remaining volume in the selection was labelled as aquiferous system because it matched threshold levels of the background solution, and was quantified using the same approach. The number of sediment particles in each sample was standardised to the selected volume, i.e., aquiferous system volume plus tissue and skeletal volumes. During tissue regression in *I. basta*, the choanocyte chamber density decreases and the tissue itself appears denser (Luter, Whalan & Webster, 2012b), indicating that the volume of the aquiferous system channels had decreased. The potential for rapid recovery from this regressed state implies that there is little change in the total number of sponge cells present (Luter, Whalan & Webster, 2012b). Therefore, in order to quantify tissue regression, the percent of the total volume occupied by the aquiferous system was calculated. Due to the pixel size, the aquiferous system volume analysed is more representative of the channels of the aquiferous system, i.e., incurrent channels, excurrent channels, atrium, etc., than of the choanocyte chambers, which are difficult to visualise at this resolution and within these relatively large samples.

Sediment particle position was determined by examining cross sections of the 3D volumes. A random cross section was selected for each sample. If sediment particles appeared tightly surrounded by sponge tissue, they were considered to be in the mesohyl. Particles present in the channels were also counted. The percentage of total particles in the mesohyl and in the channels was determined for each sample and averaged for each collection point to determine sediment position.

SEM analysis

Fixed sponges were dehydrated in increasing concentrations of ethanol using a PELCO Biowave microwave fitted with a PELCO Coldspot, then immersed in liquid nitrogen and fractured using a chisel (Johnston & Hildemann, 1982). This fracturing technique revealed the full aquiferous system including the choanocyte chambers. After fracturing, samples were returned to anhydrous ethanol, critical-point dried, and then mounted on stubs using carbon tape. Mounted samples were coated with 10 nm of gold and 10 nm of carbon to ensure sample conductivity. Images were acquired at 5 kV using a Zeiss 55 field emission scanning electron microscope. After 24 h exposure, all samples from the acute exposure

Table 1 AIC values for models generated for the different response variables for the acute and chronic exposures to sediment. The chosen model based on the lowest AIC score is shown in bold.

Response variable	Acute exposure to siliciclastic sediment				Chronic exposure to carbonate sediment			
	ANOVA with Tank	ANOVA without tank	GLS with tank	GLS without tank	ANOVA with Tank	ANOVA without tank	GLS with tank	GLS without tank
Sediment particles mm^{-3}	403	367	362	360	86	77	84	75
Sediment particle volume	272	270	N/A	N/A	63	61	N/A	N/A
Percent volume aquiferous system	375	354	N/A	N/A	-16	-18	N/A	N/A

experiment were assessed qualitatively for the presence of sediment. One control sample from each time point was also mounted without being freeze fractured in order to view the outer surface. Ostia, incurrent pore diameter, and surface area was determined from images using the ImageJ software package ([Rasband, 2012](#)).

Statistical analyses

Linear models were fitted to predict internal sediment variables (i.e., sediment particles mm^{-3} and sediment particle volume) and the percent volume of the sponge aquiferous system in terms of time and treatment (both as fixed factors). Control sponges had no internal sediment at any time, so control treatments from internal sediment variables data were excluded from the models. Internal sediment data were then compared between sediment treatments and over time. The percent volume of the sponge aquiferous system from control treatments was included in the models. These models were compared to linear mixed effects models with an additional random factor for tank, using the Akaike information criterion (AIC) in R ([R Development Core Team, 2016](#)). Based on the lowest AIC values, there was no indication that tank had an effect on any variable in either experiment, so the more parsimonious linear models, i.e., without tank as a random factor, were used ([Table 1](#)). In order to minimise genetic effects, sponge explants from each original replicate were randomly distributed between the tanks. However, due to the low number of original replicates ($n = 5$), there was still a chance of false positives in the models due the limited genetic independence of the explants. For models of sediment particles mm^{-3} over time and treatment, variances were weighted using a power law function within a generalised least squares (GLS) model for data from both acute and chronic exposure, in order to ensure homogenous variance of standardised residuals. Power-law weighted GLS models were the best fit according to AIC value for sediment particles mm^{-3} in both exposures. All other variables were modelled using linear models, i.e., analyses of variance (ANOVA). Data were arcsine transformed to model the percent volume of aquiferous system relative to tissue and skeletal volume over time and treatment in the chronic exposure, to meet the assumption of a normal distribution; otherwise raw data were used. Significance of model terms was evaluated using F -tests following the standard ANOVA approach. Tukey HSD was used to test for differences between time points and treatments. Welch t -tests were performed for each time point to identify differences in

internal sediment mm^{-3} in each treatment level, i.e., medium and high sediment, in the acute exposure. Unless otherwise specified, reported values represent mean plus or minus standard error.

RESULTS

Acute exposure to sediments

After 24 h of exposure, sediment was present in *I. basta* from both high and medium SSC treatments, but was not evident in control sponges (Figs. 2–4). No sediment particles were evident in the control sponges at any time point (Figs. 2–4). Internal sediment particles per cubic millimetre of the total volume, i.e., of the sponge tissue and the aquiferous system, (sediment particles mm^{-3}) increased significantly following exposure and then decreased during the recovery ($P < 0.01$, Table 2A), and there was a significant interaction of treatment (i.e., sediment level) with time ($P < 0.05$, Table 2A). After the first hour of exposure, the number of sediment particles in the high treatment sponges (180 ± 61 particles mm^{-3}) was double that of the medium treatment (90 ± 32 particles mm^{-3}), however this was not significantly different ($P > 0.05$). After 48 h of exposure and 1 h of recovery, sponges in the high and medium treatments had accumulated 500 ± 218 and 435 ± 118 particles mm^{-3} respectively, and again there was no significant difference between the two sediment treatments ($P > 0.05$, Table 2A, Fig. 2). Two dimensional (2D) cross-sections, of 3D X-ray microscopy images for all treatments are shown in Fig. 3. These cross-sections show the sponge skeletal and aquiferous system elements as well as the mesohyl and any internal sediments. Representative 3D X-ray microscopy images, thresholded to show only internal sediments are shown in Fig. 4. Full 3D renderings of sponges and sediments are presented in Movies S1–S5 .

After ~ 24 h recovery (78 h after initial sediment exposure), sediment levels inside samples from the high treatment (747 ± 146 particles mm^{-3}) remained significantly higher than those of the medium treatment (39 ± 10 particles mm^{-3} , Welch two sample t -test $P < 0.05$, Table 2A Fig. 2). After 3 w of recovery, little to no sediment was detected in either of the sediment treatments or the controls (13 ± 8 , 21 ± 21 , and 0 ± 0 particles mm^{-3} for the high, medium, and control treatments respectively).

All sediment exposed sponges ($n = 3$ per time point) closed all of their oscula within the first 24 h of sediment dosing in the high and medium treatments, but re-opened them at differing times. In the medium treatment, oscula reopened 1 h after sediment exposure ended, i.e., 49 h after the start of the experiment. Whereas, in the high treatment, oscula stayed closed for 3 h after sediment exposure ended. Control sponges did not exhibit closed oscula at any of the sampling times.

The size of sediments (volume: $41 \pm 10 \mu\text{m}^3$, diameter: $4.2 \pm 0.8 \mu\text{m}$) inside the sponge changed very little over time for either sediment treatment. Although there was a significant effect of time on sediment size ($P < 0.05$ Table 2B), this effect was likely caused by the decrease in particle volume in the medium treatment after 3 w (Fig. 2B). However this decrease was not significant in the Welch t -test ($P > 0.05$), and no other post hoc comparisons were significantly different. The percentage of sponge aquiferous volume

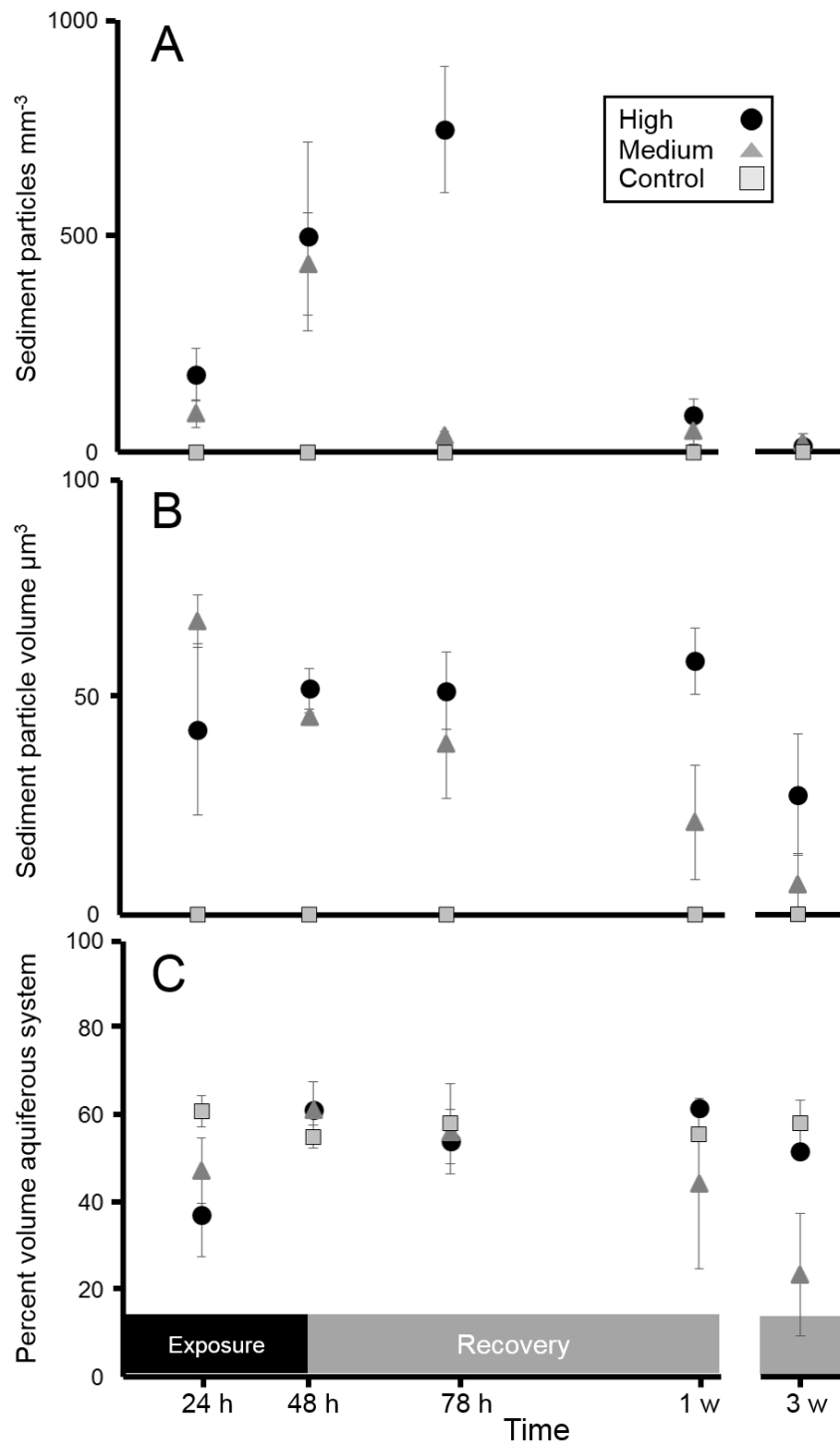


Figure 2 Siliciclastic sediment inside *I. basta* during the acute 48 h exposure experiment and subsequent recovery. Data (mean \pm SE) show (A) the number of internal sediment particles mm^{-3} , (B) sediment particle volume (μm^3), and (C) volume of aquiferous system relative to tissue and skeletal volume (%), during the exposure and recovery periods (black and grey bars, respectively) for the control (0 mg L^{-1} , grey squares), medium ($42 \pm 8 \text{ mg L}^{-1}$, dark grey triangles), and high sediment ($135 \pm 30 \text{ mg L}^{-1}$, black circles) treatments.

Full-size DOI: [10.7717/peerj.3904/fig-2](https://doi.org/10.7717/peerj.3904/fig-2)

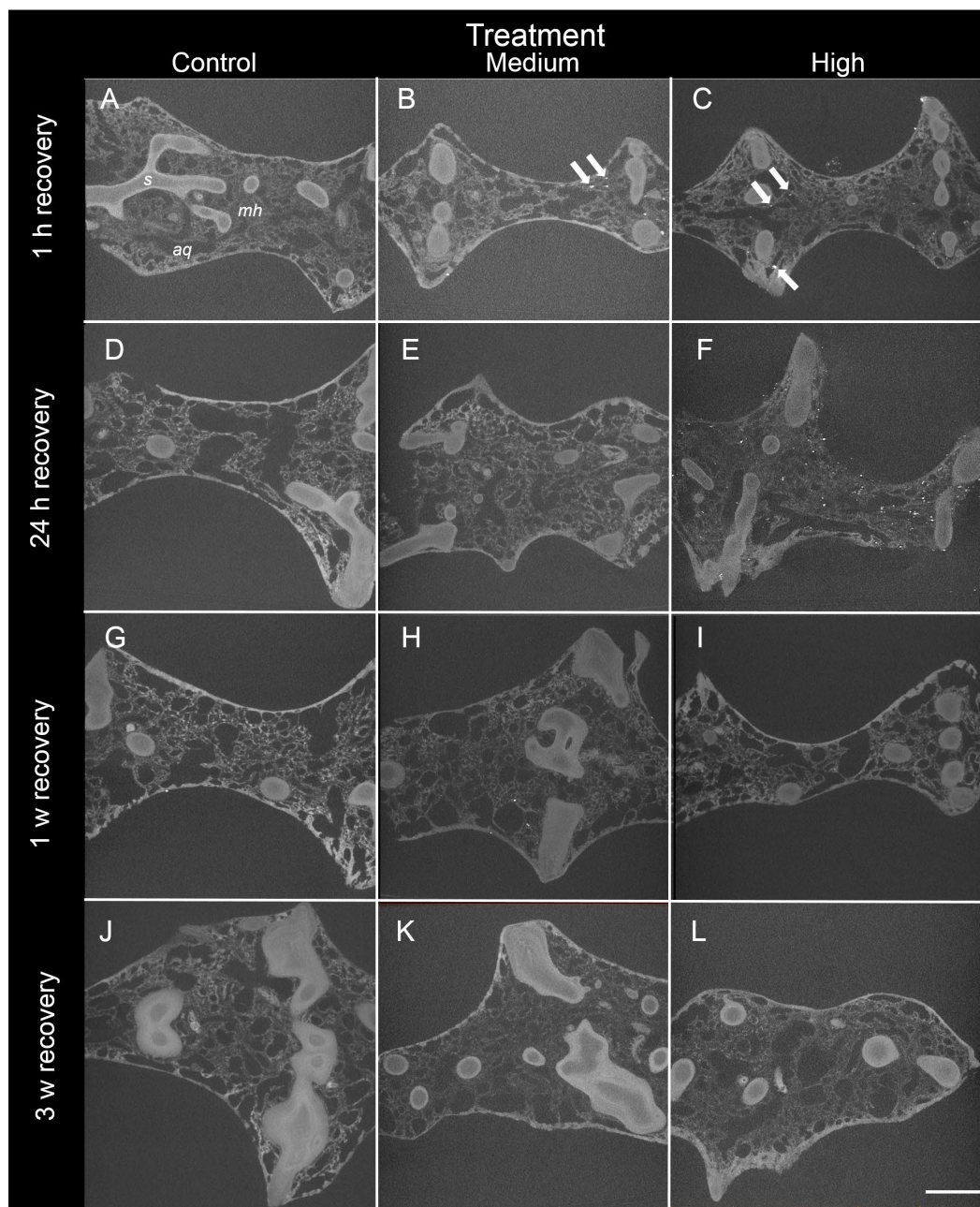


Figure 3 Representative 2D X-ray cross-sections of *I. basta* during the recovery period after 1 h, 24 h, 1 w, and 3 w for the control (0 mg L^{-1}), medium ($42 \pm 8 \text{ mg L}^{-1}$), and high siliciclastic sediment ($135 \pm 30 \text{ mg L}^{-1}$) treatments. The sponge skeletal fibres (s), mesohyl (mh) and aquiferous system channels (aq) are visible in all treatments. As recovery time increases, the sediment (white particles indicated by arrows) becomes less concentrated, and no sediment was observed in the control sponges (scale = 1 mm).

Full-size [DOI: 10.7717/peerj.3904/fig-3](https://doi.org/10.7717/peerj.3904/fig-3)

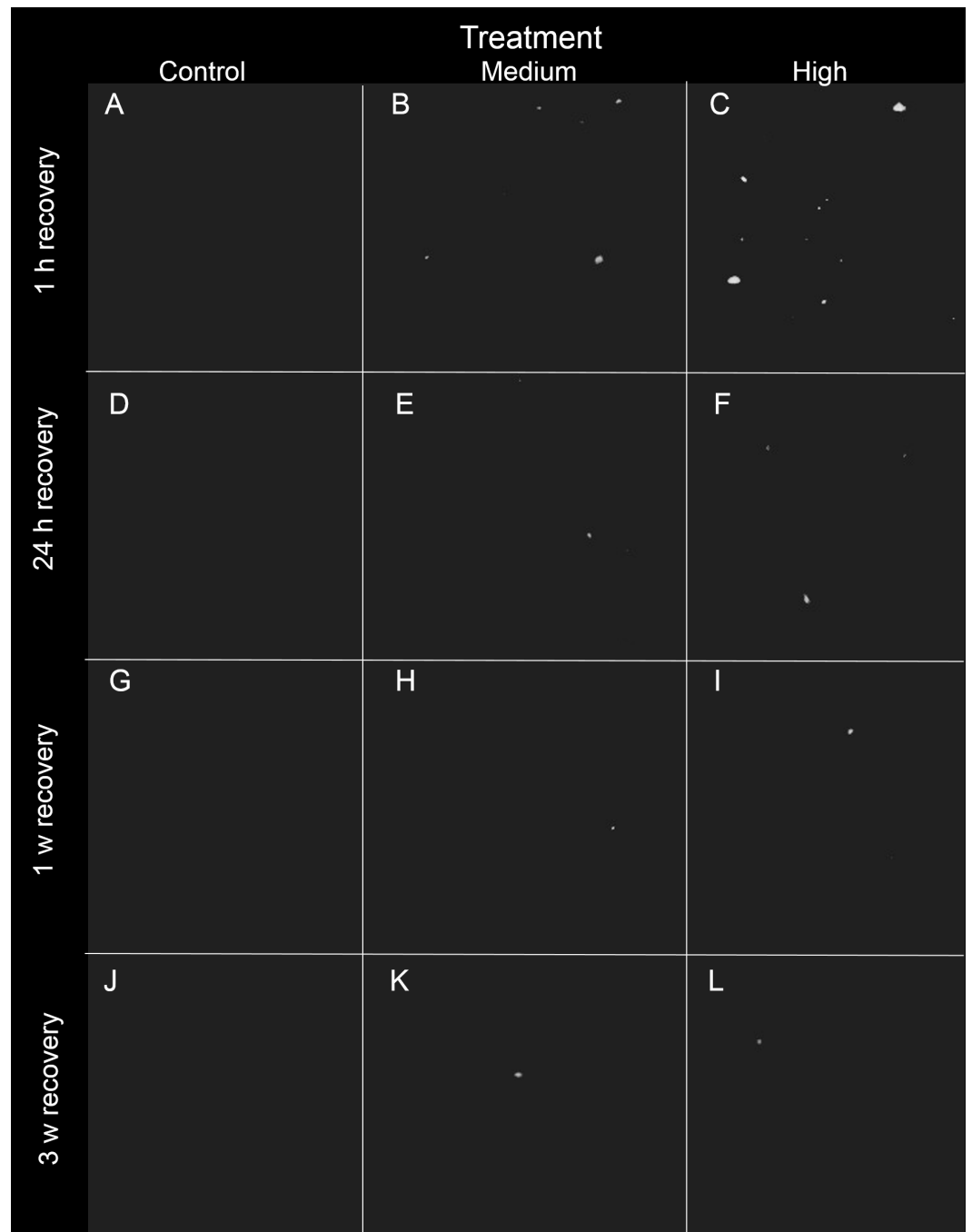


Figure 4 Representative 3D X-ray images of siliciclastic sediments within *I. basta* during the recovery period after 1 h, 24 h, 1 w, and 3 w for the control (0 mg L^{-1}), medium ($42 \pm 8 \text{ mg L}^{-1}$), and high ($135 \pm 30 \text{ mg L}^{-1}$) sediment treatments. Sponge tissue (removed via thresholding) is not shown in order to emphasise sediment particles and distribution. As recovery time increases, the sediment (white) becomes less concentrated, and no sediment was observed in the control sponges (no scale is shown because the particles are distributed in 3D).

Full-size  DOI: [10.7717/peerj.3904/fig-4](https://doi.org/10.7717/peerj.3904/fig-4)

Table 2 ANOVA summaries for the acute exposure to siliciclastic sediments. (A) A generalised least squares (GLS) model with power law weighted variance of sediment particles mm^{-3} in the tissue over time and sediment treatment level. Welch *t*-test results are shown if significant. Time point 3, i.e., ~24 h recovery (78 h after initial sediment exposure), is abbreviated as T3, and the high and medium sediment treatments are abbreviated as H and M, respectively. (B) ANOVA of sediment particle volume over time and sediment treatment level. Data from control sponges were excluded from the analysis in (A) and (B) because there were no sediments present and the values for the controls were all zero. (C) ANOVA of the arcsine transformed percent volume of the aquiferous system based on time and treatment. Control data was included in (C).

	<i>df</i>	<i>F</i>	<i>P</i>
(A) Sediment particles mm^{-3}			
Treatment	1	0.59	0.45
Time	4	7.30	<0.001
Treatment: time	4	3.627	0.02
Residuals	20		
Welch <i>t</i> -test			
Treatment: time	M:T3 < H:T3; $t = 4.84$, $df = 2.02$, $P = 0.04$		
(B) Sediment particle volume			
Treatment	1	2.30	0.15
Time	4	3.63	0.02
Treatment: time	4	2.25	0.01
Residuals	20		
(C) Percent volume aquiferous system			
Treatment	2	0.19	0.83
Time	4	0.50	0.73
Treatment: time	8	1.31	0.27

relative to tissue and skeletal volume similarly did not significantly decrease ($P > 0.05$, Table 2C) in any treatment, remaining at ~56% throughout the experiment and recovery period for all treatments (Fig. 2C).

In the high sediment treatment, internal sediment was mostly located (93%) in the mesohyl of sponges after 24 h. After 48 h of exposure and during recovery, most internal sediment (61–93%) was found in the channels of the aquiferous system. In the medium sediment treatment, the majority (>65%) of internal sediments were located in the channels of the aquiferous system at all time points.

SEM revealed that all sponges, including those not exposed to sediments, produced considerable amounts of mucus on their outer surfaces (Figs. 5A and 5B). Rates of mucus sloughing and production were not determined in this study. Mucus in the control treatment appeared to trap and facilitate any fouling on the sponge surface or pinacoderm (Fig. 5A). The mucus in the siliciclastic sediment treated sponges also appeared to trap and facilitate the removal of sediment particles on the sponge's outer surface (Fig. 5B). For the siliciclastic sediment, no major differences were observed in choanocytes of sediment-treated and control sponges (Figs. 5C and 5D). In sediment-treated and control sponges, choanocyte chambers were present and not clogged with sediments. Some sediment-like particles were observed in the channels of the aquiferous system and choanocytes,

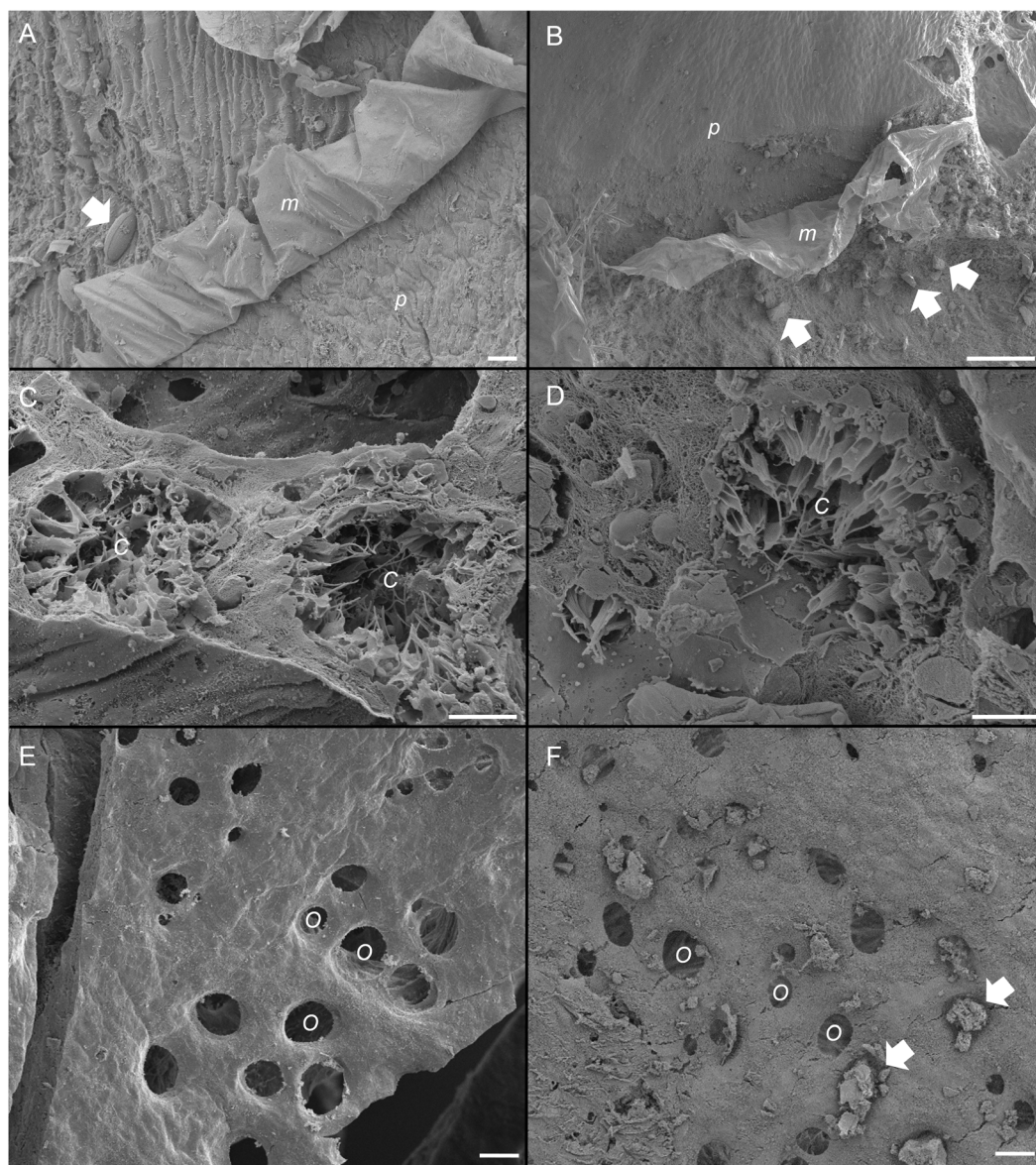


Figure 5 Scanning electron micrographs of the sponge, *Ianthella basta* in control (0 mg L^{-1}) (A, C, E) and acute siliciclastic sediment exposure (B, D, F). (A) Mucus (*m*) production in a control sponge, trapping a diatom (arrow). Mucus sloughing cleaned an area of pinacoderm (*p*) (Scale = $10 \text{ }\mu\text{m}$). (B) Mucus (*m*) production in *I. basta* from the high sediment ($135 \pm 30 \text{ mg L}^{-1}$) treatment after 48 h exposure and 1 h recovery. Sediments (arrows) were trapped in mucus (*m*). Mucus sloughing cleaned sediments off an area of pinacoderm (*p*) (Scale = $10 \text{ }\mu\text{m}$). (C) Choanocyte chambers (*C*) in the control treatment after 24 h (Scale = $10 \text{ }\mu\text{m}$). (D) Choanocyte chamber (*C*) from the high sediment treatment after 24 h of exposure to sediments (Scale = $10 \text{ }\mu\text{m}$). (E) Surface and ostia (*O*, incurrent pores) from a control after 24 h of exposure to control conditions (Scale = $20 \text{ }\mu\text{m}$). (F) Surface and ostia (*O*) from the medium sediment treatment ($42 \pm 8 \text{ mg L}^{-1}$) after 24 h of exposure to sediment (Scale = $20 \text{ }\mu\text{m}$, arrows indicate sediment particles blocking ostia).

Full-size  DOI: [10.7717/peerj.3904/fig-5](https://doi.org/10.7717/peerj.3904/fig-5)

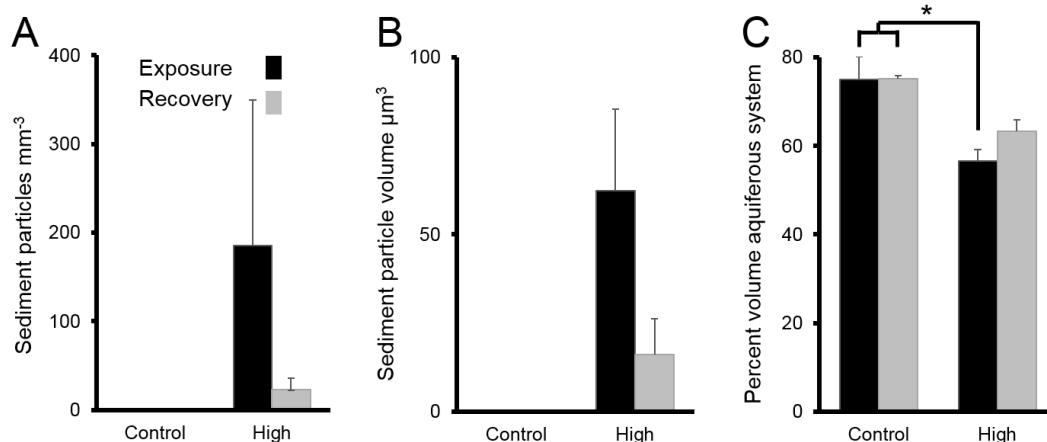


Figure 6 Sediments inside *Ianthella basta* after 4 w exposure (black bars) to carbonate sediments (High; 76 mg L⁻¹) and control conditions (Control; 0 mg L⁻¹), as well as after 2 w recovery in control conditions (grey bars). Data (mean ± SE) show the number of (A) internal sediment particles mm⁻³, (B) internal sediment particle volume (μm³), and (C) volume of aquiferous system relative to tissue and skeletal volume (%). Statistically significant differences are noted with an asterisk.

Full-size [DOI: 10.7717/peerj.3904/fig-6](https://doi.org/10.7717/peerj.3904/fig-6)

but internal sediment levels were not quantifiable. The ostia of some sponges exposed to sediment were clogged with sediment particles (Fig. 5F), whereas the ostia of control sponges were always clear (Fig. 5E). In general, ostia ($n = 15$) in control sponges were found to be ellipsoid with an average diameter of $20 \pm 1 \mu\text{m}$ and an average area of $268 \pm 34 \mu\text{m}^2$.

Chronic exposure to sediments

Following chronic exposure to carbonate sediments, no sediment was detected in control sponges. There was accumulation of sediment, with high internal sediment concentrations of $185 \pm 165 \text{ particles mm}^{-3}$, in the treated sponges after 4 w of exposure to elevated suspended sediments, light attenuation, and increased sedimentation. Internal sediment concentrations decreased to a very low level of $23 \pm 13 \text{ particles mm}^{-3}$ after 2 w of recovery in control conditions (Fig. 6A); however, this reduction was not statistically significant ($P > 0.05$, Table 3A).

The average amount of sediment particles mm^{-3} in sponges from the chronic treatments after 4 w of sediment treatment ($185 \pm 165 \text{ particles mm}^{-3}$) was approximately 63% lower than the highest observed value in the acute treatments, despite the longer exposure time. The average particle volume of internal sediments in the chronic exposure was $62 \pm 23 \mu\text{m}^3$ (diameter: 5.0 ± 1.3 ; Fig. 6B), and it did not significantly change over time ($P > 0.05$, Table 3B).

The percent volume of the aquiferous system (relative to the tissue and skeletal volumes) in the high sediment treatment ($56 \pm 3\%$) was significantly lower after 4 w exposures than that of control treatments ($75 \pm 5\%$) (Tukey HSD: $P < 0.01$, Table 3C Fig. 6C). The percent volume of the aquiferous system did not fully recover to control levels by the end of the recovery period, returning to $63 \pm 3\%$ ($P = 0.075$). After 4 w of chronic exposure,

Table 3 ANOVA summaries for chronic exposure to carbonate sediments. (A) A generalised least squares (GLS) model with power law weighted variance of sediment particles mm^{-3} in the tissue over time, i.e., 4 w exposure or 2 w recovery, in the high sediment (76 mg L^{-1}) treatment. (B) ANOVA of sediment particle volume over time high sediment treatment. Data from control sponges were excluded from the analysis in (A) and (B) because there were no sediments present and the values for the controls were all zero. (C) ANOVA of the arcsine transformed percent volume of the aquiferous system based on time and treatment. Control data was included in (C). A Tukey HSD test was performed to determine differences between the high sediment treatment and the control sponges, abbreviated H and C, respectively.

	<i>df</i>	<i>F</i>	<i>P</i>
(A) Sediment particles mm^{-3}			
Time	1	0.96	0.38
Residuals	4		
(B) Sediment particle volume			
Time	1	3.42	0.14
Residuals	4		
(C) Percent volume aquiferous system			
Treatment	1	12.9	<0.01
Time	1	0.30	0.60
Treatment: time	1	0.27	0.62
Residuals	8		
Tukey HSD			
Treatment	$H > C, P < 0.01$		

the majority of internal sediments appeared within channels ($66 \pm 33\%$). After the 2 w recovery, the majority of internal sediments appeared in the mesohyl ($75 \pm 20\%$).

DISCUSSION

The sponge *Ianthella basta* was tolerant of both short term acute and longer term chronic increases in suspended sediments. *I. basta* was able to survive using a combination of passive and active strategies, specifically through the production of mucus to trap and remove surface sediment, exclude large particles from its aquiferous system via its ostia, close its oscula to limit pumping, eliminate any particles that did enter the aquiferous system, and enter into a regressed state wherein the size of the aquiferous system was reduced. These mechanisms have been reported or hypothesised in other sponge species (Bell et al., 2015; Schönberg, 2015; Schönberg, 2016), and this study extends our knowledge by providing a comprehensive account of these mechanisms occurring concurrently within a single species. This suite of mechanisms likely underpins the ecological tolerance and resilience exhibited by *I. basta* to sediment pressures (Luter, Whalan & Webster, 2012b; Pineda et al., 2017a; Pineda et al., 2017b).

Previous analyses by Pineda et al. (2017a) revealed that mucus cover on the surface of *I. basta* significantly increased from nearly zero to $21 \pm 9\%$ in the highest sediment treatment, in the chronic exposure, compared to pre-exposure and control sponges. Mucus was present on both the incurrent and excurrent side of the sponge. *I. basta* mucus

likely functions as an anti-fouling mechanism as seen in corals ([Erftemeijer et al., 2012](#); [Jones et al., 2016](#); [Bessell-Browne et al., 2017a](#)) and as proposed in the sponges *Carteriospongia foliascens* ([Pineda et al., 2017a](#)) and *Lamellodysidea herbacea* ([Biggerstaff et al., 2017](#)). In *I. basta*, mucus likely functioned to remove sediments in the treated sponges and remove surface fouling organisms such as diatoms in untreated sponges. The chemical composition and metabolic cost of this mucus production remains to be determined. However, based on the increased respiration rates in *L. herbacea* following chronic sediment exposure ([Biggerstaff et al., 2017](#)) and the high energetic cost of mucus production in corals (e.g., [Riegl & Branch, 1995](#)), the increased mucus production in *I. basta* may also be energetically costly. It also remains unclear how sponges slough or remove mucus. Corals use ciliated surfaces to remove mucus sheets ([Stafford-Smith & Ormond, 1992](#)), but sponges do not have ciliated outer surfaces ([Bergquist, 1978](#)). High ambient currents, such as those created in this study and in [Pineda et al. \(2017a\)](#), [Pineda et al. \(2017b\)](#) and [Pineda et al. \(2017c\)](#), could facilitate the removal of mucus and the particles trapped therein; however, *L. herbacea* was still able to slough mucus and trapped sediments in low-flow conditions ([Biggerstaff et al., 2017](#)). The dynamics of sponge mucus production warrant future research, for which *I. basta* would be an excellent model species.

The ostia of *I. basta* also form a passive, physical barrier against the entrance of foreign particles larger than $\sim 20 \mu\text{m}$ in diameter. Sponges in the acute exposure had higher internal sediment concentrations than those in the chronic treatments, which may reflect the different sediment types and sizes used in the acute and chronic experiments. The smaller particles in the siliciclastic sediment used in the acute exposure likely entered the aquiferous system more easily. However, the particle size of the internal sediments in both experiments was similar, indicating that the ostia formed a size-selection barrier for larger sediments. With the ostia acting as a sieve, the majority of internal particles had a diameter of 4–5 μm , which corresponds to very fine silts and clay. In dredge and flood plumes, sediment is typically fine and comprised of medium silts and clays ($< 60 \mu\text{m}$; [Bainbridge et al., 2012](#); [Jones et al., 2016](#)). In addition to introducing smaller sediments to the aquiferous system, dredge and flood plumes could also potentially clog ostia of *I. basta* with larger sediment particles. This clogging of ostia has been previously hypothesised to negatively impact sponges ([Bell et al., 2015](#); [Schönberg, 2015](#); [Schönberg, 2016](#)), although we now provide experimental evidence that this occurs under sediment exposure. Sponge ostia can range from 1–50 μm in diameter across taxa ([Simpson, 1984](#)). Species with larger ostia and higher choanocyte chamber density are likely to be more vulnerable to high sediment exposure, since they also have comparatively high particle clearance rates ([Turon, Galera & Uriz, 1997](#)), meaning that they can filter out more particles, including sediments. For example, the sponge *Rhopaloeides odorabile* would be susceptible by this criteria, and this vulnerability may partially explain its reduced abundance in inner-shelf reefs of the GBR, where fine-grained sediment loads are high ([Bannister, Battershill & De Nys, 2012](#)). While some sponge species can contract their ostia (reviewed in [Leys & Meech, 2006](#); [Elliott & Leys, 2007](#)), this was not observed in *I. basta*. However, the possibility of ostia contraction in *I. basta*, particularly during coordinated tissue regression (see below), also warrants further investigation.

In *I. basta*, sediments that are not trapped in mucus or excluded by ostia can still potentially enter the aquiferous system. Once inside, they could reduce pumping efficiency and affect food uptake and gas exchange. While many studies have examined the rate at which sponges can remove particles from water, few have determined the rates at which these particles are expelled. [Strehlow et al. \(2016b\)](#) demonstrated that introduced *Symbiodinium* (~10 μm in diameter) could persist in the tissues and aquiferous system of *Amphimedon erina* for five days after inoculation, which was comparable to the 3 day persistence of sediment in *I. basta* from the high sediment treatment. The majority of sediments were observed in the channels of the aquiferous system as opposed to the sponge mesohyl. The increase in mesohyl sediments in the chronic exposure following the recovery period may have occurred when sediments on the surface of the sponge were engulfed as the sponge tissues expanded to recover from regression.

Due to the high filtration efficiencies of sponges, it is likely that the sediments were taken up by the choanocytes and then expelled via exocytosis into the exhalant system. Furthermore, no clumping sediments, and no corresponding increase in sediment particle volume, were observed within the scans, which would have been expected if sediments were clogging the aquiferous system elements. This indicated efficient processing of sediments. Additionally, the lack of significant changes in the aquiferous system volume in the acute exposure indicated that a coordinated contraction of aquiferous system elements to remove clumps of material, i.e., 'sneezing' ([Elliott & Leys, 2007](#); [Ludeman et al., 2014](#)), may not occur in *I. basta*. However, increasing the temporal resolution of the scans could yield further insights into this coordinated behaviour in future studies. Targeted increases in spatial resolution could also be used to better identify the various elements of the aquiferous system in the future. It may also be possible that internal sediments pass directly through the aquiferous system, without ingestion, and out through the oscula. Prosopyles and apopyles, i.e., the openings leading into and out of choanocyte chambers, respectively, were 7–8 μm in diameter (B Strehlow, pers. obs., 2017), suggesting that the small internal particles, i.e., fine silts and clays, could pass directly through the smallest part of the sponge filtration system. Sediment may also have egressed through canals that bypass choanocytes to prevent clogging ([Bavestrello, Burlando & Sara, 1988](#); [Hammel et al., 2012](#)). Although no direct evidence of sediment ingestion, i.e., phagocytosis or intracellular sediments, was observed in these experiments, it is possible that sediment was ingested, processed and egressed, particularly sediment smaller than 10 μm ([Turon, Galera & Uriz, 1997](#); [Yahel et al., 2007](#); [Topçu et al., 2010](#)). In order to verify sediment ingestion, future experiments would need to verify intracellular sediment using sectioning and transmission electron microscopy (TEM).

Sponges exposed to acute sediment exposures closed their oscula within 24 h, indicating a cessation of pumping. Internal sediments could have entered the aquiferous system before full oscula closure. To our knowledge, this is the first report of oscula closure in this species, and the first report of closure in response to sediment exposure. A preliminary experiment found no sediment inside dead and anaesthetised sponges, indicating active pumping by the sponge is necessary for sediments to enter the sponges. Therefore, osculum closure is a clear response to limit sediment uptake. This closure may even impose a threshold of maximum

sediment uptake, which would explain why there was no significant difference in internal sediment concentrations between the high and medium treatments in the acute exposure experiment after 48 h of sediment exposure and 1 h of recovery. Oscula closure leading to cessation of pumping has been observed in a number of other sponge species (e.g., *Reiswig, 1971*), particularly in response to acute and chronic SSC exposures (*Strehlow et al., 2016a; Pineda et al., 2017a*). With this prolonged closure, tissue regression and necrosis of sponges was significantly higher in the chronic, highest sediment treatment ($45 \pm 12\%$) than in the control treatments ($4 \pm 1\%$), and continued to be high throughout the recovery period ($30 \pm 5\%$, *Pineda et al., 2017b*). This regression corresponded to a decrease in the percentage volume of the aquiferous system. Sponge tissue regression results in a dormant state where choanocyte chamber density decreases (*Luter, Whalan & Webster, 2012b*), the volume of the aquiferous system decreases and, presumably, active pumping all but ceases as there are no longer visible oscula (B Strehlow, pers. obs., 2016). Necrosis, on the other hand, was characterised by a loss of cells which resulted in exposure of the sponge skeletal elements. Tissue regression has also been observed in sponges undergoing physiologically stressful events such as spawning (*Abdul Wahab et al., 2016*), yet *I. basta* has a remarkable recovery capacity, exhibiting complete recovery within 72 h of being in a fully regressed state (*Luter, Whalan & Webster, 2012b*).

This dormant state would be detrimental to *I. basta* in the long term as they depend on pumping for vital physiological processes (*Bell et al., 2015; Schönberg, 2015; Schönberg, 2016*). However, entering into a short-term regressed or dormant state may be beneficial or preferential under chronic sediment pressure. Pumping is energetically costly (*Leys et al., 2011*), and previous experiments have shown that sponges decrease or cease pumping when exposed to suspended sediments (*Gerrodette & Flechsig, 1979; Tompkins-MacDonald & Leys, 2008; Strehlow et al., 2016a*). Sponge choanocytes have the fastest cell cycle noted for a multicellular organism, and old cells are constantly expelled (*De Goeij et al., 2009*). With such a high rate of cellular turnover, maintaining the aquiferous system is likely to be energetically costly. Entering this dormant state would not only decrease the energetic cost of pumping but also the costs of maintaining choanocyte turnover.

CONCLUSION

X-ray microscopy proved a useful tool for studying sediment stress and uptake in filter feeders. The resolution (micrometres) that can be achieved over large volumes (millimetres) allowed for sensitive and accurate detection and quantification of introduced particles. The non-destructive nature of the approach allowed sponges to be visualised and quantified without disturbing internal structures or the positioning of introduced particles. Using this tool, we demonstrated that *I. basta* can readily accumulate and expel introduced sediments in short time frames. Coupling X-ray microscopy data with SEM observations led to the identification of five mechanisms that control sediment rejection and elimination in *I. basta* and underpin the tolerance and resilience of this species to sediment related stressors. These mechanisms include: (i) mucus production, (ii) exclusion of particles by incurrent pores, (iii) closure of oscula and pumping cessation, (iv) expulsion of particles

from the aquiferous system, and (v) tissue regression to reduce the volume of the aquiferous system, limiting pumping and filtration capacity, thereby entering a dormant state. These mechanisms, combined with the compact ultrastructure and relative sediment tolerance of *I. basta*, make it an excellent model species for studying sediment response mechanisms in sponges. Understanding these mechanisms contributes to our general knowledge of the effects of dredging and increased sediment loads on sponges, which will inform effective management of coastal areas given the increasing sediment loads therein.

ACKNOWLEDGEMENTS

We acknowledge the facilities, and the scientific and technical assistance of the Australian Microscopy & Microanalysis Research Facility at the Centre for Microscopy, Characterisation & Analysis, at UWA, a facility funded by the University, State and Commonwealth Governments. Special thanks to J Shaw and A Mehnert for assistance and expertise regarding X-ray microscopy and to L Kirilak and J Murphy for technical support. We also thank the staff at the AIMS National Sea Simulator for their expertise and assistance, in particular A Severati, T Baker, G Milton, E Arias, and J Hochen.

ADDITIONAL INFORMATION AND DECLARATIONS

Funding

This research was funded by the Western Australian Marine Science Institution (WAMSI) as part of the WAMSI Dredging Science Node, and made possible through investment from Chevron Australia, Woodside Energy Limited, BHP Billiton as environmental offsets and by co-investment from the WAMSI Joint Venture partners. The views expressed herein are those of the authors and not necessarily those of WAMSI. Nicole S. Webster was funded by an Australian Research Council Future Fellowship FT120100480. Brian W. Strehlow was supported by a University of Western Australia (UWA) Scholarship for International Research Fees, University International Stipend, and UWA Safety-Net Top-Up Scholarships. The funders had no role in study design, data collection and analysis, decision to publish, or preparation of the manuscript.

Grant Disclosures

The following grant information was disclosed by the authors:
Western Australian Marine Science Institution (WAMSI) Dredging Science Node.
Australian Research Council Future Fellowship: FT120100480.
University of Western Australia (UWA).

Competing Interests

The authors declare there are no competing interests.

Author Contributions

- Brian W. Strehlow conceived and designed the experiments, performed the experiments, analyzed the data, contributed reagents/materials/analysis tools, wrote the paper, prepared figures and/or tables, reviewed drafts of the paper.

- Mari-Carmen Pineda conceived and designed the experiments, performed the experiments, contributed reagents/materials/analysis tools, wrote the paper, reviewed drafts of the paper.
- Alan Duckworth, Gary A. Kendrick, Nicole S. Webster and Peta L. Clode conceived and designed the experiments, contributed reagents/materials/analysis tools, wrote the paper, reviewed drafts of the paper.
- Michael Renton conceived and designed the experiments, analyzed the data, contributed reagents/materials/analysis tools, wrote the paper, reviewed drafts of the paper.
- Muhammad Azmi Abdul Wahab contributed reagents/materials/analysis tools, wrote the paper, reviewed drafts of the paper.

Field Study Permissions

The following information was supplied relating to field study approvals (i.e., approving body and any reference numbers):

All collections from the Great Barrier Reef were performed under Great Barrier Reef Marine Park Regulations 1983 (Commonwealth) and Marine Parks regulations 2006 (Queensland).

Data Availability

The following information was supplied regarding data availability:

The raw data for Figures 2 and 6 are included as [Supplementary Files](#). Raw 3D data from X-ray microscopy scans can be accessed at: [10.4225/23/59f7d191d7c0e](https://doi.org/10.4225/23/59f7d191d7c0e).

Supplemental Information

Supplemental information for this article can be found online at <http://dx.doi.org/10.7717/peerj.3904#supplemental-information>.

REFERENCES

- Abdul Wahab MA, De Nys R, Holzman R, Schneider CL, Whalan S. 2016.** Patterns of reproduction in two co-occurring Great Barrier Reef sponges. *Marine and Freshwater Research* **68**(7):1233–1244 DOI [10.1071/MF16272](https://doi.org/10.1071/MF16272).
- Abdul Wahab MA, Fromont J, Gomez O, Fisher R, Jones R. 2017.** Comparisons of benthic filter feeder communities before and after a large-scale capital dredging program. *Marine Pollution Bulletin* **122**(1–2):176–193 DOI [10.1016/j.marpolbul.2017.06.041](https://doi.org/10.1016/j.marpolbul.2017.06.041).
- Andreakis N, Luter HM, Webster NS. 2012.** Cryptic speciation and phylogeographic relationships in the elephant ear sponge *Ianthella basta* (Porifera, Ianthellidae) from northern Australia. *Zoological Journal of the Linnean Society* **166**:225–235 DOI [10.1111/j.1096-3642.2012.00848.x](https://doi.org/10.1111/j.1096-3642.2012.00848.x).
- Bainbridge ZT, Wolanski E, Álvarez-Romero JG, Lewis SE, Brodie JE. 2012.** Fine sediment and nutrient dynamics related to particle size and floc formation in a Burdekin River flood plume, Australia. *Marine Pollution Bulletin* **65**:236–248 DOI [10.1016/j.marpolbul.2012.01.043](https://doi.org/10.1016/j.marpolbul.2012.01.043).

- Bannister RJ, Battershill CN, De Nys R. 2012.** Suspended sediment grain size and mineralogy across the continental shelf of the Great Barrier Reef: impacts on the physiology of a coral reef sponge. *Continental Shelf Research* **32**:86–95 DOI [10.1016/j.csr.2011.10.018](https://doi.org/10.1016/j.csr.2011.10.018).
- Bavestrello G, Burlando B, Sara M. 1988.** The architecture of the canal systems of *Petrosia ficiformis* and *Chondrosia reniformis* studied by corrosion casts (Porifera, Demospongiae). *Zoomorphology* **108**:161–166 DOI [10.1007/BF00363932](https://doi.org/10.1007/BF00363932).
- Bell JJ. 2004.** Evidence for morphology-induced sediment settlement prevention on the tubular sponge *Haliclona urceolus*. *Marine Biology* **146**:29–38 DOI [10.1007/s00227-004-1429-0](https://doi.org/10.1007/s00227-004-1429-0).
- Bell JJ. 2008.** The functional roles of marine sponges. *Estuarine, Coastal and Shelf Science* **79**:341–353 DOI [10.1016/j.ecss.2008.05.002](https://doi.org/10.1016/j.ecss.2008.05.002).
- Bell JJ, McGrath E, Biggerstaff A, Bates T, Bennett H, Marlow J, Shaffer M. 2015.** Sediment impacts on marine sponges. *Marine Pollution Bulletin* **94**:5–13 DOI [10.1016/j.marpolbul.2015.03.030](https://doi.org/10.1016/j.marpolbul.2015.03.030).
- Bergquist PR. 1978.** *Sponges*. Berkley and Los Angeles: University of California Press.
- Bessell-Browne P, Fisher R, Duckworth A, Jones R. 2017a.** Mucous sheet production in *Porites*: an effective bioindicator of sediment related pressures. *Ecological Indicators* **77**:276–285 DOI [10.1016/j.ecolind.2017.02.023](https://doi.org/10.1016/j.ecolind.2017.02.023).
- Bessell-Browne P, Negri AP, Fisher R, Clode PL, Jones R. 2017b.** Cumulative impacts: thermally bleached corals have reduced capacity to clear deposited sediment. *Scientific Reports* **7**:2716 DOI [10.1038/s41598-017-02810-0](https://doi.org/10.1038/s41598-017-02810-0).
- Biggerstaff A, Smith DJ, Jompa J, Bell JJ. 2017.** Metabolic responses of a phototrophic sponge to sedimentation supports transitions to sponge-dominated reefs. *Scientific Reports* **7**:2725 DOI [10.1038/s41598-017-03018-y](https://doi.org/10.1038/s41598-017-03018-y).
- Bythell JC, Wild C. 2011.** Biology and ecology of coral mucus release. *Journal of Experimental Marine Biology and Ecology* **408**:88–93 DOI [10.1016/j.jembe.2011.07.028](https://doi.org/10.1016/j.jembe.2011.07.028).
- De Goeij JM, De Kluijver A, Van Duyl FC, Vacelet J, Wijffels RH, De Goeij AFPM, Cleutjens JPM, Schutte B. 2009.** Cell kinetics of the marine sponge *Halisarca caerulea* reveal rapid cell turnover and shedding. *The Journal of Experimental Biology* **212**:3892–3900 DOI [10.1242/jeb.034561](https://doi.org/10.1242/jeb.034561).
- De Goeij JM, Van Oevelen D, Vermeij MJA, Osinga R, Middelburg JJ, De Goeij AFPM, Admiraal W. 2013.** Surviving in a marine desert: the sponge loop retains resources within coral reefs. *Science* **342**:108–110 DOI [10.1126/science.1241981](https://doi.org/10.1126/science.1241981).
- Diaz MC, Rützler K. 2001.** Sponges: an essential component of Caribbean coral reefs. *Bulletin of Marine Science* **69**:535–546.
- Duckworth AR. 2003.** Effect of wound size on the growth and regeneration of two temperate subtidal sponges. *Journal of Experimental Marine Biology and Ecology* **287**:139–153 DOI [10.1016/S0022-0981\(02\)00552-X](https://doi.org/10.1016/S0022-0981(02)00552-X).
- Elliott GRD, Leys SP. 2007.** Coordinated contractions effectively expel water from the aquiferous system of a freshwater sponge. *The Journal of Experimental Biology* **210**:3736–3748 DOI [10.1242/jeb.003392](https://doi.org/10.1242/jeb.003392).

- Erfteimeijer PLA, Riegl B, Hoeksema BW, Todd PA. 2012.** Environmental impacts of dredging and other sediment disturbances on corals: a review. *Marine Pollution Bulletin* **64**:1737–1765 DOI [10.1016/j.marpolbul.2012.05.008](https://doi.org/10.1016/j.marpolbul.2012.05.008).
- Field ME, Chezar H, Storlazzi CD. 2013.** SedPods: a low-cost coral proxy for measuring net sedimentation. *Coral Reefs* **32**:155–159 DOI [10.1007/s00338-012-0953-5](https://doi.org/10.1007/s00338-012-0953-5).
- Fisher R, Stark C, Ridd P, Jones R. 2015.** Spatial patterns in water quality changes during dredging in tropical environments. *PLOS ONE* **10**:e0143309 DOI [10.1371/journal.pone.0143309](https://doi.org/10.1371/journal.pone.0143309).
- Flach E, Lavaleye M, De Stigter H, Thomsen L. 1998.** Feeding types of the benthic community and particle transport across the slope of the N.W. European Continental Margin (Goban Spur). *Progress in Oceanography* **42**:209–231 DOI [10.1016/S0079-6611\(98\)00035-4](https://doi.org/10.1016/S0079-6611(98)00035-4).
- Fraser MW, Short J, Kendrick G, McLean D, Keesing J, Byrne M, Caley MJ, Clarke D, Davis AR, Erfteimeijer PLA, Field S, Gustin-Craig S, Huisman J, Keough M, Lavery PS, Masini R, McMahan K, Mengersen K, Rasheed M, Statton J, Stoddart J, Wu P. 2017.** Effects of dredging on critical ecological processes for marine invertebrates, seagrasses and macroalgae, and the potential for management with environmental windows using Western Australia as a case study. *Ecological Indicators* **78**:229–242 DOI [10.1016/j.ecolind.2017.03.026](https://doi.org/10.1016/j.ecolind.2017.03.026).
- Gerrodette T, Flechsig AO. 1979.** Sediment-induced reduction in the pumping rate of the tropical sponge *Verongia lacunosa*. *Marine Biology* **55**:103–110 DOI [10.1007/BF00397305](https://doi.org/10.1007/BF00397305).
- Gray JE. 1869.** Note on *Ianthella*, a new genus of keratose sponges. *Proceedings of the Zoological Society of London* **37**(1):49–51.
- Hammel JU, Filatov MV, Herzen J, Beckmann F, Kaandorp JA, Nickel M. 2012.** The non-hierarchical, non-uniformly branching topology of a leuconoid sponge aquiferous system revealed by 3D reconstruction and morphometrics using corrosion casting and X-ray microtomography. *Acta Zoologica* **93**:160–170 DOI [10.1111/j.1463-6395.2010.00492.x](https://doi.org/10.1111/j.1463-6395.2010.00492.x).
- Heyward A, Fromont J, Schönberg C, Colquhoun J, Radford B, Gomez O. 2010.** The sponge gardens of Ningaloo Reef, Western Australia. *The Open Marine Biology Journal* **4**:3–11 DOI [10.2174/1874450801004010003](https://doi.org/10.2174/1874450801004010003).
- Johnston IS, Hildemann WH. 1982.** Cellular organization in the marine demosponge *Callyspongia diffusa*. *Marine Biology* **67**:1–7 DOI [10.1007/BF00397088](https://doi.org/10.1007/BF00397088).
- Jones R, Bessell-Browne P, Fisher R, Klonowski W, Slivkoff M. 2016.** Assessing the impacts of sediments from dredging on corals. *Marine Pollution Bulletin* **102**:9–29 DOI [10.1016/j.marpolbul.2015.10.049](https://doi.org/10.1016/j.marpolbul.2015.10.049).
- Jones R, Fisher R, Stark C, Ridd P. 2015.** Temporal patterns in seawater quality from dredging in tropical environments. *PLOS ONE* **10**:e0137112 DOI [10.1371/journal.pone.0137112](https://doi.org/10.1371/journal.pone.0137112).
- Jones R, Ricardo GF, Negri AP. 2015.** Effects of sediments on the reproductive cycle of corals. *Marine Pollution Bulletin* **100**:13–33 DOI [10.1016/j.marpolbul.2015.08.021](https://doi.org/10.1016/j.marpolbul.2015.08.021).

- Kroon FJ, Kuhnert PM, Henderson BL, Wilkinson SN, Kinsey-henderson A, Abbott B, Brodie JE, Turner RDR. 2013.** River loads of suspended solids, nitrogen, phosphorus and herbicides delivered to the Great Barrier Reef lagoon. *Marine Pollution Bulletin* **65**:167–181 DOI [10.1016/j.marpolbul.2011.10.018](https://doi.org/10.1016/j.marpolbul.2011.10.018).
- Leys SP, Meech RW. 2006.** Physiology of coordination in sponges. *Canadian Journal of Zoology* **84**:288–306 DOI [10.1139/z05-171](https://doi.org/10.1139/z05-171).
- Leys SP, Yahel G, Reidenbach MA, Tunnicliffe V, Shavit U, Reiswig HM. 2011.** The sponge pump: the role of current induced flow in the design of the sponge body plan. *PLOS ONE* **6**:e27787 DOI [10.1371/journal.pone.0027787](https://doi.org/10.1371/journal.pone.0027787).
- Ludeman DA, Farrar N, Riesgo A, Paps J, Leys SP. 2014.** Evolutionary origins of sensation in metazoans: functional evidence for a new sensory organ in sponges. *BMC Evolutionary Biology* **14**:1–11 DOI [10.1186/1471-2148-14-1](https://doi.org/10.1186/1471-2148-14-1).
- Luter H, Whalan S, Webster N. 2012a.** Thermal and sedimentation stress are unlikely causes of brown spot syndrome in the coral reef sponge, *Ianthella basta*. *PLOS ONE* **7**:e39779 DOI [10.1371/journal.pone.0039779](https://doi.org/10.1371/journal.pone.0039779).
- Luter HM, Whalan S, Webster NS. 2012b.** The marine sponge *Ianthella basta* can recover from stress-induced tissue regression. *Hydrobiologia* **687**:227–235 DOI [10.1007/s10750-011-0887-x](https://doi.org/10.1007/s10750-011-0887-x).
- Maldonado M. 2016.** Sponge waste that fuels marine oligotrophic food webs: a re-assessment of its origin and nature. *Marine Ecology* **37**:477–491 DOI [10.1111/maec.12256](https://doi.org/10.1111/maec.12256).
- Maldonado M, Giraud K, Carmona C. 2008.** Effects of sediment on the survival of asexually produced sponge recruits. *Marine Biology* **154**:631–641 DOI [10.1007/s00227-008-0956-5](https://doi.org/10.1007/s00227-008-0956-5).
- McMurray SE, Pawlik JR, Finelli CM. 2014.** Trait-mediated ecosystem impacts: how morphology and size affect pumping rates of the Caribbean giant barrel sponge. *Aquatic Biology* **23**:1–13 DOI [10.3354/ab00612](https://doi.org/10.3354/ab00612).
- Messenger JB, Nixon M, Ryan KP. 1985.** Magnesium chloride as an anaesthetic for chephalopods. *Comparative Biochemistry and Physiology* **82**:203–205 DOI [10.1016/0742-8413\(85\)90230-0](https://doi.org/10.1016/0742-8413(85)90230-0).
- Pile AJ, Savarese M, Chernykh VI, Fialkov VA. 1997.** Trophic effects of sponge feeding within Lake Baikal's littoral zone. 2. Sponge abundance, diet, feeding efficiency, and carbon flux. *Limnology and Oceanography* **42**:184–192 DOI [10.4319/lo.1997.42.1.0184](https://doi.org/10.4319/lo.1997.42.1.0184).
- Pineda MC, Duckworth A, Webster N. 2016.** Appearance matters: sedimentation effects on different sponge morphologies. *Journal of the Marine Biological Association of the United Kingdom* **96**:481–492 DOI [10.1017/S0025315414001787](https://doi.org/10.1017/S0025315414001787).
- Pineda MC, Strehlow B, Duckworth A, Doyle J, Jones R, Webster NS. 2016.** Effects of light attenuation on the sponge holobiont-implications for dredging management. *Scientific Reports* **6**:39038 DOI [10.1038/srep39038](https://doi.org/10.1038/srep39038).
- Pineda MC, Strehlow B, Kamp J, Duckworth A, Jones R, Webster NS. 2017a.** Effects of combined dredging-related stressors on sponges: a laboratory approach using realistic scenarios. *Scientific Reports* **7**(1):5155 DOI [10.1038/s41598-017-05251-x](https://doi.org/10.1038/s41598-017-05251-x).

- Pineda MC, Strehlow B, Sternel M, Duckworth A, Jones R, Webster NS. 2017b.** Effects of suspended sediments on the sponge holobiont with implications for dredging management. *Scientific Reports* 7(1):4925 DOI 10.1038/s41598-017-05241-z.
- Pineda MC, Strehlow B, Sternel M, Duckworth A, Den Haan J, Jones R, Webster NS. 2017c.** Effect of sediment smothering on the sponge holobiont with implications for dredging management. *Scientific Reports* 7(1):5156 DOI 10.1038/s41598-017-05243-x.
- Ports Australia. 2014.** Dredging and Australian ports subtropical and tropical ports. Available at <http://www.portsaustralia.com.au/assets/Publications/Dredge-Report-Low-Res.pdf> (accessed on 01 May 2016).
- Ports Australia. 2015.** Dredging and Australian Temperate Ports. Available at <http://www.portsaustralia.com.au/assets/Publications/Dredge-Report-Temperate-ports-Low-respdf.pdf> (accessed on 01 May 2016).
- R Development Core Team. 2016.** R: a language and environment for statistical computing. Vienna: R Foundation for Statistical Computing.
- Rasband W. 2012.** ImageJ. Bethesda: US National Institutes of Health..
- Reiswig HM. 1971.** *In situ* pumping activities of tropical Demospongiae. *Marine Biology* 9:38–50 DOI 10.1007/BF00348816.
- Reiswig HM. 1974.** Water transport, respiration and energetics of three tropical marine sponges. *Journal of Experimental Marine Biology and Ecology* 14:231–249 DOI 10.1016/0022-0981(74)90005-7.
- Reiswig HM. 1975.** The aquiferous systems of three marine Demospongiae. *Journal of Morphology* 145:493–502 DOI 10.1002/jmor.1051450407.
- Ricardo GF, Jones RJ, Clode PL, Humanes A, Negri AP. 2015.** Suspended sediments limit coral sperm availability. *Scientific Reports* 5:18084 DOI 10.1038/srep18084.
- Riegl B, Branch GM. 1995.** Effects of sediment on the energy budgets of four scleractinian (Bourne 1900) and five alcyonacean (Lamouroux 1816) corals. *Journal of Experimental Marine Biology and Ecology* 186:259–275 DOI 10.1016/0022-0981(94)00164-9.
- Savarese M, Patterson MR, Chernykh VI, Fialkov VA. 1997.** Trophic effects of sponge feeding within Lake Baikal's littoral zone .1. *In situ* pumping rates. *Limnology and Oceanography* 42:171–178 DOI 10.4319/lo.1997.42.1.0171.
- Schönberg CHL. 2015.** Happy relationships of marine sponges with sediments—a review and some observations from Australia. *Journal of the Marine Biological Association of the United Kingdom* 96:493–514 DOI 10.1017/S0025315415001411.
- Schönberg CHL. 2016.** Effects of dredging on benthic filter feeder communities, with a focus on sponges. Report of theme 6-project 6.1.1 prepared for the dredging science node. Western Australian Marine Science Institution, Perth, 139. Available at http://www.wamsi.org.au/sites/wamsi.org.au/files/files/Effects%20of%20Dredging%20on%20Filter%20Feeders%20Review_WAMSI%20DSN%20Report%206_1_Sch%20B%20C3%2082nberg%202016%20FINAL.pdf (accessed on 01 May 2016).
- Simpson TL. 1984.** *The cell biology of sponges*. Berlin: Springer Verlag.

- Stafford-Smith MG, Ormond RFG. 1992.** Sediment-rejection mechanisms of 42 species of australian scleractinian corals. *Marine and Freshwater Research* **43**:683–705 DOI [10.1071/MF9920683](https://doi.org/10.1071/MF9920683).
- Strehlow B, Friday S, McCauley M, Hill M. 2016b.** The potential of azooxanthellate poriferan hosts to assess the fundamental and realized Symbiodinium niche: evaluating a novel method to initiate Symbiodinium associations. *Coral Reefs* **35**(4):1201–1212 DOI [10.1007/s00338-016-1465-5](https://doi.org/10.1007/s00338-016-1465-5).
- Strehlow BW, Jorgensen D, Webster NS, Pineda MC, Duckworth A. 2016a.** Using a thermistor flowmeter with attached video camera for monitoring sponge excurrent speed and oscular behaviour. *PeerJ* **4**:e2761 DOI [10.7717/peerj.2761](https://doi.org/10.7717/peerj.2761).
- Tompkins-MacDonald GJ, Leys SP. 2008.** Glass sponges arrest pumping in response to sediment: implications for the physiology of the hexactinellid conduction system. *Marine Biology* **154**:973–984 DOI [10.1007/s00227-008-0987-y](https://doi.org/10.1007/s00227-008-0987-y).
- Topçu NE, Pérez T, Grégori G, Harmelin-Vivien M. 2010.** *In situ* investigation of *Spongia officinalis* (Demospongiae) particle feeding: coupling flow cytometry and stable isotope analysis. *Journal of Experimental Marine Biology and Ecology* **389**:61–69 DOI [10.1016/j.jembe.2010.03.017](https://doi.org/10.1016/j.jembe.2010.03.017).
- Turon X, Galera J, Uriz MJ. 1997.** Clearance rates and aquiferous systems in two sponges with contrasting life-history strategies. *Journal of Experimental Zoology* **278**:22–36 DOI [10.1002/\(SICI\)1097-010X\(19970501\)278:1<22::AID-JEZ3>3.0.CO;2-8](https://doi.org/10.1002/(SICI)1097-010X(19970501)278:1<22::AID-JEZ3>3.0.CO;2-8).
- Van Soest RW, Boury-Esnault N, Hooper JNA, Rützler K, De Voogd NJ, Alvarez de Glasby B, Hajdu E, Pisera AB, Manconi R, Schoenberg C, Klautau M, Picton B, Kelly M, Vacelet J, Dohrmann M, Díaz M-C, Cárdenas P, Carballo JL. 2017.** World Porifera database. Available at <http://www.marinespecies.org/porifera> (accessed on 08 February 2017).
- Yahel G, Whitney F, Reiswig HM, Eerkes-Medrano DI, Leys SP. 2007.** *In situ* feeding and metabolism of glass sponges (Hexactinellida, Porifera) studied in a deep temperate fjord with a remotely operated submersible. *Limnology and Oceanography* **52**:428–440 DOI [10.4319/lo.2007.52.1.0428](https://doi.org/10.4319/lo.2007.52.1.0428).